TECHNICAL REPORT STANDARD PAGE

1. Report No.	2. Government Accession No.	3. Recipient's Catalog No.
FHWA/LA-88/210		

4. Title and Subtitle	5. Report Date
Development of Design Criteria for the Prevention of Slope Failures	March 1990
	6. Performing Organization Code

7. Author(s)	8. Performing Organization Report No.
Scott F. Burns, William O. Hadley, Jack W. Mutchler, Schaun M. Smith, Adnan Siddiqui, and Mike Hernandez	210

9. Performing Organization Name and Address	10. Work Unit No.
Dept. of Petroleum Engineering and Geosciences Louisiana Tech University Ruston, LA 71272	11. Contract or Grant No. STUDY NO. LA HPR 86-2GT(B)

12. Sponsoring Agency Name and Address	13. Type of Report and Period Covered
Louisiana Transportation Research Center, DOTD 4101 Gourrier Avenue Baton Rouge, LA 70808	Final Report Feb. 1986 - June 1988
	14. Sponsoring Agency Code

15. Supplementary Notes
Conducted in cooperation with the U.S. Department of Transportation, Federal Highway Administration

16. Abstract

A total of 242 embankments were examined along a 122-mile transect of I-10 AND I-20 highways in Louisiana. A total of 99 slope failures had occurred 8-15 years after construction (mean volume = 15,105 cubic feet). Most of the failures occurred on slopes greater than 16 degrees. Over 70% of the failures were found in modern alluvium parent material as compared to loess, sandy alluvium and Priairie Terrace alluvium. It is believed that the high amount of smectite in these soils created most of failures when the slope moisture content rose. A predictive model for the first 15 years after construction was developed. A high-rise slope has an 85-90% chance of failure and is constructed of soil with: 47% clay content, a plasticity index (PI) 29%, a liquid limit (LL) 54%, and net smectite 33%. Low-risk slopes have a chance of less that 5% of failure and are constructed of soils with: 32% clay, 16% PI, 36% LL, and net smectite 18%. Determination of the risk category can be done easily in the laboratory using Atterberg limits. Control of slope stability depends upon control of expansive clays in the high- and intermediate-risk slope soils. It is recommended to lime stabilize these soils or use a new slope design. A map of the distribution of these soils in Louisiana is included. Four different design nomographs based on a stability model of the slopes is presented for soils in the high- and intermediate-risk categories. Depending upon the availability of space and economy, the designs include constant slope configuration, broken-back design, and soil-stabilized layers below the above two.

17. Key Words	18. Distribution Statement
embankment, slope failure, landslides, shrink-swell clays, smectite, expansion clay, Atterberg limits, slope stabilization	No restrictions. This document is available to the public through the National Technical Information Service, Springfield, VA 22161.

19. Security Classif. (of this report)	20. Security Classif. (of this page)	21. No. of Pages	22. Price
Unclassified	Unclassified	231	

Form DOT F1700.7 (1-92)

DEVELOPMENT OF DESIGN CRITERIA FOR PREVENTION OF SLOPE FAILURES

FINAL REPORT

by

SCOTT F. BURNS, PH.D.
ASSOCIATE PROFESSOR OF GEOLOGY
LOUISIANA TECH UNIVERSITY
RUSTON, LOUISIANA 71272

WILLIAM O. HADLEY, PH.D., P.E.
PROFESSOR OF CIVIL ENGINEERING
LOUISIANA TECH UNIVERSITY
RUSTON, LOUISIANA 71272

JACK W. MUTCHLER, SCHAUN M. SMITH, ADNAN SIDDIQUI, MIKE HERNANDEZ
DEPT. OF PETROLEUM ENGINEERING AND GEOSCIENCES
LOUISIANA TECH UNIVERSITY
RUSTON, LOUISIANA 71272

RESEARCH PROJECT NO. 210
STATE PROJECT NO. 737-07-0009
RESEARCH PROJECT NO. 86-2GT(B)

CONDUCTED FOR

LOUISIANA DEPARTMENT OF TRANSPORTATION AND DEVELOPMENT
LOUISIANA TRANSPORTATION RESEARCH CENTER
in Cooperation with
U.S. Department of Transportation
FEDERAL HIGHWAY ADMINISTRATION

MARCH 1990

ACKNOWLEDGMENTS

This work was made possible by a contract from the Louisiana Department of Transportation and Development through the Louisiana Transportation Research Center and the Federal Highway Administration, Washington D.C. - Louisiana State Project No. 737-07-09 and Research Project No. 86-2GT(B). Mr. Paul Griffin of LTRC provided continued support, advice, guidance, and always appreciated encouragement throughout the project which was most valued by the researchers. During the early stages of the project and prior to their retirement from LTRC, Mr. S.C. Shah and Mr. James Melancon helped with advice and guidance that was needed.

In the field, we had good support from the field crews and DOTD administrators. Mr. Odis Gunn of the Tallulah office was most helpful when we were working in the I-20 study area. Mr. M.E. "Skipper" Cryer provided many good ideas and an abundance of data for the I-10 study area.

Mrs. Diane Zumwalt drafted many of the maps of the I-20 study area. Adnan Siddiqui compiled and drafted the map of the distribution of shrink-swell clay soils in Louisiana.

Support from this project helped three students receive their Master of Science degrees. Jack Mutchler and Schaun Smith did high-quality theses directly related to this project. Mike Hernandez is completing his thesis on landslides in northeast Louisiana as a direct outgrowth of this project.

We would like to extend thanks to the late Dr. Bobby J. Miller of LSU for confirming clay mineral identifications and to Dr. Patricia Steinhilber of Louisiana Tech University for aiding us in organic carbon determinations. Facilities for this project were supplied by the Dept. of Petroleum Engineering and Geosciences, the Dept. of Civil Engineering, and the Dept. of Soil Sciences of Louisiana Tech University. Many thanks also go to Dr. Leo Herrmann and Dr. Robert Mack Caruthers, the department heads who were in charge of this research group for its duration. Much appreciation goes to Delaine Pylant, Dean Williams and Darla Knapp for their help in retyping most of the report. The entire project was a challenge and was most enjoyable.

ABSTRACT

A total of 242 embankments were examined along a 122- mile transect on I-10 and I-20 highways in Louisiana. A total of 99 slope failures had occurred on some of the embankments. They were classified as slumps (32), slump-earthflows (44), and earthflows (23). The mean volume for all of the failures was 15,105 cubic feet. All of the embankment failures had occurred 8-15 years after their construction. Most of the failures happened on slopes greater than 16 degrees (>3.5:1). The parent materials of the slopes were: modern alluvium, Prairie Terrace alluvium, Mississippi Valley Train alluvium, and loess. Over 70% of the failures occurred in the modern alluvium slopes. It is believed that the high amount of smectite in the modern alluvium soils caused most of the failures when the slope moisture content rose.

Using T-tests, ANOVA tests, and risk model ranking, a predictive model for the first 15 years after construction was developed. High risk slopes have an 85-90% chance of failure and are constructed of soil with: > 47% clay content, a plasticity index > 29%, a liquid limit > 54%, and a net smectite value > 33%. Intermediate risk slopes have a 55-60% chance of failure and are constructed of soil with: a clay content 32-47%, a plasticity index of 16-29%, a liquid limit value of 36-54%, and a net smectite value of 18-33%. Low risk slopes have a chance of less than 5% failure and are constructed of soils with: < 32% clay content, < 16% plasticity index, < 36% liquid limit, and a net smectite value < 18%. Determination of the risk category can be easily done in the laboratory by obtaining Atterberg limits.

Control of slope stability centers around control of the shrink-swell clay in the slope soils. It is recommended to lime- stabilize the soils to inactivate the smectite clays. A map of the distribution of these clays in Louisiana is included in the report. It is not recommended to drive pilings or push the failed soil back up onto the slope. It is also recommended to have adequate drainage to control surface run-off on these slopes. It is also suggested to extend the header revetment aprons under the bridges onto the sides.

A slope stability model is presented here that adequately characterizes the embankment cross section as a three-soil layer system. When applied to 31 existing slopes, it accurately predicted the stability state of 90% of the slopes. In the cross section, soil layer 1 is the top zone of vegetation and soil covering the slopes and is considered to be a foot thick. Soil layer 2 is the embankment fill, and soil layer 3 is the natural soil surface upon which the embankment has been constructed. Soil layers 2 and 3 are characterized by cohesive strength only.

From the computer characterizations of the slopes, about 2/3 of the cases resulted in failure surfaces that extended well below the ground surface (i.e., deep-seated) and originated close to the pavement edge. Designs of slopes must take these two ideas into account.

Four different design nomographs are presented which represent design and reconstruction techniques of embankments which can be utilized for embankments composed of high smectite clays. A constant embankment slope configuration can be used when there is plenty of space. The broken-back design can be used when right-of-way is difficult to obtain. When there is a problem with upward movement of water into the embankment section, the broken-back design

with a stabilized soil layer or a constant embankment slope with a stable subgrade might be used (i.e., a lime-stabilized subgrade). For stabilization of existing embankments, installation of full embankment width soil reinforcement ties is also prescribed.

Overall, problem soils must be noted first using the risk model, and then the soils must be altered or the design changed to fit the situation to prevent slope failures.

TABLE OF CONTENTS

TABLE OF CONTENTS (CONT'D)

TABLE OF CONTENTS (CONT'D)

TABLE OF CONTENTS (CONT'D)

PAGE NO.

LIST OF TABLES

LIST OF TABLES (CONT'D)

LIST OF TABLES (CONT'D)

LIST OF TABLES (CONT'D)

LIST OF FIGURES

LIST OF FIGURES (CONT'D)

LIST OF FIGURES (CONT'D)

LIST OF FIGURES (CONT'D)

LIST OF FIGURES (CONT'D)

INTRODUCTION

An enduring problem which plagues many regions throughout the United States is slope instability on embankments along interstate highway systems. The term "embankment" as used in this report is defined as a man-made slope constructed of earthen fill excavated from adjacent parent material. Based on Federal Highway Administration estimates, landslides along federal highways in the United States result in an annual loss in excess of $50 million for tangible damage (1). Intangible costs which cannot be accurately evaluated but are often more valuable than actual physical destruction include disruptions and delays to interstate traffic flow, in addition to safety hazards to motorists. Chassie and Goughnour (2) have illustrated, in the state of New York, that with improvement and utilization of geological and geotechnical investigative techniques in slope stability analysis, losses both tangible and intangible may be sustantially reduced.

In Louisiana, over 100 embankments have failed in the last ten years along the states two major interstate highway systems. Over sixty slope failures have occurred along Interstate Highway 10 between Lafayette and Lake Charles in the southern part of the state. In the northeast part of the state along Interstate Highway 20, over 40 landslides have occurred in the past six years, primarily in Madison Parish.

The extent of the problem is manifest dramatically in the economic impact to Louisiana's budget by maintenance and remedial repair costs. Cumulative repair costs from landslides for this section of I-10 have reached approximately $1,225,000. This value only includes four of the 37 embankments in Acadia Parish where future remedial repair costs are projected in the tens of millions of dollars (3). Repair costs for the I-20 section to date are $780,000 and future repair costs are estimated to exceed $1 million. Projections are based on the costs incurred for repairs completed in the past. The solution to the problem of embankment slope instability and the resultant reduction or elimination of large capital expenditures lie in the understanding of why these embankment slopes fail.

The ultimate objectives of this study are to determine why these embankments have failed along the interstate highway systems and to recommend ways of repairing them and preventing their occurrence on other slopes. The ultimate objectives are accomplished through the following steps:

1) Characterize failed and non-failed slopes according to slope angles, size of failures, sedimentology, clay properties, and geotechnical properties.
2) Classify the types of slope failures using the Varnes system (4).

3) Statistically compare the characteristics of the two types of slopes to determine why some slopes failed and others have not failed.

4) Make predictions as to future slope failures.

5) Make recommendations about construction and repair of highway embankments.

Research conducted comparing the properties of failed and non-failed embankments will expand understanding of the reasons behind embankment slope failure. With this understanding will come improved solutions to embankment slope stability problems by the designers, engineers, and maintenance crews of the state and federal highway agencies.

STUDY AREA

INTRODUCTION

Although slope failures have occurred on embankments along all highways in Louisiana, the majority have happened in two main stretches of I-10 and I-20. Along I-10 between Lafayette and Lake Charles, over 60 slope failures have been recorded, so this area was selected as the southern study area. The majority of landslides on I-20 have occurred in Madison Parish, so a section of the highway from Monroe to Tallulah in Madison Parish was chosen for the northern study site. The slopes found in these areas give a good, representative cross section of embankments built in the state on many different parent materials. The following sections describe the boundaries, sites, soils, climate and geology of the two study areas.

THE I-20 STUDY AREA, NORTHEAST LOUISIANA

Boundaries

The I-20 study area consists of representative embankments at most interchanges and overpasses along an east-west transect from Tallulah to Monroe, Louisiana, along I-20 (Figs.1,2). The description of each of these embankment locations giving structure number, date of construction, latitude and longitude, township and range, slope angles, site of sampling, soil type, and location of the borrow pit is located in the Appendix in Tables 1 and 2. These sites are found in Ouachita, Richland, and Madison Parishes. Intensive study has been done in Madison Parish, where 42 slope failures have occurred on these man-made slopes. No failures have occurred within Richland Parish to date, and two failures have occurred in Ouachita Parish. Samples within these last two parishes were taken to compare to those in Madison Parish, to aid in understanding why the slopes have failed there.

Climate

The climate of the study area is a "subtropical, transitional, climatic region that is alternately affected by cold, dry air flowing southward and by warm moist air flowing northward" (5). Changes in the flow direction can cause sudden weather changes.

The summer, May to October, can be characterized as warm, with temperatures of 32+ degrees C (90+ degrees F) being normal and 38+ degrees C (100+ degrees F) temperatures being somewhat rare. The number of days per year when the temperatures hit 32+ degrees C normally ranges between 50 to 120. During these warmer months, hot, dry periods or droughts

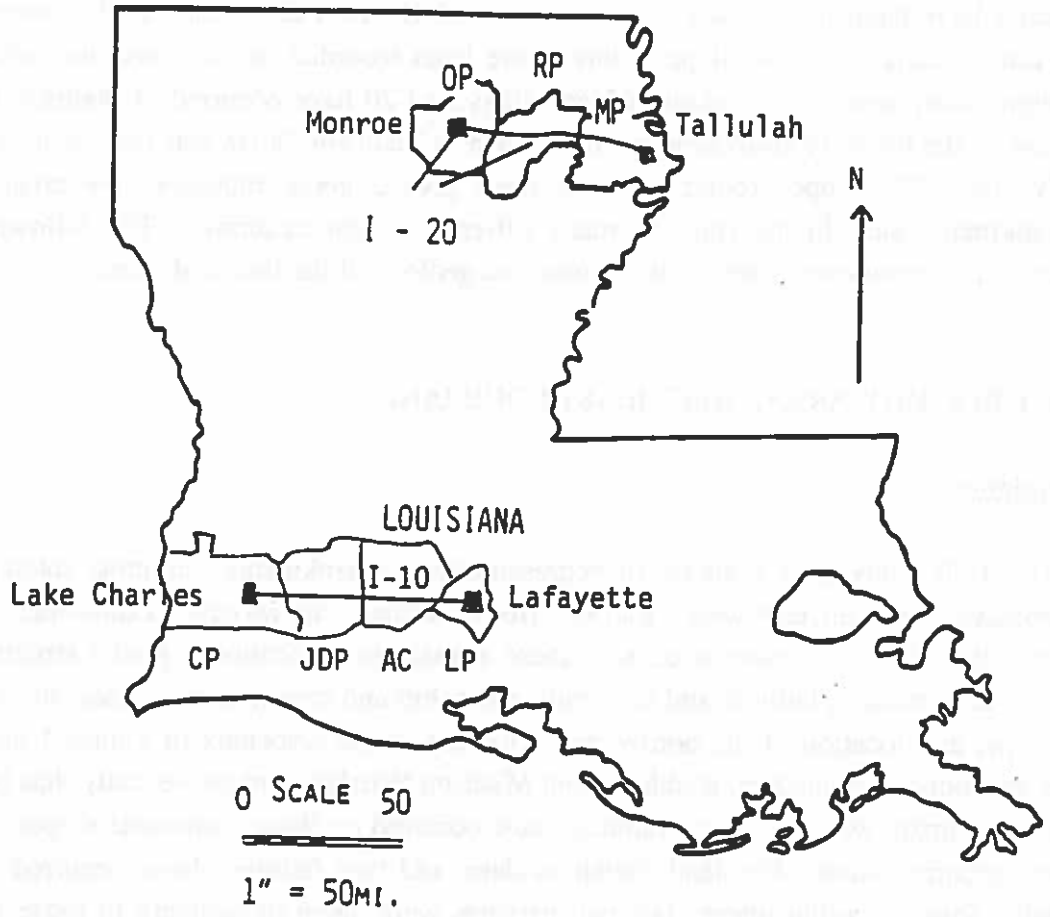

Figure 1. Location map of study areas within the state. The I-20 study area transect connects Monroe and Tallulah through Ouachita Parish (OP), Richland Parish (RP), and Madison Parish (MP). The I-10 study area connects Lake Charles and Lafayette through Calcasieu Parish (CP), Jefferson Davis Parish (JDP), Acadia Parish (AC), and Lafayette Parish (LP).

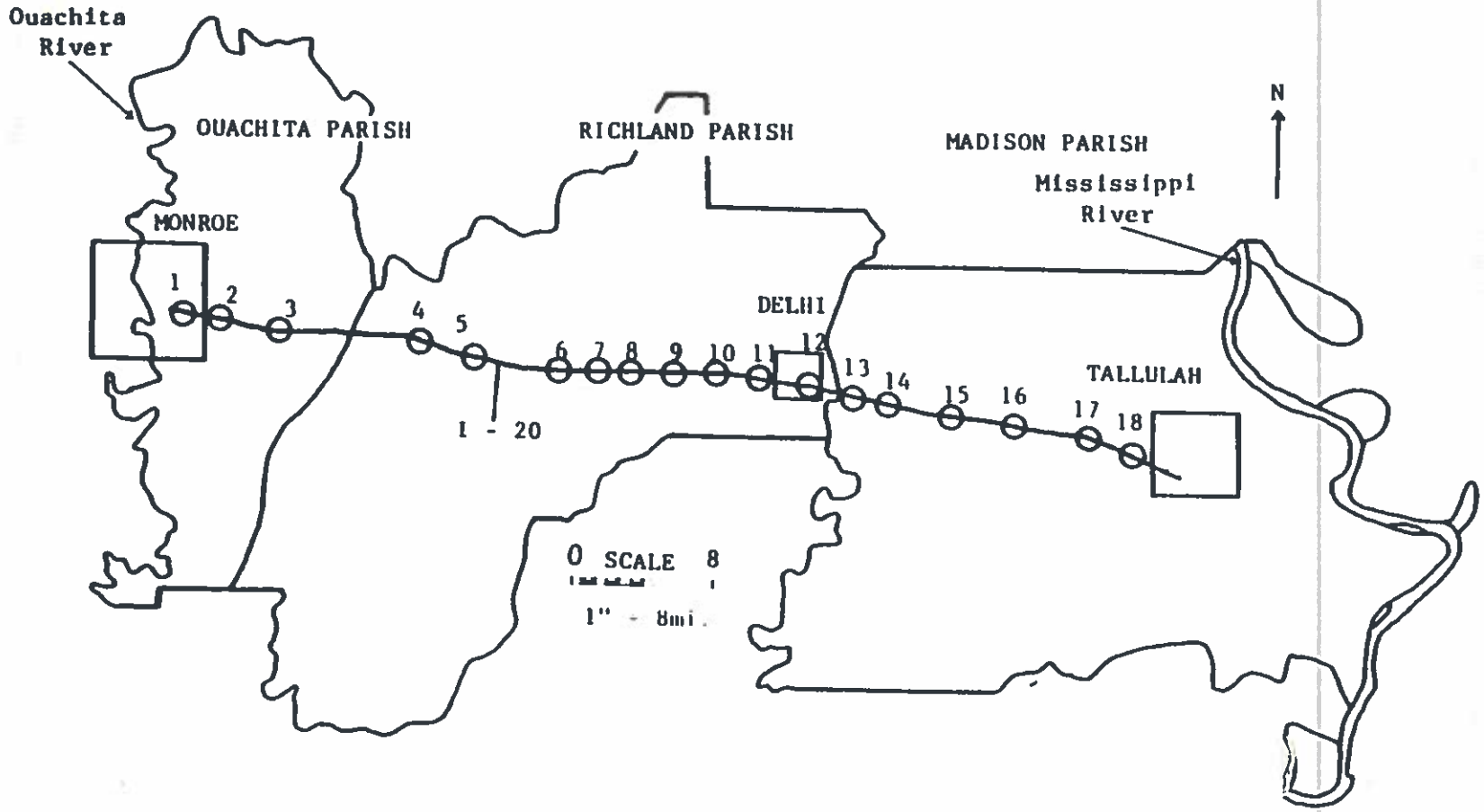

Figure 2. Sample locations along I-20 study area. Site descriptions of the numbers are explained in Table A1 and Table A2 of the Appendix. Location numbers all should have "N" in front of them.

can occur because of northerly and westerly winds, but droughts usually do not exceed one month in length (5).

The winters are mild, with temperatures of zero degrees C (32 degrees F) or less from October to early April. The number of days per year when temperatures are zero degrees C or less normally ranges between 30-65 days. Most years have at least one day when temperatures dip below -7 degrees C (20 degrees F), but cold spells are usually short lived causing the ground to freeze only to a shallow depth (5).

On the annual average, it rains two out of seven days, and extended periods of steady rain occur during the winter and spring. The weather pattern for the cooler months is usually rainy, with low to moderate temperatures, followed by a few clear, mild days, followed by more rain. Thunderstorms can occur during any season and average 60 to 70 days out of the year (5).

Snowfall is rare, and measurable amounts can be expected one out of every two years, which averages about two inches a year. However, several years may pass without any snow. Annual precipitation ranges between 36 inches (914 mm) and 67 inches (1701 mm) 90% of the time, with the annual average of 51 inches (1295 mm) computed from monthly averages (5).

The annual mean for relative humidity is 72%, and humidity greater than 80% occurs over 40% of the total hours of the year. The sun shines on an average of 63% of the possible daylight hours. Wind speed is usually less than 10 mi/hr (16 km/hr), but can gust up to 40 mi/hr (64 km/hr) during storms. Southerly winds occur during the summer and northerly winds occur during the winter (5).

Physiography and Geology

The study area is located between the Mississippi and Ouachita river systems, which have greatly influenced the region (Fig.3). Madison Parish is situated within the alluvial plain of the Mississippi River. The eastern boundary of the parish is formed by the Mississippi River and its abandoned river channels, while the western boundary is Bayou Macon. Madison Parish contains several abandoned river courses of the Mississippi River: the Tensas River, Walnut Bayou, and Roundaway Bayou (5).

The parish is made up of natural levee and alluvial deposits of fine-grained sediments. Elevations range from 80 feet (24m) above mean sea level in the north to 60 feet (18 m) above mean sea level in the south, and elevations can be up to 10 feet higher along natural levees of the Mississippi River in the eastern part of the Parish (5). Relief is very slight, ranging from flat to one degree, with possibly 2.5 degrees in ridge and swale features.

Richland Parish is situated between Madison and Ouachita Parishes. A soil survey has not been published for Richland Parish, so specific soil information is not available. Richland Parish is bounded to the east by Bayou Macon and to the west by Bayou LaFourche (6). The geology of the parish is dominated by the Macon Ridge, which is composed of braided stream terraces and glacial outwash of the ancestral Mississippi River (7). Approximately one-third to one-half of the eastern side of Macon Ridge is veneered by a loess sheet. The braided stream

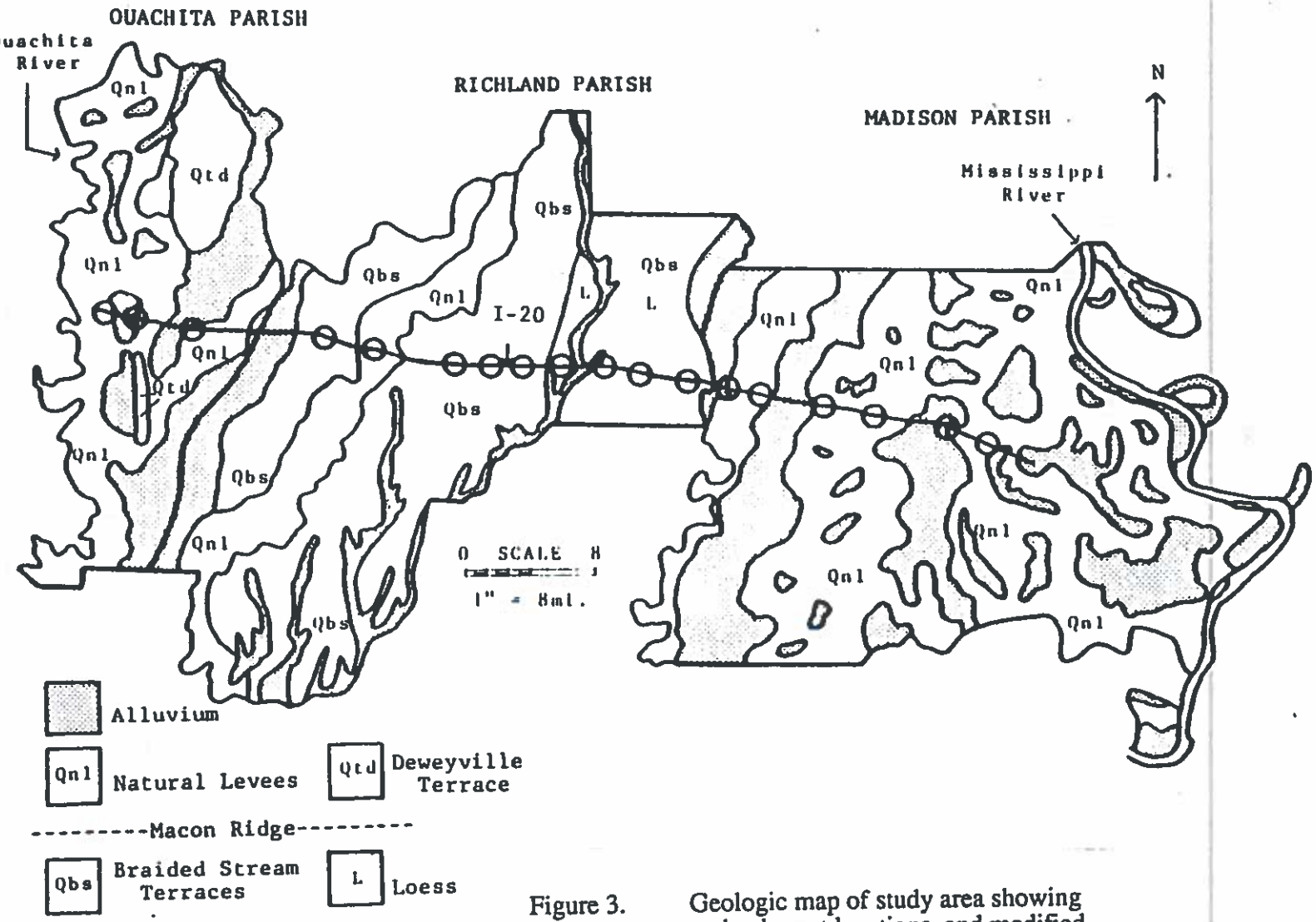

Figure 3. Geologic map of study area showing embankment locations and modified from Snead and McCulloh (6).

terrace is interrupted towards the western part of the Parish by the Boeuf River and its associated natural levee deposits. At the extreme eastern boundary of the parish, are alluvial deposits associated with the floodplain environment of Ouachita Parish. The relief of the Parish is mostly low. The parish appears to be drained by the Boeuf River and Big Creek. Many bayous feed Big Creek, including Bee Bayou, Muddy Bayou, Little Creek, Cypress Creek, and Colewa Bayou. Big Creek then feeds into the Boeuf River to the south.

Ouachita Parish has three physiographic divisions: the Hilly Coastal Plain Uplands, the Deweyville, Prairie, Montgomery, and Bentley Terrace formations, and the recent flood plains (8). This study is concerned only with that part of the parish that is to the east of the Ouachita River, since this river is the western boundary of the study area. This primarily includes the flood plain of the Ouachita River (Fig.3).

The Ouachita Parish flood plain area, which makes up one-third of the parish, contains two types of recent alluvium. The purplish-red clay and silts were possibly transported from the Ozark area by the Arkansas River (8,9). Secondly, the light to dark gray and dark bluish-gray clay and silt has been transported by the Ouachita River from the Ouachita Mountains. The bluish-gray clays can be calcareous and graveliferous locally (9). These two types of deposits are interbedded in the eastern part of the parish.

Occupying former channels of possibly the Arkansas River are the Ouachita River, which drains the whole parish, Bayou Bartholomew, Bayou De Siard, and Youngs Bayou. This area also contains oxbow lakes, meander scars, natural levees, alluvium, back swamps, and rim swamps formed from the shifting course of possibly the Arkansas River (9). Rim swamps are formed when drainage from the terraces is sealed off by natural levees of the larger streams. Black Bayou is an example of a rim swamp and backswamp. Elevations within the floodplain area range from 14 m (45 feet) to 28 m (90 feet) above mean sea level. The eastern part of the parish is primarily drained by Bayou LaFourche, which drains into the Boeuf River which, empties into the Ouachita River (8).

Soils

In this region, the warm and moist climate causes rapid soil development. Along with the climate, the vegetation also plays an active role in the soil development (5,9). The high rainfall can cause intense leaching, which moves soluble and colloidal material through the soil. Clay mineral development and the removal of carbonates are accelerated by the production of organic acids from rapidly decaying plant remains (5). These processes are also aided by lack of freezing.

The parent material for soil development in Madison Parish is alluvium of the Mississippi River flood plain. In Ouachita Parish, the parent material is alluvium of the Ouachita River flood plain. Alluvium has a wide range of textures, with the coarser particles being deposited

close to the river on the natural levees and the finer-grained sediments being deposited out over the flood plain as slackwater deposits. The finer sediments are primarily clays, with some silt and fine sands. The natural levee deposits consist of fine sands and some silts (5). The pattern of coarser material deposited close to the river channel and the finer sediments deposited in the the backswamp is repeated several times in Madison Parish because of the many abandoned river courses and bayous (5).

The parent material for soil development in Richland Parish is the Macon Ridge Valley train deposits. These have a coarser sediment content as compared to the flood plain environments, with high silt and sand content low clay content.

Long periods of time are usually required for advanced soil development. Madison Parish primarily contains young soils that have little or no development. None of the soils are over 10,000 years old, with many being less than 1,000 years old, having formed since the Mississippi River deposited the sediments.

The relief of the area is also important to soil formation, inasmuch as it affects drainage, erosion, plant cover, and soil temperature (5). Madison and Ouachita parishes are mostly flat, or in areas of ridge and swale features, the slope is up to 2.5 degrees. This does not seem like a great deal of slope, but it is enough to affect the soils of the parish by causing poor drainage and a high water table. Richland Parish has slightly more relief, because of the presence of Macon Ridge, and therefore better drainage, which is enhanced by the coarser sediment content.

The soils of the study area range from little or no development of young soils to medium development in the Macon Ridge soils. These soils have been classified using primarily the diagnostic horizons of ochric epipedons, cambic horizons, and argillic horizons according to Soil Taxonomy (10). Ochric epipedons are described as light-colored surface horizons that contain some organic matter, and all of the soils in the study area have these. A cambic horizon (Bw horizon) is a subsoil horizon that has been altered enough by soil processes to have structure, free iron oxides, and silicate clay formation, but only slight evidence of clay translocation (5). An argillic horizon is also a subsoil horizon and is characterized as having a "significant accumulation of silicate clay" that shows little or no similarities to the parent material (5).

THE I-10 STUDY AREA, SOUTHWESTERN LOUISIANA

Boundaries

The I-10 study area (Fig. 4) includes representative embankments along Interstate Highway 10 in southwestern Louisiana. I-10 makes a transect of approximately 71 miles (114 km) in length through a portion of the French Acadiana region of Louisiana. From Lake Charles in Calcasieu Parish, the study area transect extends to the eastern boundary of Lafayette Parish

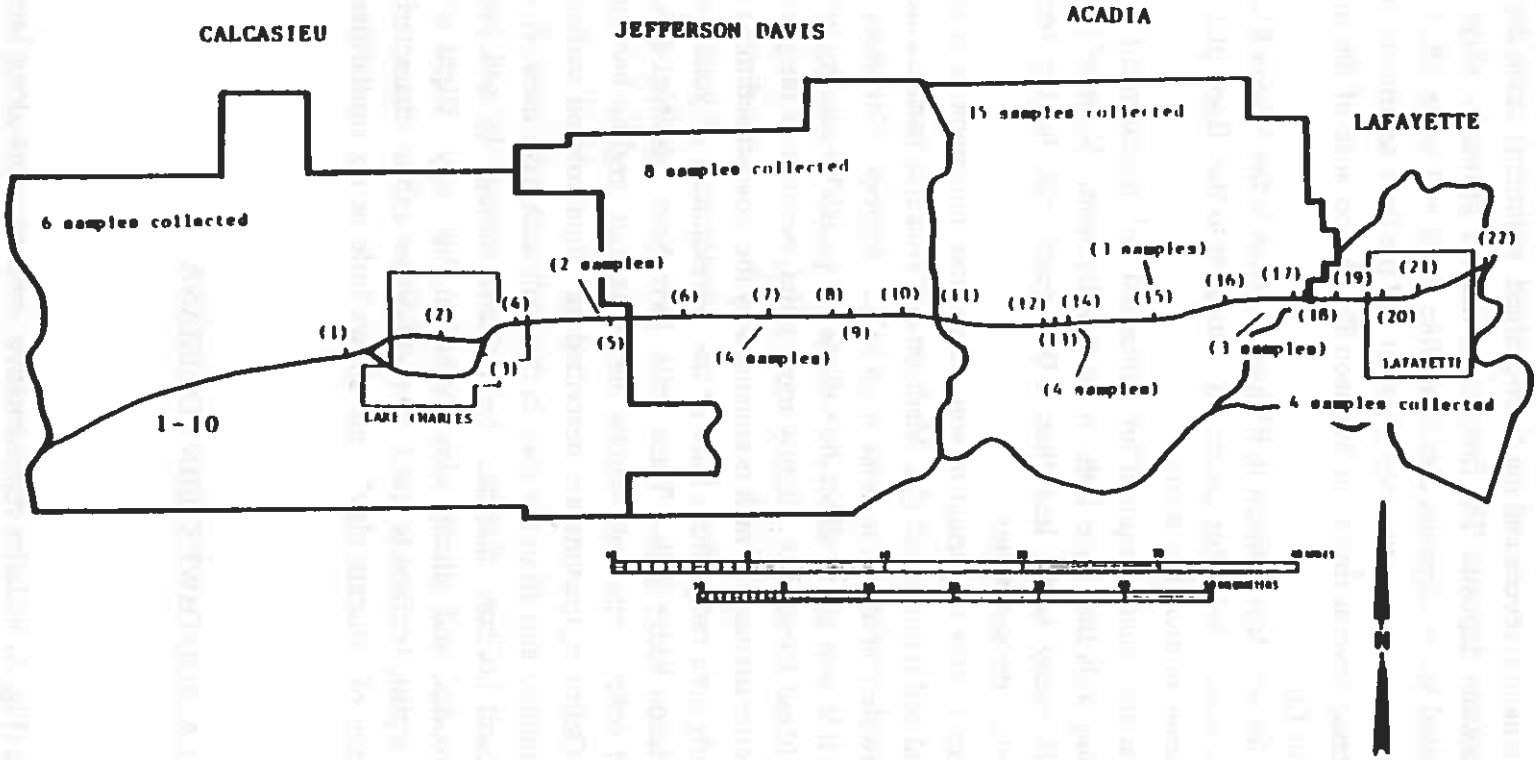

Figure 4. Highway I-10 study area transect showing sample localities S1 through S22 in parentheses. One sample was collected at each locality unless otherwise noted. The total number of samples collected in each parish is also indicated. All numbers should have an "S" in front of them.

(Fig. 1). Intermediate parishes that were studied include Jefferson Davis and Acadia. A total of 33 separate samples were collected (Fig. 4) at 22 embankment localities.

The particular slopes sampled were selected to give an equal geographical distribution across the transect with a mixture of failed (19) and non-failed (14) slopes. A summary of each embankment location and pertinent data on the structure (overpass bridge) with which it is associated is provided in Table A3 in Appendix 1.

The majority of slopes that have failed at the overpasses and interchanges of the study area transect occurred in Acadia Parish. As such, this parish is emphasized in terms of data collection (15 samples) and subsequent computer statistical modeling of embankment slope failure characteristics and trends.

During development of I-10, nearby soil was excavated for utilization in embankment construction. The soil was taken from borrow pits and transported a short distance, usually less than 0.6 miles (1 km), to the embankment site.

Climate

Southwestern Louisiana is characterized by a humid, subtropical climate. The warm waters of the Gulf of Mexico have a dominant influence on the region. During the summer months prevailing southeasterly winds off the Gulf pump warm, moist air inland. Relative humidity is generally in excess of 60 percent for three-fourths of the year. Temperatures are mild, averaging 27.8 degrees C (82 degrees F) during the summer and 12.8 degrees C (55 degrees F) in the winter (11). During the winter months, sporadic invasions of cold, Arctic air displace the moist tropical Gulf air. However, these invasions of Arctic air generally do not last longer than 72 to 96 hours,with temperatures rarely dropping into the teens (12).

Precipitation is typically associated with the fluctuating cold and warm frontal systems during the winter. Heavy showers occur in areas in front of these passing cold fronts and are generally from 60 to 120 minutes in duration (12). Winter precipitation averages approximately 16 inches (40.6 cm) (11). In the summer, precipitation averages approximately 17 inches (43 cm) and usually occurs in isolated periodic thunderstorms in the afternoon (12). These isolated thunderstorms usually affect small, local areas and result in widely variable soil moisture conditions. Heavy showers are typically associated with the introduction of tropical disturbances of hurricanes from the Gulf of Mexico during the late summer and early autumn. Although these severe weather conditions have the capability of producing flooding and excessive soil moisture conditions, they affect the parishes of the study area approximately 38 years out of every 100 (11). The average yearly rainfall, combining all seasons, is approximately 59 inches (150 cm).

Physiography and Geology

The four parishes of the study area in southwestern Louisiana are (from west to east) Calcasieu, Jefferson Davis, Acadia, and Lafayette. The surficial geology of these parishes consists almost entirely of the upper Pleistocene Prairie Terrace Complex (Fig. 5). The exception is Lafayette Parish, where the Prairie Terrace is overlain by varying amounts (one to nine meters) of loess deposit (6).

The Prairie Terrace consists predominantly of fine- grained clays, silts, and argillaceous sands that were deposited in a fluvial-deltaic environment. These deposits partially form the expansive, broad, gently dipping physiographic region termed the Great Southwest Prairies (13). This region has also been labeled the High Coastwise Terrace and the Praire Coastwise Terrace (14).

The Prairie Terrace alluvium deposits are incised by four main drainage systems in the study area: the Calcasieu River, Bayou Lacassine, Mermentau Bayou, and the Vermillion River. With its large network of tributaries, the Calcasieu River deposits modern alluvium throughout Calcasieu Parish and into northwestern Jefferson Davis Parish. Located in southern Jefferson Davis Parish is the northernmost reaches of Bayou Lacassine and its associated modern alluvium deposits. Extending north and east through Acadia Parish is the extensive Mermentau Bayou system. Cutting across cental Lafayette Parish are the modern alluvial deposits of the Vermillion River.

Parent material utilized in the construction of embankment slopes is therefore of three main types: Prairie Terrace alluvium, modern alluvium, and loess. This material is extracted from borrow pits along the transect of I-10. Depending upon the locality, it would include fine-grained clays, silts, sands, recent alluvial sediments and loess. An extensive review of the Quaternary stratigraphy of the I-10 study area is found in a recent thesis (15).

Soils

The dominant soils of each association described in this section are summarized in Table 1. Calcasieu Parish, localities 1 - 5, are composed predominantly of the Wrightsville, Mowata, and Morey soil series. These soils have a liquid limit ranging from 35 - 60% , plasticity index ranging from 15 - 36 percent, a high shrink-swell potential, and a poor drainage with slow to very slow run-off. Jefferson Davis Parish, localities 6 - 10, are composed predominantly of the Crowley and Midland soil series. These soils have a liquid limit ranging from 38 - 65%, plasticity index ranging from 18 - 40%, a moderate to high shrink-swell potential, and a somewhat poor drainage with slow to very slow run-off. Acadia Parish, localities 11 -18, are composed predominantly of the Crowley and Patoutville soil series. These soils have a liquid limit ranging from 25 - 60%, plasticity index ranging from 8 - 35%, a moderate to high shrink-swell potential, and a somewhat poor drainage with slow run-off. Lafayette Parish,

TABLE 1

SOIL SERIES CHARACTERISTICS*

Site #	Soil Series	Taxonomic Classific.	% Passing Sieve # #10	#40	#200	LL	PI	Shrink Swell Potent	Hydro geol.
S1-2	Wrightsville	Typic Glossaqualf	95-100	95-100	90-100	35-55	16-30	High	PD VS
S3	Mowata	Typic Glossaqualf	100	100	95-100	37-49	18-29	High	PD VS
S4-5	Morey	Typic Argiaquoll	95-100	90-100	85-95	35-60	15-36	High	PD S-VS
S6	Crowley	Typic Albaqualf	100	95-100	85-100	38-60	18-35	Mod-High	PD S-VS
S7	Midland	Typic Ochraqualf	100	100	95-100	41-65	20-40	High	PD S-VS
S8-16	Crowley	Typic Albaqualf	100	95-100	85 100	38-60	18-35	Mod-High	SPD S
S17-18	Patoutville	Aeric Ochraqualf	100	100	95-100	25-50	8-23	Mod	SPD S

TABLE 1 (CONTINUED)

Site #	Soil Series	Taxonomic Classific.	% Passing Sieve # #10	#40	#200	LL	PI	Shrink Swell Potent	Hydro geol.
S19	Jeanerette	Typic Argiaquolls	90-100	85-100	85-100	23-40	17-24	Mod	SPD S
S20	Coteau	Glossaquic Hapludalfs	100	100	95-100	25-37	5-15	Low-Mod	SPD SM
S21	Memphis	Typic Hapludalfs	100	100	95-100	30-40	6-25	Low	WD MR
S22	Frost	Typic Glossaqualfs	100	100	90-100	25-50	15-25	Low-Mod	PD S-VS

* Modified from National Cooperative Soil Survey, Soil Interpretation Records, 1979-1984

Abbreviations: Mod (moderate), PD (poorly-drained), SPD (somewhat poorly drained), WD (well-drained), M (medium runoff), S (slow runoff), VS (very slow runoff), R (rapid runoff);

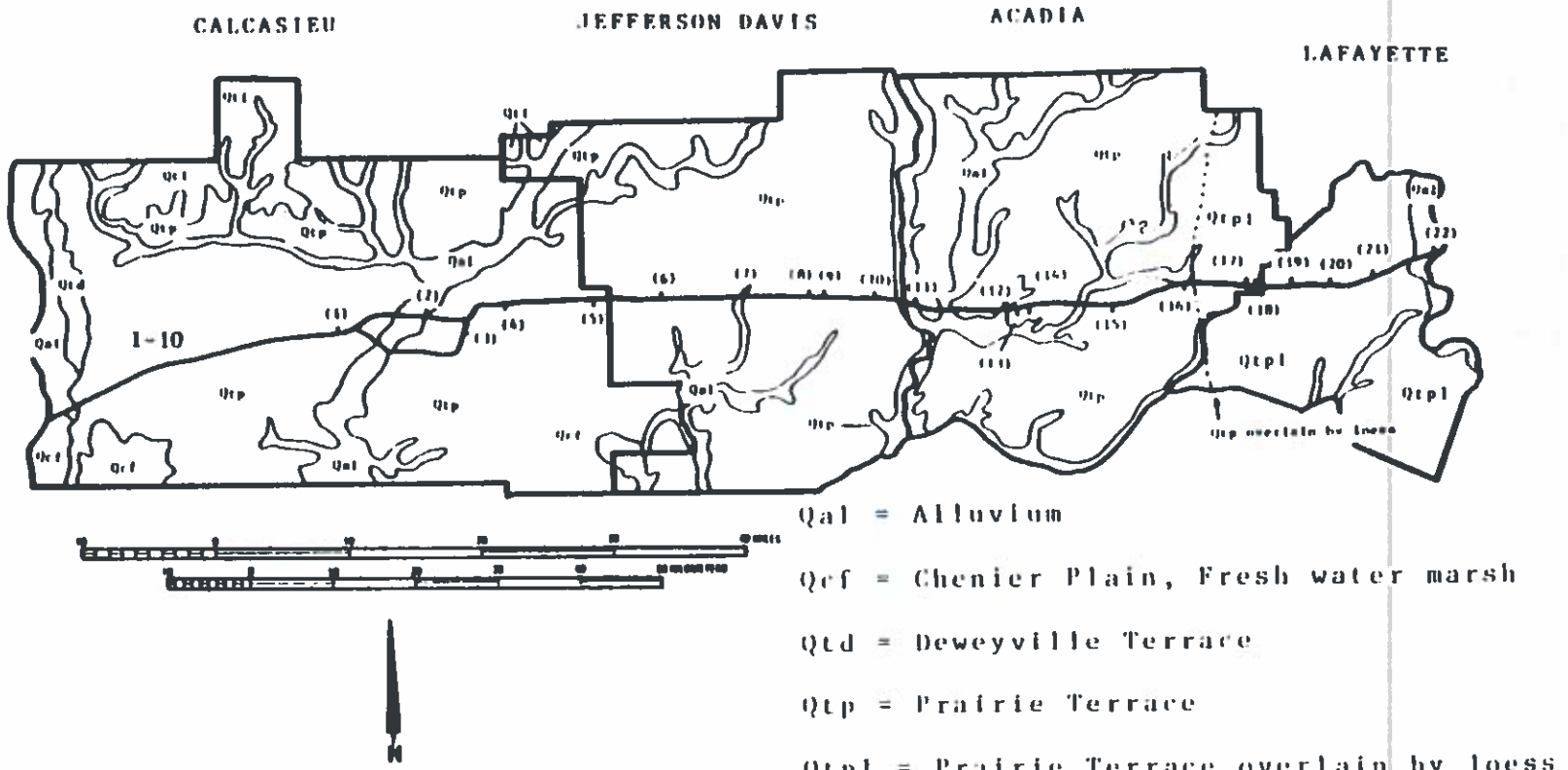

Figure 5. Map of geology and the complete transect along Highway I-10 with sample localities (S1-S22) and modified from Snead and McCulloh (6). All numbers should have an "S" in front of them.

localities 19 - 22, are composed predominantly of the Jeanerette, Coteau, Memphis, and Frost soil series. These soils have a liquid limit ranging from 23 - 50%, plasticity index ranging from 5 - 25%, a low to moderate shrink-swell potential, and a good drainage to a poor drainage with very slow to medium run-off.

METHODS

INTRODUCTION

The analysis of embankment slopes in the two study areas progressed in four stages. First, field work consisted of locating, mapping, and classifying slope failures followed by sample collection. Second, laboratory work was conducted to determine sedimentological, geotechnical, mineralogical, and hydrogeological characteristics of the samples. Third, computer models of the failures were developed using the field and laboratory data. Finally, slope designs were developed using the computer models.

FIELD METHODS

All embankments along the two transects were inspected. There are 168 slopes along the 71-mile (114 km) section of I-10 and 74 slopes along the 51-mile (82 km) portion of I-20. An elevation at each locality (height from bottom of overpass bridge to highway surface) was determined with a steel tape, and the slope angle was found with the clinometer of a Brunton compass (angle shot from the base to the top of the slope). Slope angles were confirmed with trigonometry, using the slope height and slope length, measured by a tape measure. The construction date of the slopes and identification number of each structure (overpass bridge) associated with the embankments were located and recorded. Maps of all slope failures at each sample locality were made in the field (Appendix 4). Measurements for these maps were made by pace, steel tape, and Brunton compass.

Failures were then classified as either "earth slump," "earth slump-earth flow," or "earth flow" according to Varnes (4), and map annotations were made accordingly. For facility, the three names have been shortened to slump, slump-earthflow, and earthflow.

A slump was identified as a rotational slide with movement occurring along a concave upward internal slip surface. Morphologically, a slump is characterized by a vertical scarp face at the head of the failure (Fig. 6), a central slump block that is typically rotated in toward the slope, and a toe at the base of the feature where thrusting and deformation from movement is found (Fig. 7). Concentric cracks are generally located in the slump block and are concave in the direction of movement at depth. Slumps are very common in homogeneous soils and clays on constructed embankments, as is the case in the study areas (17, 18).

If the slump scarp remains unsupported, it can result in additional failures. The top unit in the failure usually tilts backward toward the slope and provides an area for water to be collected. Repeated scarp development with water being collected can lead to an area of continuing instability. In this type of situation, material continues to move and failures become larger until a stable slope angle is obtained (4). This has been observed at the Chicago Mill (N17), Tallulah Railroad (N18), and Acadia Parish locality S11 (AC1123) sites.

Figure 6. Slump at Locality S12, Acadia Parish, east side of overpass. The slump is 32 m wide and 21 m long. Scarp is 2.5 m high. Note the displaced sections of concrete apron.

Figure 7. Slump at Locality S15, Acadia Parish, southwest quadrant. Failure morphology is well displayed: head scarp, rotated inward slump blocks, and toe above the guard rail.

An earthflow occurs when unstable material acts as a viscous fluid in which rotation is lacking and scarp development is very minor. Usually failures involve a combination of one or more types of movement and are classified as complex (4). In these study areas, complex movements are slump-earthflows and usually contain the largest volume of material. A slump-earthflow is a complex slide movement type where an earthflow is located at the foot of a slump. In this lower portion, the soil "flows" as a consequence of increased moisture content and forms a hummocky, rippled surface, many times containing radial cracks (Fig. 8). The internal slip surface is generally not seen.

Failed slopes within the I-20 study area have been mapped with a plane table and alidade, and precise measurements of each failure were used to calculate volumes (area multiplied by scarp height). Scarp height was obtained with a tape measure and is an average for the scarp. Failure areas in the I-10 study area were measured using pace distances of the length and width of each failure, while volumes were calculated by multiplying the average scarp height times the area. A study conducted by Mutchler (15) in northeast Louisiana found that mapping and calculating slope volumes by the more accurate plane table and alidade method equaled the volumes determined by the pace method multiplied by a factor of 1.1. The reported volumes for the I-10 study area are then a product of the approximate field volumes times this 1.1 factor.

Locations of the soil samples were recorded by two measurements: distance from the end of the bridge and distance down the slope. Soil samples were collected at depths of approximately 0.5 meter (20 inches) or after fresh, unaltered-original slope material was encountered. Approximately two liters (1.8 quarts) of soil volumetrically were collected and placed into labeled, air-tight storage bags for transportation back to the laboratory. Samples from failures were collected from the toe of the slope, generally. The stable slope samples were taken in mid-slope positions. In the I-10 study area, a total of 33 samples were collected from 22 separate localities (Fig. 3) during June of 1986 and February and of 1987. Nineteen of the samples that were collected are classified as failure samples with 14 being from stable portions of the slopes. The I-20 study area was sampled in the spring of 1986. In Madison Parish, where all of the failures had occurred, at least one soil sample was taken from each of the four slopes at each interchange or overpass. Usually three to five pits were sampled from each slope in order to get good, representative samples from the combined failed and non-failed portions. Along the transect of non-failed slopes from Monroe to Delhi, two samples were collected from each of the southern slopes.

An additional soil sample was taken from many of the pits. These samples were for bulk density and moisture content and were obtained by driving aluminum tubes of known volume (227.6 cc) into the sides of the sampling pits.

Figure 8. Slump-earthflow at Locality S17, Acadia Parish, northeast quadrant. Failed embankment material has "flowed" over guard rail onto shoulder of I-10.

LABORATORY METHODS

In the laboratory the soil samples were disaggregated into small pieces and allowed to air-dry for several days. Soil color of both dry and wet samples was described using the Munsell Soil Color Chart (19), and these results are found in Mutchler (15) and Smith (16). The dry samples were crushed using a Nasco-Asplin Soil Grinder. That portion of the crushed sample that passed through a No. 10 U.S. standard sieve was separated and placed into plastic storage bags awaiting sedimentologic, geotechnical and mineralogic characterization.

Particle size analysis was conducted by the pipette method (20), and the clay (<9 phi or <0.002 mm), silt (9 phi to 4 phi or 0.002 to 0.0625 mm), and sand (>4 phi to -1 phi or 0.0625 to 2.00 mm) percentage size fractions were determined. Sodium hexametaphosphate $[(NaPO_3)_6]$ was used as a dispersant. Statistical analysis and sand mineralogy of the sediment samples were completed, and their results are found in Mutchler (15) and Smith (16).

The pH of each sample was obtained with the use of a Cole Palmer Instrument Company Chemcadet 5986 pH/mV meter from a solution of 10 grams crushed sample (which passed through a number 35 U.S. standard sieve) and 10 milliliters of distilled water. The pH electrode supplied with this unit is an Ag/AgCl combination electrode. Organic carbon content percentage was determined by the "Walkley-Black" dichromate titration method (21). Appendix 2 contains the data on the physical properties described above.

Geotechnical characterization of the soil samples included determination of the Atterberg limits (liquid limit, plastic limit, and plasticity index), according to ASTM specifications (22). Bulk density is calculated by dividing the soil dry weight by the volume of the tube. Moisture content is calculated by subtracting the dry weight from the wet weight and dividing by the dry weight which is multiplied by 100 (23).

Clay (<9 phi or < 0.002 mm) mineral identification was conducted on a Norelco diffractometer. The diffractometer utilizes Cu K-alpha (nickel filtered) radiation run at one degree 2 theta per minute. Three treatments were given to each sample: untreated, glycolated, and heat treated. Quantitative calculations were made on the glycolated samples. See Appendix 3 for a summary of the clay minerals. Once quantitative clay analysis was completed, the percentage of net smectite was calculated by multiplying the clay percentage by the smectite percentage. This results in the amount of smectite in that sample.

With the physical properties of the embankment slopes determined, statistical analysis of the data was undertaken using the Statistical Analysis System (SAS), version 5.16, on the IBM 4351 Model 2 mainframe computer system. Comparisons and contrasts were made and trends were defined from all data gathered from the failed and non-failed slopes.

EMBANKMENT CONSTRUCTION

Embankments are constructed from soil that is excavated from shallow borrow pits. The borrow pits are located as close to the construction area as possible, usually within a quarter mile, to avoid large transportation costs (Fig. 9). The character of the embankments can be estimated from the type of soil used in its construction.

Excavation of soil from a borrow pit produces chunks, which must be flattened out or broken up before construction proceeds. Chunks placed in the embankment will act independently of the rest of the slope. The soil must be homogenized before it is placed on the embankment. Cohesive soils are placed and compacted at a water content close to the plastic limit (24).

Excavation, transportation, and compaction completely destroy the original structure of the soil (24). This is called remolding of the soil. It acts to weaken and soften the clay by destroying the orderly arrangement of molecules in the absorbed layers and the structure developed during sedimentation. The strength lost to remolding can slowly be regained after remolding has stopped (24). Remolding aids in homogenizing the slope material. Adequate sampling can then be done with only a few samples.

COMPUTER SLOPE STABILITY MODEL

The computer program PCSTABL4 developed at Purdue University was utilized in this study to calculate the stability number associated with particular combination of model variables.

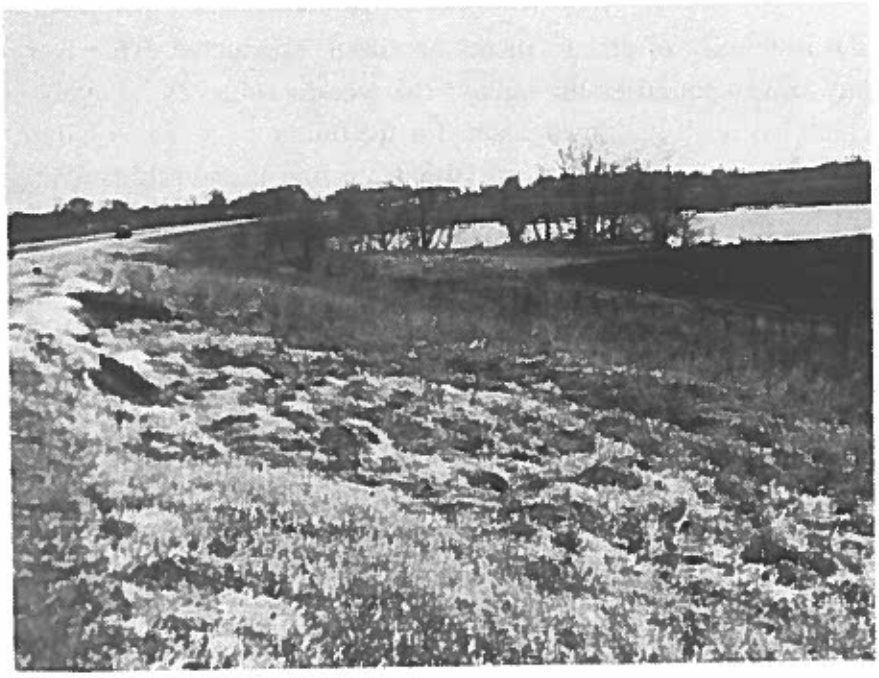

Figure 9. Water-filled borrow pit at Chicago Mill site (Locality N17), southeast quadrant, I-20 study area, Madison Parish. Note the slope failure (slump-earthflow) in foreground.

PREVIOUS WORKS

SLOPE FAILURES AND THEIR CAUSES

Research on the instability of embankments has been conducted extensively in the United States and in many other countries throughout the world (Table 2). Among other factors, much of this research has dealt with the reasons for the failure or repeated failures of particular slopes. Investigations have included detailing the geotechnical and sedimentological properties of unstable natural slopes or the parent material utilized in the construction of failed embankments in an effort to understand why failure occurred. A cross section of available publications was reviewed in which analogies could be drawn to both failed and non-failed embankment slopes in Louisiana. Table 2 summarizes the findings from the more significant and recent of these studies. Previous work on slope instability of embankments in the study areas of Louisiana is nonexistent.

FAILED EMBANKMENT

Failed embankments have been identified (Table 2) from a wide variety of locations worldwide and on differing slope types such as highway, dam, canal, and railway embankments.

A major thrust of research has been directed toward failed highway embankment slopes. Studies have focused on localities ranging from Texas to Canada and encompassing a dramatic variation of climatic and hydrogeologic conditions. Principally, failure has occurred when stiff-fissured, over-consolidated clays have been utilized in embankment construction where slope gradients have averaged approximately 2.5 to 1 (22 degrees) or more (21,25). The term "stiff" is based on the visual description of the clay's apparent resistance to compression, ranging from soft, firm and stiff to hard (46). "Fissured" simply refers to small hairline fractures or cracks in the clay.

These slopes generally display a high clay-size fraction from a minimum of 39% (33) to a maximum of 99% (43). Mineralogic investigations identified the predominant clay minerals in these slopes to be illite (mica), kaolinite, and smectite, the shrink-swell clay group. Smectite (known in the past as primarily montmorillonite) usually composed the largest percentage.

Slope instability and failure has been directly related to an increase in water content and the subsequent volume increase in the expanding shrink-swell clay (25). A high plasticity index (PI) was usually found in these failed highway embankments when testing for the geotechnical properties of the slope material. PI values averaging 45% were calculated with Atterberg liquid limit tests averaging 58%.

TABLE 2
SUMMARY OF PREVIOUS WORK
(ABBREVIATIONS AT END OF TABLE)

STUDY	LOCATION	TYPE OF SLOPE	ATTERBERGS LIMITS LL%	PL%	PI%	WC%	PARTICLE SIZE CL%	SL%	SD%	SLOPE RATIO	SLOPE MATERIAL
Abeyesekera & Lovell (25)	Indiana	FE-H	53	21	32	20	44	--	--	--	OC, KA,
Abrams & Wright (21)	Central Texas	FE-H	29-79	-	11-55	13-79	high	--	--	2.5:1-3:1	SFC, OC, PC
Cavounidis & Sotiropoulos (26)	Coastal Greece	FES	39	16	23	13	31	--	--	--	SFC, OC, CL
Degraff et al (27)	California	FES	--	--	15	--	--	--	--	--	SD, CL
Duncan & Dunlap (28)	Saskatche. Canada	FE-H	85	26	59	45	--	--	--	--	SFC, OC
Elias & Storch (29)	Coastal Massachu.	SE-H	52	26	26	45	--	--	--	--	OC, Swamp area
Henkel (30)	England	FES	--	--	42-72	--	--	--	--	--	SFC, MC
Hou (31)	Coastal China	FE, PS	47	25	22	21	high	--	low	--	SFC, IL, KA SSC
Humphrey & Leonards (32)	Illinois	FE-D	29 avg.	13 avg.	16 avg.	13 avg.	67	--	--	3:1	SD, PC
Koppula (33)	California	FS-UW	50	30	20	55	--	high	--	10:1	NC bay mud
Laguros et al (34)	Oklahoma	FES	--	--	23-38	11-23	39-70	--	--	2:1 - 3:1	OC, IL, SSC, SH, KA
Leonards (35)	Finland	FE-C	55	25	30	--	high	--	--	1:1.5	OC, GC
Leonards (35)	England	FE	55	18	37	48	--	--	--	1:1.4	CL
Marivoet (36)	Belgium	FE-R	31	18	13	20+	20	--	--	--	SL, CL, SD

TABLE 2 CONTINUED

Peterson et al (37)	Saskatch. Canada	FE-D	--	--	10-18	--	--	--	--	2:1 - 3:1	GC, PC
Ramalho-Ortigao et al (38)	Brazil	FE-H	--	--	50-100	--	--	--	--	2:1	KA, SSC, IL
Redman & Poulos (39)	Louisiana	FE-C	--	--	--	--	--	--	--	--	PC,
Roa (40)	India	FE-D	--	--	17-20	--	--	--	--	--	pebble CL
Schnabel & Grefsheim (41)	Wash. D.C. Virginia	FES	65-80	20-30	40-58	22-32	--	high	--	3.6:1	OC, SSC, CL SL
Schweizer & Wright (42)	California	FE-H	--	--	--	--	--	--	--	--	PC, SD, CL
Stauffer & Wright (43)	Texas Coast	FE-H	42-97	--	30-70	14-41	71-99	--	--	2.1:1-3.4:1	OC,SFC, SSC IL, KA, SD
Stevens & Matlock (44)	Central Texas	PS	55-70	17-29	40-41	25	98-99	--	--	--	SFC, SSC, KA IL
Wilson & Mikkelsen (45)	Minnesota	FE-H	--	--	--	--	--	--	--	--	OC, CL, SH, BT

ABBREVIATIONS:

BT:	Bentonite	GL:	Glacial Clay	SD:	Sand
CL:	Clay	KA:	Kaolinite Clay	SH:	Shale
FE:	Failed Embankment	IL:	Illite Clay	SEH:	Stable Embankment (Constructed)
FE-C:	Failed Canal Emban.	LL:	Liquid Limit (%)	SFC:	Stiff-Fissured Clay
FE-D:	Failed Dam Embank.	MC:	Moisture Content (%)	SL:	Silt
FE-H:	Failed Highway Emb.	NC:	Normally Consolidated	SSC:	Shrink-Swell Clay (Smectites)
FE-R:	Failed Railroad Emb.	OC:	Over-Consolidated	WC:	Water Content (%)
FES:	Failed Excavated/ Cutbank Slope	PC:	Plastic Clay		
		PI:	Plasticity Index (%)		
FS:	Failed Natural Slope	PL:	Plastic Limit (%)		
FS-UW:	Failed Natural Slope Under Water	PS:	Problem Soil - Prone to Failure		

Another physical property of these failed, clay-rich highway embankments which is related to the hydrogeological and concomitant climatic conditions is the percent water content. Values of this factor varied from 14% in the Texas Gulf Coastal plain (43) to 45% in Canada (28). Stauffer and Wright (43) and Abrams and Wright (21) found that slope failures are long-term processes of a progressive build-up of pore water pressures within the embankment material. Schweizer and Wright (42) found that failure was caused mainly by hydrologic conditions acting over an 11-year period in conjunction with three seasons of heavy rain which induced the failure of the plastic clays.

Additional examples of failure have occurred on constructed earthen dam, canal, and railway embankment slopes. Again, the embankments were constructed of material with a high clay size fraction content. Roa (40) studied dam embankment failures that were occurring in a predominately clay soil mixed with pebbles. In South America, Ramalho-Ortigao et al. (38) studied failures in test embankments attributed to highly plastic clays. An exception is the railway embankment site that had a clay content of only 20 percent (36). At the dam site in Illinois (32) and the canal sites in Finland (35), the parent material was derived from glacial clays. The Illinois dam embankment failure was caused by a layer of more plastic, weaker fill which caused gradual movement in the compacted clay soil. However, geotechnical tests on the Finnish embankment soil displayed relatively low plasticity indices, averaging approximately 20%, with Atterberg liquid limit tests averaging 38%. The causes of failure in these cases were related to the steepness of the embankment slope angles in conjunction with the relatively low shear strength of the construction material. Redman and Poulos (39) studied a test embankment constructed of soft plastic clays and concluded that deformation to the embankment is attributed to the nature of the parent material and is described as undrained creep.

FAILED EXCAVATED SLOPES AND FAILED NATURAL SLOPES

An excavated slope is an area where pre-existing material has been removed in comparison to an embankment slope which has been constructed of material transported from another area (46). Although excavated slopes and natural slopes are not directly analogous to the embankments of the study area, a geotechnical characteristics provide insights into the causative nature of failure which may be applied to the Louisiana transects.

A slope containing shrink-swell clays is prone to failure. Schnabel and Grefsheim (41) found that failure in the slopes of Virginia was caused by the presence of montmorillonite-rich, overconsolidated clays. Cavounidis and Sotiropoulos (26) described a failed excavated slope in coastal Greece where the failure occurred in a stiff-fissured, over-consolidated clay marl with a clay size fraction of 31 percent. They calculated a plasticity index of 29% and a liquid limit of 39% The water content was relatively low at 12.6%. The cause of the failure was determined to be from excessive pore water pressure from water that entered the soil through cracks in the expansive clays.

Koppula (33) reported the geotechnical properties of a failed natural slope in San Francisco Bay. The slope was composed of a normally-consolidated, marine, organic clayey silt. Slope gradient was a gentle 10:1 (6 degrees) and the plasticity index was low at 20% Water content, however, was relatively high at 55%, with the Atterberg liquid limit at 50%. The combination of these two conditions were the cause of failure.

Oversteepened slopes of high clay content can also lead to failures because clays lack strength. Henkel (30) determined that failures were due to the presence of overconsolidated fissured-marine clay in the slopes. Marivoet (36) found that failures were attributed to highly plastic clays disturbed by constructing the embankment.

Unconformities in excavated slopes can become failure planes for slides. DeGraff et al. (27) determined that failure was occurring at the interface of permeable slope materials and granite. Activity is directly related to the infiltration of water that moves downward until it reaches the granite. It then flows over the granite, producing a failure plane. Wilson and Mikkelsen (45) determined that slumping in a cut embankment was caused by a thin seam of bentonite that caused a failure plane to develop. Laguros et al (34) concluded that failures were occurring at the interface between weathered shale and unweathered shale. The failure plane developed due to high water content of the weathered shale and the nature of the slope material.

PROBLEM SOILS

Research on soils prone to failure add to the data base of categorizing failure disposition. Soil studies from central Texas and coastal China were particularly analogous to embankments in the study area, sedimentologically, mineralogically and geotechnically. They can contain high-clay percentages and abundant shrink-swell clays.

Hou (31) examined the physical properties of failure-prone soils in China used for construction purposes. Sedimentologically and mineralogically, these soils, situated along a broad region of the southern coast, are Quaternary in age and alluvial in origin and thus are very similar to those in our study areas in Louisiana. Hou (31) describes these soils as stiff-fissured, shrink-swell clay (smectite) containing illite (mica) and kaolinite. A high percentage of the particle fraction is clay size, with a slight percentage of sand size particles present. Geotechnically, the plasticity index averages 22% with Atterberg liquid limits averaging 47%. The water content averages 21%.

Another problem soil in central Texas, similar in characteristics to the soils of Louisiana, was reported on by Stevens and Matlock (44). The soil is composed of a 98% clay size fraction of stiff- fissured,shrink-swell clay (smectite) containing varying amounts of kaolinite and illite (mica). The geotechnical properties exhibited a high plasticity index averaging approximately 41% and Atterberg liquid limits ranging from 55 to 77%. Water content averaged approximately 25%.

SUMMARY

Comparisons of the physical properties of slope failure from a variety of locations and conditions with those of the study area help in the understanding of why slopes fail on the embankments along the Louisiana study areas. General trends established from these previous works illustrate that failure occurs in the presence of stiff-fissured, over-consolidated clays containing a high clay size fraction and primarily the shrink-swell smectite with lesser amounts of kaolinite, and illite (mica). Plasticity indices and Atterberg liquid limits are generally high,in excess of 25% and 29% respectively.

REMEDIAL MEASURES

Many workers have, quite naturally, concerned themselves with repairing and preventing these failures. Table 3 summarizes remedial measures mentioned in Schweizer and Wright (41), and brief descriptions are presented here.

Drainage

Surface drainage prevents surface run-off from entering the slide area. This is used mainly as a preventative measure in potentially unstable areas and can be used on all types of embankments (21, 42, 47, 48, 49, 50, 51). Surface drainage can be improved by reshaping the slope, constructing lined ditches, seeding or sodding, treating with bituminous material, constructing thin concrete walls, and installing flumes or conduits. Regardless of the method, the desired effect is to remove or prevent surficial water from infiltrating into the embankment and creating a reduction in shear strength which results in instability. The most successful corrective method used in an active area is drainage of surface and subsurface water.

Horizontal drains are used to divert water from its source, to lower the groundwater table in an area, to drain artesian strata, and to drain water from the interior of the slope. Drainage pipes are installed into the face of the slope at a slight inclination above horizontal and are not usually used unless a high groundwater table has been indicated. Horizontal drains are corrective and preventative and can be used in a wide range of materials.

Vertical drains are usually used in conjunction with horizontal drains as preventative and corrective measures. They are primarily used for control of unfavorable ground water conditions. These have been referred to as sand drains, vertical wells, and relief wells.

Other methods of controlling subsurface water include stripping away the unstable, saturated material, developing a drainage blanket and constructing stabilization trenches at greater depths. Drainage tunnels are used when stripping is not economical. Also used are interceptor trenches which catch subsurface water before it reaches the slope.

TABLE 3

REMEDIAL MEASURE STUDIES FOR EMBANKMENTS
GROUPED BY TYPE OF REMEDIAL MEASURE

STUDY	LOCATION	REMEDIAL MEASURE
DRAINAGE SYSTEMS		
Smith & Stafford (47)	California	Horizontal Drains
Black (48)	California	Vertical Drains
Eager (49)	Wyoming	Horizontal Drains
Downs (50)	W. Virginia	Drainage System
McKeever (51)	Oregon	Drainage Tunnel
Abrams & Wright (21)	Texas	Horizontal Drains
CHEMICAL & ELECTROCHEMICAL		
O'Bannon et al (60)	Arizona	Electrochemical
Thompson & Robnett(61)	Illinois	Chemical
Handy & Williams (62)	Iowa	Chemical
Abrams & Wright (21)	Texas	Lime & Fly Ash
Schweizer & Wright(42)	Texas	Lime & Fly Ash
Petry et al (66)	Texas	Lime, Cement & Fly Ash
Robnett & Thompson(58)	Illinois	Lime & Cement
RESTRAINT STRUCTURE		
Vidal (52)	France	Reinforced Earth
Reti (53)	California	Retaining Wall
Jessup (54)	California	Giant Spikes
Allen (55)	Indiana	Retaining Wall
Allen (56)	Indiana	Slope Baffles
Abrams & Wright (21)	Texas	Retaining Walls
Schweizer & Wright(42)	France, Africa	Retaining Walls
MISCELLANEOUS		
Rowan et al (57)	Tennessee	Excavation/Avoidance
Schroter & Maurseth(59)	California	Recommendations
Abrams & Wright (21)	Texas	Change Grade of Slope
Schweizer & Wright(42)	Russia	Thermal
Hill (67)	California	Thermal

Restraint Structures

The construction and emplacement of restraining structures have been employed as remedial measures with much success on embankments throughout the world and are perhaps some of the oldest methods of instability control (42, 52, 53, 54, 55, 56, 67). Bulkheads, cribs, buttresses, and retaining walls made of timber, concrete and steel, piling and shafts, and tie rodding are the most common structures used to increase shear strength of the embankment or to increase the resistance against movement.

Steel and timber pilings have been used extensively in an attempt at embankment stabilization in Louisiana. Locality number S11 of the I-10 study area has become known locally as "Porcupine Hill" due to the large number of pilings inserted into all embankment quadrants. Locality N17, the Chicago Mill northeast slope, had over 200 pilings in it when it was repaired in 1987 (Fig. 10). This remedial measure has met with very limited success after large expenditures. Due to the high-smectite content in the soils, the remedial measure itself increased the probability of failure. The shrink-swell clay opened fissures along the pilings, allowing surface run-off to penetrate deep into the embankment. Percent moisture content increased until driving forces (i.e., embankment weight within the failure envelope) exceeded the shear strength, at which point failure started to occur. With this example, it is obvious that in most cases, pilings are not the measures needed for solving the stability problems in parent material high in smectites.

Elimination, Avoidance, and Excavation

Elimination and avoidance involves relocating the highway to avoid the problems of slope failure, bridging over the area, removing the unstable material, and replacing it with more favorable material (56, 57, 58). Alteration of the the slope, through flattening of the slope angle and removing or substituting embankment soil, has alleviated instability problems on Texas highway embankments (21, 42). Reducing the slope angle decreases the driving forces, contributing to failure. Substituting failure-prone embankment material with low plasticity clay or cohesionless sands and gravels, particularly at the toe of the slope increases the resisting forces. This combination of forces creates a stable slope environment.

Special Measures

Special remedial measures found successful in stabilizing embankments include thermal treatment, freezing, electro-osmotic treatments, reinforced earth, and re-vegetation.

Thermal treatment has been used on embankments in such diverse localities as California and Russia (42, 66) where highly plastic clays with low permeability failed. The concept of thermal treatment is to reduce the moisture content and plasticity index of the problem soil by

Figure 10. Unsuccessful attempt at stabilizing a failed slope by use of pilings at Chicago Mill site, Locality N17, northeast slope, Madison Parish, I-20 study area. Over 250 pilings were exposed in this one slope during repairs in 1987. The pilings do little to retard the movement of material that has a high shrink-swell clay content.

forcing air heated from 300 to 500 degrees C (572 to 932 degrees F) through interconnected drainage borings. The shear strength and permeability is increased, stabilizing the material.

Slope freezing has been documented as a method of slope failure prevention during the construction of the Grand Coulee Dam in 1937 (42). Here a large slide was stabilized by pumping salt brine, cooled to -4 degrees C (25 degrees F) through pipes in the toe of the slope thereby "freezing" the slide.

Electro-osmotic treatment is a dewatering system that has been used in Canada for stabilization of a large cut embankment during the construction of the Trans-Canada Highway (42). In principle the water content of the soil is reduced by pore water migration induced by electrical current. Shear strength is increased and the slope is stabilized.

Reinforced earth involves placing thin galvanized steel strips at selected intervals within a compacted earth fill. The ends of the steel strips are fastened to a steel anchor plate. This creates a resistance to lateral movements.

The four remedial measures described above are rather exotic and are not applicable to the problems found in southwestern Louisiana, One special measure that is applicable and has had demonstrable success in the research area is slope revegetation. Vegetation inhibits weathering, decreases natural water content, and provides structural support for the embankment soils (42).

Stabilization with Chemical Additives

Embankments in central Texas, Illinois, and Iowa have been successfully stabilized with the addition or injection of lime, cement, and fly ash slurries (21, 42, 61, 62, 64). These slopes were all characterized by highly plastic, active clays which were fissured. Lime mixed into the slopes has the effect of de-activating the shrink-swell clays (smectite) and increasing the shear strength of the embankment. Injection of lime, cement, and fly ash slurries under high pressure was also found to alleviate the failure problems. These materials increase the shear strength of the embankments in several ways. The ability of the slope to retain and absorb moisture is reduced as the pore spaces are occupied with the additive, particularly cement and fly ash. The cured cement lends rigidity to the soil further increasing its strength. A major drawback to this method is expense.

REPAIRS TO MADISON PARISH SLOPES, I-20 STUDY AREA

During the study, the embankments at the Quebec, Tendal, Cow Bayou, and Chicago Mill sites were repaired. Three different techniques were used. At the Quebec site, lime was injected under high pressure into the northeast and northwest slopes. At the southeast and southwest slopes, a fly ash and lime mixture was injected into the slope.

At the Tendal and Cow Bayou sites, the slope material was stripped back from a 3:1 to a 2:1 slope. The material that was removed was spread out onto a "table," an area that is built up from the removed soil parallel to the slope, and mixed with hydrated lime. A predetermined

amount of lime is spread across the table. A machine runs over the lime and soil, acting as a large garden tiller, mixing the top nine inches of soil with the lime. Once the lime and soil is thoroughly mixed, it is put back onto the slope and compacted in nine-inch lifts. This is repeated until all the slope material has been treated. The slope is then restored to a 3:1 angle. The cost of these restorations was approximately $35,000 per slope or $140,000 for four slopes of an overpass or interchange.

Lime treatment results in an immediate reduction of the plasticity index and other long-term effects aid in soil stabilization (63, 64).

At the Chicago Mill site, the unstable material was stripped away and a "geogrid" was laid down. The geogrid was a plastic grid network used to eliminate the development of the failure plane. The geogrid is laid down, followed by a layer of soil and then compacted. This is repeated several times so there are many layers of geogrid throughout the slope. Steel and wood pilings had been previously tried at this location, unsuccessfully.

RESULTS AND DISCUSSION

INITIAL STATISTICAL ANALYSIS OF THE DATA

The first step in understanding and delineating mechanisms and contributing factors responsible for slope failures is performing a statistical analysis on the data set. The Statistical Analysis System (SAS) program, version 5.16, on the IBM 4351 Model 2 mainframe computer at Louisiana Tech University was used for this purpose.

First, it was necessary to determine what factors showed differences between failed and non-failed slopes. The factors tested were: percent clay, percent silt, percent sand, liquid limits, plastic limits, plasticity index, bulk density, percent moisture content, percent kaolinite, percent mica, percent interstratified clay, percent smectite, percent net smectite, slope angle, pH, and percent organic carbon.

Using the T test for the I-20 study area, it was determined that percent organic carbon, percent mica (illite), slope angles, and bulk density were statistically the same throughout the study area (i.e., accept the null hypothesis). The rest of the factors tested showed differences (Table 4).

Using the same T-test approach on a much smaller data set of only 33 samples for the I-10 study area, all factors were statistically the same except slope angles, plasticity index, and percent clay (15). But, from that same data set, the factors of plasticity index, bulk density, percent moisture content, percent clay, percent net smectite, and slope angle grouped into different populations when comparing stable and failed portions of the slope where the samples had actually come from. All of these results agree with the results from the I-20 study area (Table 4) except the slope angle where no difference was found in the I-20 study area.

Next, a correlation procedure (SAS CORR) was run on all of the factors that showed differences in the T test. This was done to pick out possible predictive relationships and thereby, demonstrate a linear relationship. The CORR procedure compares all the factors to each other to see how well they correlate with each other, and therefore, how well one can be used to predict the other variable . The factors that show the best correlations are percent clay, liquid limit, plasticity index, net smectite, and percent interstratified clay, and these are listed in Table 5. Because the percent of interstratified clays is so difficult to measure, this factor was eliminated from the list. The remaining four factors are to be used in the development of predictive models for the two study areas in the next section.

Last, factors showing differences between failed and non-failed slopes were used in the analysis of variance test (SAS-ANOVA), comparing more than two populations. This determines how each factor contributes to slope failure in each of the parent materials. In addition to the SAS ANOVA procedure, Duncan Waller, and LSD Tukey CLDiff significance tests were run. These tests compare the means of each factor, and group similar means together,

TABLE 4

T-TEST RESULTS OF STABLE VS. NON-STABLE SLOPES
FOR THE I-20 STUDY AREA

VARIABLE	PROB > T*	NULL HYPOTHESIS: Ho
% Clay	.0001	reject
% Silt	.0001	reject
% Sand	.0026	reject
% Kaolinite	.0018	reject
% Mica	.1014	accept
% Interstratified Clay	.0001	reject
% Smectite	.0001	reject
% Net Smectite	.0001	reject
% Liquid Limit	.0001	reject
% Plastic Limit	.0002	reject
% Plasticity Index	.0001	reject
% Organic Carbon	.4606	accept
% pH	.0479	reject
% Moisture Content	.0001	reject
Bulk Density	.0001	accept
Slope Angle	.1500	accept

* = If Pr > T is < .05, reject null hypothesis, i.e., more than one population.

TABLE 5

SAS CORR PROCEDURE RESULTS FOR I-20 STUDY AREA
FOR FACTORS THAT HAVE .0001 SIGNIFICANCE

Variables Compared	Pearson's r*	Significance 99.99% ***
% Clay vs. Liquid Limits	.97509	.0001
% Smectite vs. % Interstratified	-.92207	.0001
% Net Smectite vs. Liquid Limits	.91133	.0001
% Net Smectite vs. Plasticity Index	.89034	.0001

* = Pearson's r is the measure of strength between two variables. The closer the number to one or negative one the stronger the correlation being either positive or negative. All correlations are significant at the 99.99% confidence level (.0001).

thereby designating the number of populations for that factor in the study area. Each of the study areas have been divided into different parent material zones and the ANOVA applied to these factors for the grouping.

PREDICTION MODELS

One of the objectives of this study is to develop a method of predicting slope failures or areas prone to failure. In the last section, we determined that four variables best predict the chances of failure: net smectite, percent clay, liquid limit, and plasticity index.

Risk level tables have been established for each of these four variables (Tables 6, 7, 8, & 9). A risk level refers to a cutoff where above a particular value, the chance of failure is high and below that value, the chance of failure is significantly less. Three cutoff zones have been determined: high risk , intermediate risk, and low risk. These have been established by listing all the values of a particular variable in decreasing order. By each value an "S" or "F" is made for each sample describing whether the slope containing the sample is stable (S) or has failed (F). An "F" by itself describes a sample taken from a failure, whereas an "[F]" describes a sample coming from a stable portion of a slope that has a failure on it.

From this table three risk categories are defined. The low/intermediate risk boundary is placed below the lowest value that has a failure. By definition, the percent failure rate for these slopes is 0%. An exception to this boundary is in Table 6 (Net Smectite) where the value from locality S12 is very low, yet a failure has occurred. The x-ray diffractogram is poor for this sample, so the net smectite value is suspect. In actuality, the value is probably higher and belongs in the intermediate risk level classification. The high/intermediate risk boundary is put above the value where stable slopes become common when descending from the highest value. This boundary is placed so the high-risk category generally has a percent failure rate higher than 85%, and the intermediate-risk category has a failure rate between 55 - 60%.

These percentages also give an approximate accuracy, for if a slope is constructed of a soil that falls into the high-risk category, it has a 85% chance of failure ten to 15 years after construction. A soil sample that is in the intermediate-risk category has a 55-60% chance of failure in that same period of time.

Table 10 compares these four risk level models of samples of the I-10 study area to each other and illustrates the high consistency in predicting failure of a particular slope. The percent net smectite model has seven samples out of 33 that fall into a different failure category when compared to the other three models. The percent net smectite model has a reliability of 79%, which is the lowest. Plasticity index percent has five samples that fall into a different failure category when compared to the other models. The plasticity index percent model has a reliability of 85%. The percent clay model has an reliability of 88% with only four falling into a different risk category. The liquid limit percent model is the most reliable at 94% with only two samples falling into other categories. Therefore, all four models are consistent in defining failure trends along the I-10 transect.

TABLE 6

RISK LEVELS BASED ON PERCENT NET SMECTITE

% Slope Status	% Slope Status
71 F	33 F
69 F	32 F F [F] S S S
68 F	31 [F] S S
63 F	30 [F] [F]
62 [F]	29 F [F] S S
61 F	28 F F F INTERMEDIATE RISK
60 [F]	27 S (60 % FAILURE RATE)
59 [F] F	25 [F] S
58 [F]	24 F F
57 F F	23 [F] [F] S
56 [F] F F	22 [F]
55 F F	21 F [F]
54 F	20 S
51 [F] F HIGH RISK	19 F F S S S
50 F (90 % FAILURE RATE)	18 F S [F]
49 F F	17 S S
48 [F] F	16 S
47 [F F] F F	15 S
46 F F F S S	14 S
45 [F]	13 S LOW
44 F F F S	12 S RISK
43 [F] F F S	11 S S F
42 F F F F	10 S S S (4 % FAILURE RATE)
41 [F]	8 S S S
40 [F] F S	7 S S S
39 [F F] F F [F]	5 S S
38 F F F F F F S	4 S
37 F	3 S
36 F [F] S	
35[F] F	
34 [F] F F [F]	

Table 6: Risk of slope failure based on the percentage of net smectite of the sample. (F = sample from a failure; [F] = sample from stable portion of a slope with a failure on it; S = slope without any failure on it at this time so is at present, "stable".

TABLE 7

RISK LEVELS BASED ON PERCENT CLAY

% Slope Status		% Slope Status	
92 F		49 [F]	HIGH RISK
90 F		48 F [F]	
87 F		---	
83 F		47 F F [F] S S	
80 [F] F S		46 [F] [F] [F]	
79 F F F F S		45 [F] [F] S S S	
78 [F F]		44 [F] [F] S S	
77 [F]		43 F [F] S S	
76 F F		42 F	INTERMEDIATE
75 [F] F F F		41 F F F S	RISK
74 [F] F		40 [F] S	(56% FAILURE RISK)
72 [F] F		39 [F]	
71 F		37 F [F] S S S	
68 F F		36 [F]	
67 F	HIGH RISK	33 S	
66 S	(87% FAILURE RATE)	32 F S S	
65 F		---	
64 F		31 S	
63 [F] F F		29 S S	
62 F F F S		25 S S	LOW
61 [F] F		24 S S	RISK
60 [F F] F F S		23 S S	
59 [F]		22 S	(0% FAILURE RATE)
58 F F F S		21 S S	
57 [F] F		19 S	
56 F F		18 S S S	
55 [F F] F F		13 S	
54 F F S F F			
53 F F F			
52 F S S [F] [F]			
50 F F F S			

Table 7: Risk of slope failure based on the percentage of clay in the samples. (F = sample from a failure; [F] = sample from stable portion of a slope with a failure on it; S = slope without any failure on it at this time so is at present, "stable".

TABLE 8

RISK LEVELS BASED ON PLASTICITY INDEX

% Slope Status		% Slope Status
52 F		27 [F] F F F F F [F] S S
50 [F] F		26 [F] F F S
49 [F]		25 S S
48 F F F		24 F
47 [F]		23 F F INTERMEDIATE
46 [F] F F F F S S		22 S S RISK
45 [F] F		21 F [F] S S
44 F	HIGH RISK	20 [F] (59% FAILURE RATE)
43 F (86% FAILURE RATE)		19 [F] S S
42 F		18 F
41 [F F] S S		17 [F]
40 [F] F F F		16 [F] S
39 F F S S F		
38 [F] F F F F		15 S S
37 F F F [F]		14 S S
36 [F] F F F F		13 S
35 F [F] S		10 S
34 [F] F F S		9 S S S S
33 [F] F F F [F]		8 S S S LOW RISK
32 [F F] F F [F] S		7 S (0% FAILURE RATE)
31 [F F] F F F F F [F] S S		5 S S S
30 [F] F F F		0 S
29 [F] [F] S	INTERMEDIATE	
28 S S	RISK	

Table 8: Risk of slope failure based on the Plasticity Index percentages of the samples. (F = sample from a failure; [F] = sample from stable portion of a slope with a failure on it; S = slope without any failure on it at this time so is at present, "stable".

TABLE 9

RISK LEVELS BASED ON LIQUID LIMIT

% Slope Status		% Slope Status	
93 F		54 [F] S F	
91 F		53 S S	
89 F F		52 F F F [F]	
88 F S		51 S S	
87 [F] F		50 F F	
85 F		48 S S	
84 [F F F] F F		47 F F F [F] [F]	
83 F		46 F [F]	INTERMEDIATE
82 F		45 F [F]	RISK
81 F F		44 F F S S	(60% FAILURE RATE)
80 [F]		43 [F] S S	
79 F		42 F [F] [F]	
78 [F] F		41 [F] S	
77 F	HIGH RISK	40 S S S S	
75 F	(89% FAILURE RATE)	39 F S	
73 F S		38 F [F]	
72 [F F]		36 S [F]	
70 F S		---	
69 [F] S F			
68 F F		35 S S S S	
67 [F] F		34 S	
65 [F] F S		33 S S	
64 F		31 S	LOW RISK
63 F F F F S		29 S S	(0% FAILURE RATE)
62 F F F F		28 S	
61 F F F		27 S S S	
59 F F		25 S	
58 F [F] [F] [F] S		24 S S	
57 F F [F] S		18 S	
56 F F [F]			
55 F [F] [F] [F]			

Table 9: Risk of slope failure based on the percentage liquid limits of the samples. (F = sample from a failure; [F] = sample from stable portion of a slope with a failure on it; S = slope without any failure on it at this time so is at present, "stable".

TABLE 10

PREDICTIVE MODEL COMPARISON*

Locality/ Sample #	PI %	% Net Smec	% Clay	LL %
S1 CA-108-SE	L	L	L	L
S2 CA-90-SE	[H]	M	M	M
S3 CA-210-SW	H	H	H	H
S4 CA-EO397-SE	M	M	M	M
S5 CA-383-SW 1S	M	M	[L]	M
S5 CA-383-SE 1UC	M	M	M	M
S6 JD-101-SE	[M]	H	H	H
S7 JD-WE-SW 1UC	[M]	H	H	H
S7 JD-WE-SW UC	H	H	[M]	[M]
S7 JD-WE-NW 1S	H	[M]	[M]	H
S7 JD-WE-NW 2S	H	H	H	H
S8 JD-395-SE	H	H	H	H
S9 JD-EO395-NW	H	H	H	H
S10 JD-102-SE	H	H	H	H
S11 AC-1123-NW	H	H	H	H
S12 AC-BRIDGE UC	M	[L]	M	M
S13 AC-LA369-NW UC	M	M	M	M
S14 AC-ES-NW Stable	H	[M]	H	H
S14 AC-ES-NW Slump	[M]	H	H	H
S14 AC-ES-NE 1S	M	M	M	M
S14 AC-ES-NE 2S	[H]	M	M	M
S15 AC-EO1111-SW UC	H	H	H	H
S15 AC-EO1111-NW 1S	H	H	H	H
S15 AC-EO1111-NW 2S	H	[M]	H	[M]
S16 AC-722-SW	M	M	M	M
S17 AC-95-NE UC	H	H	H	H
S17 AC-95-NE 1UC	H	H	H	H
S17 AC-95-NW S	H	H	H	H
S18 AC-343-NW	M	[H]	M	M
S19 LA-724-NE	M	[L]	M	M
S20 LA-AC-NE	M	M	M	M
S21 LA-167-NW	L	L	L	L
S22 LA-354-NW	M	[L]	[L]	M

* H = high risk, M = medium risk, L = low risk. [ ] = sample falls into different category compared to other models. PI% = plasticity index, 85% reliability; %Net Smec = net smectite, 79% reliability; %clay, 88% reliability; LL% = liquid limit, 94% reliability.

Obtaining all of the values for these four variables can be difficult. Calculating net smectite percent requires an x-ray diffractometer, which is not easy to come by, and grain size distributions can be time-consuming. Percent clay and percent net smectite can be estimated by Atterberg limits. Linear regressions have been generated using liquid limit and plasticity index as the independent variables from which percent net smectite and percent clay could be estimated . These values are summarized in Table 11.

In the Risk Level Tables (Tables 6-9) there are samples from eight stable slopes in the high risk category. In the I-20 study area, these slopes are found at the Millhaven interchange (locality N3, OP-MH), the Girard overpass (locality N5, RP-GO), the Waverly interchange (locality N14, MP-W), and the Ouebec overpass (locality N16, MP-QU). In the I-10 study area, these slopes are found at localities S3 (CA210SW, overpass), S6 (JD101SE, interchange), S8 (JD395SE, interchange), and S17 (AC95NW, interchange). We predict that the next major slope failures will occur on these slopes. Since the study has begun, the SE slope at the Waverly interchange has already failed. It is believed that the lower slope angles at this site have only prolonged the failing process of the slope material.

A very well defined trend was also observed between slope angle and embankment slope failures (Table 12) in the I-10 study area. As the slope angle increased, the probability of failure also increased. Slopes over 19 degrees had failed, whereas slopes below 15 degrees had not failed. There was no relationship found in the I-20 study area between slope angles and chance of failure. The slopes in the I-20 study area ranged from 10 to 24 degrees, but there is a great diversity in parent material. In the I-10 study area, the slope material is much more similar so the slope angle is important.

TABLE 11

LINEAR RELATIONSHIPS BETWEEN SLOPE SAMPLE VARIABLES

REGRESSION EQUATION:	r^2	N	SIGNIFICANCE
NSM = .82 (LL) - 11.95	.83	103	.0001
PCL = .99 (LL) - 3.71	.95	103	.0001
NSM = 1.21 (PI) - .41	.79	103	.0001
PCL = 1.1 (PI) - 15.2	.74	22	.001

NSM = net smectite
PCL = percent clay
LL = liquid limit
PI = plasticity index

The first three equations are from Mutchler (16) and the last one is from Smith (15).

TABLE 12

SLOPE ANGLE COMPARED TO EMBANKMENT
SLOPE FAILURES OF THE I-10 STUDY AREA*

Locality/ Sample #	Slope Angle (degrees)		Failed/Stable Slope@
S 2 CA-90-SE	26		F
S11 AC-1123-NW	22		F
S15 AC-EO1111-SW UC	22		F
S15 AC-EO1111-NW 1S	22		F
S15 AC-EO1111-NW 2S	22		[F]
S18 AC-343-NW	21.5	PF 100%	F
S 9 JD-EO395-NW	20.5		F
S14 AC-ES-NW Slump	20		F
S10 JD-102-SE	20		[F]
S14 AC-ES-NW Stable	20		[F]
S14 AC-ES-NE 1S	19.5		F
S14 AC-ES-NE 2S	19.5		[F]
S 8 JD-395-SE	19		S
S 7 JD-WE-SW 1UC	18.5		[F]
S 7 JD-WE-SW UC	18.5		F
S 7 JD-WE-NW 1S	18.5		[F]
S 7 JD-WE-NW 2S	18.5		F
S19 LA-724-NE	18.5	PF 58%	S
S16 AC-722-SW	18		S
S22 LA-354-NW	18		S
S20 LA-AC-NE	16.5		S
S12 AC-Bridge UC	16		[F]
S17 AC-95-NE UC	16		[F]
S17 AC-95-NE 1UC	16		F
S 1 CA-108-SE	15.5		S
S 3 CA-210-SW	15		S
S 6 JD-101-SE	15		S
S17 AC-95-NW	15		S
S 4 CA-EO397-SE	14.5	PF 0%	S
S 5 CA-383-SW 1S	14.5		S
S 5 CA-383-SE 1UC	14.5		S
S13 AC-LA369-NW UC	14.5		S
S21 LA-167-NW	14.0		S

* PF = probability of failure.
@ [F] = Sample from stable portion of slope with a failure on it
F = Sample from failure on a slope
S = Sample from a stable slope

I-20 STUDY AREA

Failures And Parent Material Zones

A total of 42 embankment slope failures were mapped, studied and classified in Madison Parish, Louisiana, which is situated on the Mississippi River flood plain. Using Varnes (1978), a total of 14 slumps, 14 slump-earthflows, and 14 earthflows were classified (Figs. 11, 12, 13, 14; Appendix 5). Average volumes of failures are 14,905 cubic feet (423 cubic meters) for slumps, 25,582 cubic feet (726 cubic meters) for slump- earthflows, and 3,891 cubic feet (110 cubic meters) for earthflows. These failures occurred on slopes ranging from 13-20 degrees or 4.3-2.75:1.

One of the main causes of failure is the use of parent material that is prone to failure. Four different zones of parent material are found in the I-20 study area: Mississippi River flood plain (MRFP) fine-grained alluvium; Macon Ridge with loess (MRL) where loess overlies coarse-grained alluvium; Macon Ridge without loess (MRWL) coarse-grained alluvium; and Ouachita River flood plain (ORFP) fine-grained alluvium. The four zones have been compared to determine why failures only occurred in the MRFP zone of fine-grained alluvium.

X-ray diffractometry was conducted on all the samples. The clay minerals smectite (montmorillonite), a shrink-swell clay, mica (illite), kaolinite, and interstratified smectite-mica clays were qualitatively and quantitatively identified (Table 13).

Parent material properties from the Mississippi River flood plain (MRFP) were determined (Table 14) and then averaged (Table 15). In-depth descriptions of these sites are found in Appendix 5. This area can be characterized as clay-rich (60%) (Table 15), with large amounts of smectite and virtually no interstratified clays (Table 13). The soils are highly plastic (35% plasticity index) and moist (34.9%). The moisture content is indicative of a high clay content, which inhibits drainage and permeability of the soil and enhances water retention. All of the embankment failures had occurred within this parent material at the time of field work (Spring of 1986).

Samples of slope embankment materials were studied along the same interstate highway to the west of slopes constructed from Mississippi River flood plain parent material. These slopes were divided into three additional areas based on different parent materials, and in depth descriptions are in Appendix 6. This was done to isolate the factors of slope failure relating to parent material, which seemed to be the main cause of failure in Madison Parish.

The properties of percent organic carbon, kaolinite, mica, bulk density, and slope angles were determined to be statistically the same throughout the study area.

The first area to the west of the Mississippi River flood plain is the loess-covered Macon Ridge (MRL). Its parent material is dominated by silt (65%) and contains low percentages of sand and clay. Therefore, the Atterberg limits and moisture contents are low because of the coarser soil texture, which aids the drainage and permeability characteristics of the soils (Table

TABLE 13

AVERAGED CLAY CONTENTS OF THE FOUR PARENT MATERIAL AREAS

	MRFP*	MRL*	MRWL*	ORFP*
% Kaolinite	9	11	11	11
% Mica	18	21	20	21
% Interstratified	2	32	34	28
% Smectite	71	36	35	40
% Net Smectite	43	10	7	20

* = Parent material areas are: Mississippi River flood plain (MRFP), Macon Ridge with loess (MRL), Macon Ridge without loess (MRWL), and the Ouachita River flood plain (ORFP).

TABLE 14

AVERAGED PROPERTIES OF THE SITES
IN MADISON PARISH (MRFP)

Site	CB*	W*	TN*	QU*	CM*	TR*
Locality	N13	N14	N15	N16	N17	N18
Particle Size						
Percent Sand	8	2	8	15	3	10
Percent Silt	35	34	34	39	20	45
Percent Clay	57	64	58	46	77	45
Atterberg Limits						
Plastic limit	26	33	26	22	40	26
Liquid limit	58	73	61	50	82	55
Plasticity index	32	40	35	28	42	29
Other						
pH	7.14	7.47	6.81	6.82	7.45	7.45
Bulk density	1.35	1.39	1.39	1.47	1.14	1.51
Moisture content	34.6	29.9	34.4	25.0	44.2	25.4

* = Sites are the Cow Bayou (CB), Waverly (W), Tendal (TN), Quebec (QU), Chicago Mill (CM), and Tallulah Railroad (TR) of the Mississippi River flood plain.

TABLE 15

AVERAGED PROPERTIES OF THE FOUR PARENT MATERIAL AREAS

	MRFP*	MRL*	MRWL*	ORFP*
Particle Size				
Percent Sand	8	9	34	12
Percent Silt	32	65	45	36
Percent Clay	60	26	21	52
Atterberg Limits				
Plastic limit	30	23	20	29
Liquid limit	65	33	27	56
Plasticity index	35	10	7	27
Other				
pH	7.14	6.13	6.58	7.60
Bulk density	1.33	1.43	1.55	1.40
Moisture content	34.9	14.2	15.0	28.2

* = Parent material areas are: Mississippi River flood plain (MRFP), Macon Ridge with loess (MRL), Macon Ridge without loess (MRWL), and the Ouachita River flood plain (ORFP).

Figure 15. Polygonal cracks characteristic of high-smectite soils after dry periods. Photo taken at scarp of slump at Tendal northwest site, Locality N15, I-20 study area. The soil series is the Sharkey.

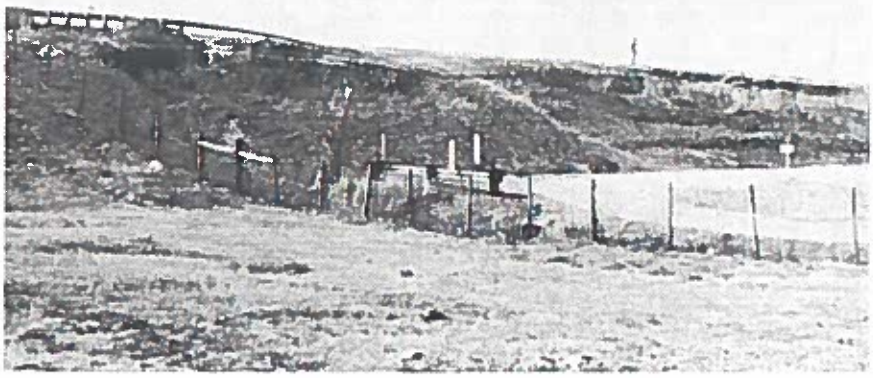

Figure 11. Failures are slump-earthflows which are separated by an earthflow. This slope is located in the I-20 study area, Tendal northeast quadrant, Locality N15, Madison Parish.

Figure 12. Prominent scarp at the head of a slump-earthflow at the Chicago Mill site, I-20 study area, Locality N17, southeast quadrant, Madison Parish.

Figure 13. Slump-earthflow at Chicago Mill, southwest quadrant, Locality N17, Madison Parish, I-20 study area. The high vegetation masks the failure. This failure continued to grow throughout the duration of the study.

Figure 14. Slump exhibiting minor scarps caused by rotation. This failure appears on the northwest quadrant of Tallulah railroad site, Locality N18, Madison Parish, I-20 study area.

15). The clay fraction contains approximately equal amounts of smectite and interstratified clays (Table 13). Therefore, with low clay and smectite values, the net smectite percentage is also low.

The Macon Ridge area without loess is the next area to the west. It has a large silt (45%) and sand (34%) fraction and a small clay percentage. This produces low Atterberg limits and moisture contents because of the coarser texture of the soil, which aids drainage and permeability of the soils (Table 15). The clay fraction contains approximately equal amounts of smectite and interstratified clays and a correspondingly low net smectite value (Table 13).

The Ouachita River flood plain (ORFP) is the last area to the west that we studied. Its parent material has a large clay constituent (52%) (Table 15). Because of the high clay content, the Atterberg limits are large. The clay fraction is dominated by smectite (40%) but has an interstratified clay content of 28%. The high clay content and low smectite value produce a net smectite value of 20% (Table 13). The moisture content is high, indicating a large clay content, poor drainage and permeability, and water retention. After returning to the field in the spring of 1987, two failures had occurred within this parent material.

Failed and non-failed embankment slopes were studied to compare parent materials of similarly built embankments to determine what characteristics were different. Stable embankments are located in the parent material of Macon Ridge, a valley train deposit, and the Ouachita River flood plain.

Stable embankments do exist in the Mississippi River flood plain, but no distinctions can be made between the characteristics of the failed and non-failed embankments. Conditions needed for failure have not been reached and the potential for failure remains high.

The Mississippi River flood plain is the site of 42 embankment failures. Several variables are statistically different from the other areas and are believed to be responsible for slope failure: high clay content, large amount of smectite clays, low amount of interstratified clays, high plasticity, and high moisture content. By comparing samples from the Mississippi River flood plain to the other parent materials, some distinctions can be made.

The stable Macon Ridge areas have a much smaller clay content, approximately equal amounts of smectite and interstratified clays, substantially lower plasticity, and a lower moisture content (Tables 13, 15). The only difference between the two Macon Ridge areas is in the silt and sand fraction resulting from the presence of a loess sheet covering the eastern part of the ridge. The high amount of interstratified clays is believed to reduce the effectiveness of the smectite clays by replacing smectite in the slope. These two clay types are highly negatively correlated, as one increases, the other decreases.

The Ouachita River flood plain parent material has properties similar to both the Mississippi River flood plain and the Macon Ridge areas. The particle size distribution, plasticity, and moisture content are all similar to the Mississippi River flood plain (Table 15). The significant differences occur within the clay fraction. The Ouachita flood plain has 40% smectite, 28% interstratified clays and a net smectite approximately half that of the Mississippi flood plain parent material and double that of the Macon Ridge area (Table 13). Therefore, the activity of smec-

tite has been halved but the plasticity remains high. Since two failures have occurred within this parent material since the study began (March 1986), the stability of the embankments here is somewhat questionable. Four embankments have been predicted to fail in this area.

The difference in clay content between the parent material areas is attributed to differing source areas for the Ouachita and Mississippi rivers and the degree of weathering of the parent material which serves to produce interstratified clays. Weathering can be indicated by the pH of the soil in that the lower the pH, usually the greater the weathering. The Macon Ridge areas have the highest amount of interstratified clays and the lowest pH.

From the comparison of the parent materials, it seems likely that slope failures are primarily due to the high clay and smectite content, which increases the plasticity of the soil.

Problem soils in the study area are the Sharkey, Portland, and Commerce soil series. However, the Commerce soil is not as much of a problem as Sharkey or Portland soils. Other soils could be prone to failure but no failures have occurred in other soils to date. These soils should not be used for embankment construction and other problem soils may be identified by comparing their properties to those of the problem soils.

Statistical Comparison of Soil Properties of The Four Parent Material Zones

The four parent material zones were compared using the analysis of variance tests to see what factors differed from zone to zone. Populations were based on the confidence level of .05 (95%) (Table 16).

Based on the total amount of clay, slope materials have two distinct populations: the flood plain environments and Macon Ridge environments. The flood plains have a large amount of clay whereas the Macon Ridge samples, either with or without loess, have much less clay in them.

The total amount of silt has three populations: the flood plain areas, as they have considerably less silt than Macon Ridge; the loess-covered part of Macon Ridge; and Macon Ridge without loess. Since the eastern portion of Macon Ridge is covered with loess, it has a higher percentage of silt because it was closer to the source area of the Mississippi valley train.

Based on the total amount of sand, there are two populations of slope materials: the flood plain environments and Macon Ridge without loess are grouped together and the loess-covered Macon Ridge is a separate population. These groupings demonstrate that the increase in silt on the loess-covered Macon Ridge is compensated for in the sand fraction. This causes the loess-covered Macon Ridge to have substantially less sand than the other environments and thus be grouped alone.

The total amount of interstratified clays has two populations: the Mississippi River flood plain is a separate population and the Macon Ridge and Ouachita River flood plain are grouped together. The Mississippi River flood plain has considerably lower amounts of interstratified clays than the Ouachita flood plain and Macon Ridge. This demonstrates the influence of two different source areas for the rivers. The Mississippi carries only small amounts of inter-

TABLE 17

SUMMARY OF FREQUENCY AND VOLUMES OF FAILURE TYPES ALONG I-10 STUDY AREA

Type of Failure	Cumulative Frequency	Volumes* Range	Mean
Slump	18	55-2,21	964
		1,929-92,400	33,970
Slump-earthflow	30	17-2,247	240
		660-79,200	8,464
Earthflow	9	13-84	27
		451-2,970	968

Total Failures of all Types =	57
Mean Failure Volume of all types =	410 cu m
	14,467 cu ft

* Top value is in cubic meters, bottom value is in cubic feet.

TABLE 16

ANALYSIS OF VARIANCE STATISTICAL GROUPINGS

Populations:

1= Mississippi River flood plain
2= Loess covered Macon Ridge
3= Eastern Macon Ridge
4= Ouachita River flood plain

VARIABLE	POPULATION GROUPING*	MEANS
% Clay	(1,4) (2,3)	1 = 61 4 = 52 2 = 26 3 = 21
% Silt	(1,4) (2) (3)	2 = 65 3 = 45 4 = 36 1 = 31
% Sand	(4,2,1) (3)	3 = 34 4 = 12 2 = 9 1 = 8
% Interstratified	(3,2,4) (1)	3 = 33 2 = 32 4 = 28 1 = 2
% Smectite	(4,2,3) (1)	1 = 71 4 = 39 2 = 36 3 = 34
% Net Smectite	(1) (4) (2,3)	1 = 43 4 = 20 2 = 10 3 = 7
% Plasticity Index	(1) (4) (2,3)	1 = 35 4 = 27 2 = 10 3 = 7

TABLE 16 (Continued)

VARIABLE	POPULATION GROUPING*	MEANS
% Plastic Limit	(1,4) (2,3)	1 = 30 4 = 29 2 = 23 3 = 20
% Liquid Limit	(1,4) (2,3)	1 = 65 4 = 56 2 = 33 3 = 27
pH	(1) (4) (2,3)	4 = 7.6 1 = 7.1 3 = 6.6 2 = 6.1
% Moisture Content	(1,4) (2,3)	1 = 30.3 4 = 28.2 3 = 14.9 2 = 14.1

* = Analysis of variance statistical groupings. Groupings are based on Duncan Waller and LSD Tukey CLDiff significance tests. ANOVA procedures determined that all the variables are significant at the 95% confidence level. PR>F is <.05 and the Null hypothesis (populations are the same) is rejected.

stratified clays, while the Ouachita River carries large amounts. Also, the Macon Ridge soils have their source from the Pleistocene valley trains and also have weathered longer, so they have more interstratified clays.

Two populations of slope material are evident when considering total smectite content, and these are the same as the interstratified clay grouping. The smectite and the interstratified content have a high negative correlation (Table 16). As smectite increases, the interstratified decreases. This is due to differing source areas and degree of weathering.

The total net smectite value is the result of multiplying the percent clay by the percent smectite in the clay fraction, and it approximates the total amount of smectite in the slope. There are statistically three different populations, which are reflections of the clay grouping and the smectite grouping. The high percent of both smectite and clay give the Mississippi flood plain the highest net smectite. The Ouachita flood plain has a substantially higher amount of clay than the Macon Ridge area but a similar amount smectite, which causes it to have the second highest net smectite value. Both Macon Ridge areas have both low clay percentages and low smectite contents and so are grouped together.

The total liquid limit and plastic limit data are grouped into two populations, the flood plain areas together and the Macon Ridge areas together, because of the higher clay contents in the flood plain areas which increase the Atterberg limits.

The Macon Ridge areas are grouped together in the plasticity index but are separated from each of the two different flood plains populations. At first glance, the failure of this program to group the plasticity index and the plastic and liquid limit data the same way appears to be a problem, since they are derived from each other. The means of the three properties must be examined to explain this. The flood plain areas in the liquid limit grouping have means that differ by nine, while the plastic limit data does not have a significant difference. When the plastic limit is subtracted from the liquid limit, the difference is the plasticity index which is eight. If there was a greater difference in the plastic limits, the grouping would be different. The difference in the liquid limit is carried into the plasticity index. Sand has a greater effect on reducing liquid limits than silt.

The total pH data are grouped into three trends rather than populations, since there does not seem to be significant difference in the means. The pH is merely an indicator of the amount of weathering. The more acidic the soil is, the greater the weathering. The pH has three trends. The two Macon Ridge areas are grouped together with the lowest, most acidic values. The Mississippi flood plain has the next highest pH, followed by the Ouachita River flood plain, which has the highest mean.

The total moisture content data is grouped into two populations: the flood plain areas grouped together and the Macon Ridge areas together. Moisture content is representative of drainage and clay content. The Macon Ridge areas have a coarser grained sediment, which allows the soils to drain more quickly. The flood plains have a higher clay percentage, which makes the soils very slow in regards to permeability, thereby allowing water to be retained.

Causes Of Failure

Usually, a single cause cannot be assigned to a landslide. All slides involve the factors of shear stress and soil strength of the embankment (43) Factors that increase the probability of slope failures include a substantial amount of clay in the slope and within the clay fraction, and a large amount of smectite with little or no interstratified clays. The presence of significant amounts of interstratified clays is believed to inactivate the smectite by reducing the amount of smectite that is in the slopes. As a result of large amounts of clay and smectite, the plasticity of the soil is increased, which favors slope failure. These factors in conjunction with a high slope angle, greatly increase the risk of failure.

Generally speaking, as the clay content in soil increases, the plasticity, shrink-swell potential, compressibility, and true cohesion increases. An increase in clay content also causes a lowering of the true angle of internal friction and permeability (65). Likewise, the swelling and shrinkage of a soil follow the same pattern as their plasticity properties. Therefore, clay minerals that exhibit high plasticity also have greater shrink-swell potential (65). Smectite has the highest shrink swell potential of the clay minerals and acts to increase the plasticity of the soil.

The high concentration of shrink-swell clays (smectites) in the soils seems to be the main difference between the failed and the non-failed slopes of the three different parent material zones. In the ANOVA tests, the only characteristic that sets the MRFP apart from the rest of the zones is essentially net smectite (Table 16). Below 17% net smectite concentration in the soil, failures were not noted (Table 6). Above 33% net smectite in the soils, over 90% of the slopes had failed (Table 4). Between 18-33% net smectite, 60% of the slopes had failed. In the field these soils are easily recognized in dry periods by their polygonal cracking (Fig. 15).

The high concentration of smectite clays in the embankments enhances extensive cracking during dry periods and swelling during wet periods, which can eventually allow a slope to fail(46). This develops large random cracks in the slope, which we noted in the field. We also noted tension cracks up to tens of feet in length, several inches wide and up to nine inches (23 cm) deep near the slope break at the top of the embankment. Terzaghi and Peck (24) report that failures in cohesive soils are usually preceded by tension cracks in the upper edge of the slope. These large cracks then enable water to penetrate into the slope to a considerable depth. When water comes in contact with the smectite, it begins to swell and reduces the shear strength of the soil. Material that has these deep cracks or fissures has a lower bearing capacity than the same material without fissures (46).

Swelling of the soils at a greater depth in the embankment takes several years and is a gradual process. Swelling partially depends on the amount and rate of water supply. Swelling can be a result of water coming in contact with the clay, from humidity, or suction from underlying material (46). Water intake is largest at the start of the swelling process and proceeds at a decreasing rate as water is accumulated within the lattice. This results in an increase in expan-

sion pressure and weight until a failure plane develops. Soil expansion is primarily due to the amount of smectite in the slope, which has a high degree of hydration and swell (25).

Many other factors affect the extent of swelling, such as the "type and amount of clay, compaction, structure of the soil, chemical properties of pore fluid, osmotic pressures, temperature, permeability, stress history, confining pressure, alternate periods of wetting and drying, time allowed for swelling, soil suction, time between compaction, and exposure to water" (25). All of these have had an effect on slope stability in the study area, but the type and amount of clay seem to be the most important factors in this study area.

After several years of building up pore water pressure, increasing shear stress and decreasing shear strength within the slope, a very heavy rapid rainfall can be enough added weight to exceed the bearing capacity of the slope or shear strength of the soil, and it will fail.

The early stage of slope failure has been observed at the Waverly site. When originally characterizing the embankments at this site, several large cracks were noted in some of the embankments, but no failures had occurred. After returning to this site approximately one year later (spring of 1987), the upper foot or so of slope material had failed in the form of a shallow earthflow on the southeast quadrant. The initial cracks were shallow and expedited the instability of the upper layer of material until this layer failed. Stauffer and Wright (43) state that soil near the surface is losing strength with time as a result of repeated wetting and drying and associated shrinking and swelling of the soil at shallow depths. The earthflow has developed a pathway for water to reach the lower soils of the embankment by exposing new material. This new, previously unexposed material will become fissured and the process will repeat itself.

I-10 STUDY AREA

Failures

Embankment failure along the 71 miles (114 km) of I-10 study area transect in southwestern Louisiana is a costly, re-occurring problem. Of the 57 failures mapped and classified between Lafayette and Lake Charles, 18 slumps were identified ranging from 1,929 to 92,400 cubic feet (55 to 2,621 cubic meters) in volume. Slumps are the largest type of failure in the I-10 study area, with a mean volume of 33,970 cubic feet (964 cubic meters) (Table 17) (Fig. 16).

Of all failure types identified along the I-10 transect, slump-earthflows had the highest frequency at 30. Volumes of material displaced had a range of 660 to 79,200 cubic feet (17 to 2,247 cubic meters) (Table 17) (Fig. 17). A mean volume of these slump-earthflows was calculated at 8,464 cubic feet (240 cubic meters). The scarps of the slumps and slump-earthflows sometimes cut into the road bed (Fig. 18).

Earthflows occurred at nine locations, the lowest frequency of all three failure types identified in the study area. They generally occurred on the headers of the embankments, that portion of the slope immediately adjacent to Highway I-10 and partially under the overpass. Of the nine total earthflows identified, eight or 89% were located on the headers. Volumes of displaced material were also the lowest, ranging from 451 to 2,970 cubic feet (13 to 84 cubic meters). The mean size of an earthflow was calculated at 968 cubic feet (27 cubic meters) (Table 17).

The mean failure volume for all types is 14,467 cubic feet (410 cubic meters), ranging from a minimum of 451 cubic feet (13 cubic meters) to a maximum of 92,400 cubic feet (2,622 cubic meters). Thirty-five percent of mapped failures occurs on the header portion of the embankment, as compared to the sides of the slope.

Geographically, Acadia Parish contained the most failures (72% of the total 57), with 66% of the total slopes in that parish having failed. Slopes were more stable in Jefferson Davis Parish (27% of the slopes had failed), Calcasieu Parish (12% of the slopes had failed), and Lafayette Parish (only 3% of the slopes had failed) (Table 18). Acadia Parish was therefore the site of the most unstable embankments and conversely, Lafayette the most stable.

Disregarding geographic boundaries and relating failure to the parent material from which the embankments were constructed, modern alluvium slopes failed most frequently (66%), with Prairie Terrace alluvium slopes next (26%), and loess slopes with the lowest frequency of failure (14%) (Table 18). Therefore, it was suspected that the parent material used for embankment construction in the different parishes was a principal cause of the observed trends in slope instability.

Figure 16. Slump failure between two bridges on I-10 (Locality S12, AC-Bridge, east side). Note the broken and displaced sections of concrete revetment apron.

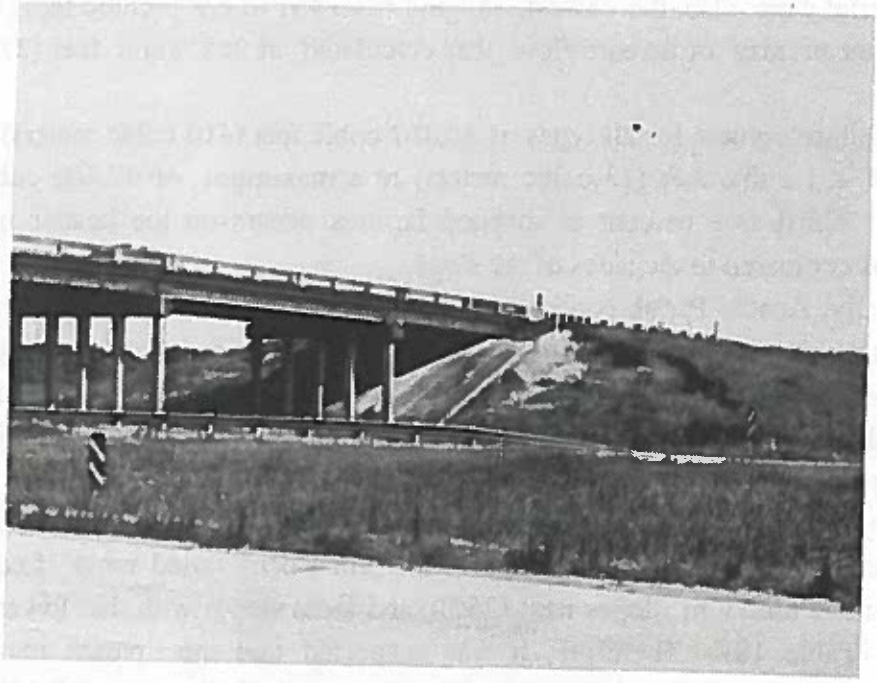

Figure 17. Slump-earthflow beginning to undermine the revetment apron at Locality S15, AC-EO1111-SW.

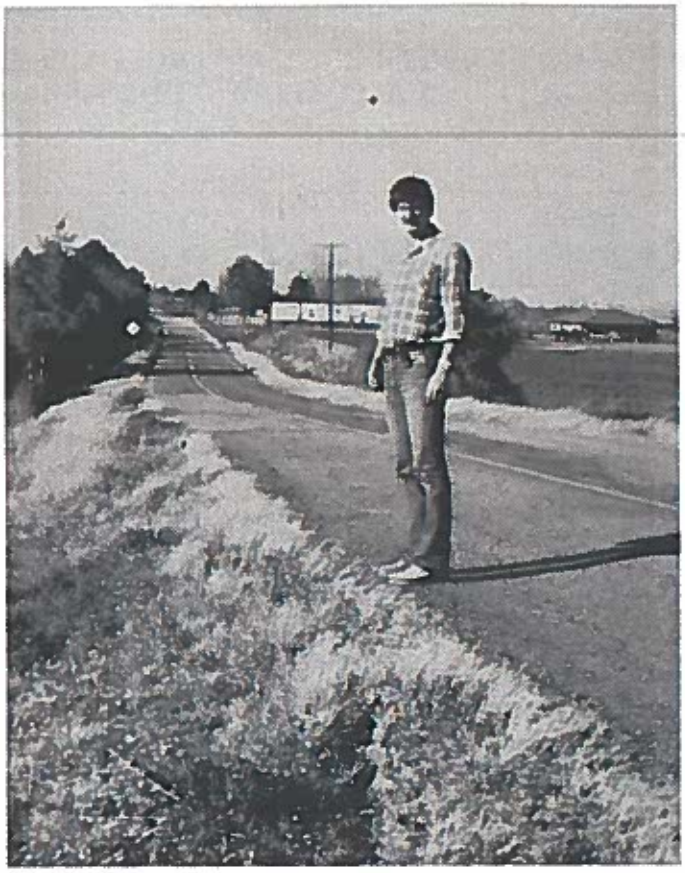

Figure 18. Upper slump scarp cutting into road in front of feet of Schaun Smith at Locality S11 (AC-1123-NW).

TABLE 18

SUMMARY OF FREQUENCY OF FAILURES BY
PARENT MATERIAL AND GEOGRAPHIC LOCATION
ALONG THE I-10 STUDY AREA

Grouping	Slump	Slump-earthflow	Earth-flow	# Slopes	% Freq@ Failures
Parish					
Calcasieu	2	1	0	26	11.5
Jefferson Davis	1	11	0	44	27.3
Acadia	14	18	9	62	66.1
Lafayette	1	0	0	36	2.7

Grouping	# Failed	# Non-Failed	Total*	% Freq Failures
Prairie Terrace Alluvium	23	65	88	26.1
Modern Alluvium	29	15	44	65.9
Loess	5	31	36	13.9

* All embankments in the study area (168) are included in this total.
@ = % Freq. Failures: percentage of the slopes that had failed for that parish or parent material.

Statistical Comparison of Soil Properties of the Three Parent Material Zones

An analysis of variance (ANOVA) was run on all 16 variables for the three parent material populations used to construct the embankment slopes: modern alluvium, Prairie Terrace alluvium, and loess. The null hypothesis was rejected for the variables plasticity index, pH, percent clay, percent silt, and percent net smectite, meaning there are different populations among the three parent material types (Table 19). The other eleven variables exhibited no differences between the three parent materials.

The Prairie Terrace alluvium embankment materials are best characterized by the following mean values: 49% clay content, 30% net smectite, 31% plasticity index, and 27% moisture content on 18 degree slopes. Modern alluvium embankment soils are characterized by the mean values: 47% clay content, 27% net smectite, 31% plasticity index, and 30% moisture content on 21 degree slopes. Loess embankments are characterized by the mean values: 33% clay content, 16% net smectite, 19% plasticity index,and 21% moisture content on 17 degree slopes. The means and ranges of the other geotechnical samples and the clay minerals of the three parent materials are summarized in Tables 20 and 21.

For the variables percent clay, percent net smectite, and plasticity index, embankments constructed of Prairie Terrace alluvium and modern alluvium behave similarly while embankments constructed of loess had different characteristics. This is indicated by the Duncan-Waller, LSD, Tukey, grouping in Table 17. The Prairie Terrace alluvium and modern alluvium slopes have relatively high plasticity index values at 31.1% and 30.7% respectively. Loess slopes on the other hand are much lower at 18.5%. Behavior of the embankment slopes is dominated by the clay size particle fraction. This component comprises approximately 50% of Prairie Terrace alluvium and modern alluvium embankment parent material types. Loess embankments, which contain the smallest clay percentage, are composed of roughly one-third clay, enough to dominate the geotechnical behavior of the slopes as well. Percent net smectite shows a corresponding relationship with Prairie Terrace alluvium and modern alluvium at 29.9% and 27.1% while loess is lower at 16.2%.

These characteristics, high clay content and smectite domination, are principal factors for slope instability in the study area. High clay percentages correspond to high liquid limit and plasticity index values which are equated with slope failure.

The variable, percent silt, illustrated that each of the three parent material embankment populations had significantly different silt percentages. Loess had the highest percentage (58.7%), followed by modern alluvium (47.8%) and the Prairie Terrace alluvium (40.6%).

In addition to these variables, pH also indicates a difference according to parent material. Loess and modern alluvium are grouped together with the statistically similar pH readings of 7.22 and 7.32, while the Prairie Terrace alluvium is considered a different population at 7.64. This relationship is not very strong, however, as the mean values are very close together.

Most of the study area consisted of the Prairie Terrace alluvium (Fig. 6). Of the 168 separate embankments along the transect, 88 were constructed of this material. The second

TABLE 19

SUMMARY OF ANOVA'S FOR PARENT MATERIAL TYPES FOR I-10 STUDY AREA

Variable	PR < F ANOVA#	Duncan-Waller, LSD Tukey, Groupings*	Mean*
PI	0.021 Reject	P A / L	P 31.1 A 30.7 L 18.5
pH	0.05 Reject	L A / P	P 7.6 A 7.3 L 7.2
% Clay	0.02 Reject	P A / L	P 48.7 A 46.9 L 32.6
% Silt	0.003 Reject	P / A / L	P 40.6 A 47.8 L 58.7
% Net Smectite	0.05 Reject	P A / L	P 29.9 A 27.2 L 16.3

* P = Prairie Terrace Alluvium
A = Modern Alluvium
L = Loess

\# If PR < F is less than 0.05, then the null hypothesis that the populations are the same must be rejected. All the other variables not listed in this table (percent kaolinite, mica, interstratified clay, smectite, liquid limit, moisture content, plastic limit, sand, bulk density, slope angle, and organic carbon) accepted the null hypothesis and are the same population.

TABLE 20

SUMMARY OF PARTICLE SIZE AND GEOTECHNICAL DATA

Embankment Parent Material Type		%Clay	%Silt	%Sand	LL	PL	PI	Bulk Density	% Mois.
Prairie Terrace Alluvium	MEAN	48.7	40.6	10.7	48.5	17.4	31.1	1.58	26.5
	MINIMA	24.0	29.8	1.5	26.9	9.6	15.1	1.29	17.8
	MAXIMA	63.1	50.9	46.2	64.3	27.5	40.4	1.80	32.4
Modern Alluvium	MEAN	46.9	47.8	5.2	48.5	17.8	30.7	1.39	29.6
	MINIMA	37.0	30.6	1.7	38.1	11.8	17.0	1.20	24.5
	MAXIMA	67.7	60.3	25.7	69.0	22.4	48.0	1.50	36.1
Loess	MEAN	32.6	58.7	8.7	37.1	18.6	18.5	1.59	20.6
	MINIMA	24.7	43.2	1.2	32.9	12.0	8.3	1.50	16.6
	MAXIMA	37.3	73.0	19.5	39.8	24.5	27.6	1.64	27.3

TABLE 21

SUMMARY OF CLAY MINERALOGY AND OTHER PHYSICAL DATA

Embankment Parent Material Type		%Kaol	%Mica	%Mxed Inter.	%Smec	%Net Smec.	%OC	pH	Slope Angle
Prairie Terrace Alluvium	MEAN	9.2	18.4	12.2	60.6	29.9	.38	7.6	18.0
	MINIMA	10.0	10.0	0.0	45.0	10.8	.16	6.9	14.5
	MAXIMA	15.0	25.0	25.0	85.0	44.0	.67	8.2	22.0
Modern Alluvium	MEAN	10.0	18.9	15.0	56.2	27.2	.45	7.3	20.6
	MINIMA	5.0	0.0	0.0	30.0	11.1	.16	6.3	14.5
	MAXIMA	20.0	30.0	30.0	75.0	44.0	.90	7.8	28.0
Loess	MEAN	8.8	21.3	20.0	50.0	16.3	.55	7.2	16.8
	MINIMA	5.0	20.0	15.0	45.0	12.4	.12	7.0	14.0
	MAXIMA	10.0	25.0	25.0	55.0	18.6	.83	7.6	18.5

most abundant construction material utilized was modern alluvium, composing 44 of the embankments along the transect. The majority of modern alluvium is found in Acadia Parish, where 45% of the embankments sampled were made of this material. Loess constituted 36 of the transect embankments. All the loess parent material samples are found on the extreme eastern end of the transect in Lafayette Parish (Fig. 6), near the Mississippi River flood plain which was its origin.

Based solely on these variables, the two parent material types would be expected to behave similarly with respect to failure versus non-failure. However, since 65.9% of embankments constructed of modern alluvium failed, contrasted to only 26.1% of Prairie Terrace alluvium embankments (Table 18), other factors must be involved.

Slope angles have a demonstrable impact on stability of the I-10 embankments where higher slope angles correspond to higher failure rates (in conjunction with the height of the embankment fill). High slope angle is obviously not the sole cause of instability, as there are stable slopes with high angles. However, failure trends corresponding to slope angle can be established (Tables 18 & 21). This is illustrated by the high percentage of failures (65.9 percent) occurring on modern alluvium slopes which have the highest mean slope angle of 20.6 degrees. The second highest failure rate (26.1 percent) occurs on Prairie Terrace alluvium embankments, which have the second highest mean slope angle of 18.0 degrees. The lowest failure rate of 13.9% occurs on loess embankments which have the lowest mean slope angle of 16.8 degrees.

Slope angle therefore is also a significant factor in embankment instability. Along the study area transect the highest occurrence of failure is associated with the highest slope angles, particularly in Acadia Parish. Additionally, a significant number of failures occur on the headers of the embankments, due to high slope angles as compared to the side slopes.

Causes of Failure

High correlations between liquid limit and clay content, plasticity index and high smectite percentage allow the use of liquid limit as a determining factor along with high moisture content and high slope angles in establishing failure prone slopes. Embankments constructed of modern alluvium parent material generally have these characteristics and consequently have the highest failure rate. Loess embankments, in comparison, have the lowest clay content, a low smectite percentage, lower liquid limit and plasticity index values, lower moisture content, and lower slope angles and a resultant low rate of failure. The embankments constructed of the Prairie Terrace alluvium parent material are very similar to modern alluvium characteristics, with the exception of having significantly lower slope angles. Prairie Terrace alluvium embankments have an approximately intermediate rate of failure between loess and modern alluvium.

As a result of high clay content, the internal drainage and permeability of the embankment material is reduced. Over ten to fifteen years, with repeated wetting and drying of the embankments in southwestern Louisiana and subsequent expansion and contraction of the shrink- swell clay, there is a reduction of shear strength. Subsequently, a large rainfall, dramatically increasing the percent moisture, will finally succeed in overcoming the strength of the embankment material. This occurs by the physical undermining of the slope through water percolation into shrinkage cracks, the building of excess pore water pressure due to poor internal drainage, and lateral expanding of smectite as it absorbs water and loses cohesion.

Embankment soil types that particularly relate to failure and high clay content are the Crowley, Patoutville, Morey and Mowata series. All of these soils have high shrink-swell potential (high smectite content), poor internal drainage, high liquid limits (ranging from 35 to 60 %), and high plasticity indices (ranging from 18 to 36 %).

STABILITY OF EMBANKMENT SLOPES

Introduction

The stability of embankment earth masses represents a serious problem in Louisiana. The extent of the problem can be ascertained from the results of embankment condition surveys conducted during this study. Stability loss or failure of an embankment slope occurs when an outer portion of the earthen mass slips downwards and outwards with respect to the original mass. The slippage generally develops along an approximate circular surface.

Slope stability studies can be used to either evaluate the safety of existing constructed or natural slopes or to design embankment slopes with adequate stability. The safety factor or stability number is used as a measure of slope stability and is defined as the ratio of the resisting soil strength (i.e., inherent soil shear strength available due to cohesion and/or frictional resistance) to the driving forces induced in the soil mass by the embankment configuration (i.e., primarily embankment height and slope). Attempts should be made to select strength characteristics representative of soil mass subjected to future environmental conditions.

A slope stability analysis generally consists of (1) an evaluation of appropriate soil strength properties and (2) an analysis of the driving and resisting forces involved in the stability/instability of earthen masses. In addition to the number, thickness and properties of soil layers existing within the soil embankment structure should be defined so that an appropriate model can be evaluated. Because of the amount of calculations involved in a slope stability analysis, computers are normally used as an aid in completing any design and/or evaluation of proposed embankment masses.

There are a number of factors which may contribute to slope instability including the strength characteristics (i.e. cohesion and frictional resistance) and properties (i.e. clay and moisture contents, density and plasticity) of the parent material, future environmental conditions (i.e., as they affect soil strength through shrink-swell and wet-dry phenomenon), unexpected load conditions (i.e., earthquakes, flooding, etc.) and embankment design and construction, including embankment height and slope angle. In general a lower slope angle would assure a more stable slope; however, the level of stability which may develop is likely related to the parent material (16).

Slope Stability Model Development

The approach utilized in the development of the model involves the establishment of soil strength properties representative of the Madison Parish area (MRFP of the I-20 study area) and the selection and evaluation of a model appropriate for an embankment cross section located in Madison Parish. The model cross section will ultimately be used in the development of a slope stability model.

TABLE 22

SOIL PROPERTIES AND CHARACTERISTICS, CHICAGO MILL SECTION MADISON PARISH, LOCALITY N17

LOCALITY	LL %	PI %	CLAY %	DEN PCF	Wn %	CS PSF	TS PSF	COHt PSF
NE Quadrant	84	45	78	85	36	1365	165	370
	87	38	75	100	25	4935	1090	2480
	84	45	78	82	35	740	130	295
	85	39	87	87	32	1350	245	605
	88	46	83	82	38	1730	295	675
	89	44	92	85	36	1630	230	525
	93	48	90	96	30	3990	850	1950
SE Quad	80	41	75	88	33	1610	365	835
	83	40	79	78	42	395	95	215
	81	37	75	79	41	1270	105	235
	82	39	92	80	39	1665	185	425
	82	39	92	85	35	1475	150	340
	81	37	74	79	38	870	130	290
SW Quad	84	50	74	81	37	675	130	290
	84	50	74	81	37	1125	140	325
	91	52	79	82	39	840	185	425
	84	43	72	75	42	780	100	225
	84	43	79	79	45	640	80	185
	84	43	79	79	35	570	60	130
	75	40	72	80	37	990	110	250
	65	31	88	89	28	1480	110	250
	65	31	88	80	37	1180	70	155
NW Quad	67	38	61	92	29	1455	230	525
	61	27	58	95	27	1095	175	400
	89	46		76	41	995	140	325
	89	46	80	78	39	960	170	385
	82	52		76	45	830	85	200
	84	53		80	39	1120	135	310

LEGEND

LL - Liquid Limit
PI - Plasticity Index
CLAY- Clay Percentage
DEN - Dry Density
Wn - Moisture Content
CS - Compressive Strength
TS - Tensile Strength
COHt- Cohesive Strength

COHt = 2.28 x TS

TABLE 23

SOIL PROPERTIES AND CHARACTERISTICS, CHICAGO MILL SITE MADISON PARISH, LOCALITY N17 LADOTD GEOTECHNICAL SOILS EVALUATION

DEPTH, FT From	To	LL %	PI %	CLAY %	DEN PCF	Wn %	CS PSF	DSS PSF	COHc PSF
Station 832 + 21									
3	6	73	45	74	86	35	2490		870
12	15				84	40		400	400
15	18	94	61	81	86	38	1266		445
18	21	33	7	25	86		2491		870
24	27				87	35	2950		1475
36	39	90	58	86	72	49	1885		660
Station 832 + 22									
6	9	88	60	80	82	38		500	500
15	18				90	33		1400	1400
18	21	93	61	77				615	615
Station 833 + 22									
9	12				92	30		495	495
15	18				82	40		500	500
30	33	93	66		72	51		540	540
Station 833 + 40									
9	12	81	47	60	88	34	4900		1715
15	18	95	67	70	83	38	1780		625
18	21	92	57	68	82	39	4320		1510
24	27	82	51	74	81	40	2000		700
27	30	66	38	56	80	32	1265		445
30	33	38	15	35		34	745		260
33	36	63	35	65	82	40	1100		770
36	39	94	58	89	70	54	1800		630
39	42	83	53	84	77		1540		540

LEGEND

LL - Liquid Limit	Wn - Moisture Content
PI - Plasticity Index	CS - Compressive Strength
CLAY- Clay Percentage	DS - Direct Shear Strength
DEN - Dry Density	COHc- Cohesive Strength

COHc = 0.35 x CS

TABLE 24

SOIL PROPERTIES AND CHARACTERISTICS
I-20 LOCATIONS IN MADISON PARISH, LOUISIANA

OVERPASS	LL %	PI %	CLAY %	DEN PCF	Wn %	CS PSF	TS PSF	COHt PSF
Cow Bayou , Locality N13								
NE Quad	46	20	43	100	25	1510	230	565
	65	30	61	101	24	1425	175	430
SE Quad	43	19	55	107	22	1500	260	645
	61	33	58	99	26	1040	170	415
	70	42	67	91	30	950	165	415
SW Quad	43	23	40	102	21	1555	190	475
NW Quad	41	21	39	90	26	1940	360	815
	42	23	43				1410	3490
Quebec , Locality N16								
NE Quad	47	29	46	94	25	2950	450	1115
	54	30	32	103	17	3930	615	1520
SE Quad	55	32	46	104	18	3415	385	950
	54	30	48	103	17	2450	355	885
SW Quad	44	23	43	111	12	9835	920	2280
	51	32	44	111	14	5195	350	870
NW Quad	44	21	45	105	16	11090	1030	2550
	51	31	45	100	21	2255	400	990
Tendal , Locality N15								
NE Quad	36	16	36	102	14	3850	515	1275
SE Quad	58	31	57	108	17		610	1515
SW Quad	56	31	49	96	14	1600	365	835
	67	36	64	95	23	2620	430	975
NW Quad	65	41	60	107	10	4405	710	1615

LEGEND

LL - Liquid Limit
PI - Plasticity Index
CLAY- Clay Percentage
DEN - Dry Density
Wn - Moisture Content
CS - Compressive Strength
TS - Tensile Strength
COHt- Cohesive Strength

$$COHt = 2.28 \times \frac{TS}{75}$$

The slope stability model will be developed, improved and calibrated for the Chicago Mill embankment section (Locality N17). This site was selected because of the transition in both embankment height and slope which exists in the vicinity of the Chicago Mill box culvert. The variety of combinations of embankment height and slope then allows ample opportunity for comparisons of the predicted slope stability numbers obtained by computer analysis with the results of the slope condition surveys which illustrate stability/instability of the existing embankment slopes (i.e., at time of inventory in 1986-87).

Subsequent to calibration, the slope stability model will be used to predict the slope stability/instability for Cow Bayou (N13), Quebec (N16) and Tendal (N15) overpasses, also located in Madison Parish of the I-20 study area. Comparisons of these predictions developed from a computer analysis with condition survey results will establish the reliability of the slope stability model.

Available Soil Strength Information

The development of soil strength estimates to be used in the subsequent slope stability analysis involved consideration of results of in situ sampling and laboratory testing by project personnel and geotechnical information provided by LaDOTD personnel. The in situ soil samples that were obtained by project personnel were considered to be representative of the surficial soils, since they were extracted from the top of the second soil layer (and below the organic grassy blanket). On the other hand, the geotechnical results provided by LADOTD were developed from soil borings carried to depths of 40 feet and would be representative of soil conditions in and below the existing embankment mass.

Indirect tensile and unconfined compression tests were completed by project personnel on the surficial soil samples extracted from the Chicago Mill area (Table 22), as well as from the Cow Bayou, Quebec and Tendal overpass areas (Table 24). At the time of testing, moisture content and dry density were determined for each sample. In addition Atterberg limits data (i.e., plastic limit, liquid limit and plasticity index), as well as clay content and type, were established for each soil sample. Cohesion or cohesive strength of the various soil samples was estimated by multiplying the tensile strength by a factor of 2.28. This factored value represents that uniaxial stress required to develop the same tensile strain as that developed in the biaxial stress state created in the indirect tensile test.

Unconfined compression, confined triaxial and direct shear tests were completed by LADOTD personnel on soil samples extracted from the embankment sections of the Chicago Mill area, as well as Cow Bayou (N13), Tendal (N15) and Quebec (N16) overpasses. Some of the results of the LADOTD testing program for the Chicago Mill area (N17) are presented in Table 23. Atterberg limit data, clay content, in situ moisture contents and dry density are presented in the table, along with compressive strength and direct shear strengths for soil samples obtained at depths ranging from 3' to 42' below the top of the embankment section. In

addition, cohesion or cohesive strength estimates (based on the compressive strength values) are listed in the last column of the table. The cohesion estimate for the soil samples (at varying depths below embankment top) was obtained by multiplying the compressive strength values by a factor of 0.35. This factored value is less than the value of 0.5 normally used to estimate cohesion from compressive strength for a purely cohesive material but represents a more reasonable estimate of the tensile strains produced in the compression test configuration by the rigid load platens (69).

Selection of Representative Soil Properties-Chicago Mill, N17

Since the Chicago Mill section was designated as the principal source of information in the development and calibration of the slope stability model, it was essential that a comprehensive sampling and testing program be conducted to establish representative soil properties. The results of this program for the Chicago Mill section of I-20 are presented in Table 22. From this information it can be seen that the soils encountered in the program consisted of high clay content soils (i.e., 58% or greater) with existing moisture contents ranging from 25 to 45%. These surficial soils generally exhibited low cohesive strengths with the lower values falling in the range of 130 to 185 pounds per square foot. Individual test data was analyzed to determine if the low cohesive strengths were related to certain isolated conditions, e.g., high moisture content with low clay content, or related to the general soil conditions.

In order to ascertain any general relationship between cohesion and soil characteristics, scatter diagrams portraying soil cohesion of the Chicago Mill surficial soils versus dry density, moisture content and clay content were developed and are presented in Figure 19. From these three scatter plots it can be seen that low cohesive strength values were obtained for varying clay contents (i.e., 60 to 95%), moisture contents ranging from 27 to 46% and dry densities between 75 and 95 pcf. Similarly, low cohesive strength values were found for wide ranges in plastic limit, liquid limit and plasticity index (Figure 20). The scatter diagrams for measures of relative moisture (Figure 21) illustrate that the low cohesive strengths occur for high relative moisture contents (e.g., liquidity index greater than -10, moisture content/plastic limit greater than 85% and ratio of moisture content to liquid limit of 42%). From this information it can be ascertained that the cohesive strength of the surficial soils at Chicago Mill can be as low as approximately 175 psf when relatively high moisture contents are attained.

In the soils data collected for the Chicago Mill area, there was no direct measurement of the soil swelling which had occurred. The dry density values would provide some measure of soil swelling. Since the soil properties (i.e., clay content, liquid limit and plasticity index) of the samples reported in Table 22 are essentially the same, it is expected that they exhibit practically the same dry density at optimum moisture-density conditions. Based on this premise, the lower dry density values are indicative of greater amounts of soil swelling. As the clays attract moisture, the clay platelets are forced further apart by the accumulation of water, resulting in a reduction in the electrical charges (or attraction) and a lower cohesive strength. This can be seen in

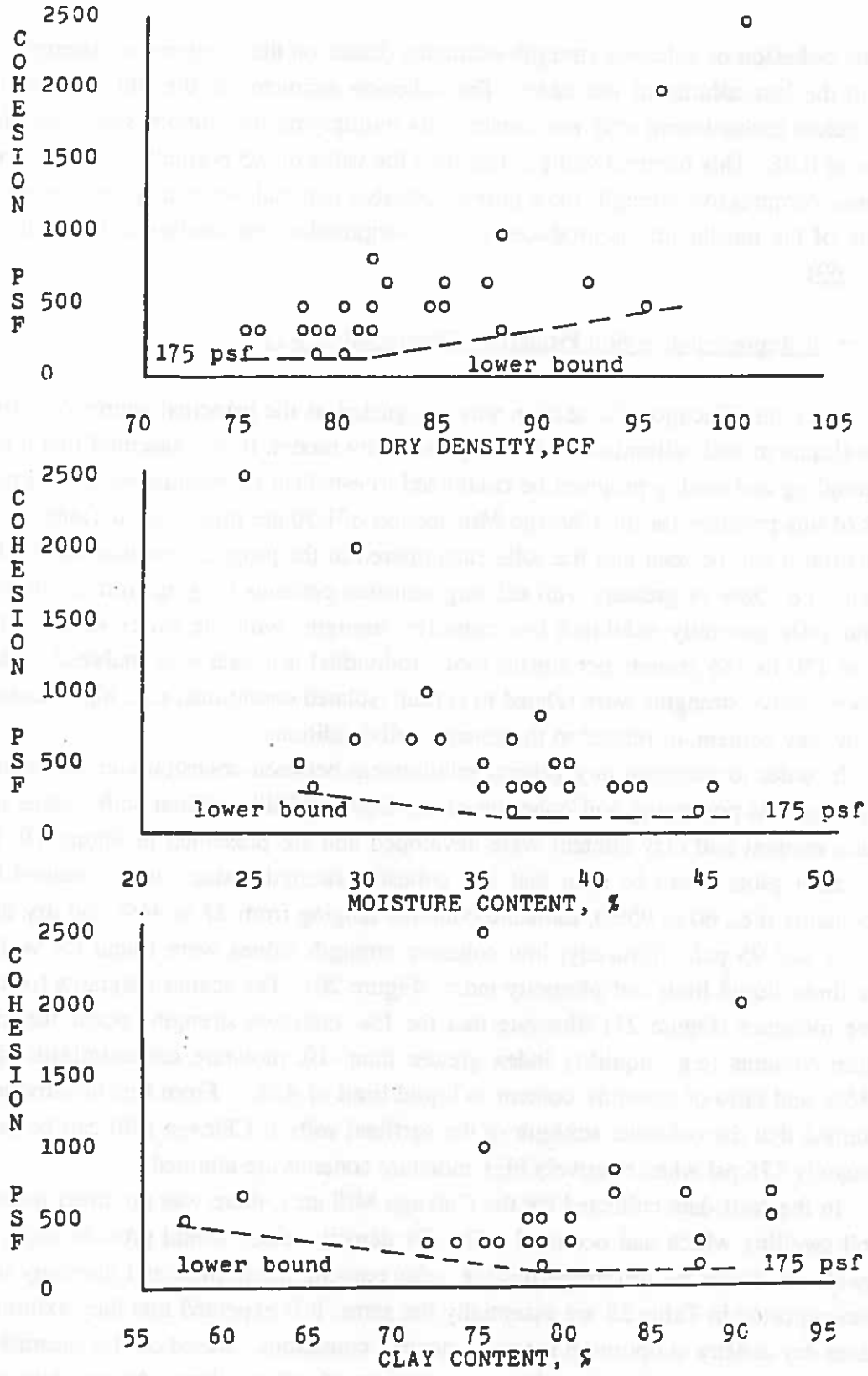

Figure 19. Scatter diagrams for various soil characteristics Chicago Mill section of I-20, Madison Parish, N17.

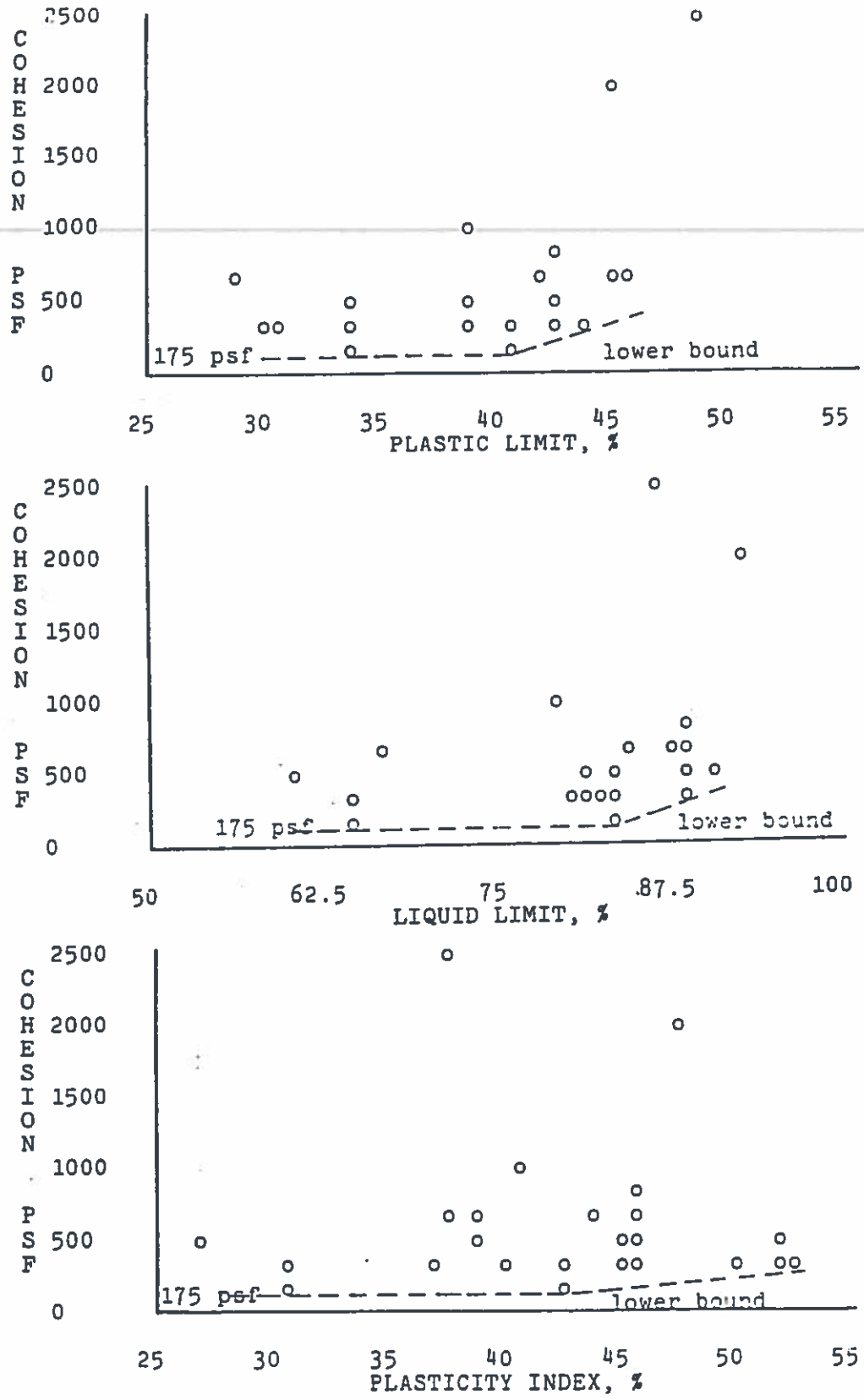

Figure 20. Scatter diagrams for soil Atterberg limits Chicago Mill section of I-20, Madison Parish, N17.

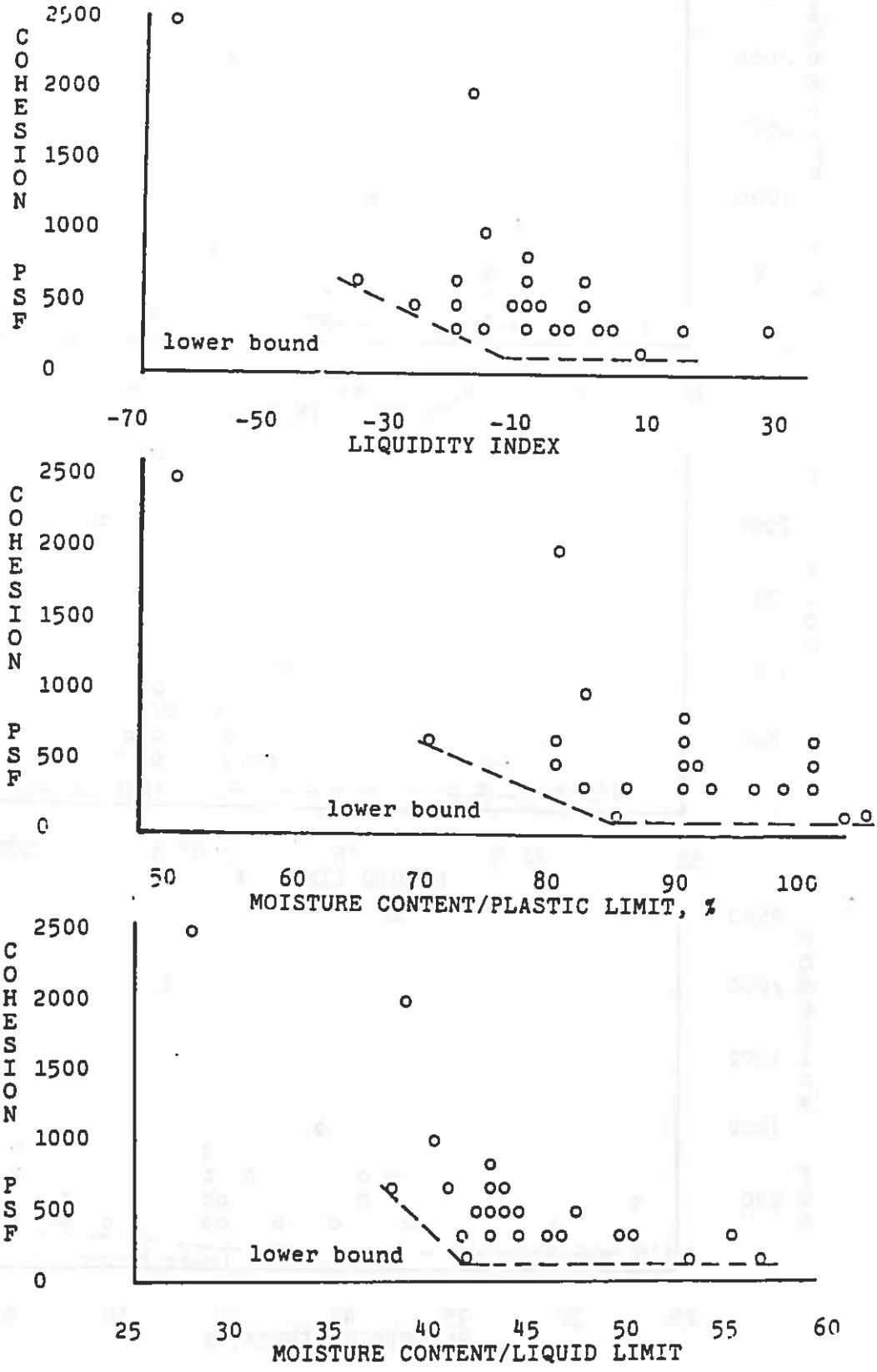

Figure 21. Scatter diagrams for relative moisture levels Chicago Mill section of I-20, Madison Parish, N17. Lafayette and Lake Charles, Louisiana.

the top section of Figure 19 where the cohesive strength values are lower for the lower dry densities. It is apparent that a majority of the surficial soil samples from the Chicago Mill area have undergone significant swelling.

The results of the geotechnical soils evaluation completed by LADOTD (Table 23) indicate that soils similar to the surficial soils at Chicago Mill (Table 22) were found in depths up to 42 ft below the top of the Chicago Mill embankment. There were only two instances where the soils did not match. These two include the soils at depths of 18 to 21 ft at station 832 + 21 and the 27 to 33 ft depth at station 833 + 40. It should be noted that the cohesive strength estimates from Table 23 are generally higher than the surficial soil strengths (Table 22). Nevertheless low values of cohesive strengths were found at depths of 27 to 33 ft below the top of embankment at station 833 + 40. At this level the soils exhibit lower Atterberg data (i.e., P.I. less than 38 and liquid limit less than 66) and lower estimates of cohesive strength. From Table 23 it can be seen that an average cohesion estimate of about 350 psf would be representative of the soils between 27 and 33 ft below embankment top at station 833 + 40. This soil layer location (i.e., 27 ft depth) represents a position approximately 9' below the toe of slope elevation.

A limited sampling and laboratory testing program was established for the Cow Bayou, Quebec and Tendal overpasses. The results of this program are presented in Table 24 and indicate that the soils obtained from these three sites may be different from those soils found in the Chicago Mill area. For these soils the clay contents varied from 32 to 67%, while the moisture contents varied from 12 to 30%. The cohesive strengths were also generally higher than the cohesion values for those soils from the Chicago Mill area. The differences in the strength values, however, can probably be related to the differences in the moisture contents, since these samples were taken during a seasonally dry period.

Soil Properties and Characteristics, I-10 Locations

Because embankment instability and failures had occurred at various overpass and bridge locations on Interstate Highway 10 between Lafayette and Lake Charles in south Louisiana, an embankment condition survey along this section of I-10 was conducted, along with a limited sampling and laboratory testing program of the surficial soils located in the upper portion of the second soil layer (i.e., the second layers is considered to be located just below the grassy vegetation surface). The results of the sampling and laboratory testing program are presented in Table 25, which includes Atterberg limit data (i.e., liquid limit and plasticity index values), soil properties (i.e., clay content, dry density, and moisture content), and soil strength characteristics (i.e., compressive, tensile and cohesive strengths).

Although the soils in this area of the state exhibit soil characteristics different than those from Chicago Mill of the I-20 study area (i.e., the liquid limits, plasticity indices and clay contents are all lower than the Chicago Mill results), these surficial soils also display low cohesive strength values (i.e., a lower bound value of 180 psf).

TABLE 25

SOIL PROPERTIES AND CHARACTERISTICS OF VARIOUS OVERPASSES ALONG I-10 BETWEEN LAFAYETTE AND LAKE CHARLES, LOUISIANA

#	LOCALITY	LL %	PI %	CLAY %	DEN PCF	Wn %	CS PSF	TS PSF	COHt PSF
S5	CA-383-SE	40	21	45	114	15	3145	480	1085
S7	JD-WE-SW	47	27	52	107	17	1560	230	530
S7	JD-WE-SW	41	31	41	105	17	1825	240	540
S12	AC-BRIDGE	38	17	37	108	18	1125	155	360
S13	AC-369-NW	43	28	40	112	18	2775	310	705
S14	AC-ES-NW	58	35	46	94	24	820	90	200
S14	AC-ES-NW	45	26	54	94	28	825	85	195
S14	AC-ES-NE	39	21	41	93	29	845	80	180
S15	AC-E01111	64	39	63	95	28	855	150	345
S15	AC-E01111	64	39	63	97	23	870	95	215
S17	AC-95-NE	52	33	52	100	25	805	80	180
S17	AC-95-NE	69	48	52	92	29	845	80	180
S20	LA-AC-NE	36	19	37	114	18	2010	200	455

LEGEND

LL - Liquid Limit
PI - Plasticity Index
CLAY- Clay Percentage
DEN - Dry Density
Wn - Moisture Content
CS - Compressive Strength
TS - Tensile Strength
COHt- Cohesive Strength

$$COHt = 2.28 \times TS$$

From the scatter diagrams presented in Figures 22, 23 and 24, it can be seen that the low cohesion values develop over a range of moisture and clay contents (Fig. 22), a variety of Atterberg limits data (Fig. 23) and a number of relative moisture measurements (Fig. 24). Based on higher dry density values (e.g., higher by 20 pcf) and lower clay contents (e.g., lower by 25 to 35%) it can be assumed that the soils from the I-10 area have undergone an amount of swelling less than those soils from the Chicago Mill area of I-20.

Soil Properties and Characteristics, Combined I-10 & I-20 Data

In order to provide a comprehensive evaluation of soil cohesive strength for a greater range of soil properties and characteristics, scatter diagrams were generated for combined I-10 and I-20 Chicago Mill test results. The scatter diagrams for density, moisture content and clay content are presented in Figure 25, while scatter plots for plastic limit, liquid limit and plasticity index are included in Figure 26. The relative moisture contents with respect to liquid limit and plastic limit, as well as liquidity index, are plotted versus cohesive strength in Figure 27.

From Figure 25 it can be seen that low cohesive strengths can develop for a wide range of dry densities, moisture contents and clay contents. From the plots there appear to be target values of dry density, moisture content and clay content that result in a cohesion of approximately 175 psf. A value of dry density less than or equal to 90 psf results in a low cohesive strength, while a moisture content greater than or equal to approximately 30% yields the same effect. In fact, it is believed that these are compatible values and represent the same effect (i.e., a dry unit weight of 90 pcf corresponds with a moisture content of 30%). In addition, based on the results presented here any, soils with clay contents exceeding 50% could result in low cohesive strengths probably created by soil swelling.

There does not appear to be a strong relationship between cohesive strength and Atterberg limits data. Low cohesion was observed for plastic limits ranging from 15 to 50% and liquid limits ranging from 50 to 90%. There may be target values for liquid limit (i.e., 50%) and plasticity index (i.e., 30%) that delineate the conditions that could produce low cohesion in soils after some sustained exposure to environmental conditions.

In reviewing the scatter plots of Figure 27, it can be seen that there are target values for the three relative moisture measurements which delineate expected changes in soil cohesive strength. A ratio of moisture content to plastic limit of 35% or a ratio of moisture content to liquid limit of 38% appear to be the limiting values resulting in low cohesive strengths. A liquidity index of approximately -10% heralds the same soil condition as the previous relative moisture measurements.

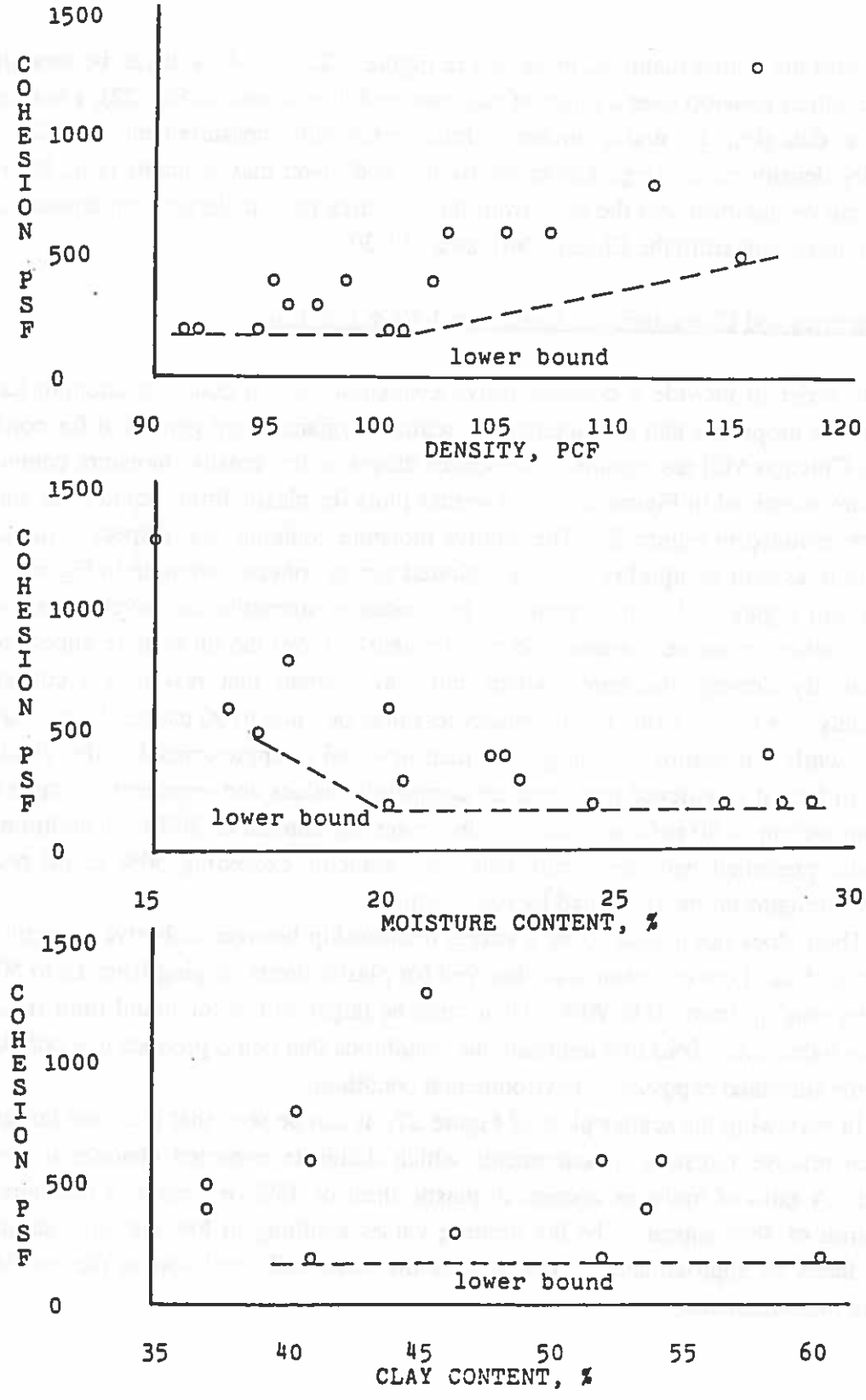

Figure 22. Scatter diagrams for various soil characteristics of various highway overpasses along I-10 between

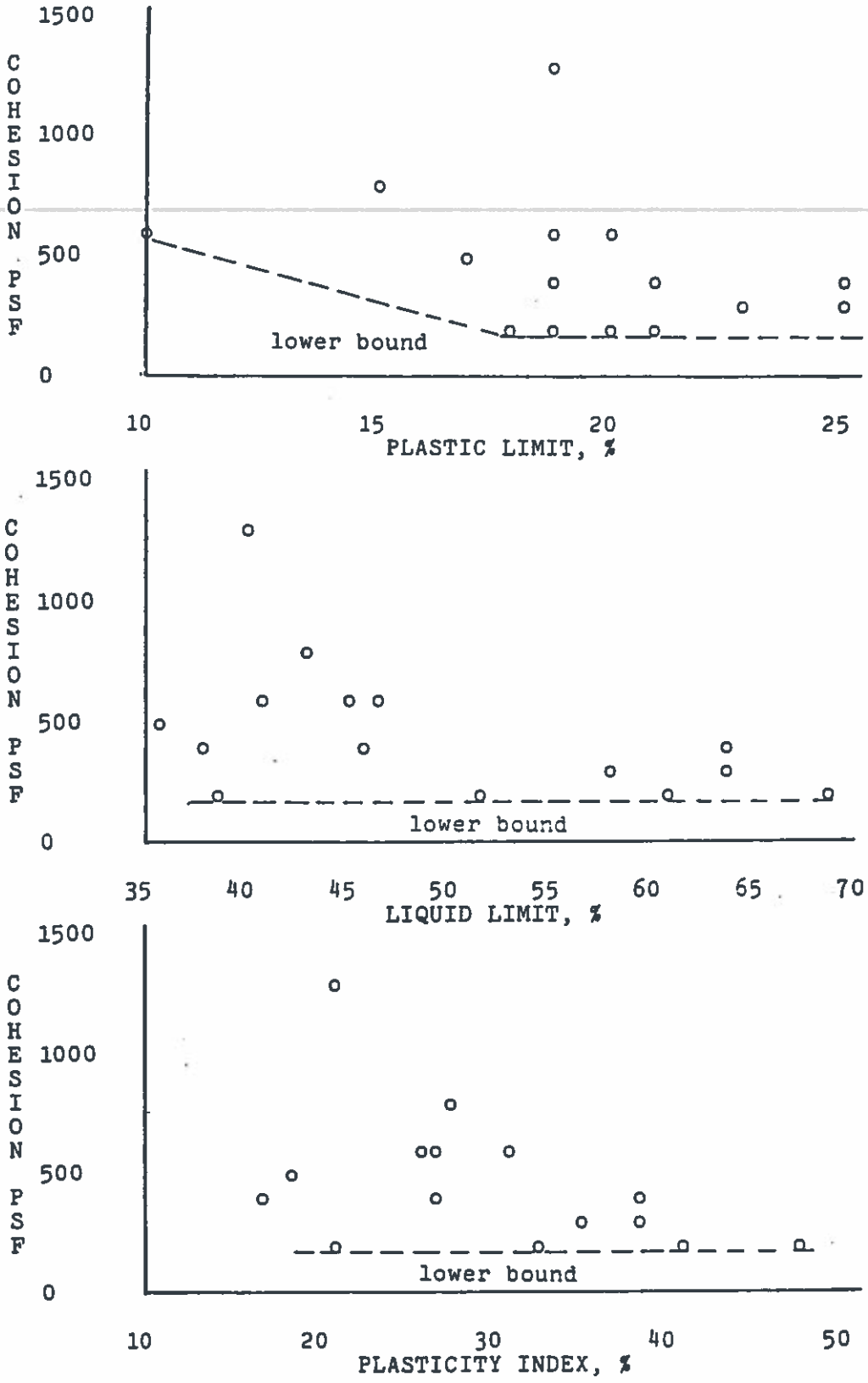

Figure 23. Scatter diagrams for soil Atterberg limits of various highway overpasses along I-10 between Lafayette and Lake Charles, Louisiana.

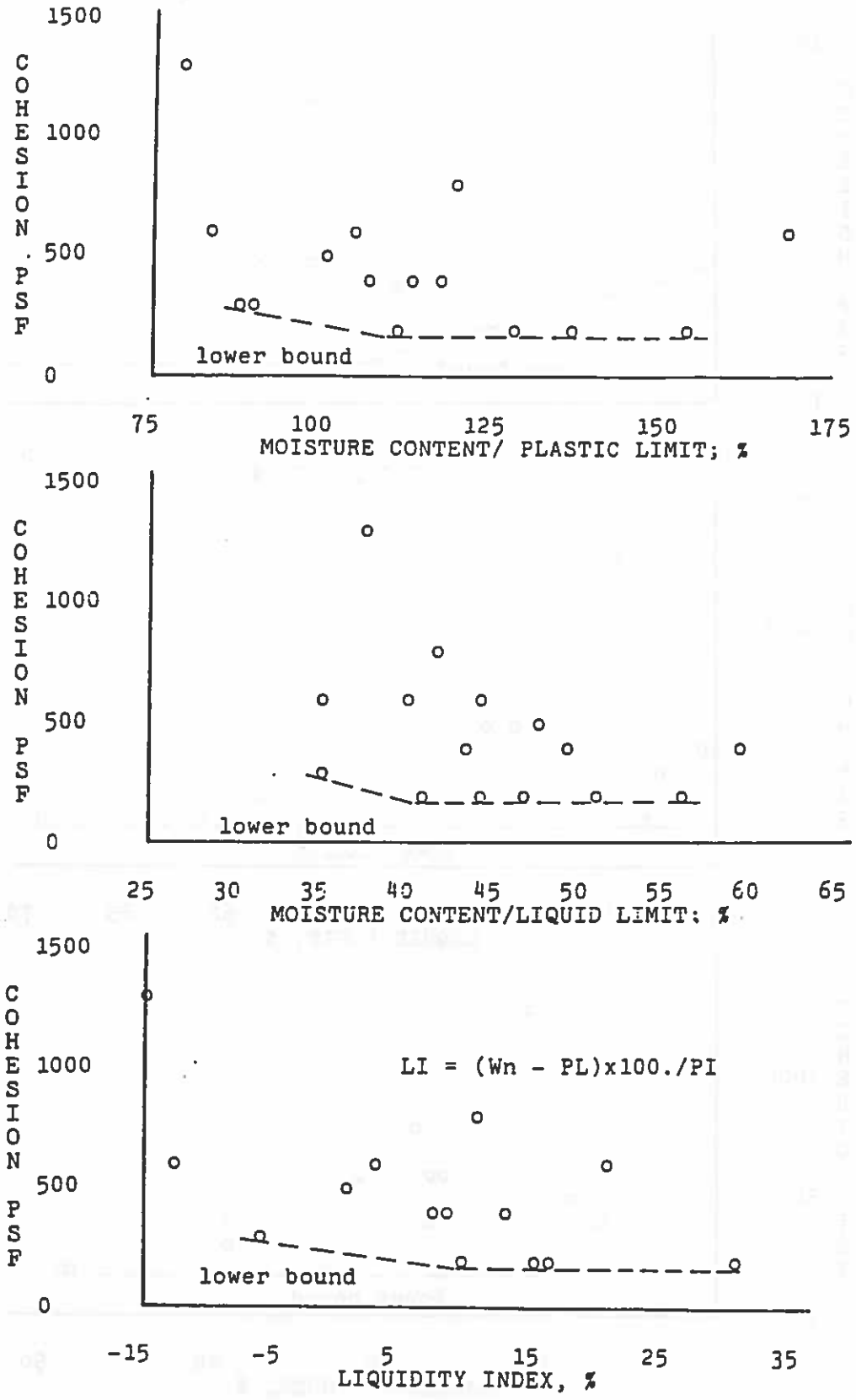

Figure 24. Scatter diagrams for relative moisture levels of various highway overpasses along I-10 between Lafayette and Lake Charles, Louisiana.

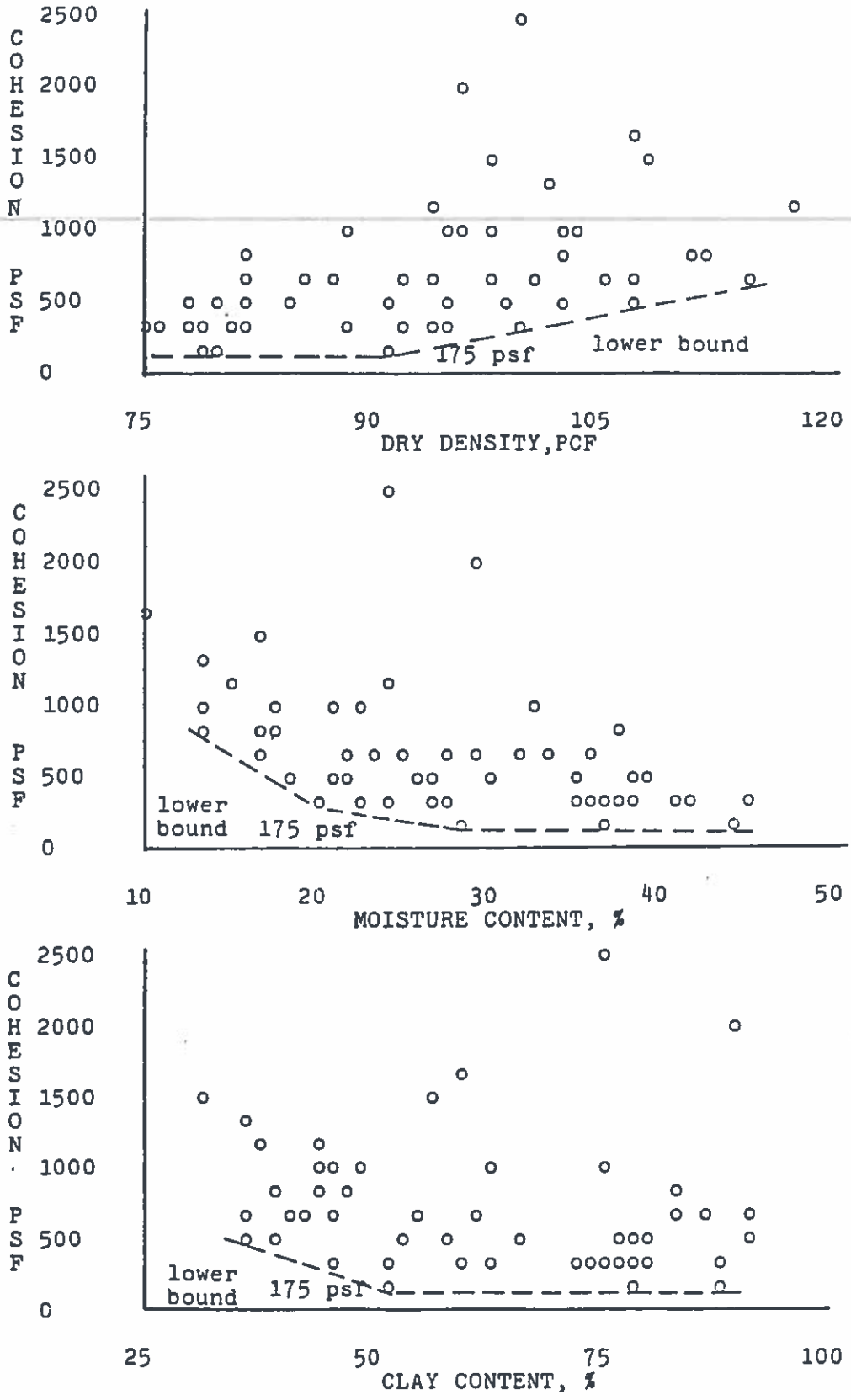

Figure 25. Scatter diagrams for various soil characteristics, combined data from Chicago Mill and I-10 overpasses.

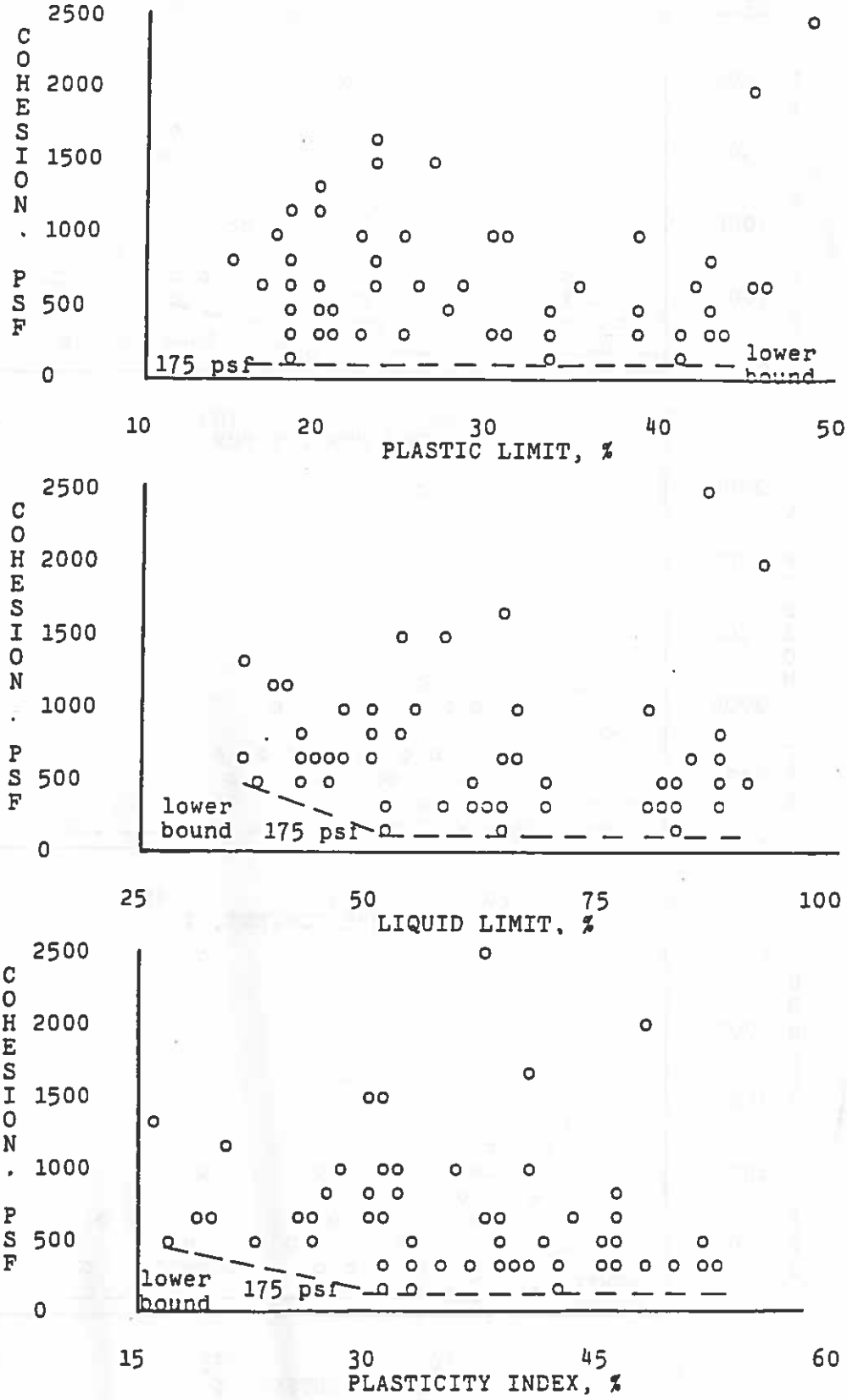

Figure 26. Scatter diagrams for soil Atterberg limits, combined data from Chicago Mill and I-10 overpasses.

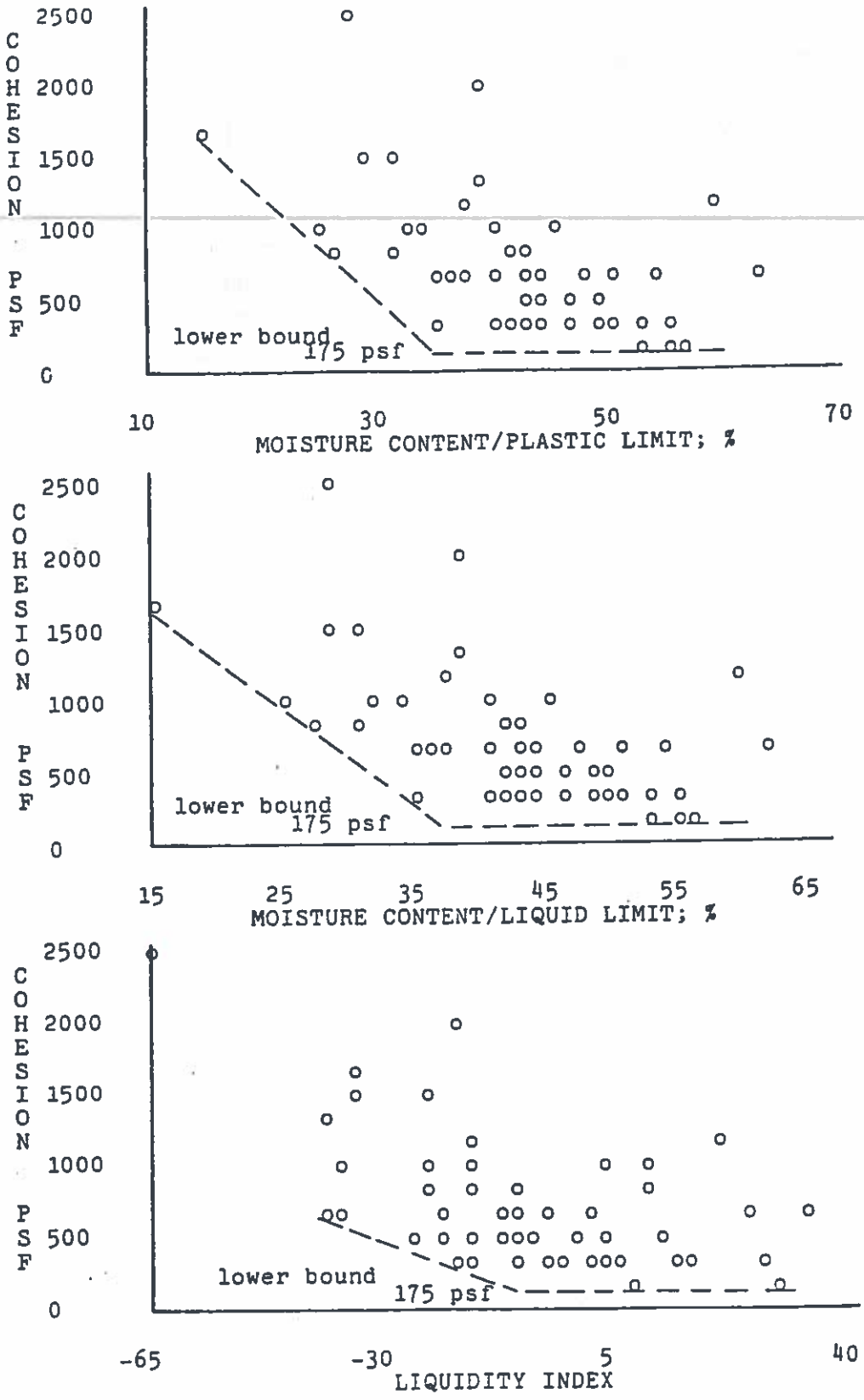

Figure 27. Scatter diagrams for relative moisture levels, combined data from Chicago Mill and I-10 overpasses.

Selection of Slope Stability Model

The slope stability model representative of a Madison Parish, I-20 study area embankment was developed from cross section information provided by LADOTD personnel and soils strength data generated in this project. The initial slope stability model selected for further evaluation and calibration is presented in Figure 28. The model was developed for station 830 + 00 of Chicago Mill, utilizing LADOTD's elevation cross section and side slope results.

This Chicago Mill location was selected based on the results of a slope condition survey completed by project personnel (Fig. 30). Station 830 + 00 was selected because it represented a position along Chicago Mill at which there was evidence of a transition from a stable embankment status (i.e., for stations below 830) to an unstable condition (i.e., for positions beyond station 830). It was, therefore, expected that a stability number of 1.0 would be appropriate for station 830 + 00. The model could then be adjusted to yield the same stability number.

The embankment cross section was assumed to be composed of three distinct layers as indicated in Figure 28. The top layer consists of the vegetation covering the embankment top and sloping sides, is assumed to be 1 ft in thickness and to provide no structural support to the embankment. This premise is based upon the fact that the vegetation layer developed significant surface shrinkage cracking, which extended to depths approaching 1 foot. On the other hand, this vegetation layer was thought to form a part of the driving forces since in a saturated state (i.e., wet unit weight) it would exert significant vertical forces on the embankment.

The second layer was believed to consist of a soil represented by the surficial soil data listed in Table 22. A single layer was assumed because the soil properties and characteristics of the Chicago Mill surficial soils (Table 22) are similar to those found at depths extending to 27 ft below the top of embankment (see LADOTD results in Table 23). The soil in this layer was established as a strictly cohesive clay, with a cohesive strength of 175 psf. Since the soils were composed of very high clay contents and long-term loading would develop in a slope stability situation, it was felt that the effective angle of friction would be very low or negligible. A cohesive strength of 175 psf was selected because it represents the approximate lower bound value obtained in laboratory testing for Chicago Mill soils.

A third layer was established because of the change in soil properties and characteristics observed in the LADOTD results for Chicago Mill station 833 + 40. At this station there was a distinct change in the soil at depths of 27 to 33 ft below the embankment top. As a result, a third layer was established as a strictly cohesive clay. For this layer, too, it was believed that the long-term loading conditions produced in a slope stability situation would negate any effects of soil friction. The cohesive strength value was to be varied between 175 and 525 psf. An intermediate cohesion value of 350 psf was also to be evaluated during calibration of the overall slope stability model. This latter value corresponds to the average cohesive strength of the 27 to 30 ft level (i.e., 445 psf) and the 30 to 33 ft level (i.e., 260 psf).

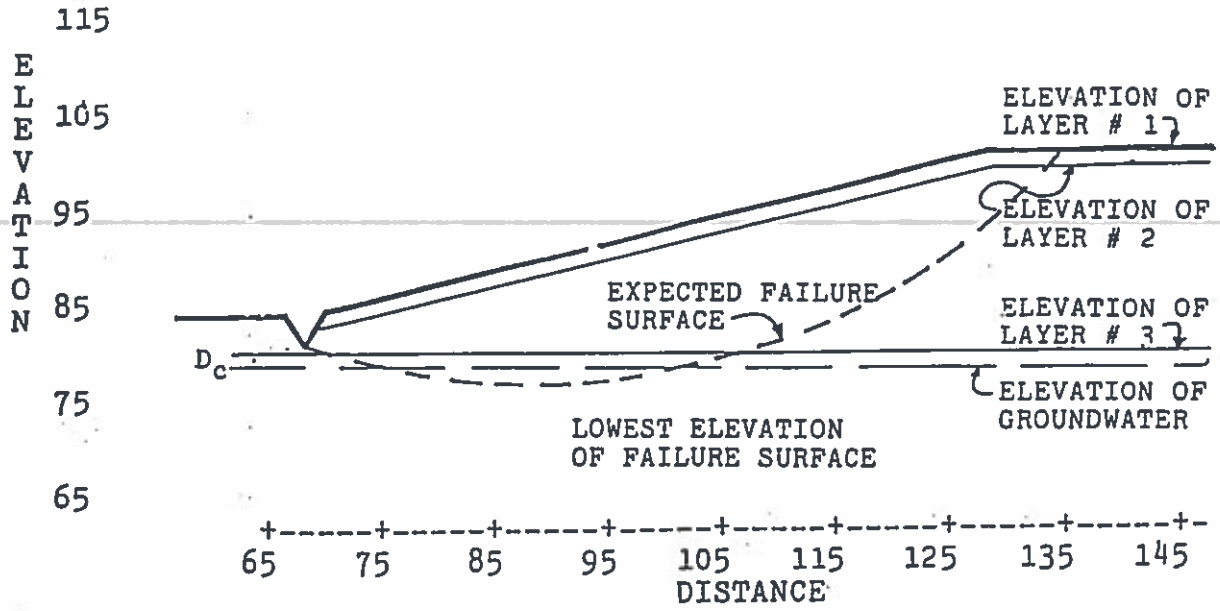

Figure 28. Slope stability model utilized in establishing final evaluation model.

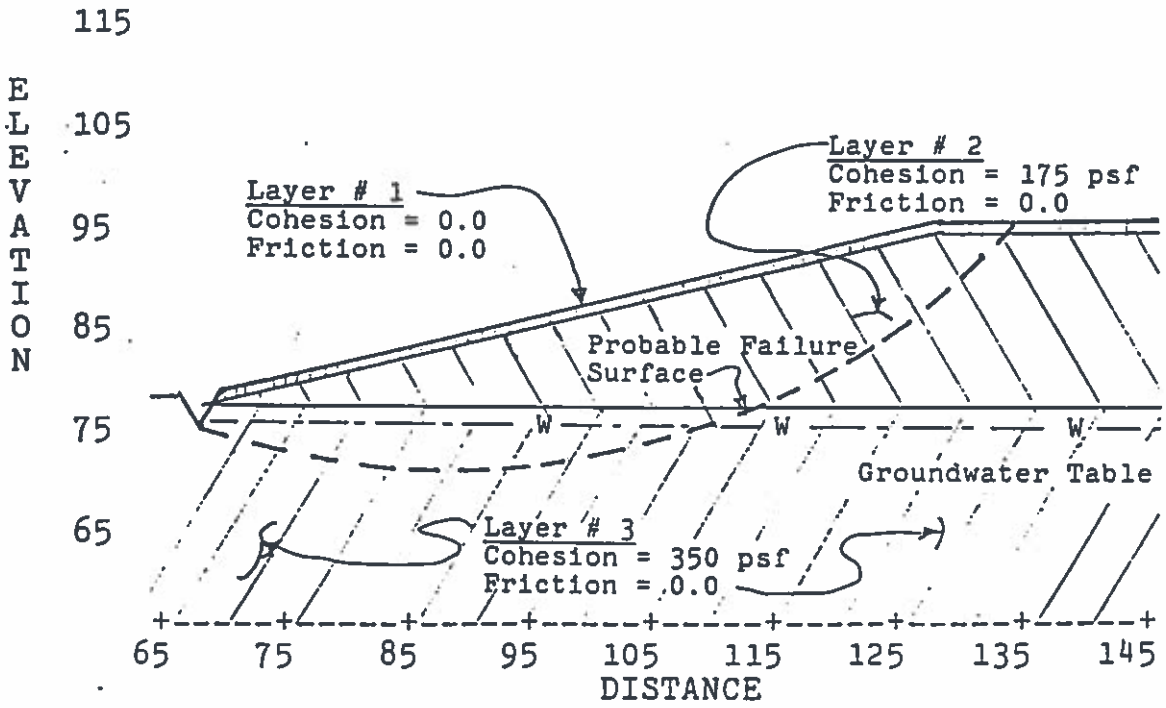

Figure 29. Selected slope stability model for calibration purposes.

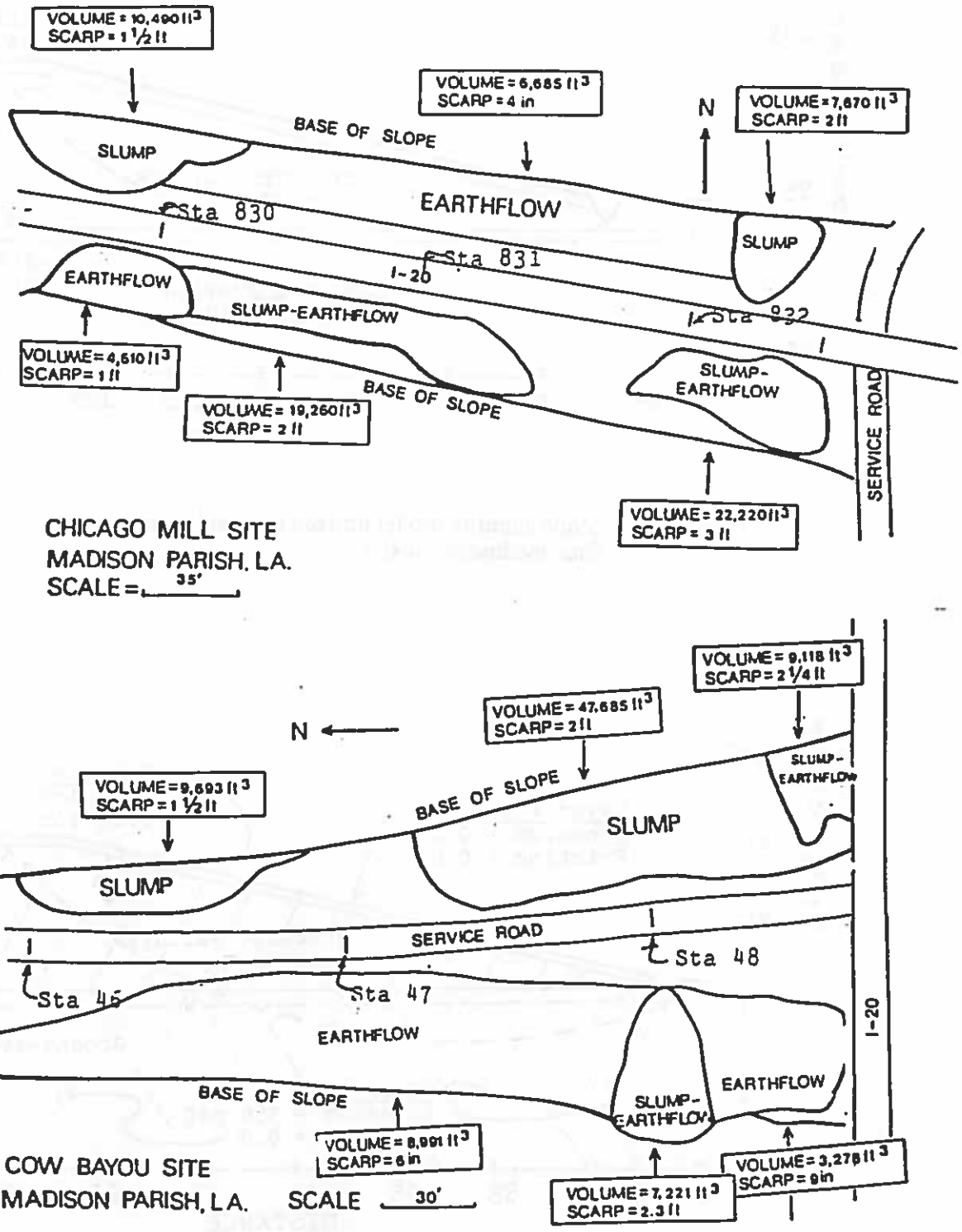

Figure 30. Embankment slope condition survey results for Chicago Mill (N17) and Cow Bayou (N13) sites.

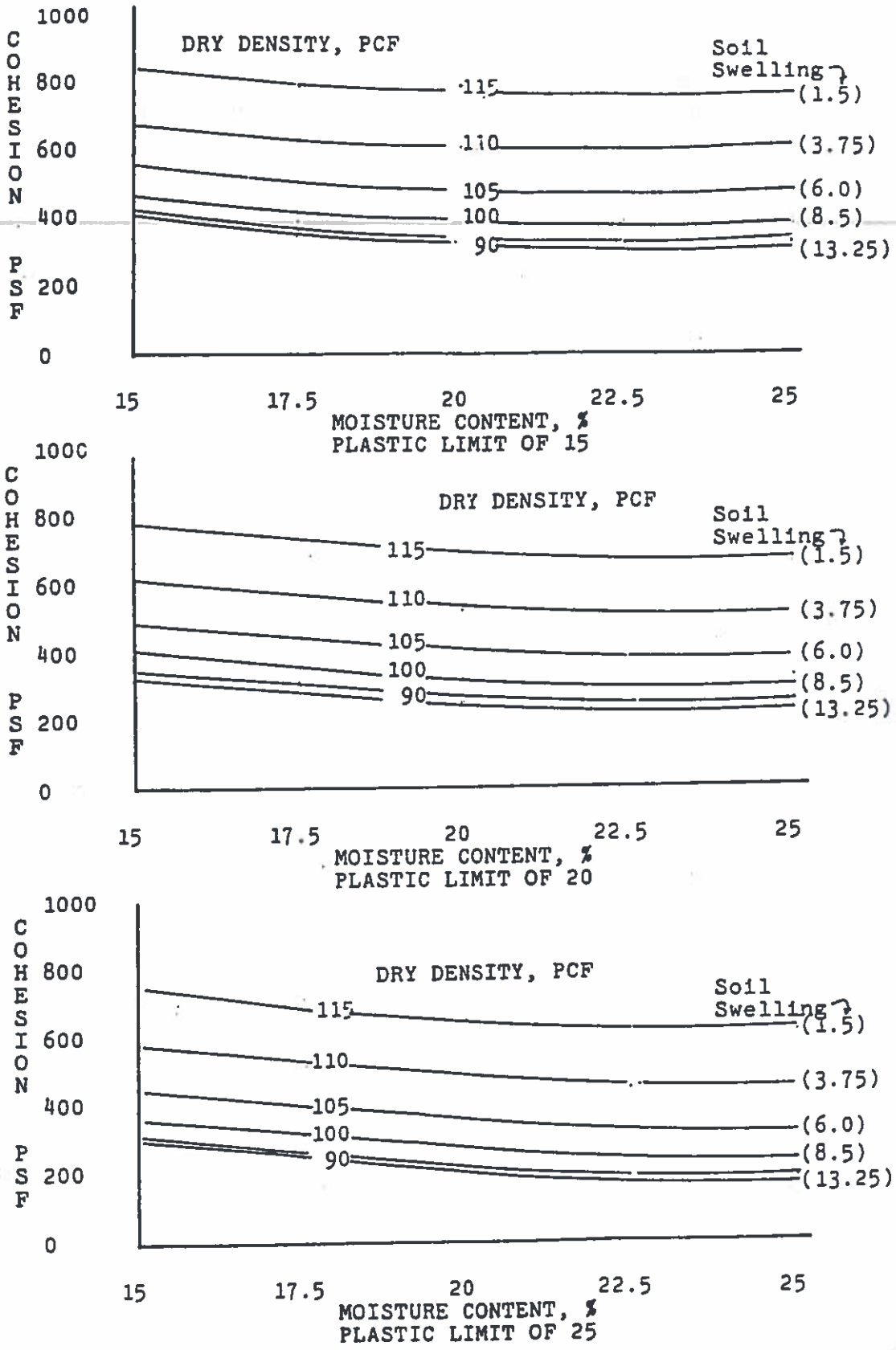

Figure 34. Soil cohesion estimates for low and medium plasticity clays (CL) for varying moisture, density and plastic limits. No slope design or redesign should be attempted using this method alone.

The thickness of Layer 2 would be established by the elevation of the top of Layer 3. During calibration of the slope stability model, three different positions of the top of layer three were investigated. The elevations under consideration were 75.0, 71.0 and 70.0 ft. All are relative to an elevation of 95.0 ft for top of embankment. The 75.0 elevation was selected because it represents an elevation about 1 1/2 ft below surrounding ground elevation. In this situation Layer 3 would represent the existing ground, while the second layer would be representative of embankment fill. The 71.0 and 70.0 ft elevations correspond to the depth of approximate soil change observed by LADOTD personnel at station 833 + 40 (Table 23). In all three situations it was assumed that the groundwater table was located 1 ft below the top elevation of Layer 3.

Calibration of Slope Stability Model

The factors used in the initial calibration of the slope stability model included the cohesion and friction angle of Layer 2 and the cohesion and elevation of Layer 3. The computer program PCSTABL4 developed at Purdue University, was utilized in this study to calculate the stability number associated with particular combination of model variables. The seven cases evaluated in the calibration of the slope stability model are presented in Table 26. From this table it can be seen that the model which yields a safety factor of 1.0 would fall between cases 5 and 6.

As a result of this evaluation, the calibrated model was established (Fig. 29) as a three-layer system, with the bottom two layers composed of strictly cohesive soils (i.e., friction effects are nil). The top layer has no friction or tensile strength, while layers 2 and 3 have cohesion values of 175 and 350 psf respectively. The depth of Layer 2 was set at 22.5 feet, while the groundwater level was fixed at 1 ft below the top elevation of Layer 3.

Reliability of the Calibrated Slope Stability Model

Since the model was calibrated for a single location along I-20 at the Chicago Mill, it was considered essential that the calibrated model be used to project stability numbers for other locations along Chicago Mill, as well as for some of the overpass locations in Madison Parish. Comparisons between calculated stability numbers and the stability status as designated in the condition survey would certainly shed light on the reliability and universality of the calibrated model.

With this in mind, the results of the condition surveys were perused to establish areas along Chicago Mill (N17) and at Cow Bayou (N13), Quebec (N16) and Tendal (N15) overpasses which were stable and unstable. Visual representations of the results of the embankment condition surveys are presented in Figure 30 for Chicago Mill section and Cow Bayou overpass site and in Figure 31 for Quebec and Tendal overpass sites.

TABLE 26

CALIBRATION MODELS FOR SLOPE STABILITY EVALUATION
STATION 830+00 AT CHICAGO MILL, MADISON PARISH, N17

CASE NUMB	SECOND SOIL LAYER COHES (psf)	ANGLE (degs)	ELEV (ft)	THIRD SOIL LAYER COHES (psf)	ANGLE (degs)	ELEV (ft)	GW ELEV (ft)	STABILITY NUMBER
1	175	2	94.0	575	0	75.0	74.0	1.50
2	175	0	94.0	575	0	75.0	74.0	1.33
3	175	0	94.0	175	0	75.0	74.0	0.81
4	175	0	94.0	350	0	75.0	74.0	1.33
5	175	0	94.0	350	0	71.0	70.0	1.02
6	175	0	94.0	350	0	70.0	69.0	0.98
7	175	0	94.0	225	0	70.0	69.0	0.80

GENERAL INFORMATION & ASSUMPTIONS

Embankment height - 18.3'
Layer # 1 Cohesion - 0
Layer # 1 Friction Angle - 0
Layer # 1 Thickness - 1'
Cohes is short for Cohesion
Angle is short for Friction Angle
GW is short for Groundwater

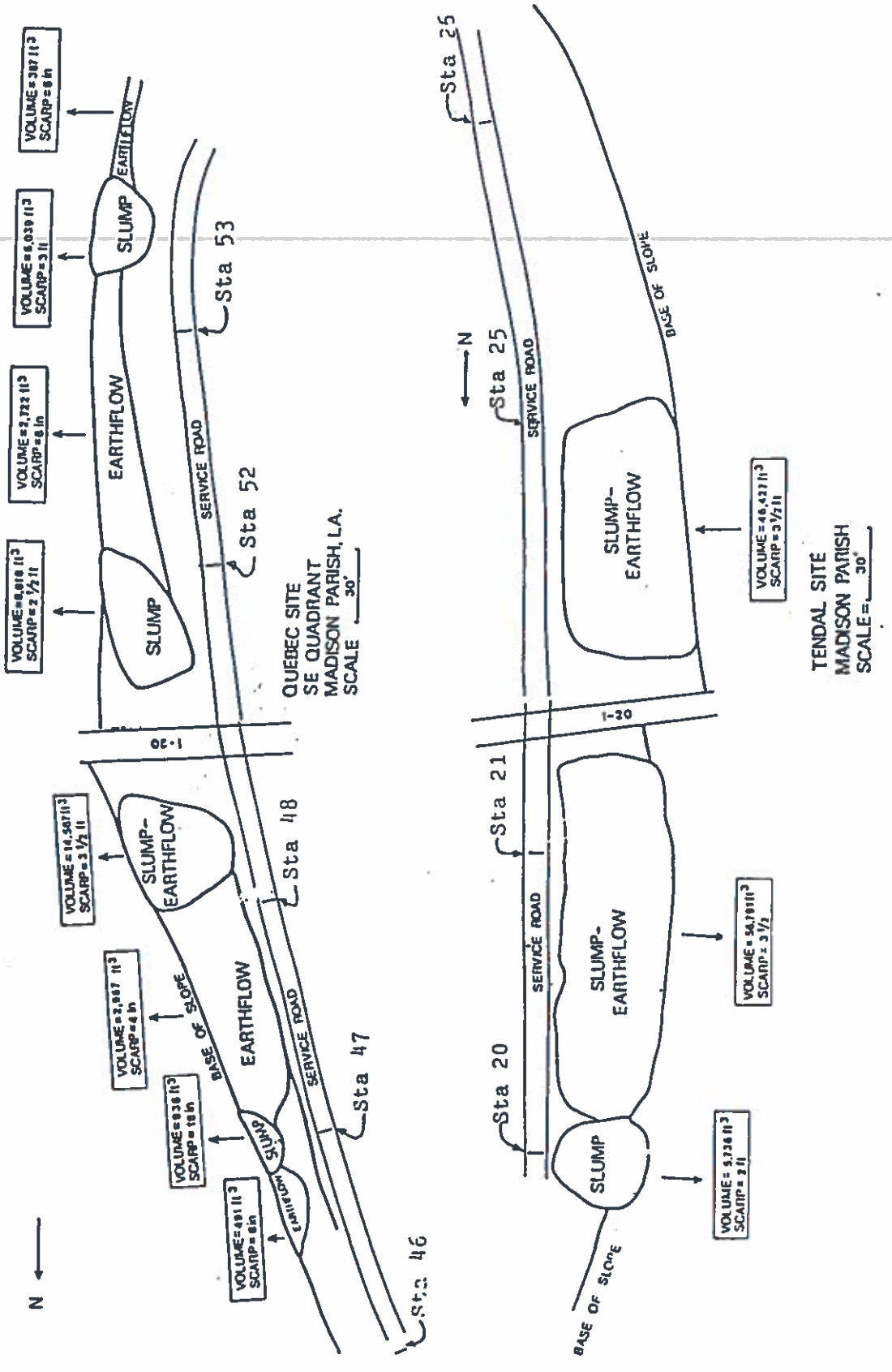

Figure 31. Embankment slope condition survey results for Quebec (N16) and Tendal (N15) sites.

A number of locations along Chicago Mill and at the three overpass locations were selected to aid in a reliability check of the slope stability model. The locations designated stations are presented in Table 27. The table also includes pertinent information related to the embankment cross section, including embankment height and slope angle, elevation of the embankment top and toe, and the stability or condition status. The condition status is presented in the last column of the table as N for a stable (or non-fail) slope or Y representing an unstable (or failed) slope.

Additional information related to the slope stability results obtained from the computer analysis is included under the headings of "FAIL ELEV". and "CIRCLE DEPTH". FAIL ELEV. refers to the elevation of the lowest point of the circular failure surface, while CIRCLE DEPTH represents the depth of the FAIL ELEV. below the surrounding surface. This latter quantity, i.e., CIRCLE DEPTH, is an important bit of information, since it can be used to provide guidance as to the depth of soil borings necessary to develop the geotechnical information needed to complete a slope stability analysis.

Five locations at Chicago Mill section (N17) were selected using condition survey results (Table 27). Four of the embankment locations exhibited stable slopes, while the remaining embankment site (sta 830) is located in a transition area. The stability numbers generated by the slope stability computer program essentially matched the condition or status of the corresponding embankment location. In the first two cases, stability numbers exceeding 1.0 were obtained and corresponded to the stable status defined in the condition survey. In the next two cases (i.e., stations 826 + 00 and 828 + 00), stability numbers of 0.99 were determined for those areas classified as stable in the condition survey. These stability numbers are so very close to a value of 1.01 that it is accepted that the slope stability model evaluated in the PCSTABL4 computer program reasonably modeled actual slope stability conditions. The final station location was 830 + 00 and was designated as the beginning of an unstable area. The stability number established with the computer for this location was 0.98, which indicates a probability of slope instability. Based on these comparisons, the slope stability model then adequately characterized the stability of the embankment slopes of Chicago Mill. It should be noted that all predicted failure surfaces were shallow-based (i.e., CIRCLE DEPTHs are less than 8.0).

Six station locations were investigated for the Cow Bayou overpass (N13). Two of the locations were selected from an area with stable embankments, while four were designated in unstable embankment areas. A comparison of the stability number and the status or condition indicates that the slope stability model adequately projected both the stable and unstable conditions. It should be noted that the embankment height of the Cow Bayou station 48 + 23 reached a value of 30.5 ft and a deep-seated slope failure was projected since the expected failure surface extended to a depth of 25 ft below the surrounding ground. Two of the expected failure surfaces were shallow-based, while the remaining four were deep-seated.

Thirteen station locations were established for the Quebec overpass (N16). Seven of the stations were located in areas of stable slope conditions, while the remaining six locations were selected from the portions of the overpass displaying unstable embankments. In the case of the

TABLE 27

SLOPE STABILITY EVALUATIONS FOR FOUR EMBANKMENT AREAS ALONG I-20 IN MADISON PARISH, LOUISIANA

STATION NUMBER	EMBANKMENT HGT	EMBANKMENT SLP	ELEVATION TOP	ELEVATION TOE	STAB NUMB	FAIL. ELEV	CIRCLE DEPTH	INSITU FAIL.
Chicago Mill, Locality N17								
822+72N	8.3	20	85.08	75.75	1.53	69.39	6.36	N
824+00S	13.0	25	87.49	74.50	1.21	69.94	4.56	N
826+00S	14.8	24	89.91	75.50	0.99	69.18	6.32	N
828+00N	15.6	23	93.50	77.50	0.99	70.28	7.22	N
830+00S	18.3	21	95.03	76.75	0.98	70.41	7.34	Y
Cow Bayou, Locality N13								
44+00W	9.7	28	83.57	73.84	1.84	71.06	2.78	N
44+73E	12.5	32	86.33	73.37	1.15	71.25	2.12	N
46+00E	19.8	28	92.59	72.29	0.99	56.08	16.21	Y
47+00E	25.1	28	98.90	71.51	0.75	52.47	19.04	Y
48+00E	29.6	28	99.59	69.98	0.71	46.91	23.07	Y
48+23E	30.5	27	100.05	70.00	0.71	44.47	25.53	Y
Quebec, Locality N16								
31+00W	2.7	17	83.25	80.47	4.92	80.11	0.36	N
31+00E	4.5	8	83.77	78.97	6.38	59.37	19.60	N
44+00W	8.4	23	87.14	78.84	2.88	66.43	12.41	N
45+40E	15.1	17	93.86	78.74	1.52	79.46	-0.72	N
46+00W	18.0	19	96.58	78.56	1.28	67.96	10.60	N
48+00W	21.9	30	102.74	80.84	0.86	79.74	1.10	Y
48+84E	23.5	29	103.52	80.07	0.84	79.75	0.32	Y
51+35E	28.7	27	103.47	74.72	0.73	75.10	-0.38	Y
51+80E	26.5	28	102.42	75.92	0.82	58.22	17.70	Y
52+25E	25.0	28	101.46	76.42	0.79	74.61	1.81	Y
53+00E	23.1	29	99.47	76.41	0.88	76.70	-0.29	Y
54+00E	19.0	28	95.21	76.71	1.07	75.18	1.53	N
55+00E	13.8	26	90.58	76.81	1.37	75.28	1.53	N
Tendal, Locality N15								
16+00W	8.4	25	87.05	78.67	1.90	77.13	1.54	N
17+00W	11.4	26	89.98	78.57	1.65	66.93	11.64	N
18+00W	14.7	28	93.57	78.06	1.21	64.50	13.56	N
18+60W	18.3	29	95.99	77.69	1.07	62.08	15.61	N
19+00W	21.1	29	98.86	77.69	0.98	62.42	15.27	N
20+50W	19.6	31	101.78	82.28	0.88	76.52	5.76	Y
21+00W	24.0	32	102.78	78.78	0.82	58.88	19.90	Y

LEGEND

HGT is short for Height and SLP is short for Slope
FAIL. ELEV is the lowest point of failure surface
CIRCLE DEPTH is the depth of FAIL. ELEV below surrounding area
INSITU FAIL. represents insitu status of slope; Y indicates a slope failure and N indicates a stable slope

seven stable locations, the slope stability model yielded stability numbers greater than 1.0, while stability numbers less than 1.0 were obtained for those stations exhibiting slope instability. From these results it is obvious that the slope stability model adequately characterizes the existing embankment stability. Four of the expected circular failure surfaces are deep seated, since large CIRCLE DEPTHs were calculated.

For the Tendal overpass (N15), seven station locations were selected for a reliability check on the slope stability model. Five of the stations were situated in stable embankment areas, while two were located in areas with unstable embankment slopes. For four of the locations with stable slopes, stability values greater than 1.0 were calculated. In a single case (i.e., station 19 + 00W), a stability value of 0.98 was calculated for an area which was classified as stable in the condition survey. Even though a stability number greater than 1.0 was not obtained in this case, it is still considered to be a reasonable characterization of the slope stability because of the very close proximity to a value of 1.01. In the remaining two cases, calculated stability values were less than 1.0 and corresponded with the unstable condition observed in the slope condition survey. Most of the stations evaluated for Tendal overpass resulted in deep seated circular failure surfaces (i.e., CIRCLE DEPTHs of -11.64 to -19.90 for five of the cases).

When comparing the calculated stability numbers with the stability/instability status established in the condition survey, it was found that slope stability model accurately predicted the slope stability or instability in 28 of the 31 cases undertaken. In the other three cases stability numbers very slightly below 1.00 were calculated for existing stable embankment conditions. When rounded to the nearest tenth, all three values would have been rounded to 1.0. In the eleven cases dealing with areas sustaining embankment slope failures, the slope stability model produced stability numbers less than 1.0 in every situation. Furthermore, the slope stability predicted both shallow-based and deep-seated failures.

It is therefore believed that the slope stability model presented in Figure 29 adequately characterizes the embankment cross section, and more importantly, that the model adequately and accurately predicts embankment slope stability.

DESIGN, REPAIR AND REHABILITATION OF EMBANKMENT SLOPES

Introduction

The slope stability problem encountered in northeast and southern Louisiana necessitates the development of new design techniques for use in future embankment construction projects, as well as in the development of repair and rehabilitation options for reconstruction of unstable embankment areas. The slope stability model developed and calibrated for the Madison Parish, Louisiana area offers a useful tool in the development of design techniques and repair/rehabilitation schemes.

Important Considerations

Placement of the failure surface was influenced by local conditions and the use of PCSTABL4. For the cases chosen, results were so similar that it was used as an example to establish the design guide. As a result, the failure surface that was chosen was deep-seated in most cases. Current actual slope failures do not all support this placement.

These designs are applicable for the specified cases within the limits of PCSTABL4. Applicability to other sites requires further investigation by a geotechnical engineer. No slope design or redesign should be attempted using this method alone.

Soil Characteristics

One of the more important soil characteristics required in slope stability evaluations is the future cohesive soil strength that will evolve over the expected design life. The design and stabilization nomographs presented in this section were developed for the soil conditions shown in Figure 32 (i.e., cohesion values of 0, 175, and 350 for Layers 1, 2 and 3 respectively). Some adjustments can be made in the procedures for higher soil strengths.

In order to provide estimates of soil cohesion for varying conditions, the results of laboratory evaluations of surficial soils from the Chicago Mill area of Madison Parish (Table 22) and from various overpass locations along I-10 (Table 25) were analyzed using regression analysis techniques to develop the relationships presented in Figures 33 and 34.

The relationship between soil cohesive strength and the soil properties of dry density and liquid limit for the high plasticity soils (i.e., soils classified as CH) is presented in Figure 33. From this figure it can be seen that a lower cohesive strength can be related with lower liquid limits and dry density. The dry density in this situation is essentially a measure of the amount of soil swelling over time, since the surficial soils in the Chicago Mill area are uniform in composition and would have essentially the same unit weight for the soil particles. For the same total volume and unit weight of soil particles, changes in the dry density would be indicative of the buildup of soil moisture and concomitant soil swelling. With this in mind, approximate values of soil swelling based on the changes in wet unit weight were obtained and added to the nomograph (i.e., the numbers within the parentheses).

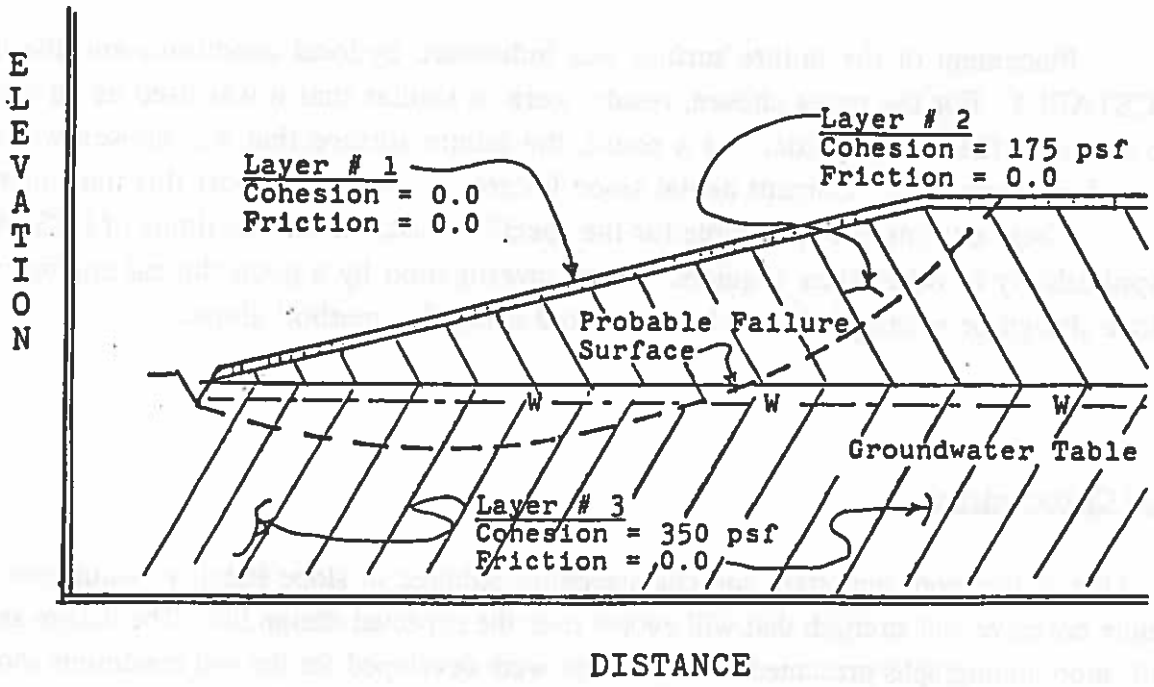

Figure 32. General soil-embankment conditions for slope stability model cross section.

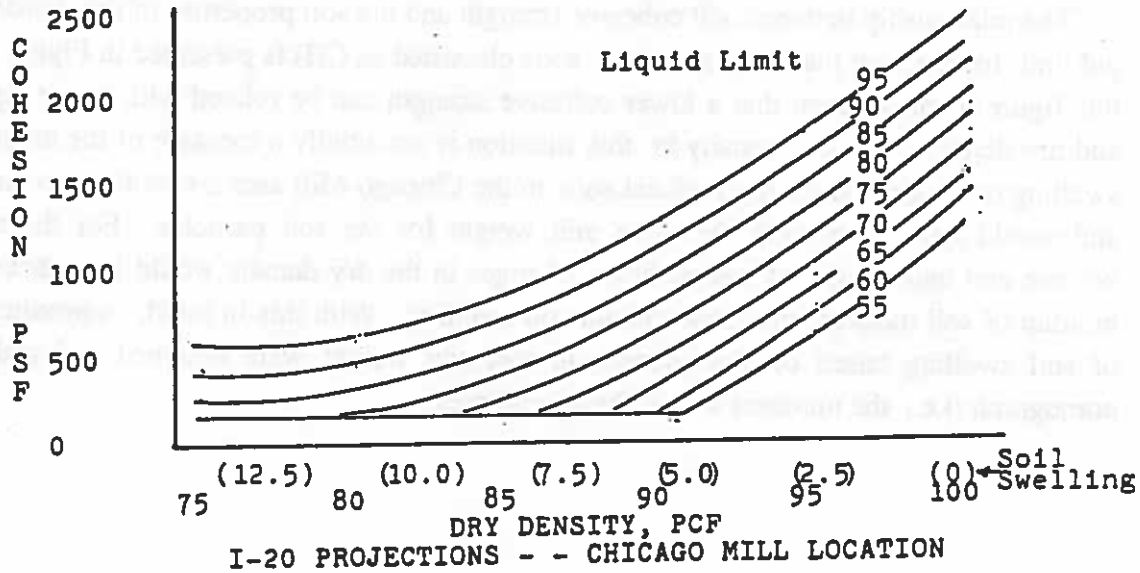

Figure 33. Soil cohesion estimates for high plasticity clays (CH) for varying density and liquid limits. No slope design or redesign should be attempted using this method alone.

Relationships between soil cohesive strength and the soil properties of dry density, moisture content, and plastic limit for low-to-medium-plasticity clays (i.e., CL classification) are presented in Figure 34. From this figure it can be seen that lower cohesive strengths could be expected for low dry density, high plastic limits and high moisture contents. As the case for the CH clays, the variation in dry density values probably represents a measure of the amount of soil swelling. Estimates of soil swelling were calculated and are also included in parentheses in Figure 34.

The nomographs presented in Figures 33 and 34 can be used to estimate a soil cohesive strength for situations in which soil swelling will be actively controlled through construction techniques aimed at reducing upward flow of water in clay embankment materials produced by capillary action, soil suction or surcharge loading. Intermediate granular layers, wick installations and french drain installations could fall within this category. It should be noted, however, that estimates of soil cohesion would not be necessary if such corrective actions are not anticipated.

Design and Reconstruction of Embankment Slopes

There are four different embankment conditions considered in the development of design procedures for construction of new embankments and reconstruction procedures for rehabilitation of existing embankment slopes. The embankment conditions are included below:

1) constant embankment slope configuration,
2) broken-back embankment configuration,
3) broken-back embankment with stabilized soil layer,
4) constant embankment slope with stable subgrade.

The design nomograph for a constant embankment slope is presented in Figure 35. This configuration would be utilized in those situations where acquisition of right of way is not a problem. The input for this nomograph would include the height of embankment, H, and desired stability number. The intersection of a horizontal line through the stability number with a vertical line through the height, H, would yield the minimum acceptable embankment slope, S.

The broken-back configuration (Fig. 36) was developed for the case of limited right-of-way or reconstruction of an existing embankment. The broken-back term describes an embankment configuration consisting of two different slopes. The upper slope is the steeper of the two. This configuration was selected because it represented an opportunity to reduce the mass of earth captured within the failure surface and should result in a lesser driving force and a corresponding higher stability number. The nomograph is used in a fashion similar to that described above for the case of constant slope. A vertical line would be constructed from the height of embankment, H, while a horizontal line would be constructed from the desired stability number. The intersection of these two lines would yield the combination of slopes, S1 and S2, which meet the stability requirement.

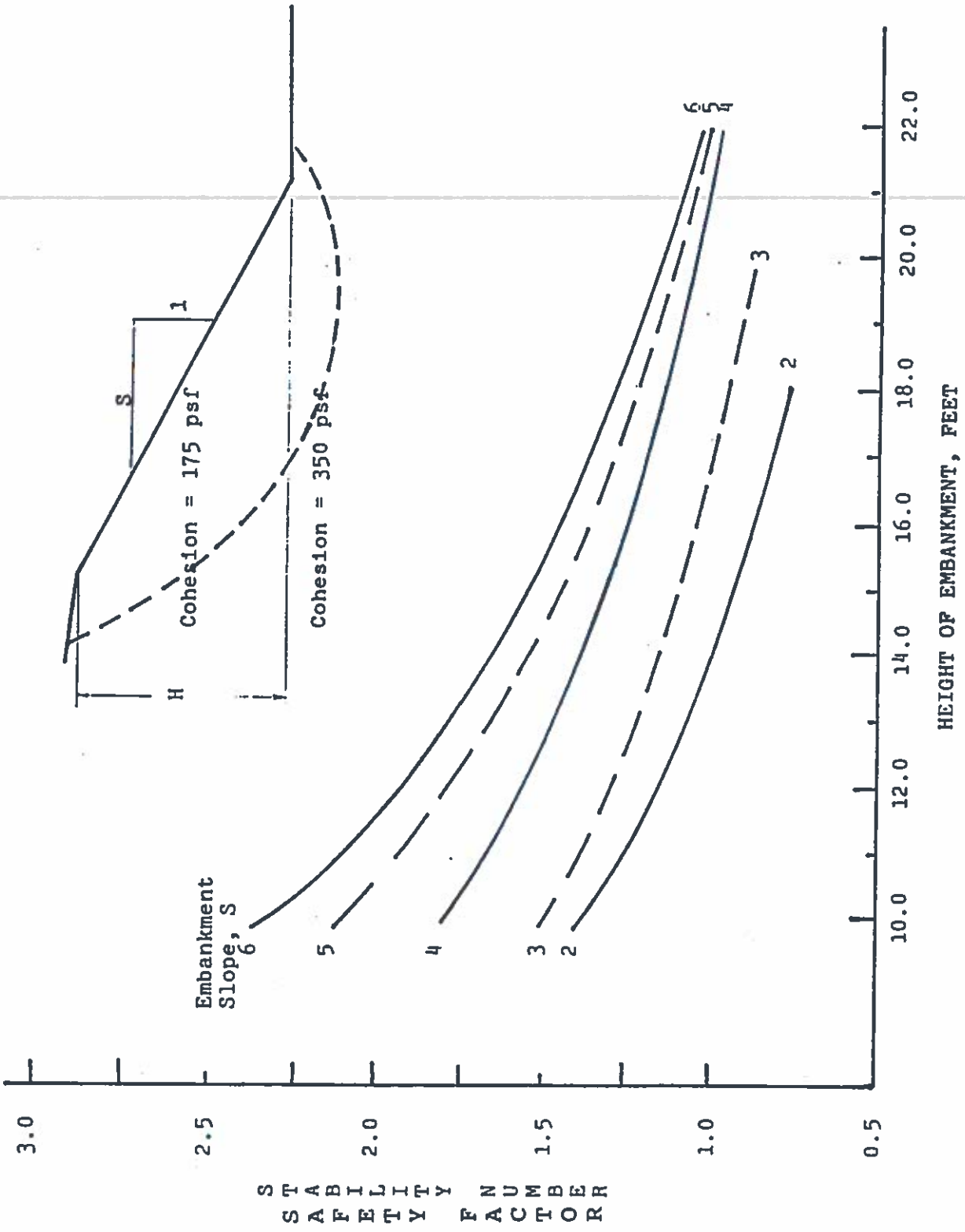

Figure 35. Stability numbers (safety factors) for constant slope of embankments and embankment height. No slope design or redesign should be attempted using this method alone.

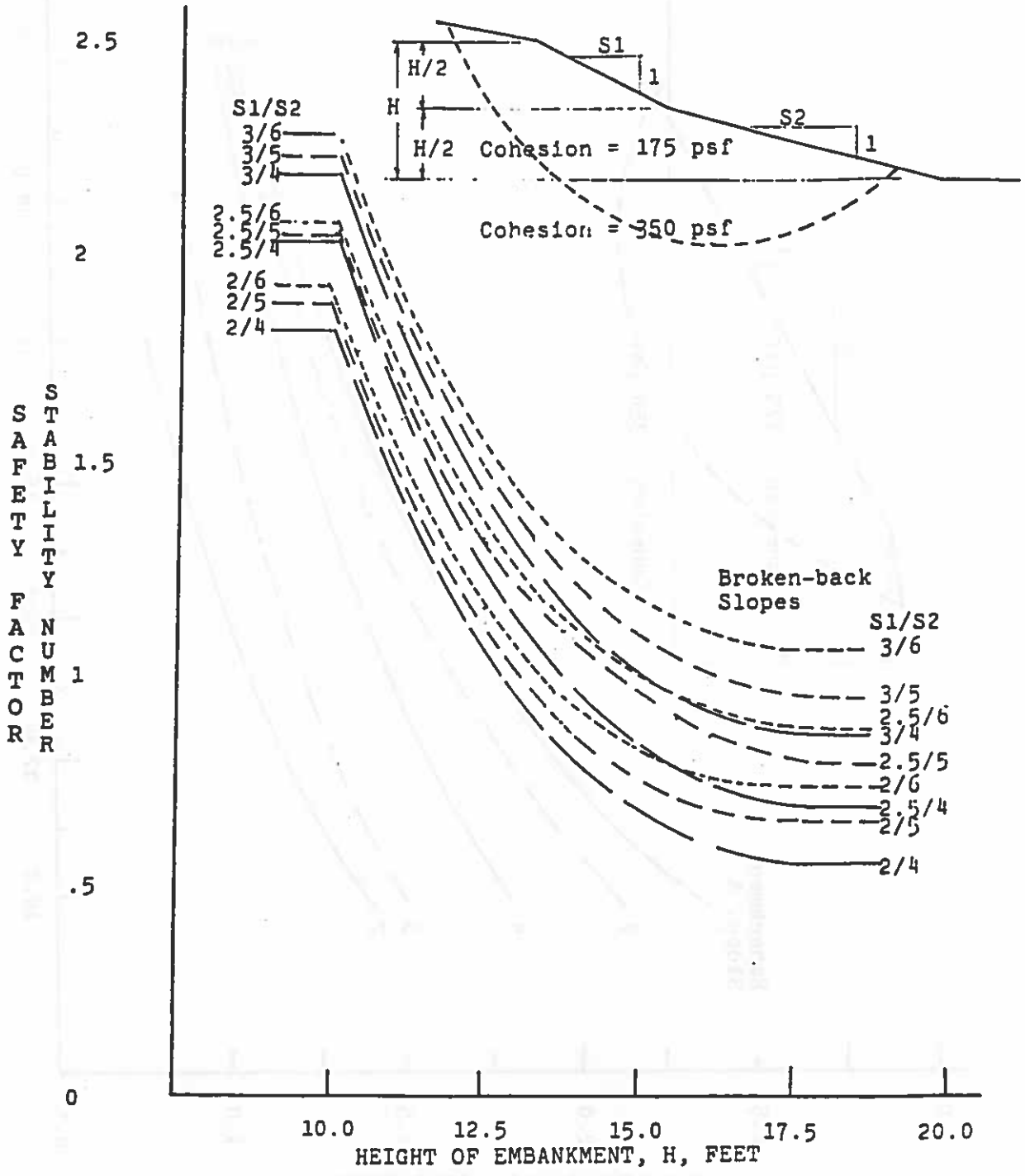

Figure 36. Stability numbers (safety factors) for broken back embankment configuration with varying heights and slopes. No slope design or redesign should be attempted using this method alone.

In both of the preceding configurations the failure surface dipped quite a bit down into the subgrade or third soil layer. This third configuration was established to create a situation in which a stabilized soil layer would limit the intrusion of the predicted failure surface into the subgrade or bottom soil layer. The nomograph developed for this configuration is presented in Figure 37. The nomograph is used in the same fashion as the preceding one. The stabilized soil layer would have to have a minimum thickness of 18 inches and more than likely, a lime-stabilized material. The stabilized layer would offer an additional advantage in that it would substantially reduce the movement of soil moisture from the subgrade or bottom layer to the upper embankment layer. Economics would, of course, play a major role in evaluating this option.

The fourth case involves the placement of a clay material as embankment over a stable subgrade with a cohesive strength of 700 psf or more. This would represent a case in which the in situ soil material is stable and unaffected by available groundwater (i.e., not a very active clay). Minimum embankment slopes for this situation can be obtained by the appropriate entry of the nomograph (Fig. 38) with embankment height and desired stability number.

For those cases where soil moisture movements can be controlled and soil cohesive strength is estimated from either Figure 33 or 34, these four nomographs presented in Figures 35 thru 38 can also be used in establishing minimum embankment slopes. The correction for the effect of increased cohesion would be handled by adjustments to the desired stability number, since an increase in soil cohesive strength would yield higher stability numbers. Consequently, the nomographs could be used in the present form by multiplying the desired stability number by the ratio of 175 to the estimated cohesive strength. For instance, a soil cohesive strength is estimated to be 280 psf and a desired stability number of 1.3 is established. An adjusted stability number of 0.81 (e.g. adjusted stability number equals 175 x 1.30 / 280 or 0.81) would then be used with an appropriate design nomograph to establish a minimum slope or slopes.

Selection of Design or Reconstruction Technique

The options considered in the selection and evaluation process will depend upon space and economy, as well as existing or projected soil strength. The amount of available or acquirable right-of-way would certainly delineate those design options which would be viable alternatives. Economy of construction would also be a consideration in the selection process along with embankment height and soil strength. As a result no rule of thumb can be offered concerning an appropriate design option. The circumstances surrounding a particular job site would therefore determine to a great extent the design option or options that would meet the project requirements.

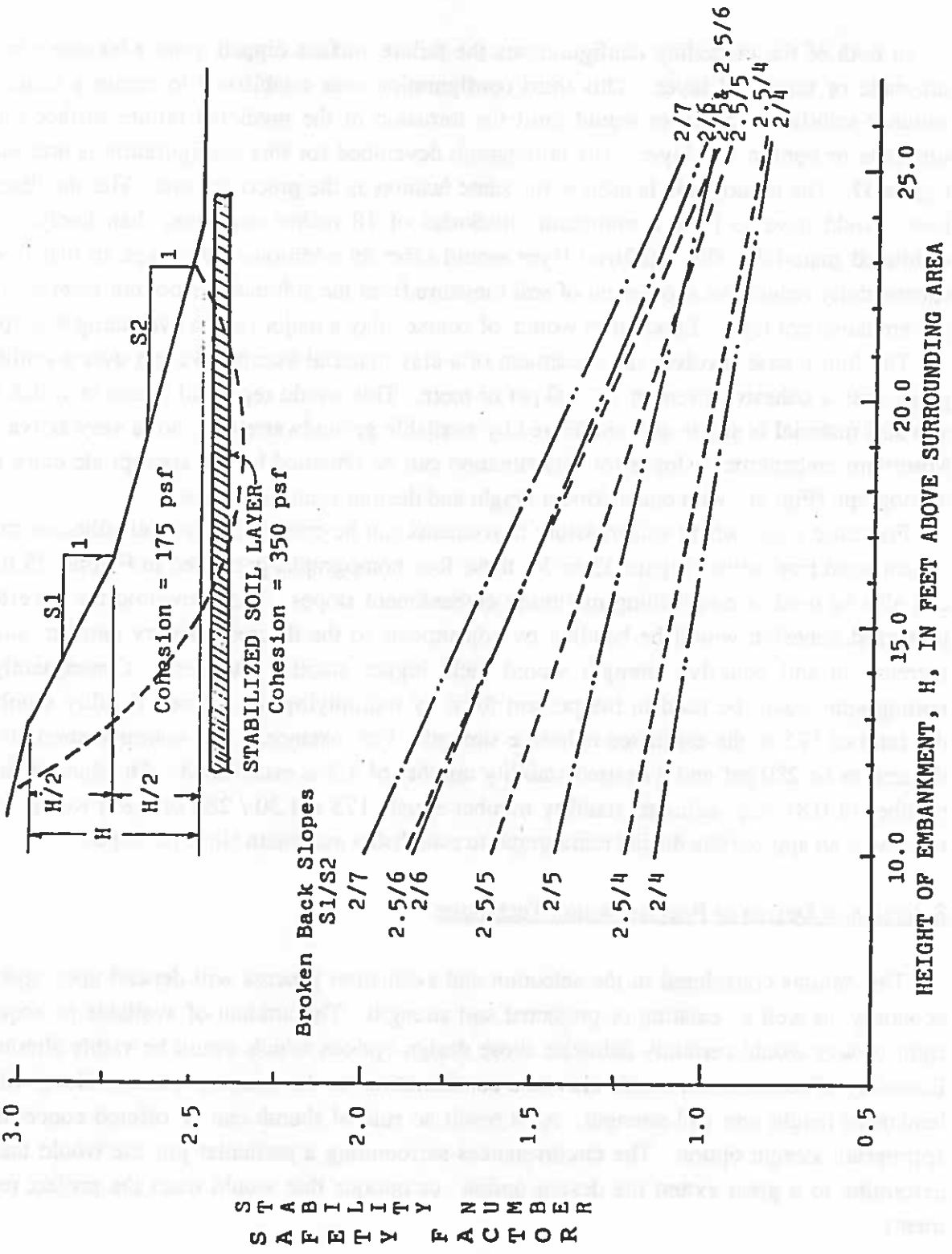

Figure 37. Stability numbers (safety factors) for broken back embankment configuration and stabilized soil layer at toe of slope; consideration of height, H, and slopes, S1 and S2. No slope design or redesign should be attempted using this method alone.

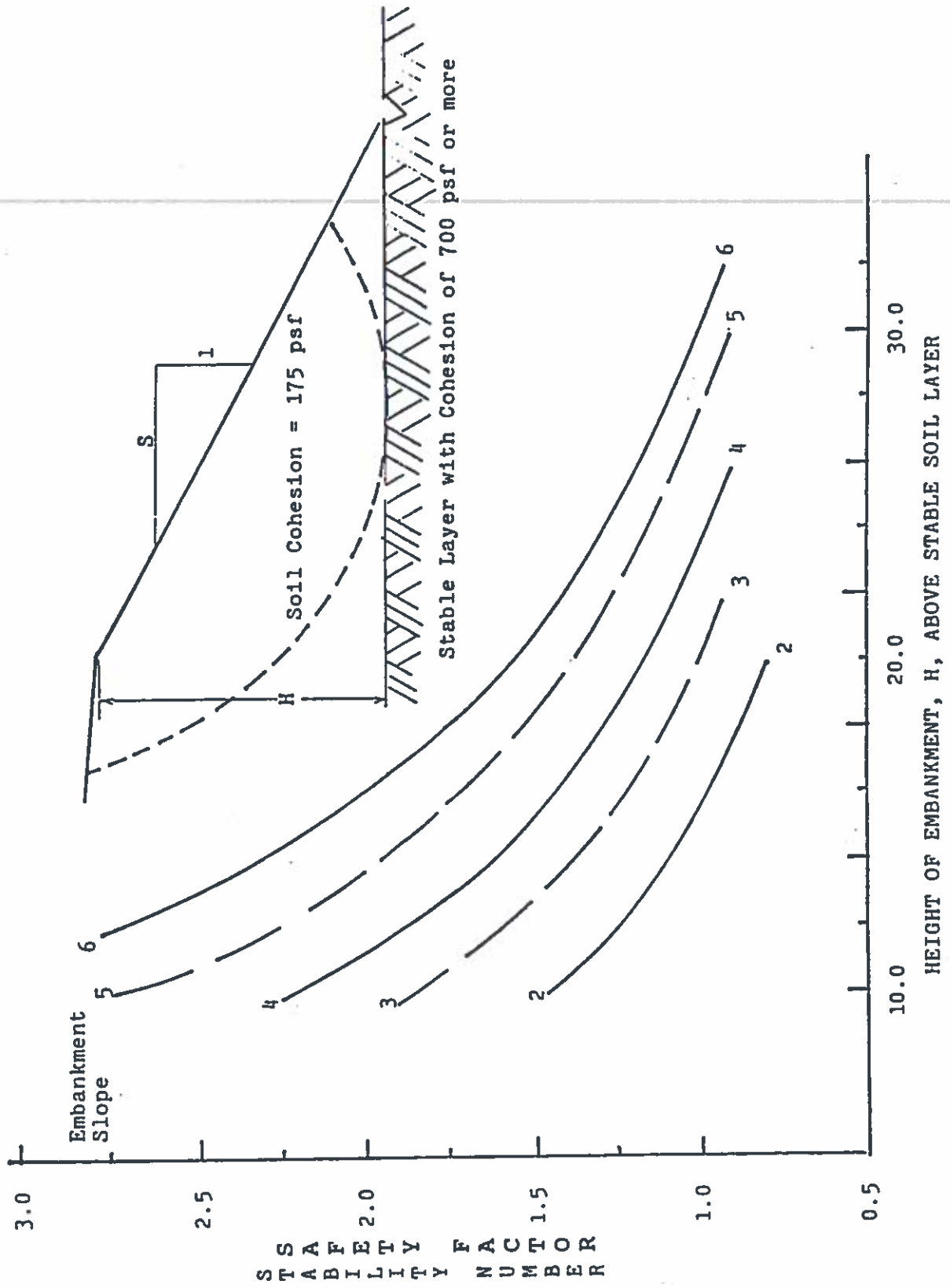

Figure 38. Stability numbers (safety factors) for embankment founded on stable subgrade. No slope design or redesign should be attempted using this method alone.

LOUISIANA MAP OF SOILS CONTAINING SHRINK-SWELL CLAYS

It became obvious during the course of the project that soils containing shrink-swell clays were one of the major factors in slope instability of embankments. We decided to produce a map of the distribution of these clays in the state of Louisiana for future use of planners. The map (Plate 1) alerts the planner to the possibility of finding expansive soils in the part of the state he is working in.

The map is a compilation of information from the different parish soil surveys produced by the Soil Conservation Service. When a soil survey was not available for a particular parish, we used information from the "General Soil Map" for that parish that was also produced by the Soil Conservation Service. If a soil series had one of three characteristics, it was considered a "soil with shrink-swell potential" and was mapped on the map.

The first characteristic we considered was that the soil had a montmorillonitic family in classification. If this character- istic was found, it had the highest potential for having large slope failure problems. Series that met this characteristic were: Acadia, Allemands, Alligator, Anacoco, Baldwin, Barbary, Beaumont, Bellpass, Bellwood, Clovelly, Eutaw, Fausse, Forbing, Forestdale, Gentilly, Harahan, Harris, Hollywood, Houston, Iberia, Ijam, Judice, Kaufman, Kisatchie, Larose, Lebeau, Mayhew, Midland, Natchitoches, Newellton, Oktibbeha, Oula, Perry, Placebo, Rita, Roebuck, Scatlake, Sharkey, Sostien, Susquehanna, Tensas, Tunica, Vaiden, Watsonia, Westwego, and Woodtell.

The second and third qualifying characteristics we searched for in a shrink-swell soil series were the presence of a "vertic subgroup" in Soil Taxonomy classification (10) or a high shrink-swell engineering class in any horizon. Series that met these characteristics but were not in a montmorillonitic family were: Bayoudan, Buxin, Ged, Latanier, Litro, Moreland, Morse, Pledger, Portland, Solier, Sumter, Una, and Wrightsville.

For a more accurate characterization of the soils before field work is begun, it is recommended that planners consult the parish soil surveys in search of the above soil series. The scale of these parish maps is much more precise in delineating shrink-swell clay problems than our general state map.

SUMMARY AND CONCLUSIONS

Over the 122-mile (195 km) transect in the two study areas along I-10 and I-20 highways, 242 embankments were examined and characterized. There were 99 slope failures that occurred in the study areas. The 32 slumps had an average volume of 25,629 cu ft (727 cu m). The 44 slump-earthflows had an average volume of 13,911 cu ft (395 cu m). The 23 earthflows had an average volume of 2747 cu ft (88 cu m). The mean volume for all of the failures was 15,105 cu ft (431 cu m).

All embankment failures have the following characteristics in common:

1) Embankment slope failures have occurred 8-15 years after construction of the embankment. This indicates that failure is a result of long-term processes of the soil losing strength as water infiltrates the slope. Gradual swelling of the smectite-rich soil proceeds and pore water pressure builds up (21, 43).

2) Most of the failures occurred after major storms had dropped abundant precipitation onto the slopes. Hurricanes have been the common sources of this moisture in the I-10 study area in the south and the storm of Christmas, 1982, was the main cause in the I-20 study area in the north.

3) As the slope angle decreases, the time required to reach a condition of failure increased. It was determined that slopes less than 16 degrees (< 3.5:1) had a very low incidence of failure, even when constructed of high risk parent material.

4) Slopes constructed of the Sharkey, Portland, and Commerce soil series (Soil Conservation Service) in the I-20 study area and the Crowley, Patoutville, Morey, and Mowata soil series in the I-10 study areas had a high degree of failure.

5) Slopes constructed of soil with a clay content > 47%, a plasticity index > 29%, a liquid limit > 54%. and a net smectite value > 33% had an 85-90% chance of failure during the first 15 years after construction.

6) Slopes constructed of soil with a clay content 32-47%, a plasticity index of 16-29%, a liquid limit of 36-54%, and a net smectite of 18-33% had a 55-60% chance of failure during the first 15 years after construction.

7) Slopes constructed of soil with a clay content < 32%, a plasticity index < 16%, a liquid limit < 36%, and a net smectite value < 18% rarely failed in the first 15 years after construction.

8) Using the last three characteristics of soils(#5, #6, & #7), one can construct a risk hazard model that can predict the chances of slope failure of an embankment constructed of a soil sample. The model can be based on Atterberg limits and clay content which can be easily obtained from the geotechnical laboratory. The risk hazard model will definitely work anywhere in Louisiana, but also should work for the whole Gulf Coast region and probably most places in the world.

9) The amount of smectite in the soil seemed to be the most important characteristic that determined slope stability of the embankments. A high clay content in the slope is not necessarily bad, but if the clay is mainly smectite, it is a major problem. A map of the extent of soils in Louisiana that contain these shrink-swell clays is found on Plate 1.

In the I-20 study area, all of the failures had occurred in the Mississippi River flood plain when the study had begun. Some additional failures happened during the study, but still 96% of the failures were in this one parent material zone. The soils there are highly susceptible to slope instability, for they contain on the average 60% clay, 43% net smectite, 35% plasticity index, 65% liquid limit and 35% moisture content. Based on the risk models, slope failures are predicted for the Millhaven interchange (N3) and the Girard overpass (N5) of the Ouachita River flood plain and the Waverly interchange (N14) of the Mississippi River flood plain. Slopes should remain stable on the Macon Ridge parent materials.

In the I-10 study area, the greatest percentage of failures have occurred on the modern alluvium parent material (66% failure rate) compared to the Prairie Terrace alluvium (26% failure rate) and the loess parent material (14% failure rate). The two alluvium parent materials are very similar, with about 50% clay content, 30% net smectite, 29% plasticity index, and 29% moisture content. The main difference is that the modern alluvium slopes tend to be more steep, with an average of 21 degrees versus 18 degrees for the Prairie Terrace alluvium. Therefore, both are considered to be candidates for slope failures, but the slope angle controls the incidence of failure considerably. The alluvium parent material along the I-10 study area had geotechnical characteristics between the Mississippi River flood plain soils and the Ouachita River flood plain soils in risk potential. Based on the risk models, slope failures are predicted for sites S3 in Calcasieu Parish, S6 and S8 in Jefferson Davis Parish and S17 in Acadia Parish, where most of the failures have occurred so far.

Control of slope stability depends upon control of shrink-swell clays in the slope soils. When these slopes were originally built, the designers were not aware of the expansive soil problems, so the embankments were not limed, only compacted during construction. For the past ten years, repair of the slopes has consisted of either cosmetically reshaping the slopes by pushing the soil failures back up the slope or driving pilings into the slope. Both of these measures have been unsuccessful and actually increase the rate of failure.

Remedial measures of slope repair which should be considered for the study areas follow this clay stabilization. They are: deactivating the shrink-swell clays (smectites) in the soils with lime; controlling surface run-off with concrete troughs and curbs; laterally extending the existing aprons particularly on the header portion of the slopes (Figure 34), and lowering the slope angle to below 16 degrees. In the case of new construction, all of the above remedial ideas should be incorporated.

Close similarities are noted when comparing failure trends in the study areas to the physical properties of slope failures from a variety of locations worldwide. Detailed scientific investigations from these other locations illustrate a general trend of embankment failure in the presence of high clay content (21, 25, 35), high smectite content (31, 34, 41, 44), plasticity indices in excess of 25% (26, 28, 35), and liquid limits in excess of 29% (29, 33, 36, 43).

The slope stability model developed in this project (Fig. 29) adequately characterizes the embankment cross sections and more importantly, accurately predicts embankment slope stability. The model when applied to slopes in the I-20 study area predicted slope failures in all of the eleven slopes used as examples. When applied to 20 stable slopes in the same area, it predicted stability in 17 of the examples. The three examples where failure was predicted had safety factors just below 1.0, so were very close.

The slope stability model cross section (Fig. 29) is composed of three distinct soil layers. The top layer consists of vegetation covering the embankment top and sides, is approximately one foot thick, and provides no structural support. The soil Layer 2 consists of the embankment fill material and is considered cohesive clay with a cohesive strength of 175 psf. The Layer 3 is the natural soil surface upon which the embankment has been constructed and is strictly cohesive clay with a cohesion of 350 psf.

Two important conclusions were made from computer characterizations of the I-20 slopes. About 2/3 of the cases investigated resulted in failure surfaces extending well below the surrounding ground surface, i.e., deep seated failures. Also, the predicted failure surface originated well back of the top of the embankment slope (i.e., approximately 6 - 8 ft from the top of the slope in the directions of the pavement edge) and approaching the edge of the pavement shoulder. This information leads one to conclude that repair and rehabilitation schemes which only designate improvements above the existing ground elevations and from the top of the slope to the toe of the embankment slope may not alleviate the slope stability problem since deep-seated failures could possibly develop behind and underneath the improved embankment.

Four different design nomographs are presented (Figs. 35-38) for different design and reconstruction of embankments with the conditions just mentioned in the previous paragraph. A constant embankment slope configuration can be used where right-of-way is not a problem and low slope angles can be used (Fig. 35). A broken-back design can be used where there is limited right-of-way or reconstruction of an existing slope is needed (Fig. 36). A third example is the broken-back design with a stabilized soil layer at the base (Fig. 37). This would be used to limit the intrusion of the predicted failure surface into the subgrade or bottom layer and would also reduce the upward movement of water into the embankment. A lime-stabilized soil zone of about 18 in. thick would supply the base of the slope. This method is more costly. The last example is the constant embankment slope with a stable subgrade (Fig. 38). The stable subgrade would have a cohesive strength of at least 700 psf and would prevent upward movement of groundwater.

For stabilization of existing embankments, one of the above four designs for reconstruction could be used. Overall, the options considered in the selection and evaluation process of embankment reconstruction, design, or stabilization will depend upon space and economy, as well as upon existing or projected soil strength.

RECOMMENDATIONS

1) It has been concluded that clay-rich embankments are unstable and prone to failure (see Previous Works section). The question always asked is, "How much clay is considered enough to make the slope unstable?" The rule of thumb found in the literature of > 50% liquid limit and > 25% plasticity index Atterberg limits is commonly used as the lower limits for indicating potential problems with expansive soils (70). This study establishes more concrete guidelines using both Atterberg limits and clay content (Table 28).

It is recommended that the Atterberg limits and clay content be calculated for any soil to be used to make an embankment. Each of the results should be compared to the risk model and categorized as to high, intermediate or low risk (Table 28). The overall sample risk category is the one that has the most examples in it. (A sample that has the liquid limit and clay content in the high risk category and the plasticity index in the intermediate category is considered high risk.) In most cases, the Atterberg limits should provide sufficient information for classification and the clay content does not have to be run.

Once the overall risk category classification has been determined, the slope designer or repairer has to make a choice. If the overall classification is low risk, the slope can be designed with standard methods in use today. If the sample falls into the high- or intermediate-risk level, the soils must be stabilized using lime or an alternative method, the slope design must change to accommodate these failure-prone soils, or a combination of the above two processes must be used.

2) In the field, the following characteristics in the soils generally indicate that they are expansive soils and that they might be high- or intermediate-risk soils for slope construction:

a) The soil is very sticky to the touch when wet.

b) Polygonal cracks form on the surface when the soil dries.

c) The soil is gray in color with red mottles.

3) The map of the distribution of shrink-swell clay soils in the state should be used before work is started in a new region to determine if expansive soils are found there (Plate 1). For more exact information, the soil survey of that particular parish should be consulted.

4) For repair of slopes that have had failures on them, there are different choices to be made. One can either mechanically or chemically alter the soil characteristics and/or control the moisture conditions. All of the following should be considered:

a) Stabilize with lime to inactivate the expansive soils.

b) Lower the slope angles if it is possible to below 16 degrees (>3.5:1).

c) Do not use pilings in the slope.

d) Extend the header apron around the sides of the embankment (Fig. 39).

e) Provide ample drainage to keep water off of the slope.

f) Revegetate the slope immediately after repair. If pampas grass (Cortaderia selloana) is available for revegetation, try this.

g) Import low-risk category soil to repair the slope.

TABLE 28

SLOPE STABILITY RISK CATEGORIES FOR EMBANKMENT SOILS

GEOTECHNICAL TEST	HIGH* RISK	INTERMEDIATE* RISK	LOW* RISK
LIQUID LIMIT	> 54%	36 - 54%	< 36%
PLASTICITY INDEX	> 29%	16 - 29%	< 16%
CLAY CONTENT	> 47%	32 - 47%	< 32%

* : HIGH RISK CATEGORY: 85-90% chance of failure in 8-15 years after construction
INTERMEDIATE RISK: 55-60% chance of failure in 8-15 years after construction
LOW RISK CATEGORY: < 5% chance of failure in 8-15 years after construction

Figure 39. Revetments on the headers. This site has not failed and is located at the interchange at Rayne in the I-10 study area. This design is recommended to reduce the large number of header failures.

5) When designing a new embankment or reconstructing one, there are four choices, depending upon the space and economy available, plus the projected soil strength. The choices are:

a) Constant embankment slope configuration (Fig. 35). This design should be used where obtaining enough right-of-way is not a problem and low slope angles can be used.

b) Broken-back design (Fig. 36). This design has two different slope angles on the same embankment and should be used where there is limited right-of-way or where reconstruction of a slope is needed.

c) Broken-back design with a stabilized soil layer at the base (Fig. 37). This method of using two slope angles on the slope with a stabilized layer at the base to prevent upward movement of water into the slope is more costly than the others.

d) Constant embankment slope with a stable subgrade (Fig. 38). The low-angle embankment is built on a stable subgrade with a cohesive strength of at least 700 psf.

FUTURE WORK

Results of this project have only touched on only a few facets of embankment stability in soils containing varying amounts of shrink-swell clays. Many additional problem areas have unfolded that need further investigation for better understanding of these slope processes. Also, some new repair procedures need to be investigated further to test their feasibility. This project furnishes a reference framework against which future embankment stability work can be compared.

Many highway embankments are built with steep slopes (>16 degrees or <3.5:1) containing more than 20% smectites. To prevent failures of these slopes, these clays must be inactivated during the construction or repair of the slope. Currently, the best method of smectite inactivation is lime stabilization (71). In the guidelines for this method, the whole slope is being removed (back to a 2:1 slope), lime-stabilized, and rebuilt. This method is costly (approximately $35,000/slope). It is possible that the depth of lime treatment does not have to extend to the 2:1 slope, but only to a portion of it. A set of criteria needs to be developed to determine the minimum depth of lime treatment on a slope that also insures slope stability.

Another method of clay stabilization should also be tested: heat inactivation of the smectites using an asphalt heater. During the construction of these slopes and after the compaction of the soils on the slopes, the asphalt heater could be pulled over the soil and could heat the soil above 550 degrees C. This will collapse the clays irreversibly. The technology is already available, and the application of this machinery to this problem should be tested for cost-effectiveness, ease of use in the field, and depth of penetration into the soil. This method could be much cheaper and longer-lasting than the lime stabilization method.

The possibility of using a different type of vegetation on the slope should also be examined. There is a need for more biomass on the slopes for they act as pumps, and through evapotranspiration, remove water from the slopes. Pampas grass (Cortaderia selloana) might be the perfect alternative, for it has been used successfully in Texas and also on the repaired slope at location S1 in the I-10 study area (Fig. 40). It has deep roots and is easily transplanted. It is an aesthetically pleasing plant that would not require mowing. The constant use of heavy machinery on these embankments to mow the grass might help cause slope failures so lack of mowing might help stabilize the slopes.

The role of climate in causing the failures should also be determined. Is there really a long-term process of soil losing strength as water infiltrates the slope (21, 43)? Or is the failure dictated by the 25- or 50-year rainfall event that has passed through the area and greatly increased the soil moisture in the slope?

Figure 40. Slope stabilization with exotic vegetation. At this Locality S1 in Calcasieu Parish in the I-10 study area, pampas grass has been successfully used to stabilize a repaired slope.

The capillary rise of water into an embankment seems to be a real problem. We have addressed this problem with two slope designs to prevent this water movement. More work needs to be done to evaluate how often this occurs and what the different ways of inhibiting this rise of water into the embankment are. Will a lime-stabilized layer be enough to prevent the water movement?

Further work needs to be done to develop an easier test than the unconfined triaxial test to evaluate the cohesion and angle of friction for cohesive soils. We have experimented here with using the indirect tensile test with the unconfined compression test. Is this a good replacement?

REFERENCES

(1) Schuster, R.L., "Introduction," Landslides - Analysis and Control, R.L. Schuster & R.J. Krizek, eds. Transportation Research Board Special Publication 176, National Academy of Science, 1978, pp. 1-9.

(2) Chassie, R.G. and Goughnour, R.D., "States Intensifying Efforts to Reduce Highway Landslides," Civil Engineering, Vol. 46, No. 4, 1976, pp. 65-66.

(3) Cryer, M. E., written communication: Louisiana Dept. of Transportation, Lake Charles, Louisiana.

(4) Varnes, D.J., "Slope Movement Types and Processes," Landslides - Analysis and Control, R.L. Schuster and R.J. Krizek, eds., Transportation Research Board Special Report 176, National Academy of Science, 1978, pp. 12-33.

(5) Weems, T.A., Reynolds, E.F., Venson, R.L., Allen, E.T., and Smith, T.J., Soil Survey of Madison Parish, Louisiana, USDA Soil Conservation Service, 1982.

(6) Snead, J.I. and McCulloh, R.P., comps, Geological Map of Louisiana, Louisiana Geological Survey, Baton Rouge, 1984.

(7) Saucier, R.T., "Geomorphology, Stratigraphy, and Chronology of the Lower Mississippi Valley," Quaternary Non-Glacial Geology of the Conterminous United States, Morrison, R.B. ed, Decade of North American Geology Series, Geological Society of America, in press.

(8) Matthews, D., Reynolds, E.F., Colvin, G.P., Weems, T.A., Ray, C.A., Seaholm, J.E., and Kilpatrick, W.W., Soil Survey of Ouachita Parish, Louisiana, USDA Soil Conservation Service, 1974.

(9) Wang, K.K., Geology of Ouachita Parish, Louisiana Geological Survey Bulletin, No. 28, 1952, pp. 11-21.

(10) Soil Survey Staff, Soil Taxonomy, USDA Soil Conservation Service, Agricultural Handbook No. 436, 1975.

(11) Clark, H.L., Haley, G.J., Herbert, E.J., Hollier, R.M., and Roy, A.J., Soil Survey of Acadia Parish, Louisiana, USDA Soil Conservation Service, 1962.

(12) Muller, R.A., "Climate," Soil Survey of Lafayette Parish, Louisiana, Murphy, K.E., Daigle, J.J., and Roetker, L.J., eds, USDA Soil Conservation Service, 1977.

(13) Autin, W.J., Saucier, R.T., and Snead, J.I., "Introduction" to Chapter on "Quaternary Geology of the Lower Mississippi Valley," Quaternary Non-Glacial Geology of the Conterminous United States, Morrison, R. B., ed.,Geological Society of America, Decade of North American Geology Series,in press.

(14) Fisk, H.N., "Geological Investigations of the Alluvial Valley of the Lower Mississippi River," U.S. Army Corps of Engineers, Mississippi River Commission, 1944.

(15) Smith, S.M., "Properties of Embankment Slope Instability in Southwestern Louisiana," Masters Thesis, Louisiana Tech University, 1987.

(16) Mutchler, J.W., "Causes of Instability on Embankments in Northeast Louisiana," Masters Thesis, Louisiana Tech University, 1987.

(17) Sowers, G.B. and Sowers, G.F., Introductory Soil Mechanics and Foundations, Macmillan, New York, 1970.

(18) United States Geological Survey, Goals and Tasks of the Landslide Part of a Ground-Failure Hazards Reduction Program, U.S. Geological Survey Circular 880, U.S. Dept. of Interior, 1982.

(19) Munsell, Soil Color Charts, USDA Handbook No. 18, Soil Survey Manual, Kollmorgen Corp., Baltimore, 1975.

(20) Day, P.R.,"Particle fractionation and particle-size analysis," Methods of Soil Analysis, Black, C.A., ed, American Society of Agronomy, Madison, Part 1, Series in Agronomy No. 9, 1965, pp. 545-567.

(21) Abrams, T.G., and S.G. Wright, A Survey of Earth Slope Failures and Remedial Measures in Texas, Center for Highway Research, The University of Texas at Austin, Research Report No. 161-1, 1972.

(22) Soil Conservation Service, Procedures for Collecting Soil Samples and Methods of Analysis for Soil Survey, Soil Survey Investigation Report 1, USDA, U.S. Governmental Printing Office, Washington, D.C., 1982.

(23) Black, G.R., "Bulk density," Methods of Soil Analysis, Black, C.A., ed. American Society of Agronomy, Madison, Part 1, Series in Agronomy No. 9, 1965, pp.383-390.

(24) Terzaghi, K., and Peck, R.B., Soil Mechanics in Engineering Practice, John Wiley and Sons, New York, 2nd Ed, 1967.

(25) Abeyesekera, R.A., and Lovell, C.W., "Volume Changes in Compacted Clays and Shales on Saturation," Shales and Swelling Clays, Transportation Research Record No. 790, 1981, pp.67-78.

(26) Cavounidis, S., and Sotiropoulos, E., "Hypothesis for Progressive Failure," Journal of Geotechnical Engineering Division, Proceedings of ASCE, Vol. 106, No. GT6, 1980, pp. 659-671.

(27) DeGraff, J.V., McKean, J., Watanabe, P.E., and McCaffrey, W.F., "Landslide Activity and Groundwater Conditions: Insights from a Road in the Central Sierra Nevada, California," Soil Reinforcement and Moisture Effect on Slope Stability, Transportation Research Record No. 965, 1984,
pp. 32-46.

(28) Duncan, J.M. and Dunlap, P., "Slopes in Stiff-Fissured Clays and Shales," Journal of the Soil Mechanics and Foundations Engineering Division, Proceedings of the ASCE, Vol. 95, No. SM2, 1969, pp. 467-492.

(29) Elias, V., and Storch, H., "Control and Performance During Construction of a Highway Embankment on Weak Soils," Landslides, Slope Protection and Stability, Embankment Design and Stability, Highway Research Record No. 323,1970, pp. 60-70.

(30) Henkel, D.J., "Investigations of Two Long-Term Failures in London Clay Slopes at Wood Green and Northolt," Fourth International Conference on Soil Mechanics and Foundation Engineering Proceedings, Vol. 2, 1957, pp. 315-320.

(31) Hou, S., "Expansive-Shrinkable Soils in China," Canadian Geotechnical Journal, Vol. 21, No. 2, 1984, pp. 375-379.

(32) Humphrey, D.N., and Leonards, G.A., "Slide in Upstream Slope of Lake Shelbyville Dam," Journal of Geotechnical Engineering, Vol. 112, No. 5, ASCE Geotechnical Engineering Division, 1986, pp. 564-577.

(33) Koppula, S.D., "On Stability of Slopes in Clays with Linearly Increasing Strength," Canadian Geotechnical Journal, Vol. 21, No. 3, 1984, pp. 577-581.

(34) Laguros, J.G., Kumar, S., and Medhani, R., "Failure of Slopes in Weathered Overconsolidated Clay," Overconsolidated Clays and Shales, Transportation Research Record No. 873, 1982, pp. 12-14.

(35) Leonards, G.A., "Investigations of Failures," Journal of Geotechnical Engineering Division, Proceedings of the ASCE, Vol. 108, No. GT2, 1982, pp. 187-246.

(36) Marivoet, L., "Control of the Stability of a Sliding Slope in a Railway Cut near Wettern," Proceedings of the Second International Conference on Soil Mechanics and Foundation Engineering, Rotterdam, Vol. 2-3, Sec. IVC, 1948, pp. 38-42.

(37) Peterson, R., Iverson, N.L., and Rivard, P.J., "Studies of Several Dam Failures on Clay Foundations," Fourth International Conference on Soil Mechanics and Foundation Engineering Proceedings, Vol. 2, 1957, pp. 348-352.

(38) Ramaltho-Ortigao, J.A., Werneck, M.L.G., and Lacerda, W.A., "Embankment Failure on Clay near Rio de Janeiro," Journal of Geotechnical Engineering, Vol. 109, No. 11, 1983, pp. 1460-1479.

(39) Redman, P.G. and Poulos, H.G., "Study of Two Field Cases Involving Undrained Creep," Journal of Geotechnical Engineering Division, ASCE, Vol. 110, No. 2, 1984, pp.1307-1320.

(40) Roa, K.L., "Behavior of Recent Earth Dams and Levees in India," Fourth International Conference on Soil Mechanics and Foundation Engineering Proceedings, Vol. 2, 1957, pp. 361-367.

(41) Schnabel, J., and Grefsheim, F., "Slope Stability in the Washington D.C. Area: Cretaceous Clays," Overconsolidated Clays, Shales, Transportation Research Record No. 873, 1982, pp. 1-8.

(42) Schweizer, R.J., and Wright, S.G., A Survey and Evaluation of Remedial Measures for Earth Slope Stabilization, Center for Highway Research, The University of Texas at Austin, Research Report No. 161-2F, 1974.

(43) Stauffer, P.A., and Wright, S.G., An Examination of Earth Slope Failures in Texas, Center for Highway Research, The University of Texas at Austin, Research Report No. 353-3F, 1984.

(44) Stevens, J.B., and Matlock, H., "Measurements Beneath the Surface of Expansive Clay," Swelling Soils, Transportation Research Record No. 568, 1976, pp. 35-47.

(45) Wilson, S.D., and Mikkelsen, P.E., Landslides - Analysis and Control, Transportation Research Board Special Report No. 176, Schuster, R.L. and Krizek, R.J. eds., National Academy of Sciences, 1978, pp. 133-137.

(46) Krynine, D.P., and Judd, W.R., Principles of Engineering Geology and Geotechnics, McGraw Hill Co., New York, 1957.

(47) Smith, T.W. and Stafford, G.V., "Horizontal Drains on California Highways," Journal of Soil Mechanics and Foundations Division, ASCE Proceedings, Vol. 83, No. SM3,1957, pp. 1301-1326.

(48) Black, J.C., "Connected Wells Installed to Stabilize California Hillside," Roads and Streets, Vol. 99, No. 1, 1956, pp. 104-107.

(49) Eager, W.L., "Slide Stabilized with Drilled Horizontal Drains," Roads and Streets, Vol. 99, No. 2, 1956, pp. 87-95.

(50) Downs, W.S., "Earth Slip Hazards and Control in Highway Maintenance," Engineering News Record, Vol. 104, No. 19, 1930, pp. 794-798.

(51) McKeever, H.J., "Curing Slides with Drainage Tunnels," Roads and Streets, Vol. 90, No. 4, 1947, pp. 73-76.

(52) Vidal, H., "Reinforced Earth Steel Retaining Wall Used on High Steep Slope in France," Civil Engineering, Vol. 40, No. 2, Pt. 1, 1970, pp. 72-73.

(53) Reti, G.A., "Slope Stabilized by Anchored Retaining Wall," Civil Engineering, Vol. 34, No.4, 1964, pp. 49-53.

(54) Jessup, W.J., "Giant Spikes Halt Earth Movement in California," Civil Engineering, Vol. 28, No. 1, 1958, p. 96.

(55) Allen, G.H., "Steel Baffles Stop Sliding Fill," Engineering News Record, Vol. 119, No. 1, 1937, pp. 32-33.

(56) Allen, G.H., "Old Slide Compels Radical Remedy," Engineering News Record, Vol. 123, No. 6, 1939, pp. 70-71.

(57) Rowan, W.H., Pierce, T.R., and Webb, R., "Failure of a Side-Hill Highway Fill," Civil Engineering, Vol. 33, No. 5, 1963, pp. 40-41.

(58) Robnett, Q.L., and Thompson, M.R., "Concepts for Developing Stabilization Recommendations for the Soils of an Area," Soil Stabilization: Multiple Aspects, Highway Research Record No. 315, 1970, pp. 1-13.

(59) Schroter, G.A., and Maurseth, R.O., "Hillside Stability - the Modern Approach," Civil Engineering, Vol. 30, No. 6, 1960, pp. 66-69.

(60) O'Bannon, C.E., "Electrochemical Hardening of Expansive Clays," Use of Waste Materials and Soil Stabilization, Transportation Research Record No. 593, 1976, pp. 46-50.

(61) Thompson, M.R., and Robnett, Q.R., "Pressure Injected Lime for Treatment of Swelling Soils," Swelling Soils, Transportation Research Record No. 568, 1976, pp. 24-34.

(62) Handy, R.L. and Williams, W.W., "Chemical Stabilization of an Active Landslide," Civil Engineering, Vol. 37, No. 8, 1967, pp. 62-65.

(63) Diamond, S., and Kinter, E.B., "Mechanisms of Soil-Lime Stabilization, an Interpretive Review," Lime Stabilization, Highway Research Record No. 92, 1965, pp. 83-95.

(64) Petry, T.M., Armstrong, J.C., and Chang, T.D., "Short-Term Active Soil Property Changes Caused by Injection of Lime and Fly Ash," Soil Stabilization, Transportation Research Record No. 839, 1982, pp. 26-33.

(65) Mitchell, J.K., Fundamentals of Soil Behavior, John Wiley and Sons, New York. 1976.

(66) Hill, R.A., "Clay Stratum Dried Out to Prevent Landslips," Civil Engineering, Vol. 4, No. 8, 1934, pp. 403-407.

(67) Reti, G.A., "Slope Stabilized by Anchored Retaining Wall," Civil Engineering, Vol. 34, No. 4, 1964, pp. 49-53.

(68) Bowles, J.E., "Slope Stability," Analytical and Computer Methods in Foundation Engineering, Chapter 14, McGraw Hill, New York, 1974.

(69) Hadley, W.O., Special Studies -- Fundamental Engineering Properties of Construction Materials, Research Report No. 78-3, Materials Research Laboratory, Louisiana Tech University, Ruston, Louisiana, 1983.

(70) Snethen, D.R., "Expansive Soils," Ground Failure, National Research Council Commission on Ground Failure Hazards, No. 3, 1986, pp. 12-16.

APPENDICES

APPENDIX 1

SITE DESCRIPTIONS

Characterization of the embankments of the I-20 study area is summarized in Tables A1 and A2. Included in these descriptions are locality numbers, structure numbers, date of construction, latitude and longitude, township and range, form of the structure, slope angles, site of sample collection, soil type, and location of the borrow pit.

The embankment descriptions for the I-10 study area are summarized in Table A3. The following items are described in this table: locality numbers, soil sample numbers, structure numbers, date of construction, latitude and longitude, township and range, form of the structure, and slope activity (failed or stable).

TABLE A1

EMBANKMENT LOCATION AND IDENTIFICATION OF
OVERPASSES (OP) AND INTERCHANGES (INT)
IN THE STUDY AREA

#	SYMBOL &* NAME	STRUCTURE #	DATE CONSTRUCTED	LATITUDE & LONGITUDE	TOWNSHIP & RANGE	FORM**
			OUACHITA PARISH			
N1	OP-SF* State Farm	451-06-2032-1	1966	32°29'51"N 92°04'12"W	SW1/4 Sec 33 T18N R4E	OP
N2	OP-PM Pecanland Mall	451-06-2158-1	1966	32°29'36"N 92°03'15"W	NW1/4 Sec 2 T17N R5E	OP
N3	OP-MH Millhaven	451-06-2532-1	1966	32°29'13"N 91°59'25"W	NE1/4 Sec 6 T17N R5E	INT
			RICHLAND PARISH			
N4	RP-SI Start	451-07-0441-1	1967	32°28'34"N 91°51'43"W	NE1/4 Sec 9 T17N R6E	INT
N5	RP-GO Girard	451-07-0607-1	1967	32°28'11"N 91°49'37"W	SE1/4 Sec 11 T17N R6E	OP
N6	RP-RE Rayville East	451-07-1184-1	1968	32°27'17"N 91°43'47"W	SE1/4 Sec 15 T17N R7E	OP
N7	RP-BB Bee Bayou	451-07-1419-1	1968	32°27'15"N 91°41'34"W	SW1/4 Sec 18 T17N R8E	INT

TABLE A1 (CONTINUED)

#	SYMBOL &* NAME	STRUCTURE #	DATE CONSTRUCTED	LATITUDE & LONGITUDE	TOWNSHIP & RANGE	FORM**
			RICHLAND PARISH (continued)			
N8	RP-BH Bee Bayou/Holly Ridge	451-07-1594-1	1968	32°27'15"N 91°39'59"W	SE1/4 Sec 17 T17N R8E	OP
N9	RP-HR Holly Ridge	451-07-1820-1	1970	32°27'15"N 91°37'41"W	SE1/4 Sec 15 T17N R8E	INT
N10	RP-DI Dunn	451-07-2091-1	1970	32°27'00"N 91°34'56"W	SE1/4 Sec 18 T17N R9E	INT
N11	RP-DD Dunn/Delhi	451-07-2413-1	1969	32°26'41"N 91°29'33"W	NW1/4 Sec 22 T17N R9E	OP
N12	RP-DO Dunn	451-07-2606-2	1970	32°26'31"N 91°29'33"W	NE1/4 Sec 24 T17N R9E	OP
			MADISON PARISH			
N13	MP-CB Cow Bayou	451-08-0086-1	1970	32°26'20"N 91°27'30"W	SE1/4 Sec 20 T17N R10E	OP
N14	MP-W Waverly	451-08-0317-1	1970	32°25'50"N 91°25'12"W	NW1/4 Sec 26 T17N R10E	INT

TABLE A1 (CONTINUED)

#	SYMBOL &* NAME	STRUCTURE #	DATE CONSTRUCTED	LATITUDE & LONGITUDE	TOWNSHIP & RANGE	FORM**
			MADISON PARISH (continued)			
N15	MP-TN Tendal	451-08-0611-1	1974	32°25'25"N 91°22'08"W	SW1/4 Sec 29 T17N R11E	OP
N16	MP-QU Quebec	451-08-1007-1	1974	32°25'04"N 91°18'12"W	NW1/4 Sec 36 T17N R11E	OP
N17	MP-CM Chicago Mill	451-08-1451-1	1970	32°24'20"N 91°13'30"W	NW1/4 Sec 33 T16N R12E	OP
N18	MP-TR Tallulah Railroad	451-08-1588-1	1974	32°23'15"N 91°12'10"W	SE1/4 Sec 32 T16N R12E	OP

* = The first part of the symbol name is the parish: (OP) Ouachita, (RP) Richland, and (MP) Madison Parishes. The second part of the symbol is the geographical name.

** = Forms are overpasses (OP) and interchanges (INT).

TABLE A2

SAMPLE SITE LOCATIONS ON THE EMBANKMENTS
AND SOIL TYPES USED IN CONSTRUCTION
OF THE EMBANKMENTS

NUMBER &* SYMBOL	SLOPE ANGLES QUAD/DEG^{O}/RATIO	DIRECTION & DISTANCE FROM BRIDGE	DISTANCE DOWN SLOPE	SOIL TYPE	LOCATION OF BORROW PIT
		OUACHITA PARISH			
N1 OP-SF*	SW 18-3:1	S-25' (7.6m)	50' (15.3m)	Portland	1/4 mi SE
	SW 18-3:1	S-70' (21.4m)	40' (12.2m)		
N2 OP-PM	SW 23-2.35:1	S-55' (16.8m)	25' (7.6m)	Herbert & Portland	Directly NW
	SE 23-2.35:1	S-55' (16.8m)	25' (7.6m)		
N3 OP-MH	SW 17-3.25:1	S-50' (15.3m)	50' (15.3m)	Portland & or Herbert	Directly SE & SW
	SE 17-3.35:1	S-50' (15.3m)	50' (15.3m)		
		RICHLAND PARISH			
N4 RP-SI	SW 17-3.25:1	S-50' (15.3m)	40' (12.2m)	Rilla-Herbert -Sterlington	1/4 mi SE
	SE 17-3.25:1	S-50' (15.3m)	40' (12.2m)		
N5 RP-GO	SW 21-2.6:1	S-65' (19.8m)	30' (9.1m)	Rilla-Herbert -Sterlington	Directly NE
	SE 21-2.6:1	S-65' (19.8m)	35' (10.7m)		
N6 RP-RE	SW 24-2.25:1	S-40' (12.2m)	35' (10.7m)	Grenada-Foley -Calhoun	1/4 mi SW
	SE 24-2.25:1	S-60' (18.3m)	30' (9.1m)		

TABLE A2 (Continued)

NUMBER &* SYMBOL	SLOPE ANGLES QUAD/DEG°/RATIO	DIRECTION & DISTANCE FROM BRIDGE	DISTANCE DOWN SLOPE	SOIL TYPE	LOCATION OF BORROW PIT
		RICHLAND PARISH (continued)			
N7 RP-BB	SW 19-2.9:1	S-60' (18.3m)	30' (9.1m)	Grenada-Foley -Calhoun	Directly NE
	SW 19-2:9:1	S-60' (18.3m)	25' (7.6m)		
N8 RP-BH	SW 19-2.9:1	S-65' (19.8m)	33' (10.1m)	Grenada-Foley -Calhoun	Directly SW & SW
	SE 19-2.9:1	S-65' (19.8m)	35' (10.7m)		
N9 RP-HR	SW 10-5.6:1	S-45' (13.7m)	65' (19.8m)	Grenada-Foley -Calhoun	1/4 mi SW
	SE 10-5.6:1	S-69' (21.0m)	51' (15.6m)		
N10 RP-DI	SW 12-4.7:1	S-70' (21.4m)	60' (18.3m)	Grenada-Calhoun	1/4 mi SE
	SE 12-4.7:1	S-70' (21.4m)	60' (18.3m)		
N11 RP-DD	SW 21-2.6:1	S-55' (16.8m)	35' (10.7m)	Grenada-Calhoun	Directly SW
	SE 21-2.6:1	S-55' (16.8m)	30' (9.1m)		
N12 RP-DO	SW 14-4:1	S-60' (18.3m)	40' (12.2m)	Grenada-Calhoun -Memphis	1/4 mi NW
	SE 14-4:1	S-65' (19.3m)	35' (10.7m)		

TABLE A2 (Continued)

NUMBER &* SYMBOL	SLOPE ANGLES QUAD/DEG°/RATIO	DIRECTION & DISTANCE FROM BRIDGE	DISTANCE DOWN SLOPE	SOIL TYPE	LOCATION OF BORROW PIT
		MADISON PARISH			
N13 MP-CB	NE 13-18, 4.3-3:1			Sharkey	Directly NW
	NW 17-18, 3.25-3:1	SEE APPENDIX I (Fig. I-1 to 4)			
	SE 18-3:1				
	SW 16-3.5:1				
N14 MP-W	NE 14-4:1	N-145' (44.2m)	37' (11.3m)	Sharkey	1/4 mi NW & SE
	NW 15-3.75:1	N-120' (36.6m)	45' (13.7m)		
	SE 13-4.3:1	S-120' (36.6m)	45' (13.7m)		
	SW 16-3.5:1	S-120' (36.6m)	45' (13.7m)		
N15 MP-TN	NE 16-17, 3.5-3.25:1			Sharkey	1/4 mi SW
	NW 19-2.9:1	SEE APPENDIX I (Fig. I-5 to 8)			
	SE 18-3:1				
	SW 15-17, 3.75-3.25:1				

TABLE A2 (Continued)

NUMBER &* SYMBOL	SLOPE ANGLES QUAD/DEG°/RATIO	DIRECTION & DISTANCE FROM BRIDGE	DISTANCE DOWN SLOPE	SOIL TYPE	LOCATION OF BORROW PIT
		MADISON PARISH (continued)			
N16 MP-QU	NE 18-3:1	SEE APPENDIX I (Fig. I-9)		Sharkey & Dundee	1/4 mi SE
	NW 19-2.9:1	1) N-50' (15.3m) 2) N-75' (22.9m) 3) N-75' (22.9m)	50' (15.3m) 30' (9.1m) 62' (18.9m)		
	SE 18-20, 3-2.75:1	SEE APPENDIX I (Fig. I-10)			
	SW 19-2.9:1	1) S-100' (30.5m) 2) S-100' (30.5m) 3) S-40' (12.2m)	50' (15.3m) 30' (9.1m) 62' (18.9m)		
N17 MP-CM	NE 13-4.3:1			Sharkey	1/4 mi SE & SW
	NW 17-3.25:1	SEE APPENDIX I (Fig. I-11 to 14)			
	SE 15-3.75:1				
	SW 16-3.5:1				
N18 MP-TR	NE 17-3.25:1			Commerce	1/4 mi NW
	SW 16-3.5:1	SEE APPENDIX I (Fig. I-15,16)			

* = Numbers and abbreviations are identical to those identified in Table 1.

TABLE A3

CONSTRUCTION AND LOCATION DATA OF
EMBANKMENT SLOPES OF
STUDY AREA

LOCALITY	SAMPLE #	BRIDGE #	CONSTRUCTION DATE	LAT/LONG	LOCATION TOWNSHIP/RANGE		STRUCTURE FORM	SLOPE
S1	CA108SE	4509123291	1959	30°13'00" N 93°19'30" W	SW1/4 T10S	Sec 6 R9W	interchange	stable
S2	CA90SE	4509130941	1960	30°14'15" N 93°11'30" W	NE/4 T9S	Sec 33 R8W	interchange	failed
S3	CA210SW	4503011801	1977	30°12'15" N 93°10'00" W	SW/4 T10S	Sec 10 R8W	overpass	stable
S4	CAE397SE	4509137731	1963	30°15'00" N 93°05'45" W	NW/4 T9S	Sec 28 R7W	overpass	stable
S5	CA383SE	4509142761	1963	30°14'00" N 93°00'45" W	SW/4 T9S	Sec 19 R6W	interchange	stable
"	CA383SE UC	"	"	"	"	"	"	"
S6	JD101SE	4500304071	1964	30°15'00" N 92°55'45" W	NW/4 T9S	Sec 30 R5W	interchange	stable
S7	JDWESW 1UC	4500310491	1964	30°14'45" N 92°49'15" W	NW/4 T9S	Sec 30 R4W	interchange	stable
"	JDWESW UC	4500310491	1964	"	"	"	"	failed
"	JDWENW 1S	"	"	"	"	"	"	stable

TABLE A3 (Continued)

LOCALITY	SAMPLE #	BRIDGE #	CONSTRUCTION DATE	LAT/LONG	LOCATION TOWNSHIP/RANGE		STRUCTURE FORM	SLOPE
S7	JDWENW 2S	4500310491	1964	30°14'45" N 92°45'15" W	NW/4 T9S	Sec 30 R4W	interchange	failed
S8	JD395SE	4500315351	1964	30°14'45" N 92°44'30" W	NW/4 T9S	Sec 25 R3W	interchange	stable
S9	JDE395NW	4500316351	1964	30°14'45" N 92°43'30" W	SE/4 T9S	Sec 24 R4W	overpass	failed
S10	JD102SE	4500320461	1964	30°14'45" N 92°39'15" W	NW/4 T9S	Sec 26 R5W	overpass	stable
S11	AC1123NW	4500401431	1960	30°14'00" N 92°36'00" W	SE/4 T9S	Sec 36 R2W	overpass	stable
S12	ACBRIDGE	4500407052	N/A	30°13'30" N 92°30'15" W	SW/4 T9S	Sec 30 R1W	overpass	stable
S13	ACLA369NW	4500408111	1962	30°13'30" N 92°29'25" W	SW/4 T9S	Sec 29 R1W	overpass	stable
S14	ACESNW UC (stable)	4500409671	1960	30°13'45" N 92°27'45" W	SE/4 T9S	Sec 28 R1W	interchange	stable
"	ACESNW UC (slump)	"	"	"	"	"	"	failed

TABLE A3 (Continued)

LOCALITY	SAMPLE #	BRIDGE #	CONSTRUCTION DATE	LAT/LONG	LOCATION TOWNSHIP/RANGE		STRUCTURE FORM	SLOPE
S14	ACESNE 1S	4500409671	1960	30°13'45" N 92°27'45" W	SW/4 T19S	Sec 27 R1W	interchange	failed
"	ACESNE 2S	"	"	"	"	"	"	stable
S15	ACE1111SW UC	4500416781	1966	30°13'45" N 92°20'45" W	SE/4 T9S	Sec 27 R1E	overpass	failed
"	ACE1111NW 1-S	"	"	"	"	"	"	stable
"	ACE1111NW 2-S	"	"	"	"	"	"	stable
S16	AC722SW	4500420451	1966	30°15'00" N 92°17'30" W	SE/4 T9S	Sec 19 R2E	overpass	stable
S17	AC95NE UC	4500426111	1965	30°14'20" N 92°11'30" W	SW/4 T9S	Sec 20 R3E	interchange	stable
"	AC95NE 1UC	"	"	"	"	"	"	stable
"	AC95NW S	"	"	"	"	"	"	stable
S18	AC343NW	4500500001	1968	30°14'45" N 92°10'30" W	SE/4 T9S	Sec 20 R3E	overpass	failed

TABLE A3 (Continued)

LOCALITY	SAMPLE #	BRIDGE #	CONSTRUCTION DATE	LAT/LONG	LOCATION TOWNSHIP/RANGE		STRUCTURE FORM	SLOPE
S19	LA724NE S	4500502031	1968	30°14'45" N 92°08'30" W	NE/4 T9S	Sec 22 R3E	overpass	stable
S20	LAACNE S	4500506571	1967	30°14'45" N 92°03'45" W	SE/4 T9S	Sec 21 R4E	interchange	stable
S21	LA167NW	4500509762	N/A	30°15'30" N 92°00'45" W	NW/4 T9S	Sec 52 R5W	interchange	stable
S22	LA354NW	4500600001	1970	30°16'45" N 91°57'00" W	SW/4 T9S	Sec 42 R5E	interchange	stable

APPENDIX 2

GEOTECHNICAL DATA OF THE SITES

This appendix contains Atterbergs limits (liquid limit, plastic limit, and plasticity index), moisture content, and bulk density data which have been collectively designated as geotechnical properties. Also included are particle size data, organic carbon values, and pH data.

GEOTECHNICAL DATA FOR I-20 STUDY AREA

An "*" denotes samples taken from the stable part of a failed slope. When an "*" appears within a slope quadrant, the samples without an "*" are from failures. If an "*" does not appear next to any sample numbers within a particular slope quadrant, then the slope is stable. An "NR" states that this sample is not representative of this slope. Data is arranged in order of occurrence from west to east. See Table 1 for abbreviations.

TABLE A4a

GRAIN SIZE DISTRIBUTION ORGANIC CARBON AND pH

SAMPLE & SLOPE	% SAND	% SILT	% CLAY	ORGANIC CARBON	pH
OPSFSW-1	5	43	52	.91	7.28
OPSFSE-1	5	42	53	.67	7.46
OPPMSW-1	39	43	18	.20	6.94
OPPMSE-1	25	43	32	.36	7.70
OPMHSW-1	3	18	79	.28	7.89
OPMHSE-1	3	17	80	.36	8.04
RPSISW-1	41	35	24	.0	6.65
RPSISE-1	43	36	21	.32	5.86
RPGOSW-1	5	43	52	.44	7.70
RPGOSE-1	10	43	47	.28	7.76
RPRESW-1	28	54	18	.55	6.30
RPRESE-1	30	52	18	.40	5.90
RPBBSW-1	23	55	22	.59	7.12
RPBBSE-1	29	48	23	.20	7.06
RPBHSW-1	22	49	29	.75	6.11
RPBHSE-1	54	33	13	.08	7.64
RPHRSW-1	7	64	29	.63	6.32
RPHRSE-1	10	57	33	.28	7.39
RPDISW-1	5	70	25	.28	5.68
RPDISE-1	14	54	32	.44	5.06
RPDDSW-1	4	77	19	.16	5.30
RPDDSE-1	17	62	21	.55	6.04
RPDONW-1	8	69	23	.40	7.14
RPDONE-1	58	10	32	.40	4.46

TABLE A4b

GRAIN SIZE DISTRIBUTION ORGANIC CARBON AND pH

SAMPLE & SLOPE		% SAND	% SILT	% CLAY	ORGANIC CARBON	pH
MPCBNE	1*	15	42	43	.32	7.38
	2	7	32	61	.62	7.38
	3	9	36	55	1.07	6.78
	4	9	37	54	.63	7.17
	5*	13	42	45	.32	7.21
	6	7	38	55	.24	7.42
MPCBNW	1*	11	50	39	.40	7.03
	2	3	22	75	.55	7.04
	3	5	35	60	.71	6.66
	4	8	30	62	.63	7.13
	5	6	31	63	.44	7.19
	6	13	44	43	.28	7.40
MPCBSE	1*	13	32	55	.51	7.45
	2	5	37	58	.59	6.77
	3	5	28	67	.32	7.10
	4	6	23	71	.47	7.32
	5	5	33	62	.51	7.16
	6	13	37	50	.36	7.20
	7*	36 NR	37 NR	27 NR	.44	7.03
MPCBSW	1	10 NR	50 NR	40 NR	.32	7.43
	2*	13 NR	61 NR	26 NR	.36	7.59
	3	8 NR	67 NR	25 NR	.83	6.61
	4	14 NR	53 NR	33 NR	.28	6.97
	5	16 NR	56 NR	28 NR	.28	7.27
	6	18 NR	46 NR	36 NR	.36	7.16
	7	4 NR	20 NR	76 NR	.71	6.94
MPWNE	1	3	39	58	.47	7.51
MPWNW	1	2	32	66	.59	7.47
MPWSE	1	1	20	79	.44	7.70
MPWSW	1	2	44	54	.71	7.20
MPTNNE	1*	29	35	36	.36	6.05
	2*	12	33	55	.47	6.84
	3	11	36	53	.67	6.14
	4	9	35	56	.55	6.59

* = Sample taken from stable part of failed slope.
NR = Sample not representative of parent material.

TABLE A4c

GRAIN SIZE DISTRIBUTION ORGANIC CARBON AND pH

SAMPLE & SLOPE		% SAND	% SILT	% CLAY	ORGANIC CARBON	pH
MPTNNW	1*	1	39	60	.36	7.20
	2	4	31	65	.59	7.11
	3	1	31	68	.20	6.73
	4	6	32	62	.51	7.13
	5*	4	36	60	.47	7.16
MPTNSE	1*	8	35	57	.51	6.97
	2	9	33	58	.59	6.70
	3	9	34	57	.40	7.27
MPTNSW	1*	11	40	49	.20	7.21
	2*	2	35	63	.32	7.26
	3	11	33	56	.55	6.20
	4	3	33	64	.51	6.37
MPQUNE	1*	19	35	46	.44	6.59
	2	27	41	32	.24	6.27
	3	12	34	54	.40	6.14
	4	16	34	50	.47	6.73
MPQUNW	1	13	42	45	.75	7.77
	2	14	41	45	.47	7.00
	3	17	39	44	.36	7.10
MPQUSE	1*	15	39	46	.63	6.69
	2*	13	39	48	.59	6.93
	3	15	38	47	.55	6.91
	4	13	37	50	.75	6.55
MPQUSW	1	13	44	43	.63	6.15
	2	11	45	44	.55	5.72
	3	8	45	47	.91	5.99

* = Sample taken from stable part of failed slope.

TABLE A4d

GRAIN SIZE DISTRIBUTION ORGANIC CARBON AND pH

SAMPLE & SLOPE		% SAND	% SILT	% CLAY	ORGANIC CARBON	pH
MPCMNE	1*	1	21	78	.32	7.68
	2	3	10	87	.44	7.70
	3	2	23	75	.47	7.45
	4	2	15	83	.67	7.43
	5	1	7	92	.32	7.50
	6	2	8	90	.55	7.49
	7*	3	19	78	.44	7.62
	8*	1	19	80	.32	7.52
MPCMNW	1*	14	25	61	.59	7.86
	2	2	40	58	.24	7.38
	4	2	18	20	.51	7.20
MPCMSE	1*	4	19	77	.55	7.81
	2*	3	22	75	.87	7.36
	3	2	19	79	.44	7.41
	4	1	24	75	.55	6.91
	5	1	7	92	.59	6.91
	6	1	25	74	.44	7.52
	7	3	21	76	.51	7.56
MPCMSW	1*	4	22	74	.47	7.81
	2	1	20	79	.47	7.65
	3*	8	20	72	.51	7.26
	4	1	20	79	.44	7.17
	5	2	26	72	.67	7.14
MPTRNE	1*	10	45	45	.55	7.24
	2	10	53	37	.51	7.52
MPTRSW	1*	12	44	44	.79	7.48
	2	7	39	54	.32	7.70

* = Sample taken from stable part of failed slope.

TABLE A5a

GEOTECHNICAL SAMPLES

SAMPLE & SLOPE	BULK DENSITY g/cc	MOISTURE CONTENT %	LIQUID LIMIT %	PLASTIC LIMIT %	PLASTICITY INDEX %
OPSFSW-1	1.35	32.81	63	32	31
OPSFSE-1	1.51	21.65	61	35	26
OPPMSW-1	1.43	17.48	29	20	9
OPPMSE-1	1.68	18.91	35	19	16
OPMHSW-1	1.22	37.64	88	42	46
OPMHSE-1	1.26	35.96	70	29	41
RPSISW-1	1.69	15.38	28	18	10
RPSISE-1	1.66	16.68	27	18	9
RPGOSW-1	1.25	35.69	53	28	25
RPGOSE-1	1.47	25.48	48	27	21
RPRESW-1	1.37	6.86	24	91	5
RPRESE-1	1.32	21.03	24	19	5
RPBBSW-1	1.58	16.64	31	23	8
RPBBSE-1	1.47	13.05	25	17	8
RPBHSW-1	1.46	15.45	35	21	14
RPBHSE-1	1.81	14.49	18	18	0
RPHRSW-1	1.31	10.15	35	26	9
RPHRSE-1	1.52	18.20	39	24	15
RPDISW-1	1.51	17.12	35	22	13
RPDISE-1	1.52	16.53	34	20	14
RPDDSW-1	1.24	10.37	29	22	7
RPDDSE-1	1.49	10.54	27	22	5
RPDOSW-1	1.43	16.38	33	24	9
RPDOSE-1	1.67	14.91	36	23	13

TABLE A5b

GEOTECHNICAL SAMPLES

SAMPLE & SLOPE		BULK DENSITY g/cc	MOISTURE CONTENT %	LIQUID LIMIT %	PLASTIC LIMIT %	PLASTICITY INDEX %
MPCBNE	1*	1.57	26.93	46	26	20
	2	1.26	38.35	65	35	30
	3	1.20	39.32	56	25	31
	4	1.36	33.76	58	28	30
	5*	1.46	27.57	47	20	27
	6	1.29	31.78	57	23	34
MPCBNW	1*	1.56	26.96	41	20	21
	2	1.22	42.23	79	33	46
	3	1.19	44.60	62	24	38
	4	1.33	36.23	62	27	35
	5	1.27	38.94	63	25	38
	6	1.51	25.38	42	19	23
MPCBSE	1*	1.48	28.60	43	24	19
	2	1.31	37.90	61	28	33
	3	1.19	45.20	70	28	42
	4	1.23	44.53	73	28	45
	5	1.30	37.20	68	37	31
	6	1.32	29.20	50	26	24
	7*	1.52	25.78	37 NR	18 NR	19 NR
MPCBSW	1	1.40	29.00	43 NR	20 NR	23 NR
	2*	1.29	38.20	35 NR	20 NR	15 NR
	3	1.22	41.10	37 NR	26 NR	11 NR
	4	1.48	30.32	34 NR	23 NR	11 NR
	5	1.41	27.80	35 NR	22 NR	13 NR
	6	1.55	26.00	39 NR	22 NR	17 NR
	7	1.14	47.70	76 NR	31 NR	45 NR
MPWNE	1	1.41	31.32	69	28	41
MPWNW	1	1.38	26.20	73	34	39
MPWSE	1	1.35	33.91	84	36	48
MPWSW	1	1.42	28.27	65	34	31
MPTNNE	1*	1.70	21.40	36	20	16
	2*	1.44	30.90	57	24	33
	3	1.43	28.80	55	24	31
	4	1.32	37.95	59	23	36

* = Sample taken from stable part of failed slope.
NR = Sample not representative of parent material.

TABLE A5c

GEOTECHNICAL SAMPLES

SAMPLE & SLOPE		BULK DENSITY g/cc	MOISTURE CONTENT %	LIQUID LIMIT %	PLASTIC LIMIT %	PLASTICITY INDEX %
MPTNNW	1*	1.25	41.15	72	25	47
	2	1.27	38.96	68	23	46
	3	1.15	46.88	78	18	50
	4	1.37	34.33	63	25	38
	5*	1.36	31.87	65	24	41
MPTNSE	1*	1.49	30.77	58	27	31
	2	1.30	40.10	62	26	36
	3	1.37	34.77	59	27	32
MPTNSW	1*	1.59	23.54	56	25	31
	2*	1.47	29.73	69	29	40
	3	1.41	33.23	56	30	26
	4	1.36	37.51	67	31	36
MPQUNE	1*	1.47	26.33	47	18	29
	2	1.46	21.54	54	24	30
	3	1.39	30.05	52	25	28
	4	1.38	30.00	50	23	27
MPQUNW	1	1.48	25.36	44	23	21
	2	1.52	23.54	51	20	31
	3	1.55	23.04	48	21	27
MPQUSE	1*	1.40	20.88	55	23	32
	2*	1.46	21.54	54	24	30
	3	1.39	30.05	52	25	27
	4	1.38	30.00	50	23	27
MPQUSW	1	1.54	23.58	44	22	22
	2	1.55	22.67	51	19	32
	3	1.47	25.10	57	22	35

* = Sample taken from stable part of failed slope.

TABLE A5d

GEOTECHNICAL SAMPLES

SAMPLE & SLOPE		BULK DENSITY g/cc	MOISTURE CONTENT %	LIQUID LIMIT %	PLASTIC LIMIT %	PLASTICITY INDEX %
MPCMNE	1*	1.23	43.60	84	39	45
	2	1.21	45.30	85	46	39
	3	1.03	53.50	87	49	38
	4	1.02	49.20	88	42	46
	5	1.09	49.00	89	45	44
	6	1.11	42.80	93	45	48
	7*	1.10	43.50	84	38	49
	8*	1.10	46.80	87	38	49
MPCMNW	1*	1.23	37.97	67	29	38
	2	1.25	38.25	61	34	27
	4	1.09	49.90	89	43	46
MPCMSE	1*	1.30	35.53	78	42	36
	2*	1.09	43.03	80	39	41
	3	1.17	43.7	83	43	40
	4	1.11	47.90	81	44	37
	5	1.06	45.36	82	43	39
	6	1.13	45.22	81	44	37
	7	1.07	43.53	77	40	37
MPCMSW	1*	1.35	30.58	84	34	50
	2	1.16	43.97	91	39	52
	3*	1.24	39.44	72	38	34
	4	1.04	52.95	84	41	43
	5	1.14	45.78	75	35	40
MPTRNE	1*	1.49	23.35	55	29	26
	2	1.53	22.60	46	23	23
MPTRSW	1*	1.70	22.05	55	23	32
	2	1.31	33.34	63	29	34

* = Sample taken from stable part of failed slope.

I-10 STUDY AREA GEOTECHNICAL DATA

The embankment slope characteristics determined by both field and laboratory work have been divided into four major categories and presented as Table II-1, Sedimentological Properties, which include percent clay, silt, and sand. Table A7 contains geotechnical properties such as liquid limits, plastic limits, plasticity indices, bulk density, and percent moisture. Table A8 includes percent organic carbon, pH, and slope angle.

TABLE A6

SEDIMENTOLOGICAL PROPERTIES

Locality/ Sample #	% Clay (<.002 mm)	% Silt (.002-.063 mm)	% Sand (.063-2 m)
S1 CA-108-SE	24.0	29.8	46.2
S2 CA-90-SE	42.4	31.9	2.7
S3 CA-210-S15.5	59.6	35.7	25.7
S4 CA-EO397-SE	43.0	32.1	24.9
S5 CA-383-SW, 1S	36.8	43.0	20.2
S5 CA-383-SE, 1UC	45.0	35.0	20.0
6 JD-101-SE	50.6	45.7	3.7
S7 JD-WE-SW, 1UC	52.2	40.6	7.2
S7 JD-WE-SW, UC	41.3	47.1	11.5
S7 JD-WE-NW, 1S	43.5	48.5	8.0
S7 JD-WE-NW, 2S	47.5	45.1	7.4
S8 JD-395-SE	51.9	44.2	3.9
S9 JD-EO395-NW	60.1	35.6	4.3
S10 JD-102-SE	59.2	37.8	3.0
S11 AC-1123-NW	47.3	46.5	6.1
S12 AC-Bridge, UC	37.0	60.3	2.7
S13 AC-LA369-NW, UC	40.3	54.6	5.0
S14 AC-ES-NW, UC Stable	46.2	50.0	3.8
S14 AC-ES-NW, UC Slump	53.8	44.4	1.8
S14 AC-ES-NE, 1S	40.6	53.3	6.1
S14 AC-ES-NE, 2S	39.9	57.0	3.1
S15 AC-EO1111-SW, UC	63.1	35.4	1.5
S15 AC-EO1111-NW, 1S	54.0	43.5	2.6
S15 AC-EO1111-NW, 2S	46.8	50.9	2.3
S16 AC-722-SW	40.7	54.4	4.9
S17 AC-95-NE, UC	52.2	44.6	3.2
S17 AC-95-NE, 1UC	67.7	30.6	1.8
S17 AC-95-NW, S	62.0	36.3	1.7
S18 AC-343-NW	40.5	57.5	20.0
S19 LA-724-NE, S	37.3	43.2	19.5
S20 LA-AC-NE, S	37.1	51.1	11.8
S21 LA-167-NW	24.7	73.0	2.4
S22 LA-354-NW	31.4	67.5	1.2

TABLE A7

GEOTECHNICAL PROPERTIES*

LOCALITY/ SAMPLE #	LL	PL	PI	BULK DENSITY	MOISTURE
S1 CA-108-SE	26.9	11.8	15.1	1.8	17.8
S2 CA-90-SE	43.5	13.9	29.6	1.4	34.0
S3 CA-210-SW	54.0	19.9	34.1	1.5	29.6
S4 CA-EO397-SE	41.2	14.9	26.3	1.6	22.9
S5 CA-383-SW,1S	40.0	11.7	28.3	1.7	20.7
S5 CA-383-SE, 1UC	39.9	18.5	21.4	---	----
S6 JD-101-SE	52.5	27.6	24.9	1.5	27.8
S7 JD-WE-SW, 1UC	46.8	19.4	27.4	---	----
S7 JD-WE-SW, UC	40.9	9.6	31.2	---	----
S7 JD-WE-NW, 1S	46.6	15.6	31.0	1.5	23.7
S7 JD-WE-NW, 2S	46.8	13.7	33.0	1.5	24.5
S8 JD-395-SE	57.8	18.4	39.3	1.4	32.1
S9 JD-EO395-NW	62.0	21.6	40.4	1.4	32.4
S10 JD-102-SE	58.0	20.6	37.4	1.4	32.4
S11 AC-1123-NW	51.5	19.5	32.0	1.3	36.1
S12 AC-Bridge, UC	38.1	21.1	17.0	---	----
S13 AC-LA369-NW, UC	43.4	14.9	28.5	---	----
S14 AC-ES-NW, UC Stable	57.6	22.4	35.2	---	----
S14 AC-ES-NW, UC Slump	45.3	18.8	26.5	---	----
S14 AC-ES-NE, 1S	38.9	18.0	21.0	1.2	30.6
S14 AC-ES-NE, 2S	40.6	11.8	28.9	1.5	24.5
S15 AC-EO1111-SW, UC	64.3	25.3	39.0	---	----
S15 AC-EO1111-NW, 1S	53.6	17.2	36.4	1.3	31.4
S15 AC-EO1111-NW, 2S	44.5	12.8	31.7	1.5	23.0
S16 AC-722-SW	43.1	16.5	26.6	1.5	25.2
S17 AC-95-NE, UC	51.9	18.8	33.1	---	----
S17 AC-95-NE, 1UC	69.0	21.0	48.0	---	----
S17 AC-95-NW, S	63.0	16.9	46.1	1.3	30.5
S18 AC-343-NW	44.4	17.4	27.1	1.5	26.4
S19 LA-724-NE, S	39.6	12.0	27.6	1.6	16.6
S20 LA-AC-NE, S	36.2	17.0	19.2	1.6	18.7
S21 LA-167-NW	32.9	24.5	8.3	1.5	19.9
S22 LA-354-NW	39.8	21.0	18.8	1.6	27.3

* LL = Liquid Limit
PL = Plastic Limit
PI = Plasticity Index
Bulk Density = Bulk Density
Moisture = % Moisture

TABLE A8

OTHER PHYSICAL PROPERTIES

Locality/ Sample #	% Organic Carbon	pH	Slope Angle (degrees)
S1 CA-108-SE	.18	7.6	15.5
S2 CA-90-SE	.48	7.8	26
S3 CA-210-SW	.41	7.8	15
S4 CA-EO397-SE	.28	8.0	14.5
S5 CA-383-SW, 1S	.15	7.5	14.5
S5 CA-383-SE, 1UC	.23	6.9	14.5
S6 JD-101-SE	.65	7.8	15
S7 JD-WE-SW, 1UC	.51	7.4	18.5
S7 JD-WE-SW, UC	.67	7.2	18.5
S7 JD-WE-NW, 1S	.20	7.6	18.5
S7 JD-WE-NW, 2S	.20	7.6	18.5
S8 JD-395-SE	.51	7.8	19
S9 JD-EO395-NW	.35	8.0	20.5
S10 JD-102-SE	.28	8.2	20
S11 AC-1123-NW	.61	7.6	22
S12 AC-Bridge, UC	.63	6.7	16
S13 AC-LA369-NW, UC	.36	6.3	14.5
S14 AC-ES-NW, UC Stable	.20	7.7	20
S14 AC-ES-NW, UC Slump	.16	6.8	20
S14 AC-ES-NE, 1S	.91	7.3	19.5
S14 AC-ES-NE, 2S	.59	7.1	19.5
S15 AC-EO1111-SW, UC	.20	7.5	22
S15 AC-EO1111-NW, 1S	.16	7.1	22
S15 AC-EO1111-NW, 2S	.24	7.7	22
S16 AC-722-SW	.48	7.7	18
S17 AC-95-NE, UC	.51	7.4	16
S17 AC-95-NE, 1UC	.20	7.4	16
S17 AC-95-NW, S	.28	7.7	15
S18 AC-343-NW	.38	7.8	21.5
S19 LA-724-NE, S	.12	7.2	18.5
S20 LA-AC-NE, S	.83	7.0	16.5
S21 LA-167-NW	.65	7.0	14
S22 LA-354-NW	.61	7.6	18

APPENDIX 3

CLAY MINERALOGY SUMMARIES

This appendix contains the semi-quantitative clay mineralogy analysis data. Clay minerals identified in the samples are mica, smectite, kaolinite, and mica-smectite mixed interlayer. No chlorite was identified in any of the samples. The last column contains net smectite which approximates the total amount of smectite in that sample. This is done by multiplying the clay content by the percent smectite.

Clay mineral identification was performed according to the procedures discussed in Smith (15) and Mutchler (16).

For the I-20 study area, Table A9 summarizes the clay percentages. An "*" denotes samples taken from the stable part of a failed slope. When an "*" appears within a slope quadrant, the samples without an "*" are from failures. If an "*" does not appear next to any sample numbers within a particular slope quadrant, then the slope is stable. An "NR" next to a number states that the sample is not representative for this slope because the material was probably imported to repair the slope. This data was not included in the statistics. Data is arranged in order of occurrence from west to east. See Table 1 for abbreviations.

The clay mineralogy for the I-10 study area is summarized in Table A10.

TABLE A9a

CLAY MINERALOGY

SAMPLE & SLOPE	% KAOLINITE	% MICA	% MIXED INTERLAYER	% SMECTITE	% NET SMECTITE
OPSFSW-1	10	25	25	40	21
OPSFSE-1	10	25	30	35	19
OPPMSW-1	15	15	25	45	8
OPPMSE-1	10	20	25	45	14
OPMHSW-1	10	20	30	40	32
OPMHSE-1	10	20	30	40	32
RPSISW-1	20	35	30	15	3
RPSISE-1	15	30	35	20	4
RPGOSW-1	10	25	30	35	19
RPGOSE-1	15	20	30	35	16
RPRESW-1	15	20	35	30	5
RPRESE-1	10	15	35	40	7
RPBBSW-1	5	15	30	30	7
RPBBSE-1	10	15	30	45	10
RPBHSW-1	10	15	25	50	15
RPBHSE-1	5	15	40	40	5
RPHRSW-1	10	35	20	35	10
RPHRSE-1	10	20	40	30	10
RPDISW-1	10	10	50	30	8
RPDISE-1	10	15	35	40	13
RPDDSW-1	15	15	35	35	7
RPDDSE-1	10	15	25	50	11
RPDONW-1	10	35	20	35	8
RPDONE-1	100				

TABLE A9b

CLAY MINERALOGY

SAMPLE & SLOPE		% KAOLINITE	% MICA	% MIXED INTERLAYER	% SMECTITE	% NET SMECTITE
MPCBNE	1*	10	25	--	65	30
	2	5	20	--	75	46
	3	10	20	--	65	36
	4	10	20	--	70	38
	5*	10	20	--	70	39
	6	10	20	--	70	39
MPCBNW	1*	5	20	--	75	30
	2	25	20	--	75	56
	3	10	20	5	65	39
	4	5	20	--	80	50
	5	10	20	--	70	44
	6	5	10	--	80	34
MPCBSE	1*	10	20	--	70	39
	2	10	20	5	65	38
	3	10	20	--	70	47
	4	10	10	15	65	46
	5	10	20	5	65	40
	6	15	20	10	55	28
	7*	10	20	--	70	19 NR
MPCBSW	1	10	25	--	65	26 NR
	2*	5	25	--	70	18 NR
	3	10	25	--	65	16 NR
	4	5	20	--	75	25 NR
	5	5	20	--	70	20 NR
	6	5	15	--	80	29 NR
	7	5	15	--	80	61 NR
MPWNE	1	5	15	--	80	46
MPWNW	1	10	20	--	70	46
MPWSE	1	10	20	5	65	51
MPWSW	1	10	15	--	75	40
MPTNNE	1*	10	20	5	65	23
	2*	10	15	--	75	41
	3	5	15	--	80	42
	4	5	20	--	75	40

* = Sample taken from stable part of failed slope.
NR = Sample not representative of parent material.

TABLE A9c

CLAY MINERALOGY

SAMPLE & SLOPE		% KAOLINITE	% MICA	% MIXED INTERLAYER	% SMECTITE	% NET SMECTITE
MPTNNW	1*	5	15	--	80	48
	2	10	20	--	70	46
	3	10	20	--	70	48
	4	5	20	--	75	47
	5*	5	20	--	75	45
MPTNSE	1*	10	20	--	70	40
	2	5	10	--	85	49
	3	10	20	5	65	37
MPTNSW	1*	5	15	--	80	39
	2*	10	15	--	75	47
	3	15	20	5	60	34
	4	15	20	--	65	42
MPQUNE	1*	10	20	15	55	25
	2	5	20	--	75	24
	3	15	20	5	60	32
	4	10	15	--	75	38
MPQUNW	1	10	15	20	55	25
	2	10	20	5	65	29
	3	10	20	--	70	31
MPQUSE	1*	10	15	--	75	35
	2*	10	15	--	65	31
	3	5	20	--	75	35
	4	5	20	--	75	38
MPQUSW	1	10	15	--	75	32
	2	10	25	--	65	29
	3	15	20	--	65	31
MPCMNE	1*	10	20	5	65	51
	2	10	15	5	70	61
	3	10	25	--	65	49
	4	5	10	--	85	71
	5	10	15	--	75	69
	6	10	15	--	75	68
	7*	10	10	--	80	62
	8*	10	15	--	75	60

* = Sample taken from stable part of failed slope.

TABLE A9d

CLAY MINERALOGY

SAMPLE & SLOPE		% KAOLINITE	% MICA	% MIXED INTERLAYER	% SMECTITE	% NET SMECTITE
MPCMNW	1*	10	20	--	70	43
	2	10	15	--	75	43
	4	10	20	15	55	44
MPCMSE	1*	10	15	--	75	58
	2*	10	15	--	75	56
	3	10	10	--	80	63
	4	10	15	--	75	56
	5	10	15	--	75	57
	6	10	10	--	80	59
	7	5	20	--	75	57
MPCMSW	1*	5	15	--	80	59
	2	10	20	--	70	55
	3*	5	25	5	65	47
	4	15	15	--	70	55
	5	10	15	--	75	54
MPTRNE	1*	10	10	5	75	34
	2	10	20	5	65	24
MPTRSW	1*	10	20	5	65	29
	2	5	15	--	80	43

* = Sample taken from stable part of failed slope.

TABLE A10

RELATIVE CLAY MINERAL PERCENTAGES*

Locality/ Sample #	% Kaol	% Mica	% Mixed Inter	% Smec	% Net Smec
S1 CA-108-SE	10	20	25	45	10.8
S2 CA-90-SE	5	30	20	45	19.1
S3 CA-210-SW	5	25	10	60	35.8
S4 CA-EO397-SE	10	25	20	45	19.4
S5 CA-383-SW, 1S	10	25	10	55	20.2
S5 CA-383-SE, 1UC	10	20	20	50	22.5
S6 JD-101-SE	5	15	5	75	38.0
S7 JD-WE-SW, 1UC	10	10	15	65	33.9
S7 JD-WE-SW, UC	10	10	0	80	33.0
S7 JD-WE-NW, 1S	10	15	25	50	21.8
S7 JD-WE-NW, 2S	10	15	15	60	28.5
S8 JD-395-SE	5	10	0	85	44.1
S9 JD-EO395-NW	5	20	5	70	42.1
S10 JD-102-SE	10	20	10	60	35.5
S11 AC-1123-NW	10	0	30	60	28.4
S12 AC-Bridge, UC	20	25	25	30	11.1
S13 AC-LA369-NW, UC	10	20	25	45	18.1
S14 AC-ES-NW, UC Stable	15	20	20	45	20.8
S14 AC-ES-NW, UC Slump	10	15	5	70	37.7
S14 AC-ES-NE, 1S	10	25	20	45	18.3
S14 AC-ES-NE, 2S	10	25	20	45	18.0
S15 AC-EO1111-SW, UC	5	25	20	50	31.6
S15 AC-EO1111-NW, 1S	10	20	0	70	37.8
S15 AC-EO1111-NW, 2S	15	20	15	50	23.4
S16 AC-722-SW	5	20	10	65	26.5
S17 AC-95-NE, UC	10	15	0	75	39.2
S17 AC-95-NE, 1UC	10	20	5	65	44.0
S17 AC-95-NW, S	10	20	0	70	43.4
S18 AC-343-NW	5	10	15	70	28.4
S19 LA-724-NE	10	20	25	45	16.8
S20 LA-AC-NE, S	10	25	15	50	18.6
S21 LA-167-NW	10	20	20	50	12.4
S22 LA-354-NW	5	20	20	55	17.3

* Kaol = Kaolinite, Mixed Inter = Mixed Interlayers
Smec = Smectite, Net Smec = Net Smectite

APPENDIX 4

SAMPLE LOCATION MAPS

I-10 Study Area Maps

Twenty-two embankment localities were sampled along the Interstate Highway 10 transect, which is about one half of the total embankment localities in the study area. Table III-1 lists the samples collected at each locality which correspond to the subject locality maps.

Each sample is labeled first with the abbreviated parish name (Calcasieu, CA; Jefferson Davis, JD; Acadia, AC; and Lafayette, LA) followed by the number of the identifying highway overpass, exit name, or interchange which the embankment was built to accommodate. The prefix "EO," meaning "east of," was attached to some highway numbers to clarify exact locations. For example EO1111 identifies the embankments for the overpass east of Highway 1111 along Interstate-10. The last portion of the hyphenated sample names specifies the embankment quadrant that was sampled: northeast (NE), northwest (NW), southeast (SE), and southwest (SW). Additional abbreviations on the end of the sample number include "UC," which stands for unconfined compression sample.

Each failure found has been spotted precisely on the locality maps (Figures A1 through A22) and classified according to (4). Annotations include "S" for slump, "SE" for slump-earthflow, and "EF" for earthflow. Calculated volumes, in cubic feet, and scarp heights are also noted on the maps and compiled in Table A12. Unless otherwise indicated, a blank embankment quadrant represents stable slopes or slopes with no failures of significance. Locations of sample pits are indicated by a small circle. These pits were filled and the slope surface restored as closely as possible to its original form upon completion of sampling.

TABLE A11

LOCALITY NUMBERS AND CORRESPONDING

SAMPLE NUMBERS

Parish	Locality #	Sample #
Calcasieu	S1	CA-108-SE
"	S2	CA-90-SE
"	S3	CA-210-SW
"	S4	CA-EO397-SE
"	S5	CA-383-SW,1-S
"		CA-383-SE,1-UC
Jefferson Davis	S6	JD-101-SE
"	S7	JD-WE-SW,1-UC
"	S7	JD-WE-SW,UC
"	S7	JD-WE-NW,1-S
"	S7	JD-WE-NW,2-S
"	S8	JD-395-SE
"	S9	JD-EO395-NW
"	S10	JD-102-SE
Acadia	S11	AC-1123-NW
"	S12	AC-BRIDGE,UC
"	S13	AC-La369-NW,UC
"	S14	AC-ES-NW,UC,Stable
"	S14	AC-ES-NW,UC,Slump
"	S14	AC-ES-NE,1-S
"	S14	AC-ES-NE,2-S
"	S15	AC-EO1111-SW,UC
"	S15	AC-EO1111-NW,1-S
"	S15	AC-EO1111-NW,2-S
"	S16	AC-722-SW
"	S17	AC-95-NE,UC
"	S17	AC-95-NE,1-UC
"	S17	AC-95-NW,S
"	S18	AC-343-NW
Lafayette	S19	LA-724-N
"	S20	LA-AC-NE
"	S21	LA-167-NW
"	S22	LA-354-NW

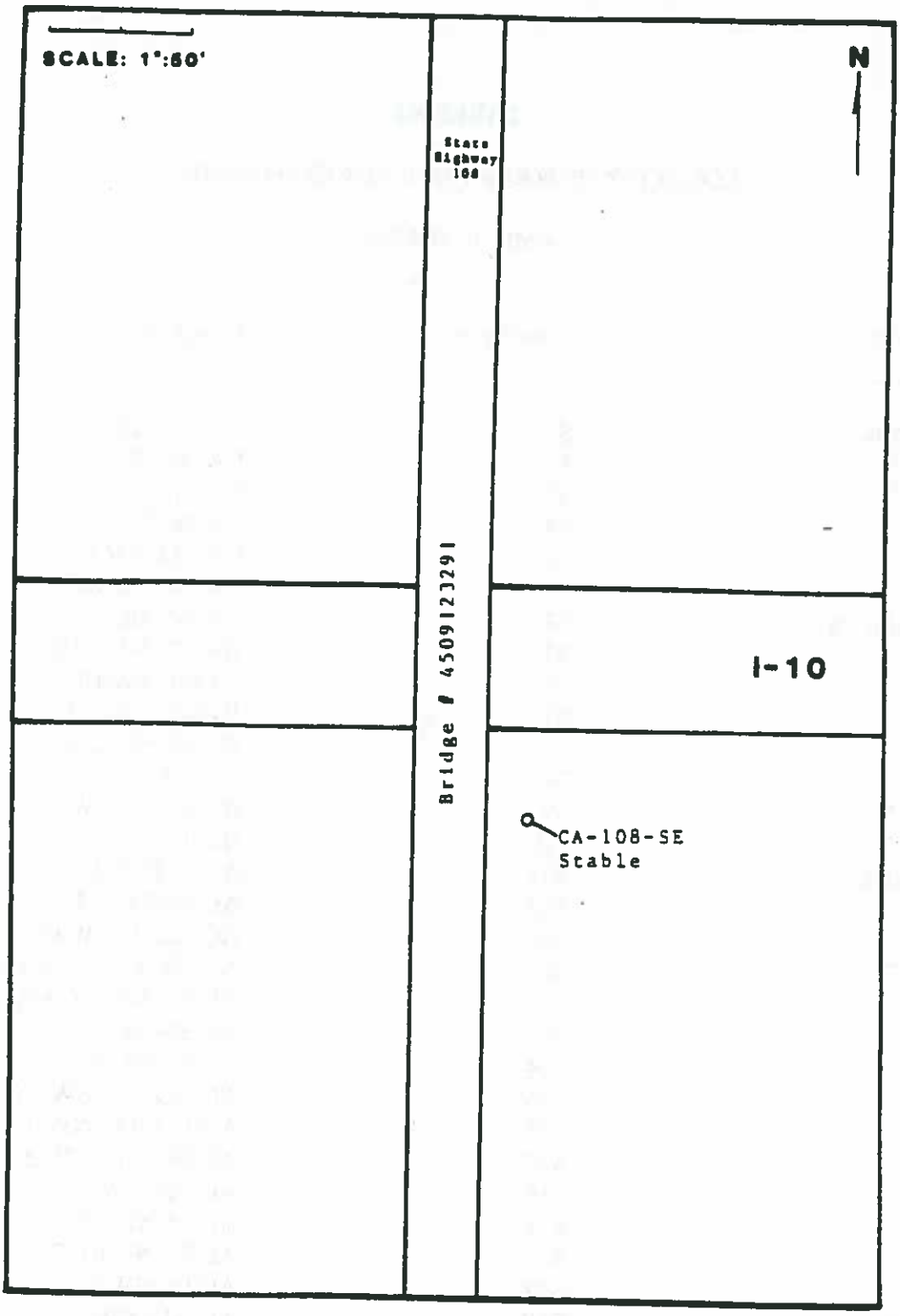

Figure A1. Locality S1, Calcasieu Parish.

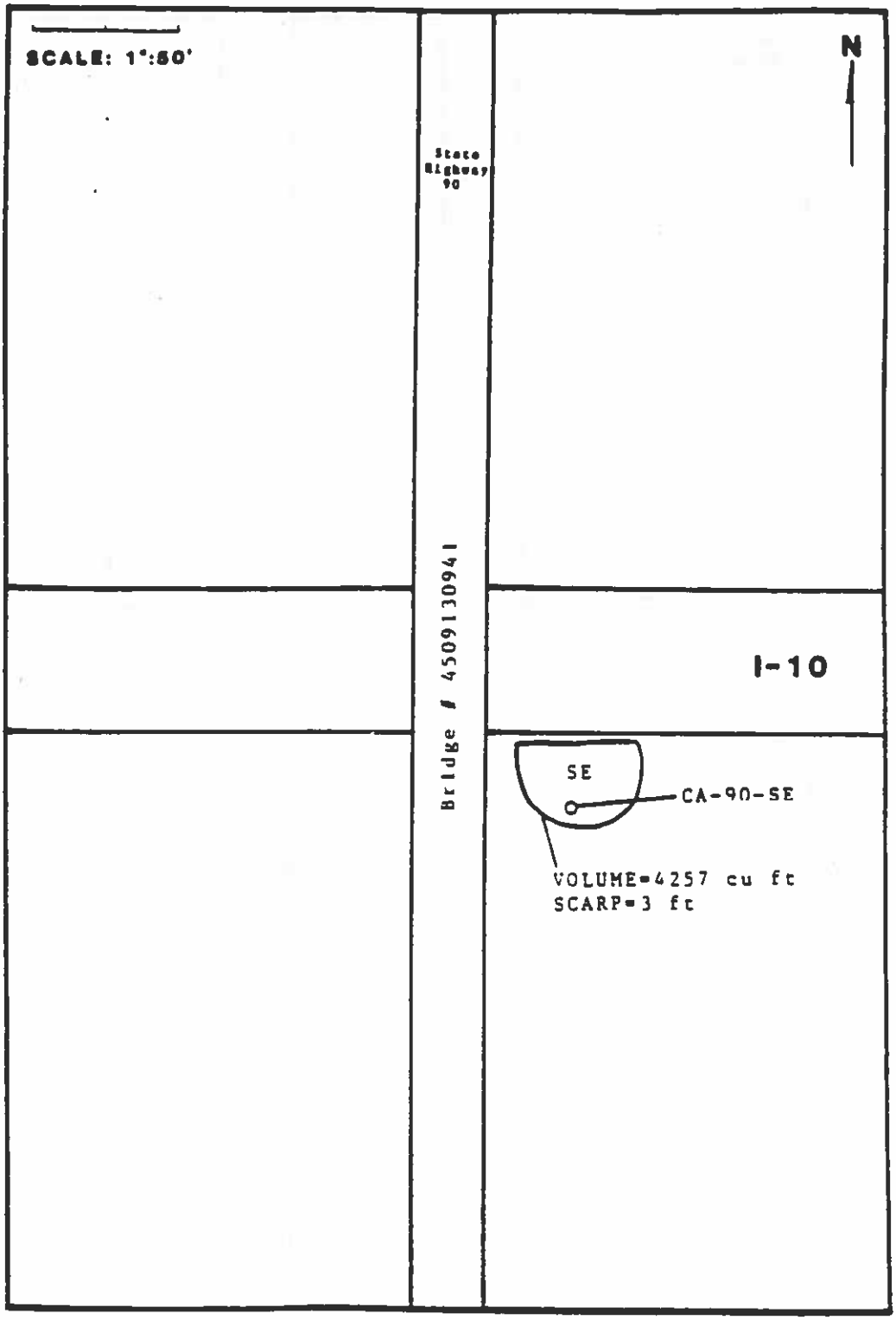

Figure A2. Locality S2, Calcasieu Parish.

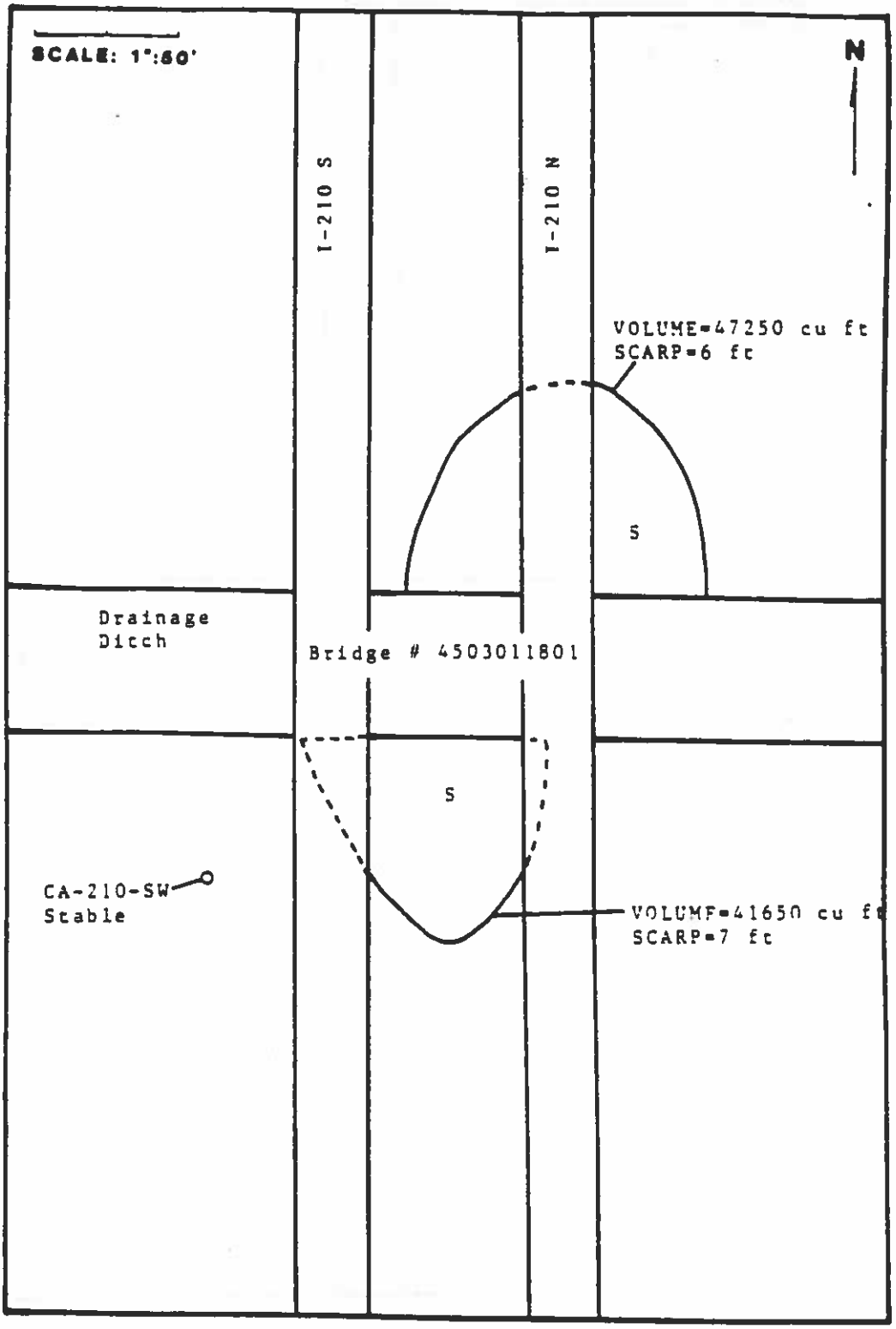

Figure A3. Locality S3, Calcasieu Parish.

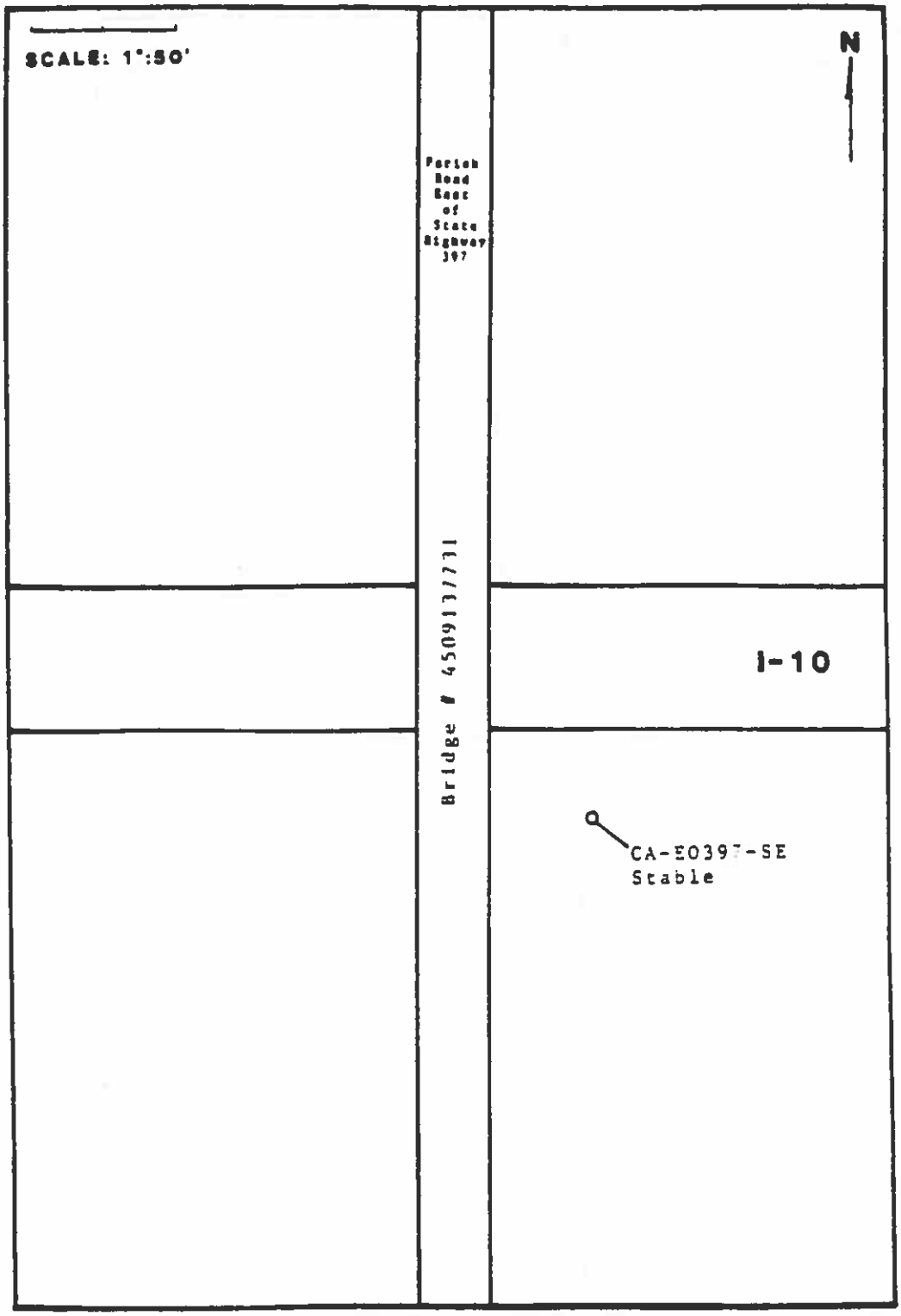

Figure A4. Locality S4, Calcasieu Parish.

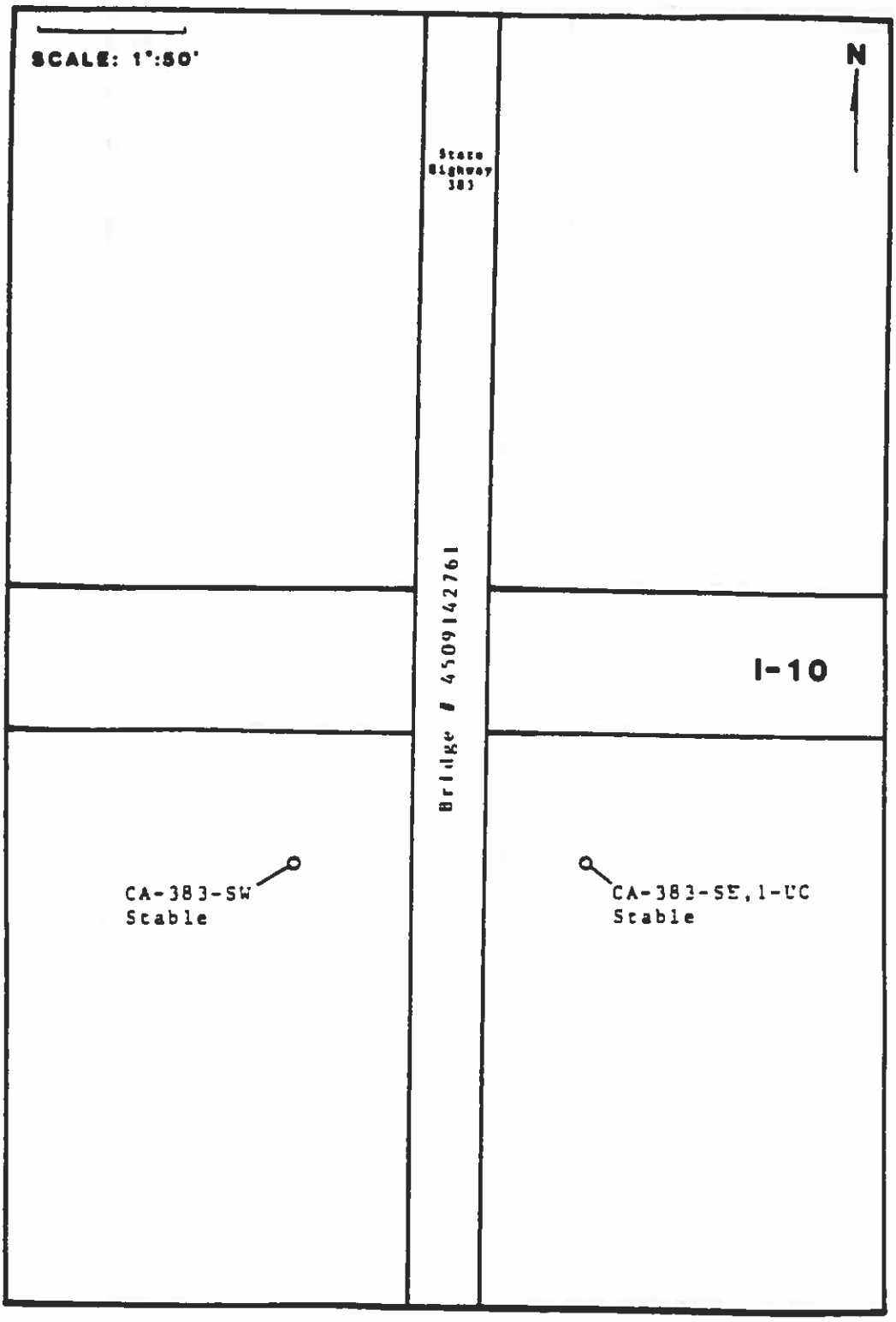

Figure A5. Locality S5, Calcasieu Parish.

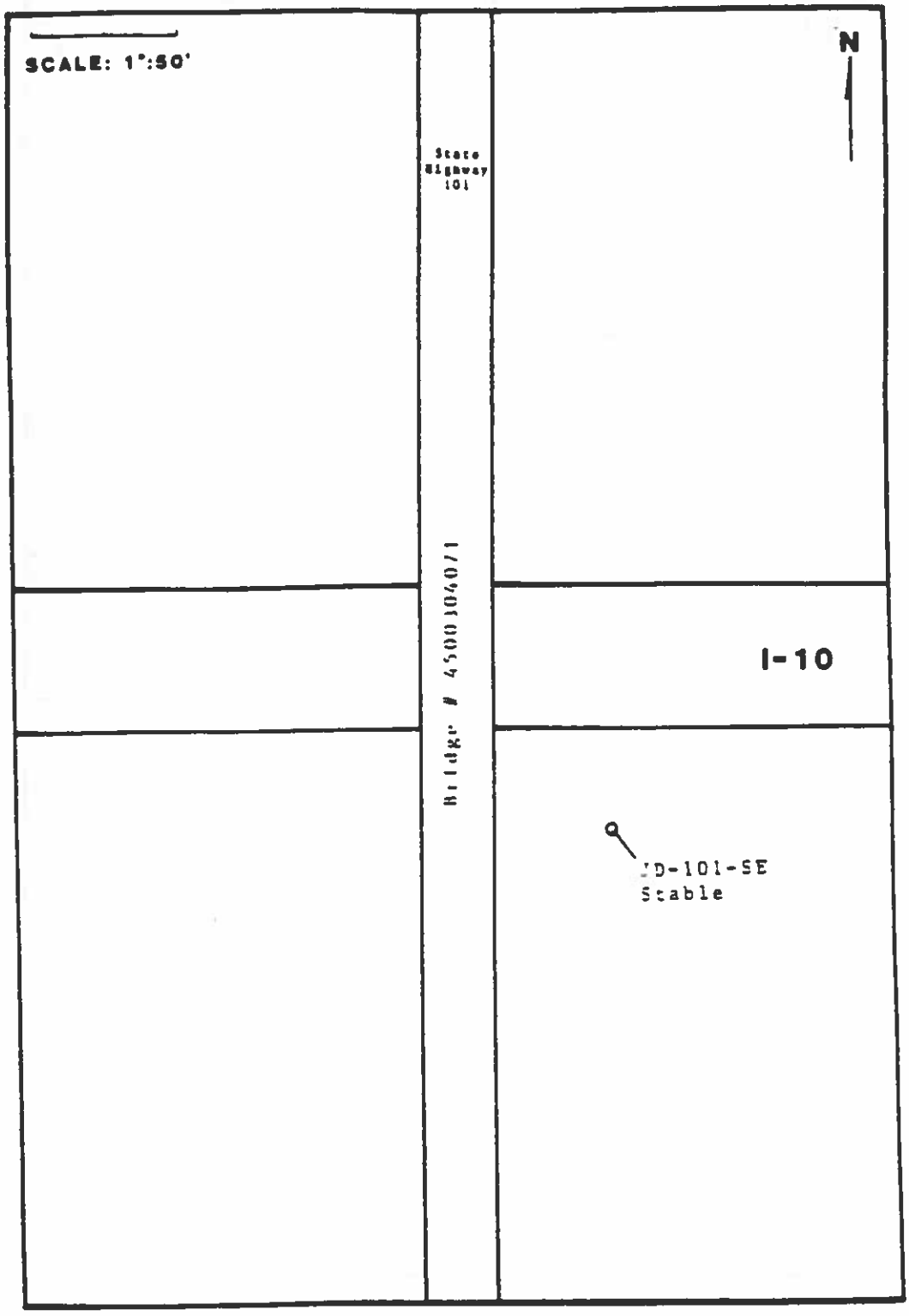

Figure A6. Locality S6, Jefferson Davis Parish.

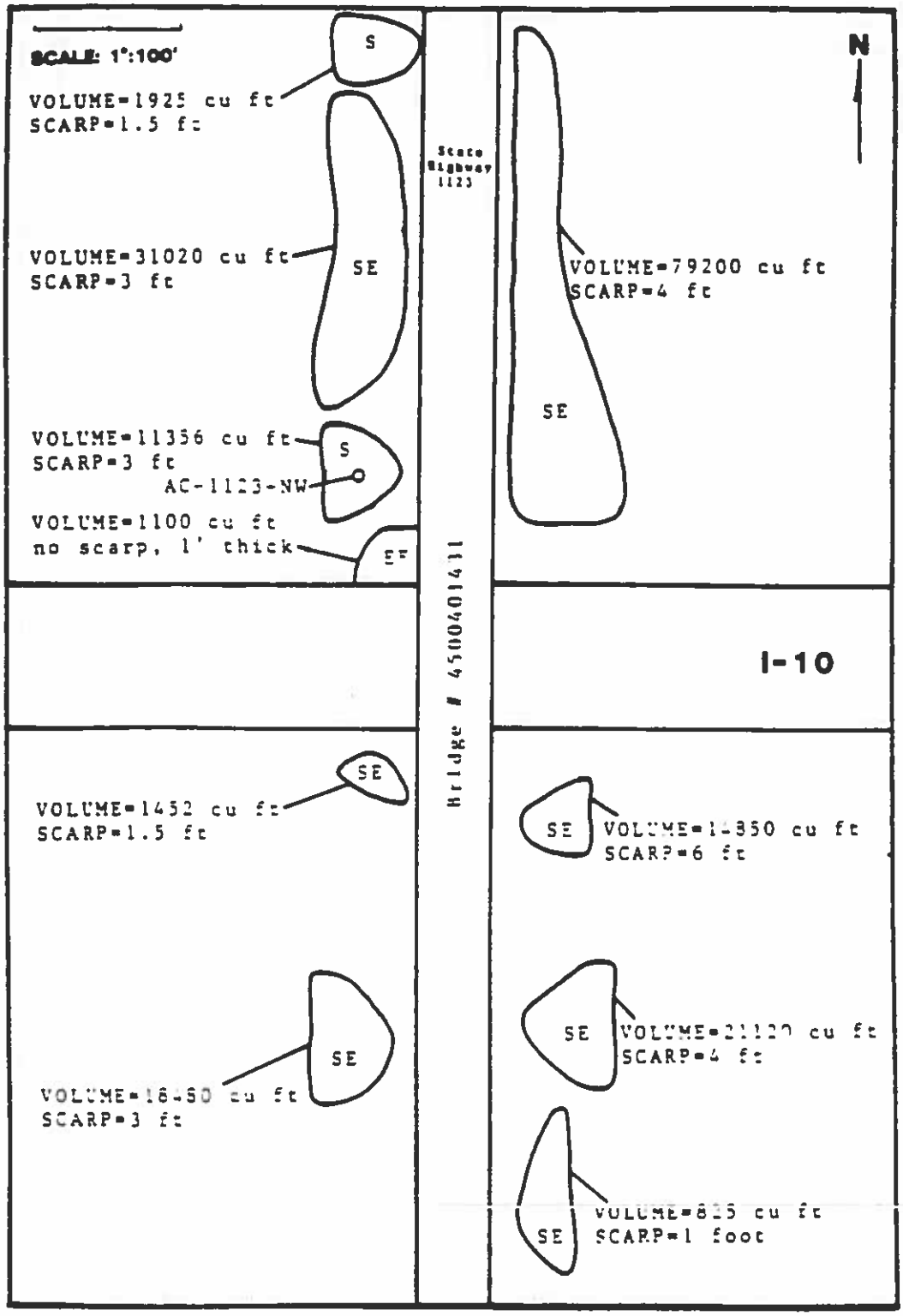

Figure A11. Locality S11, Acadia Parish.

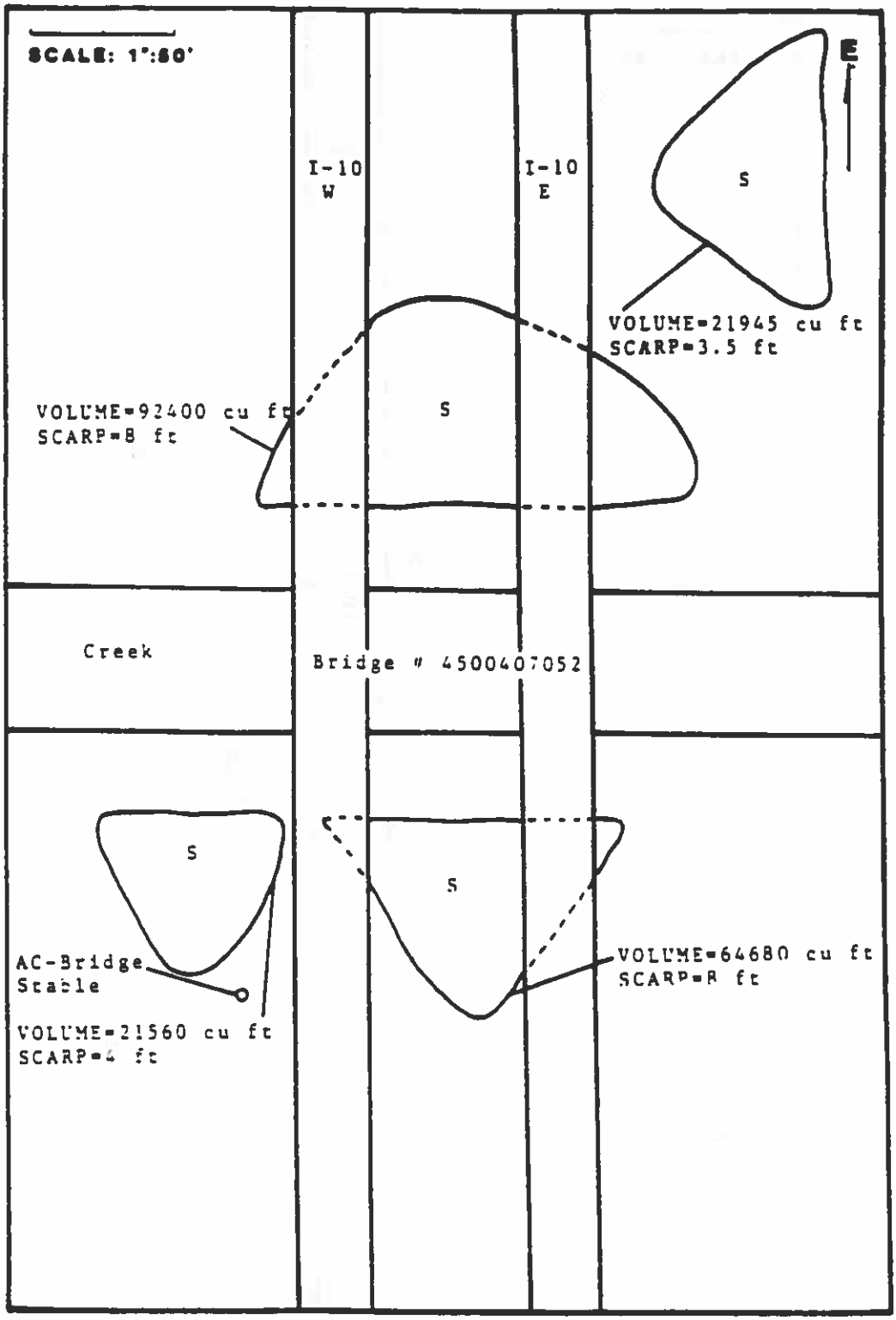

Figure A12. Locality S12, Acadia Parish.

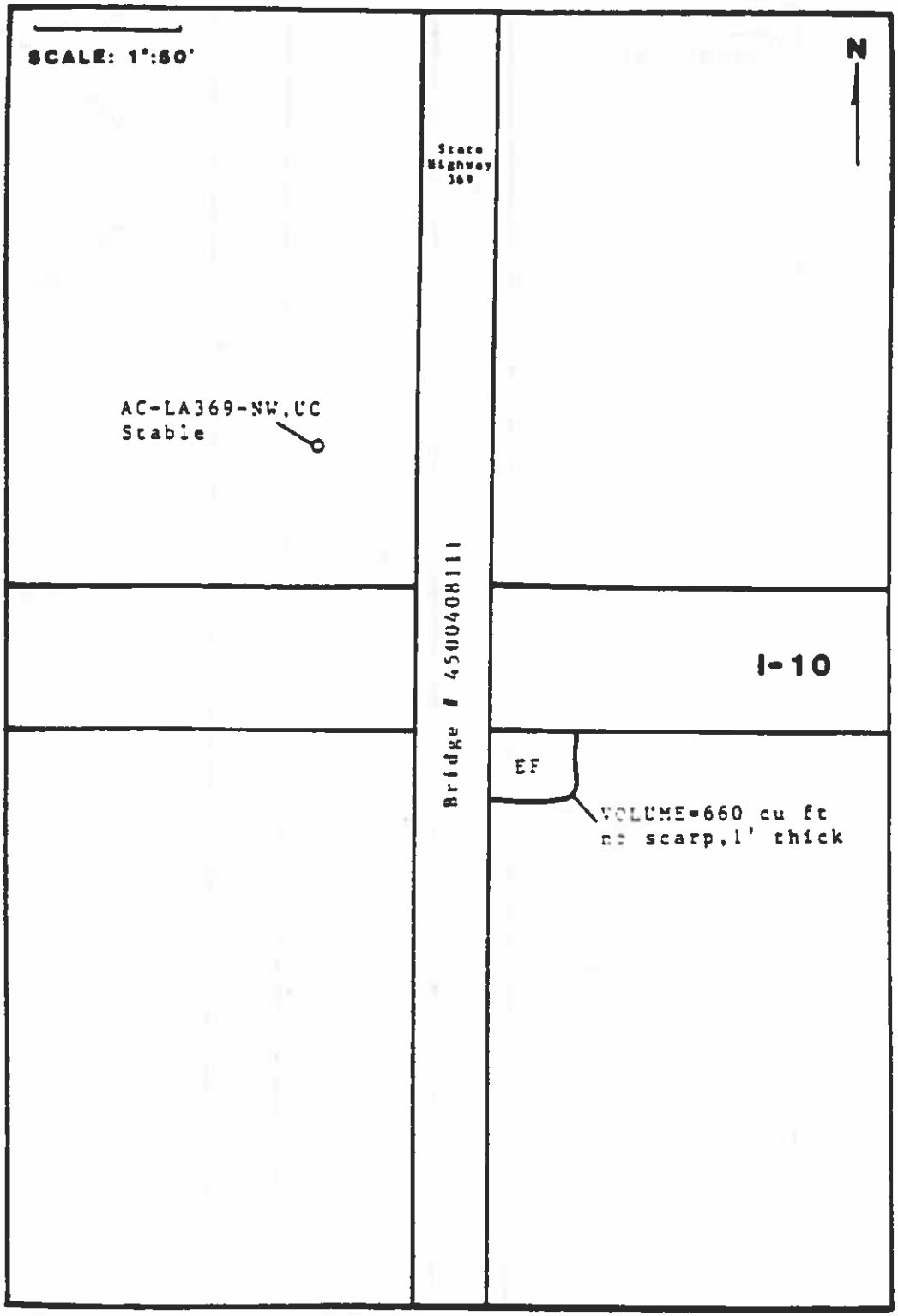

Figure A13. Locality S13, Acadia Parish.

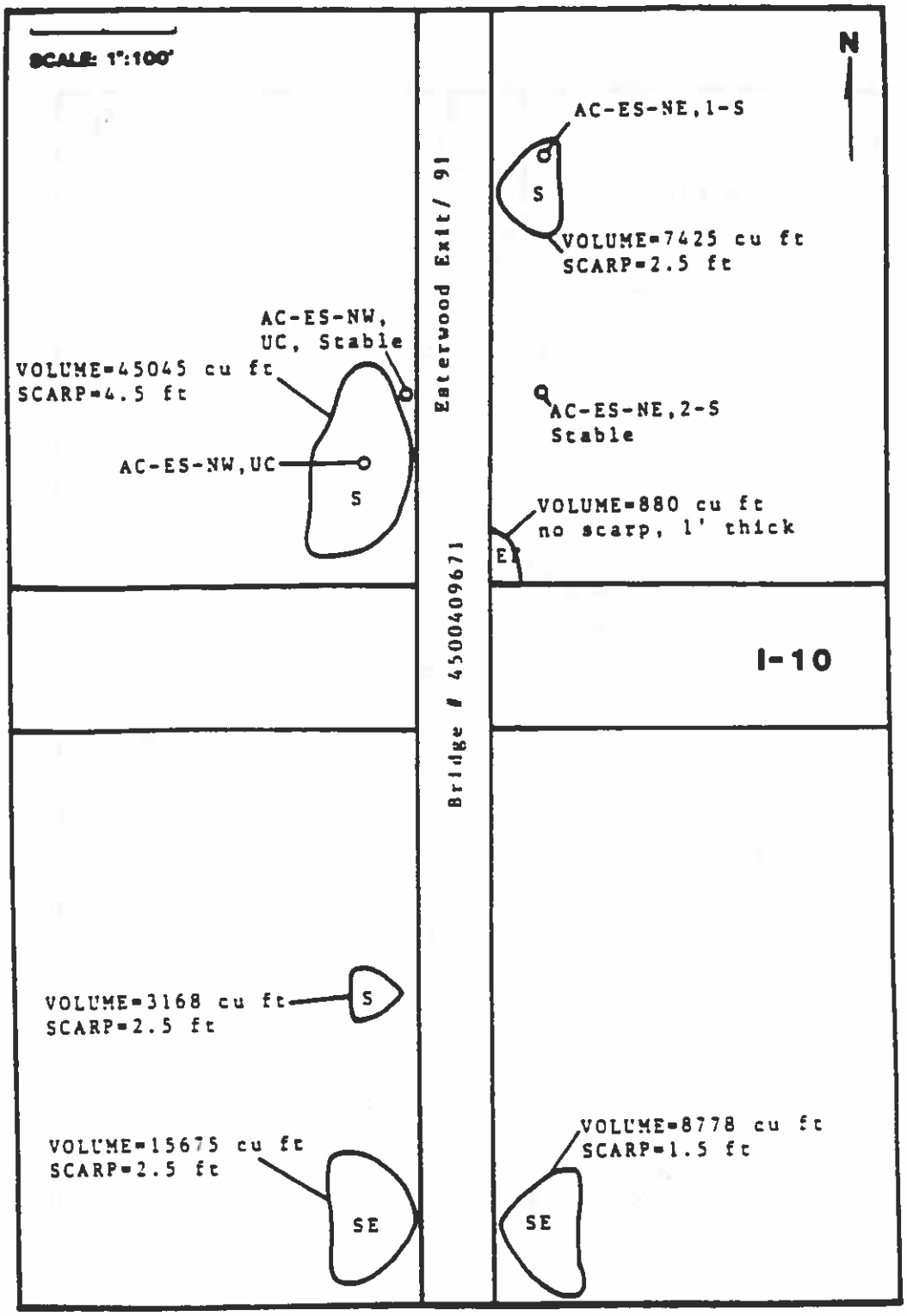

Figure A14. Locality S14, Acadia Parish.

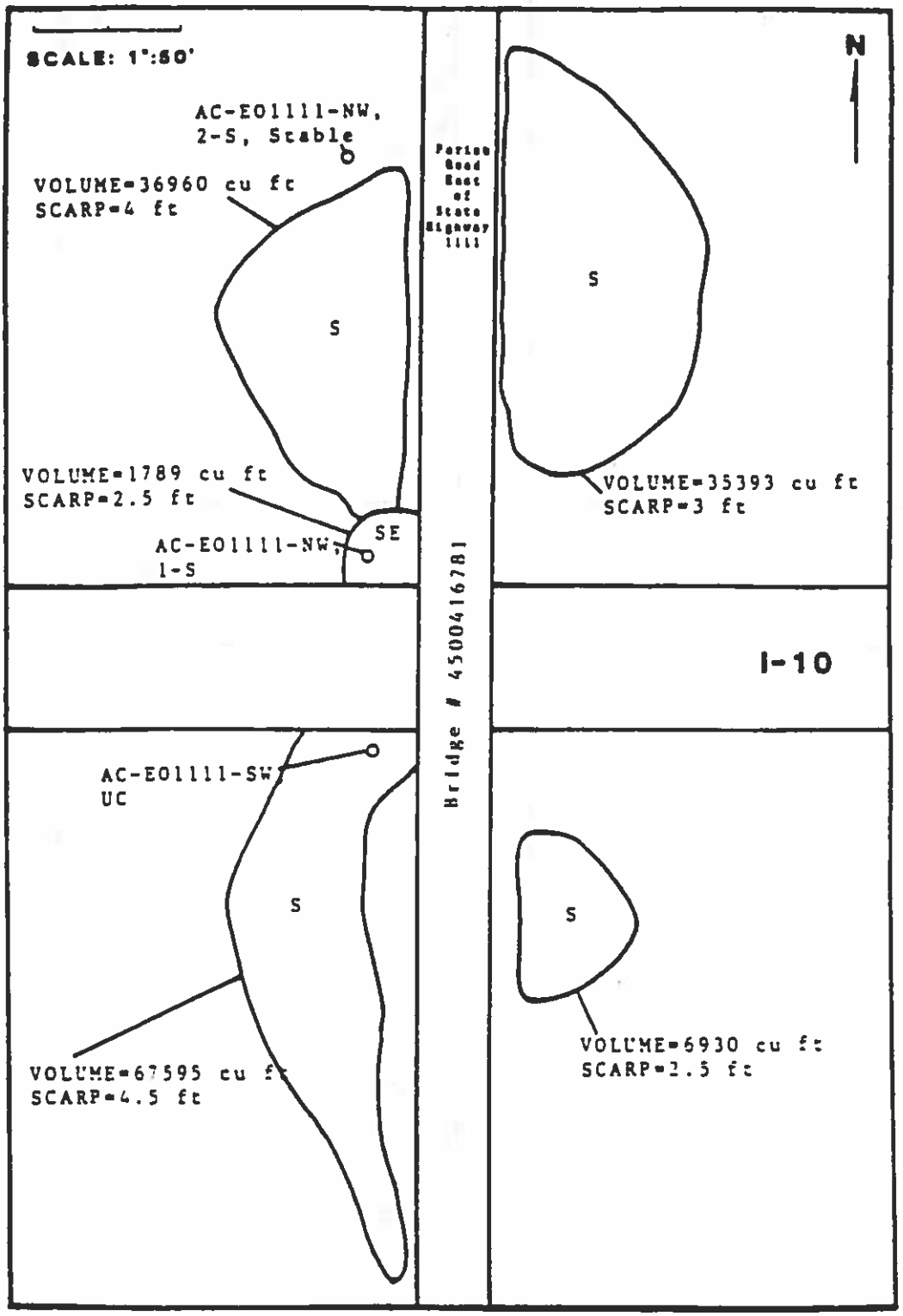

Figure A15. Locality S15, Acadia Parish.

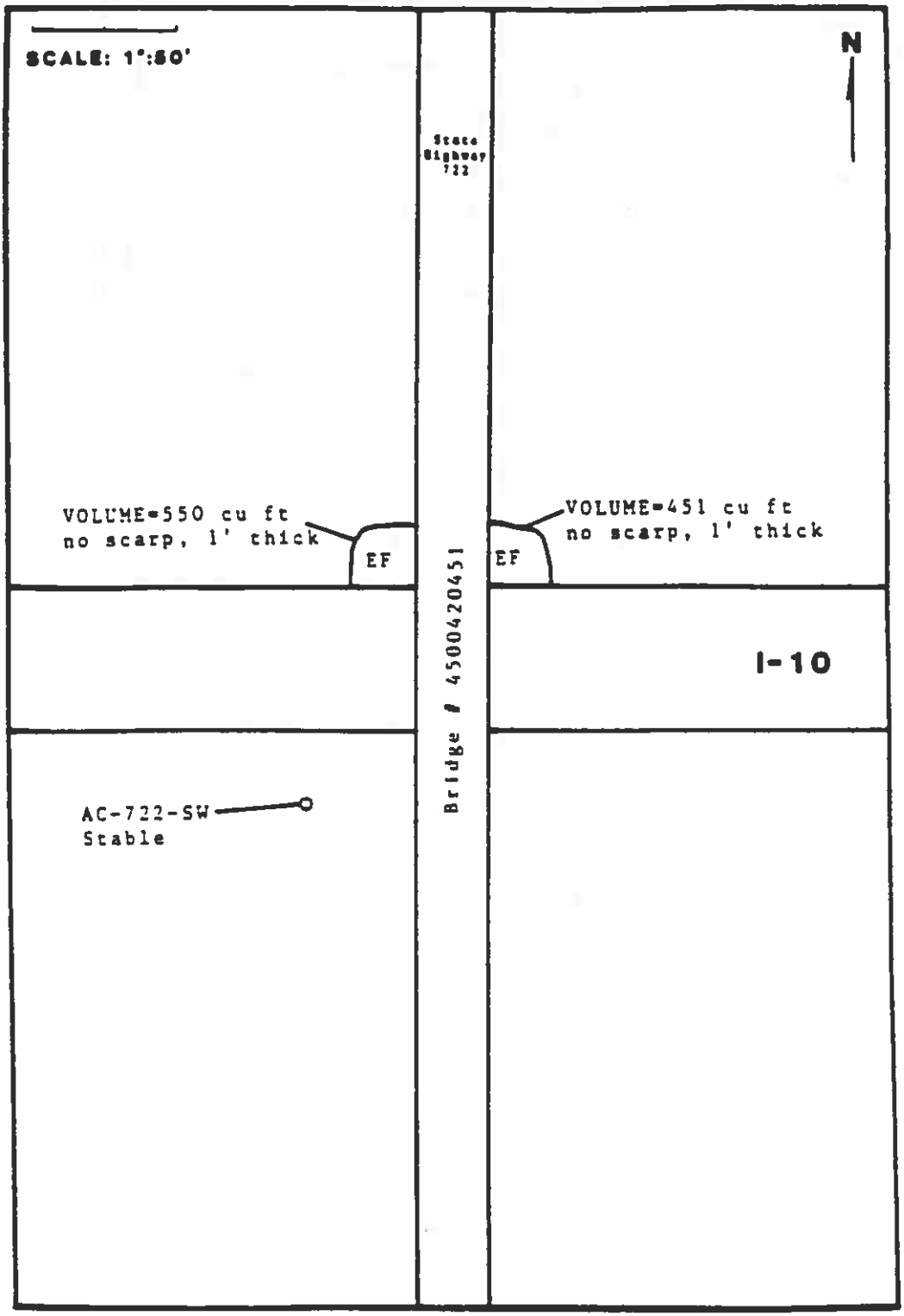

Figure A16. Locality S16, Acadia Parish.

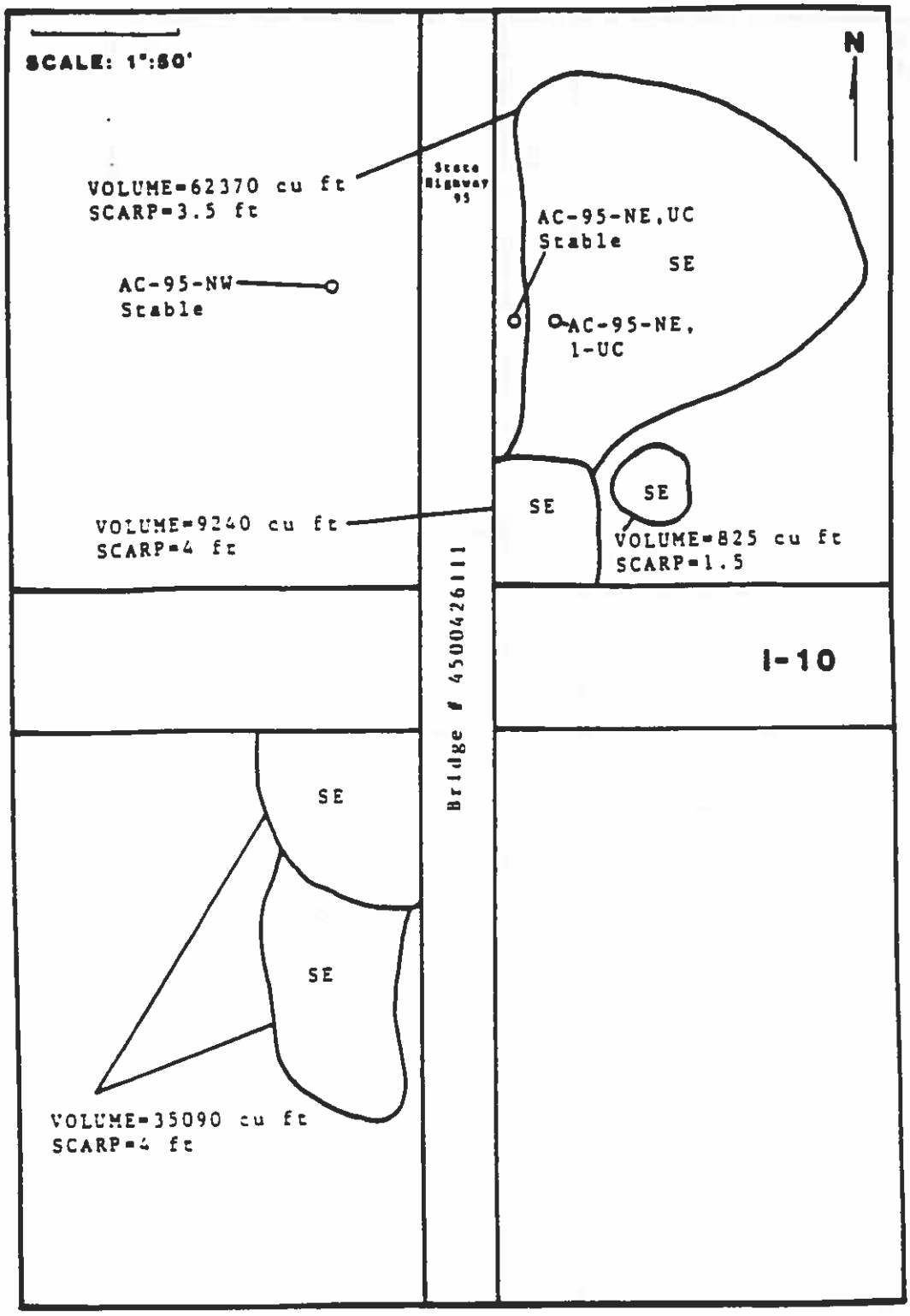

Figure A17. Locality S17, Acadia Parish.

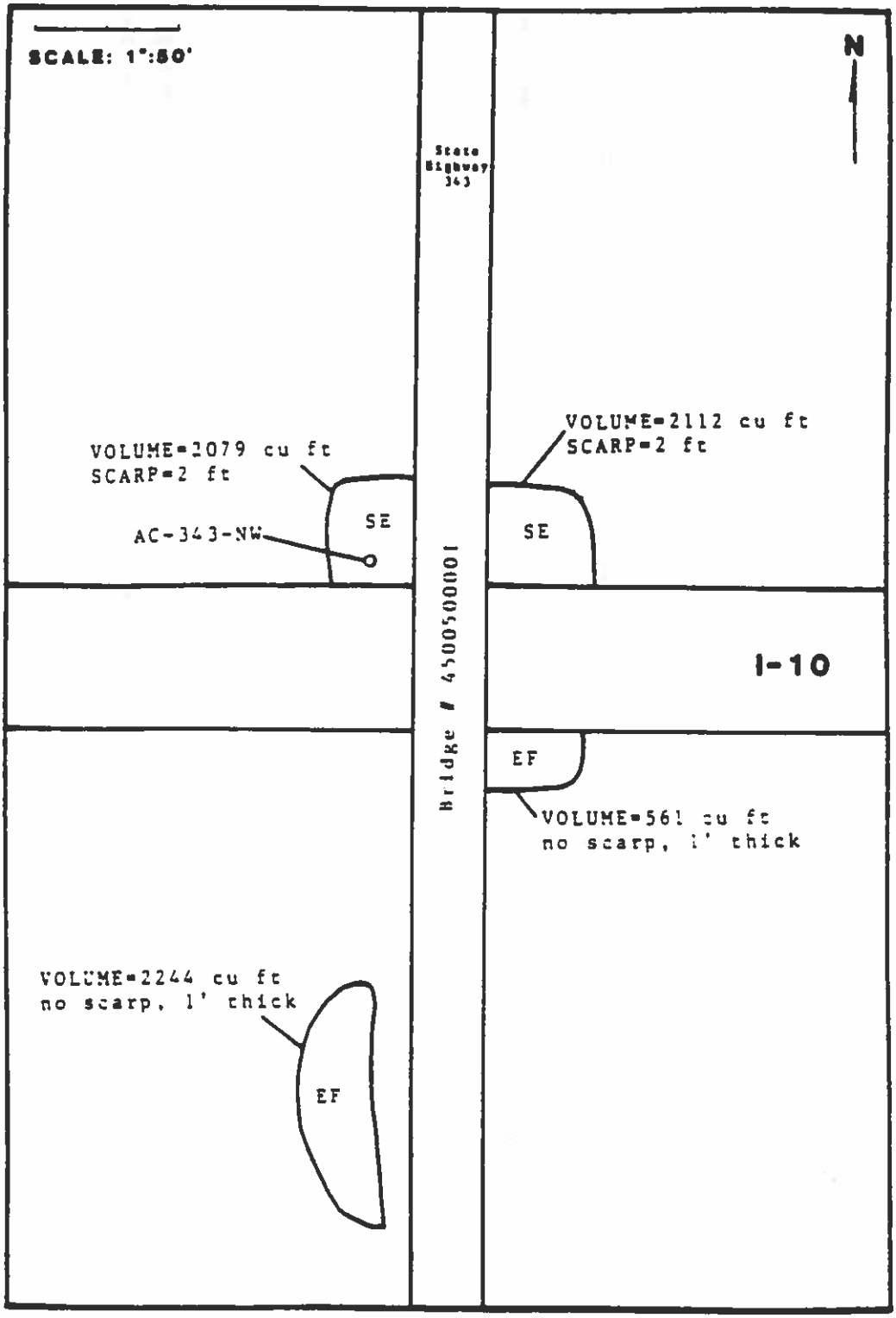

Figure A18. Locality S18, Acadia Parish.

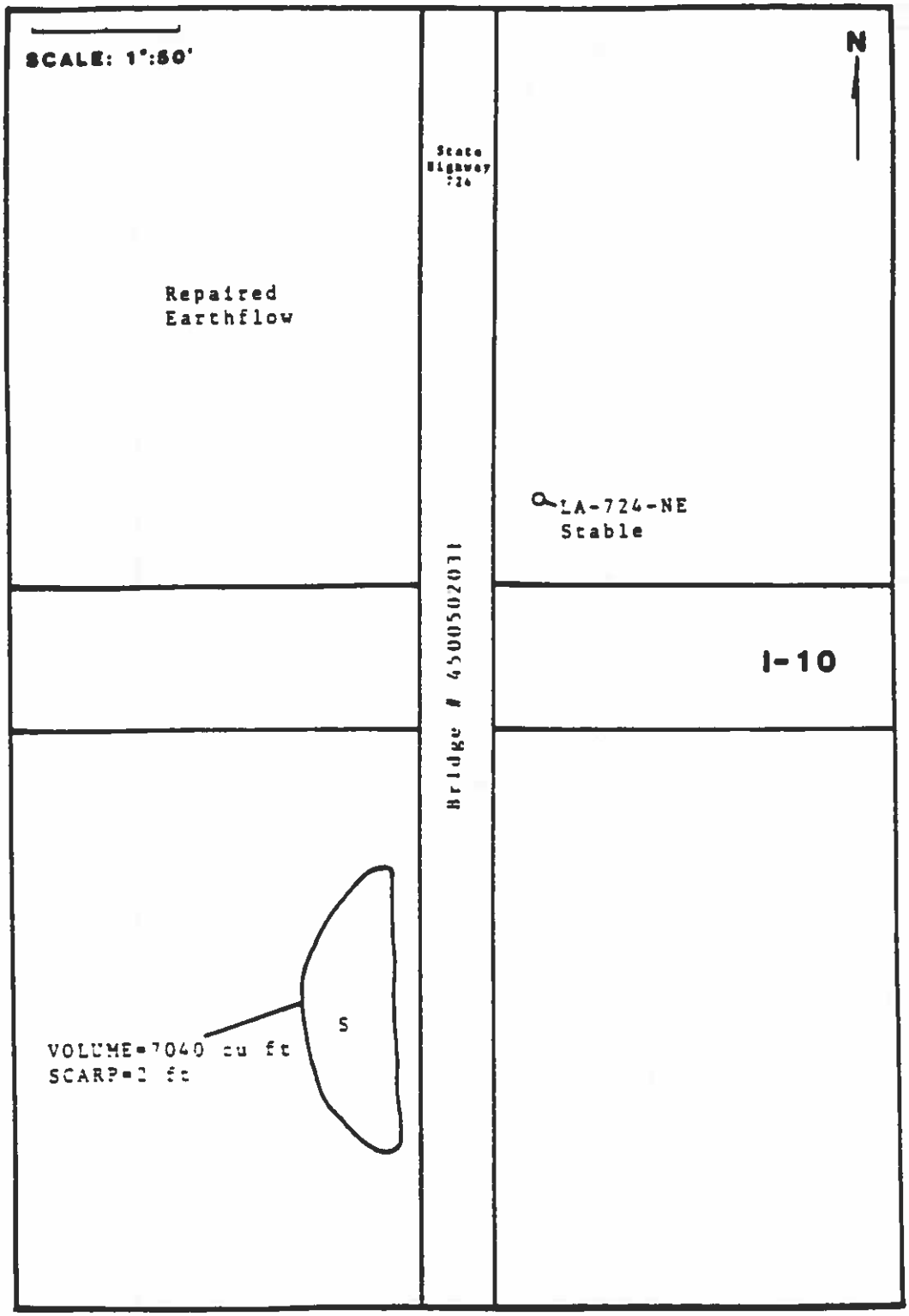

Figure A19. Locality S19, Lafayette Parish.

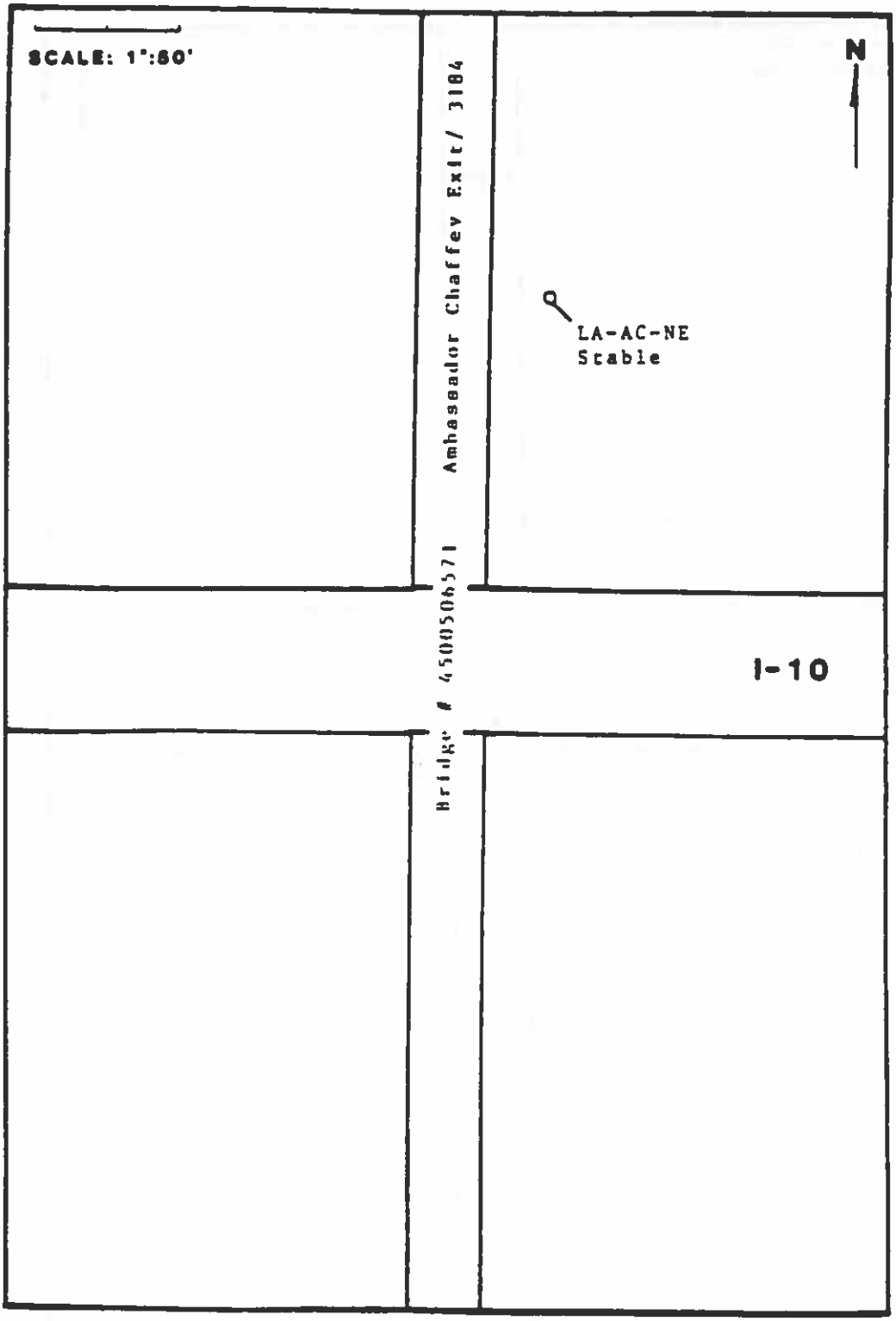

Figure A20. Locality S20, Lafayette Parish.

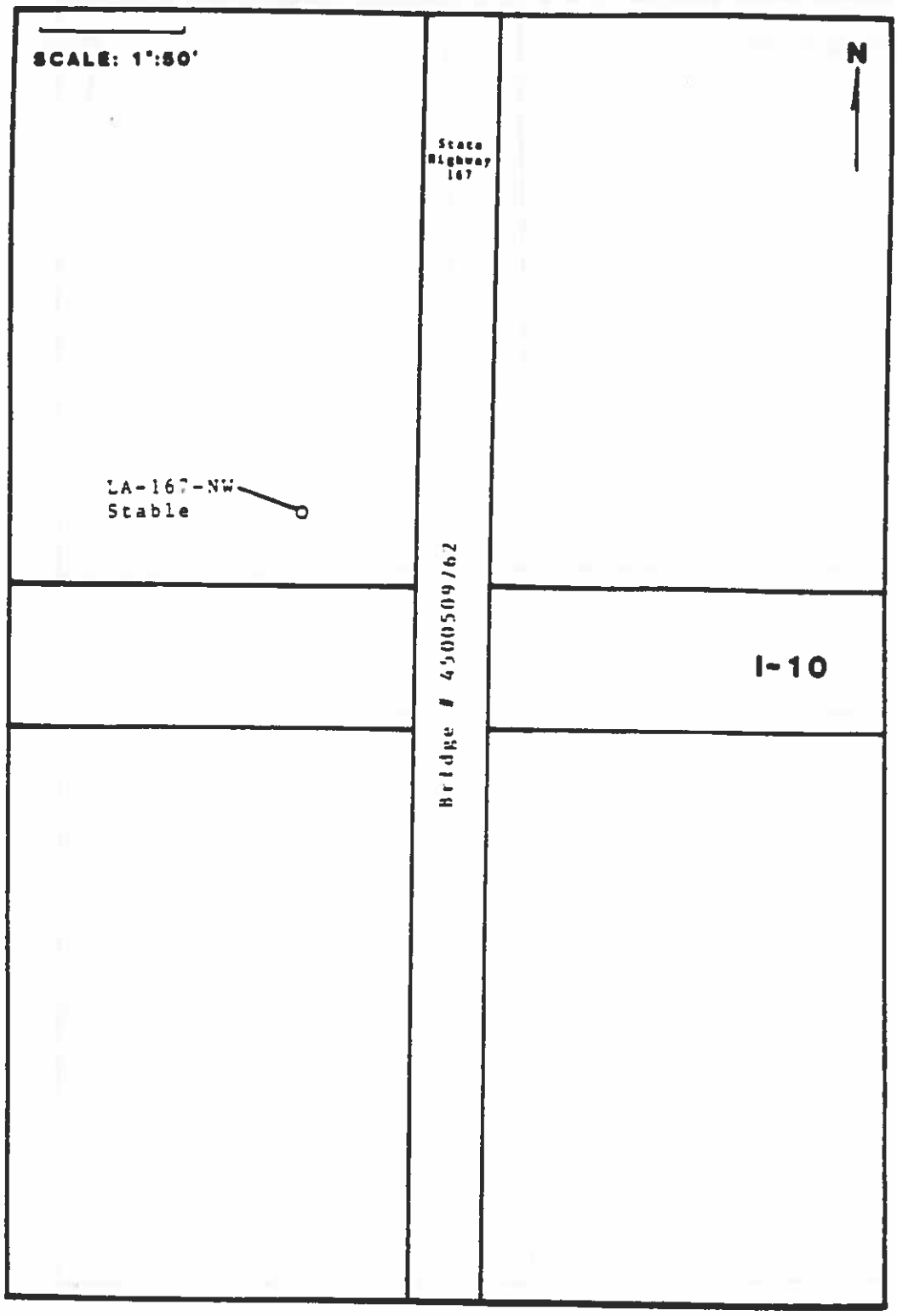

Figure A21. Locality S21, Lafayette Parish.

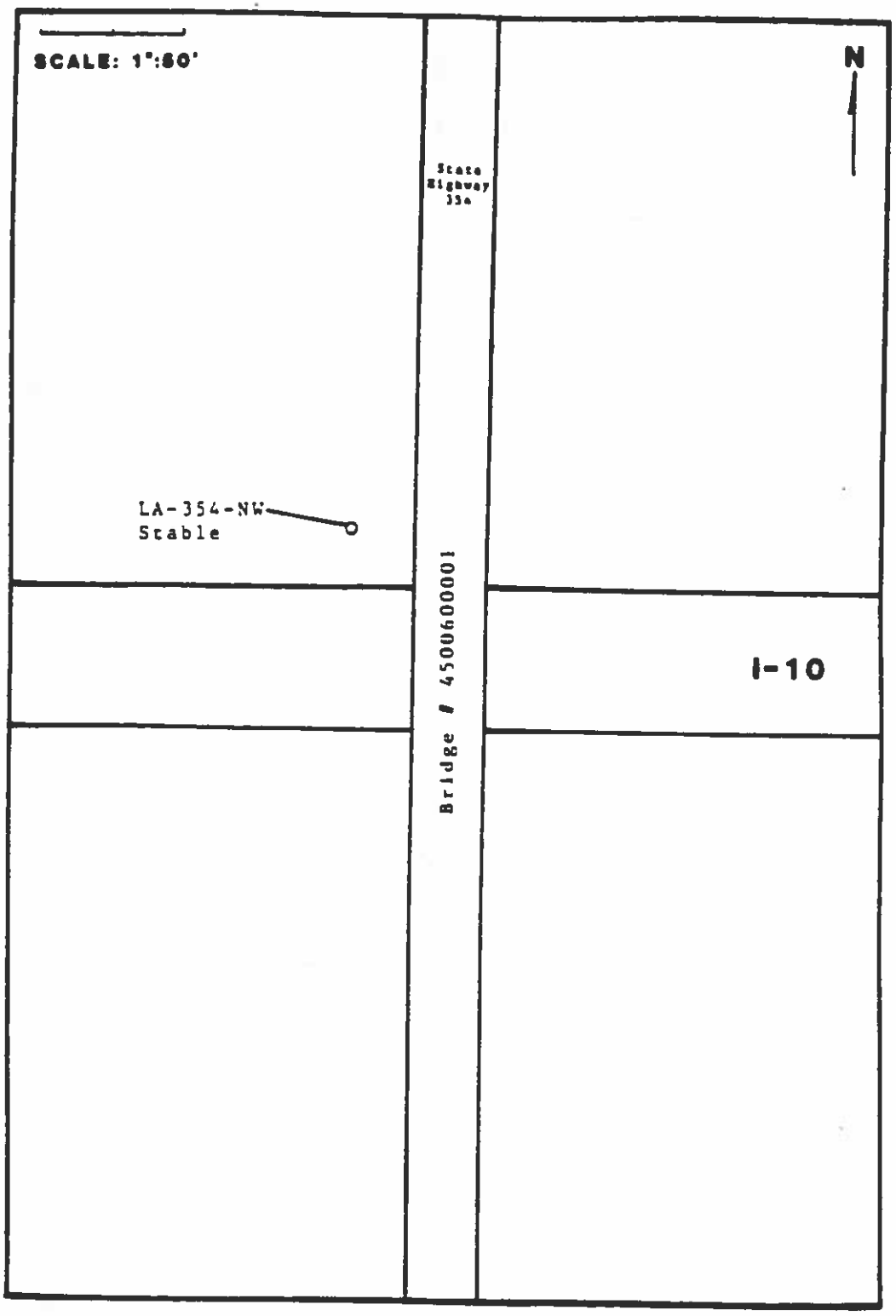

Figure A22. Locality S22, Lafayette Parish.

TABLE A12

EMBANKMENT SLOPE FAILURE DATA

Locality	Failure Type*	Frequency	Total Volume*	Range	Mean
S1	---	---	---	---	---
S2	SE	1	4257	---	4257
S3	S	2	88900	41650-47250	44450
S4	---	---	---	---	---
S5	---	---	---	---	---
S6	---	---	---	---	---
S7	SE	5	70676	5445-26400	14135
S8	---	---	---	---	---
S9	SE	2	33600	660-33000	16800
S10	SE	1	825	---	825
S11	S	2	13281	1925-11356	6641
	SE	7	166947	825-79200	23850
	EF	1	1100	---	1100
S12	S	4	200585	21560-92400	50146
S13	EF	1	660	---	660
S14	S	3	55638	3168-45045	18546
	SE	2	24453	8778-15675	12227
	EF	1	880	---	880
S15	S	4	146878	6930-67595	36720
	SE	1	1789	---	1789
S16	EF	2	1001	451-550	501
S17	SE	5	107525	825-62370	21505
S18	SE	2	4191	2079-2112	2096
	EF	2	2805	561-2244	1403
S19	S	1	7040	---	7040
S20	---	---	---	---	---
S21	---	---	---	---	---
S22	---	---	---	---	---

* S = slump
SE = slump-earthflow
EF = earthflow

All volumes in cubic feet, slope angle in degrees. Note that cost of these failures are on the header portion of the slope.

TABLE A12 CONTINUED

SLOPE FAILURE DATA OF UNSAMPLED EMBANKMENTS

Slope Location	Failure Type*	Volume*	Slope Angle*
AC-RR-SW	S	74,250	----
AC-WOB-SW	SE	1,650	26
AC-EO1123-SE	E	1,000	27
AC-EO11123-NW	E	1,238	27
JD-97-NE	SE	4,653	27.5
JD-97-SE	SE	1,100	26
JD-CG-E	S	2,970	26
JD-CG-W	SE	4,950	26

* S = slump, SE = slump-earthflow, E = earthflow. All volumes are in cubic feet, and slope angles are in degrees. Note that most of these failures are on the header (revetment) portion of the slope.

I-20 Study Area Maps

This portion of Appendix 4 contains site maps with sample locations for embankments that have failed. These embankments are those of the Cow Bayou,Quebec, Tendal, Chicago Mill, and Tallulah Railroad locations.

Sample locations are indicated by dark circles and the corresponding sample numbers. Also given are the type of failure, volume of failure, and the scarp height for individual failures. Maps are arranged according to occurrence from west to east within Madison Parish.

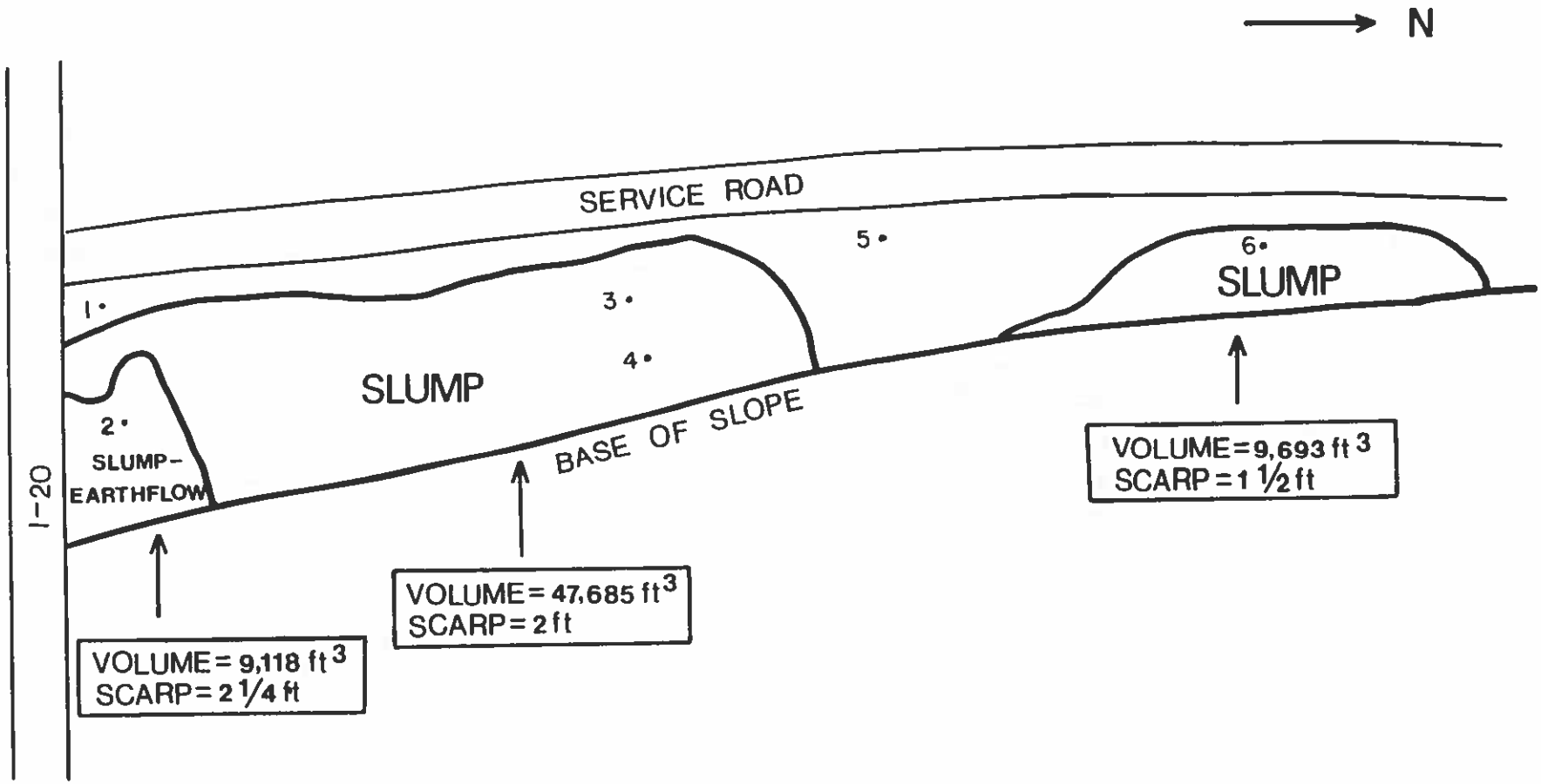

Figure A23. Locality N13, sample location and site map of Cow Bayou, northeast quadrant.

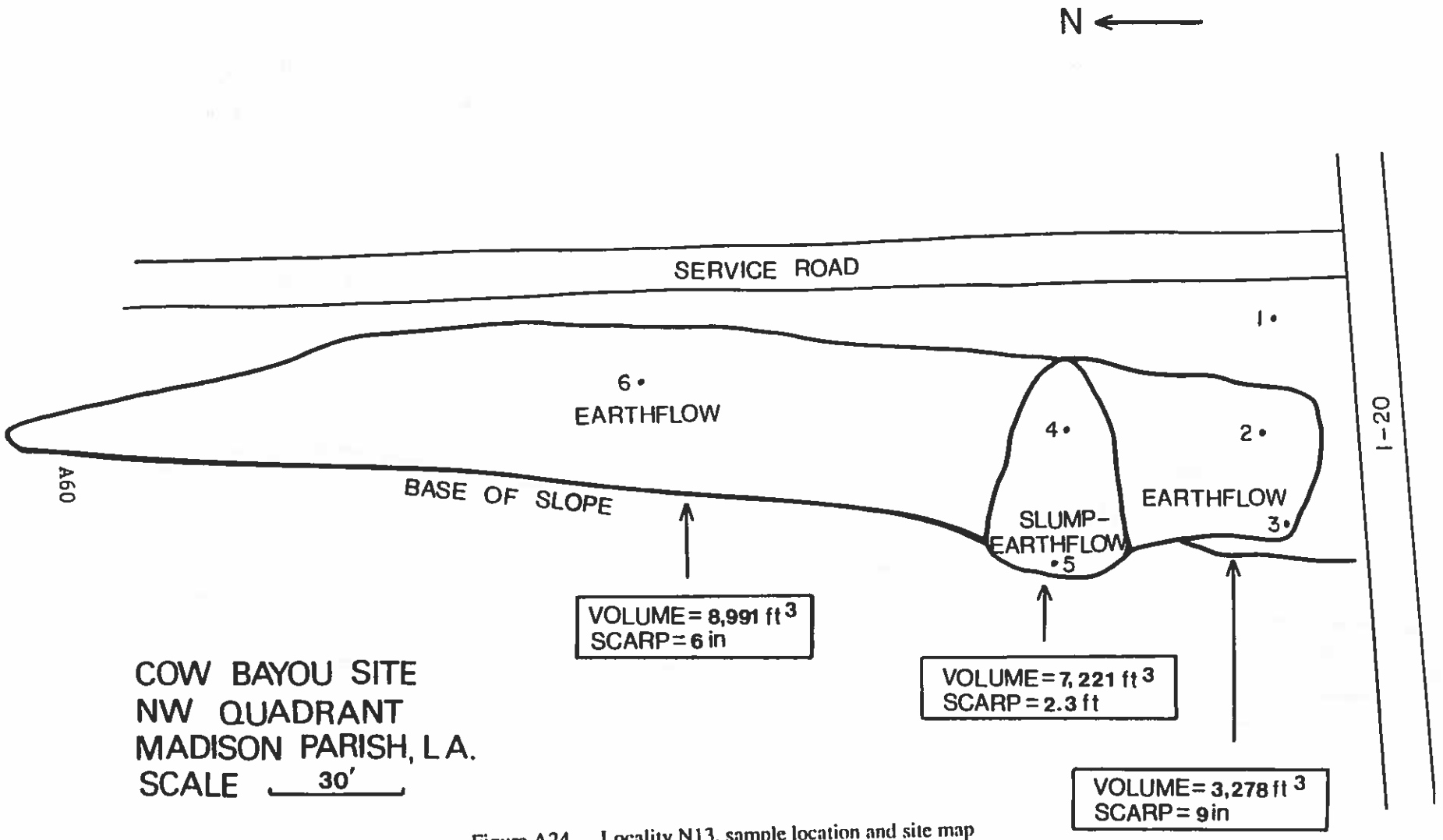

Figure A24. Locality N13, sample location and site map of Cow Bayou, northwest quadrant.

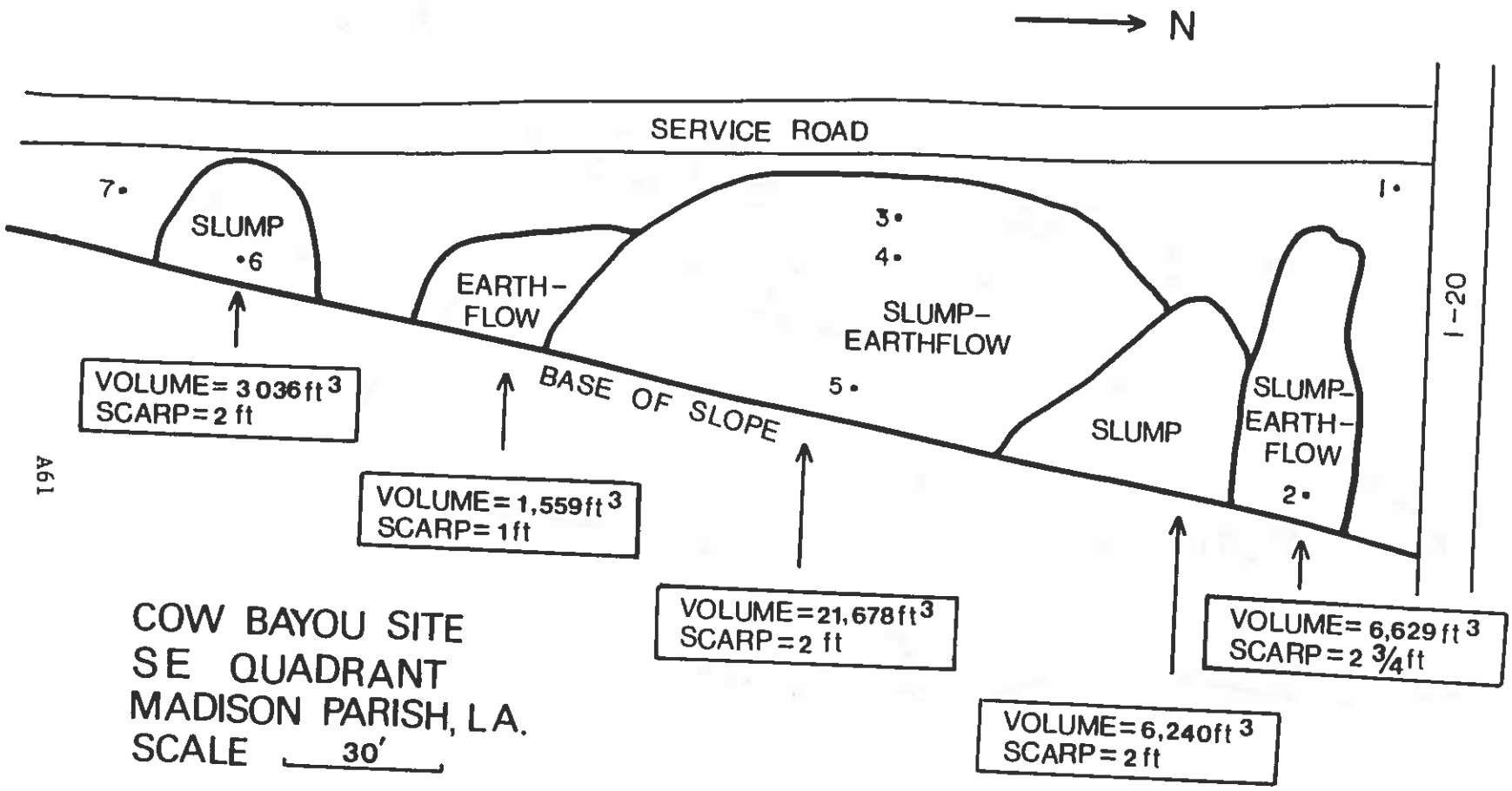

Figure A25. Locality N13, sample location and site map of Cow Bayou, southeast quadrant.

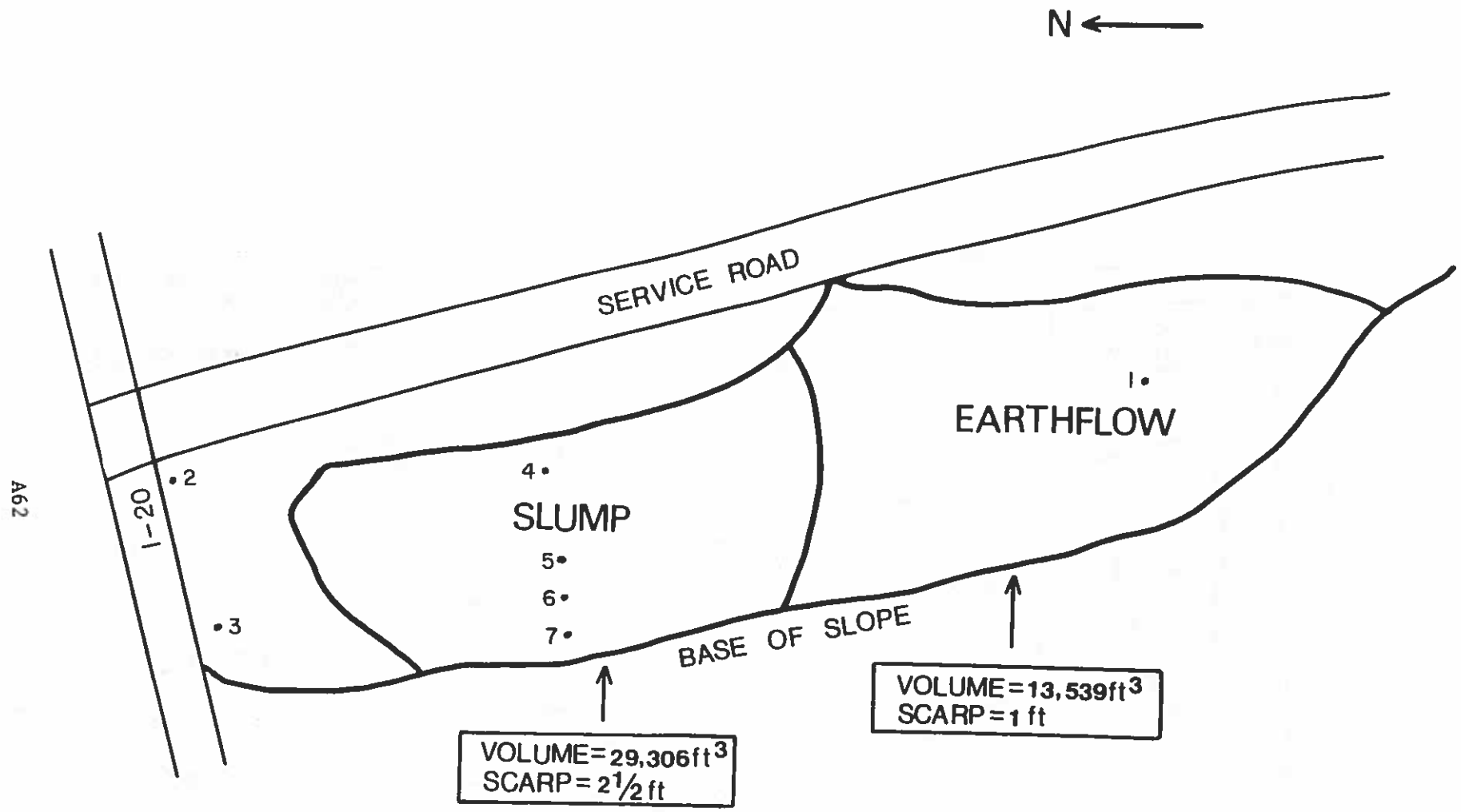

Figure A26. Locality N13, sample location and site map of Cow Bayou, southwest quadrant.

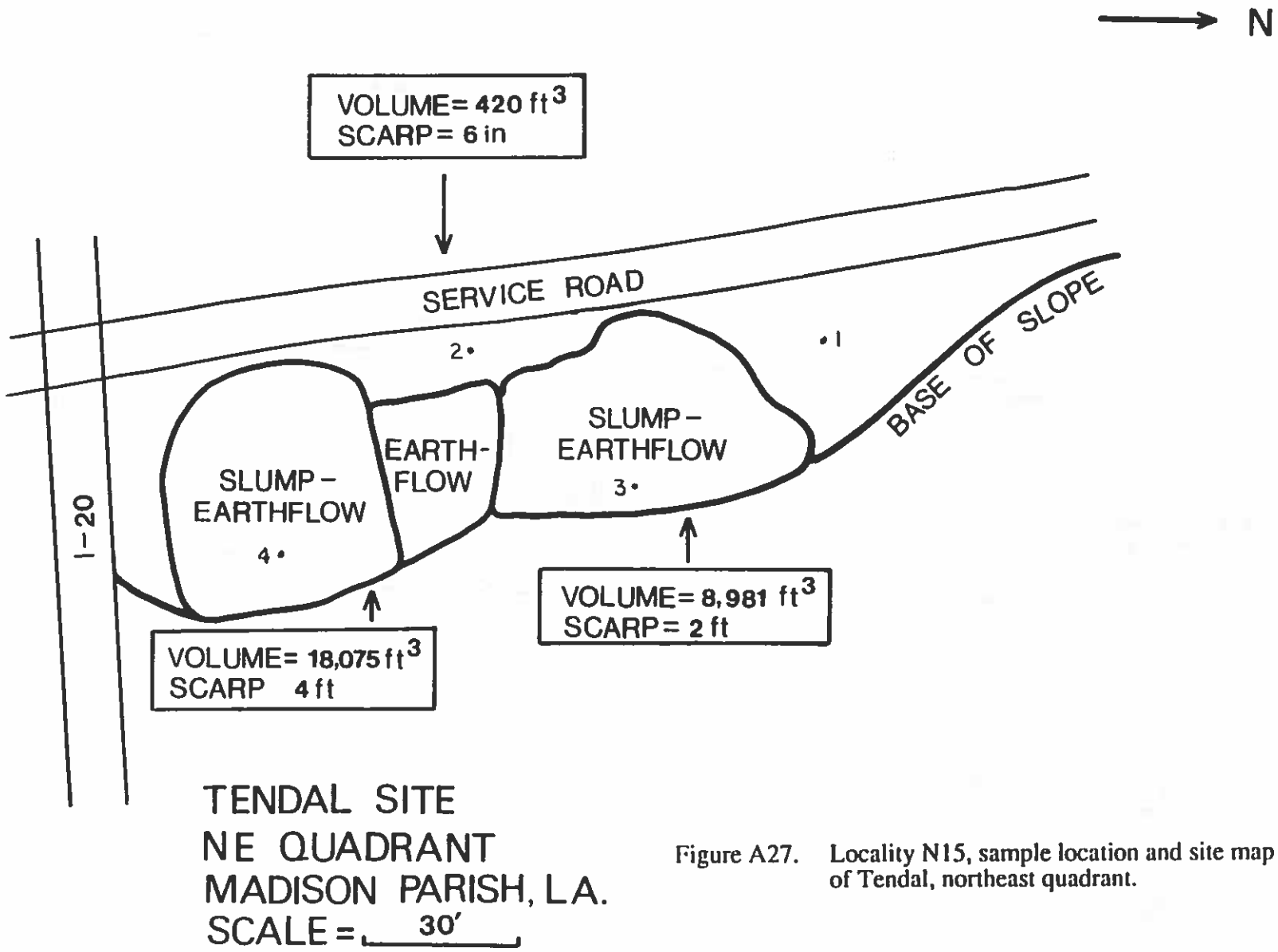

Figure A27. Locality N15, sample location and site map of Tendal, northeast quadrant.

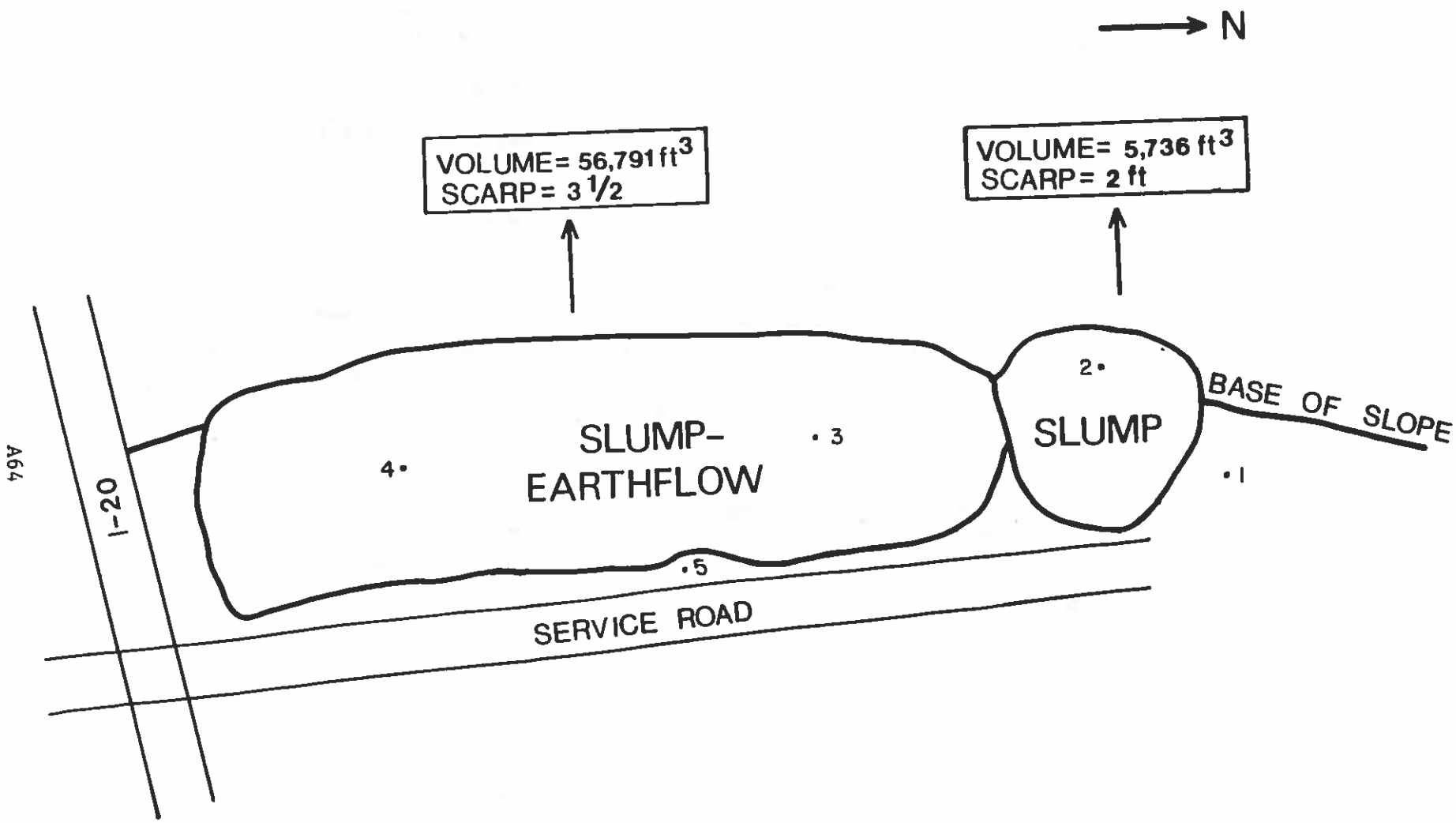

Figure A28. Locality N15, sample location and site map for Tendal, northwest quadrant.

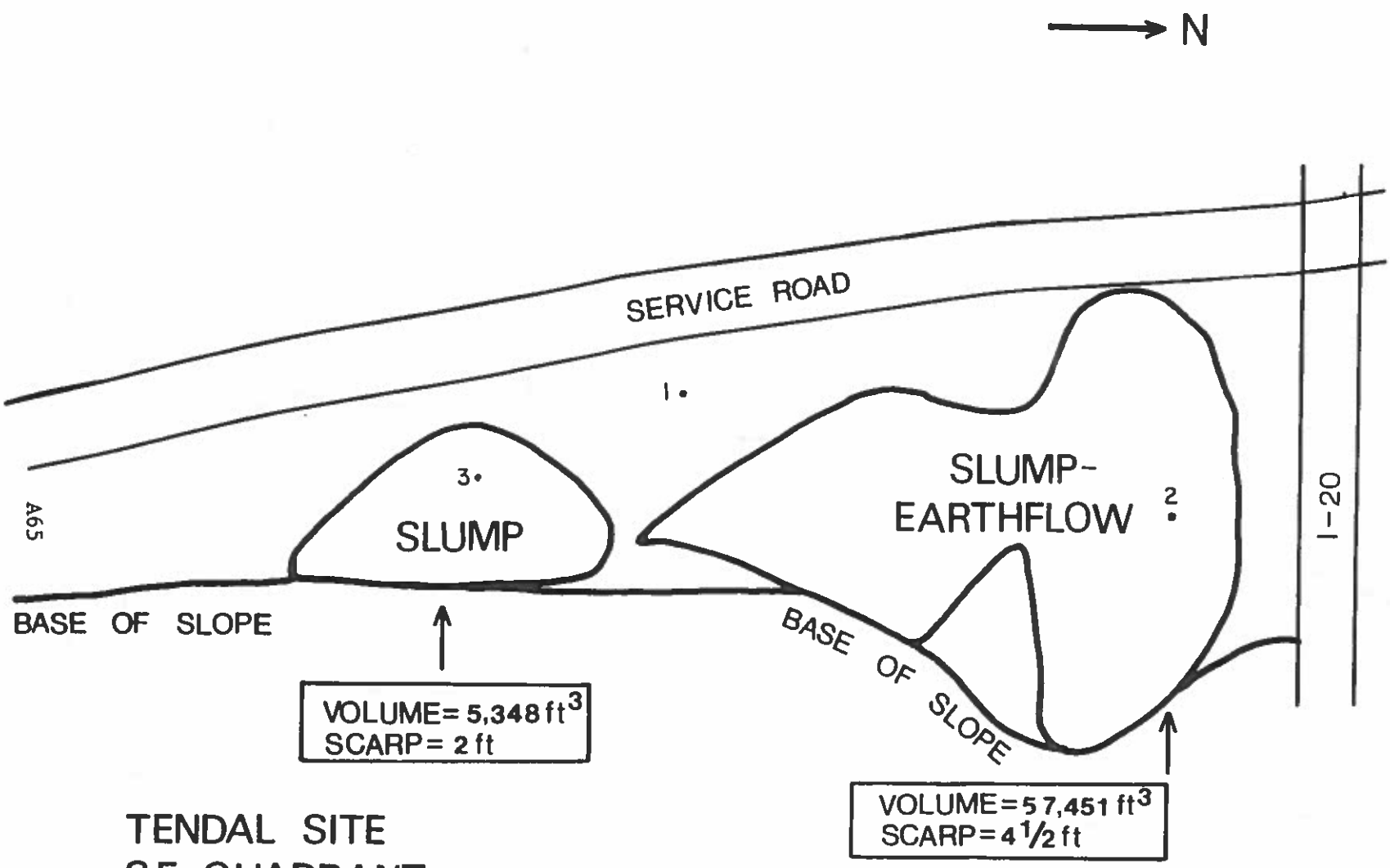

Figure A29. Locality N15, sample location and site map for Tendal, southeast quadrant.

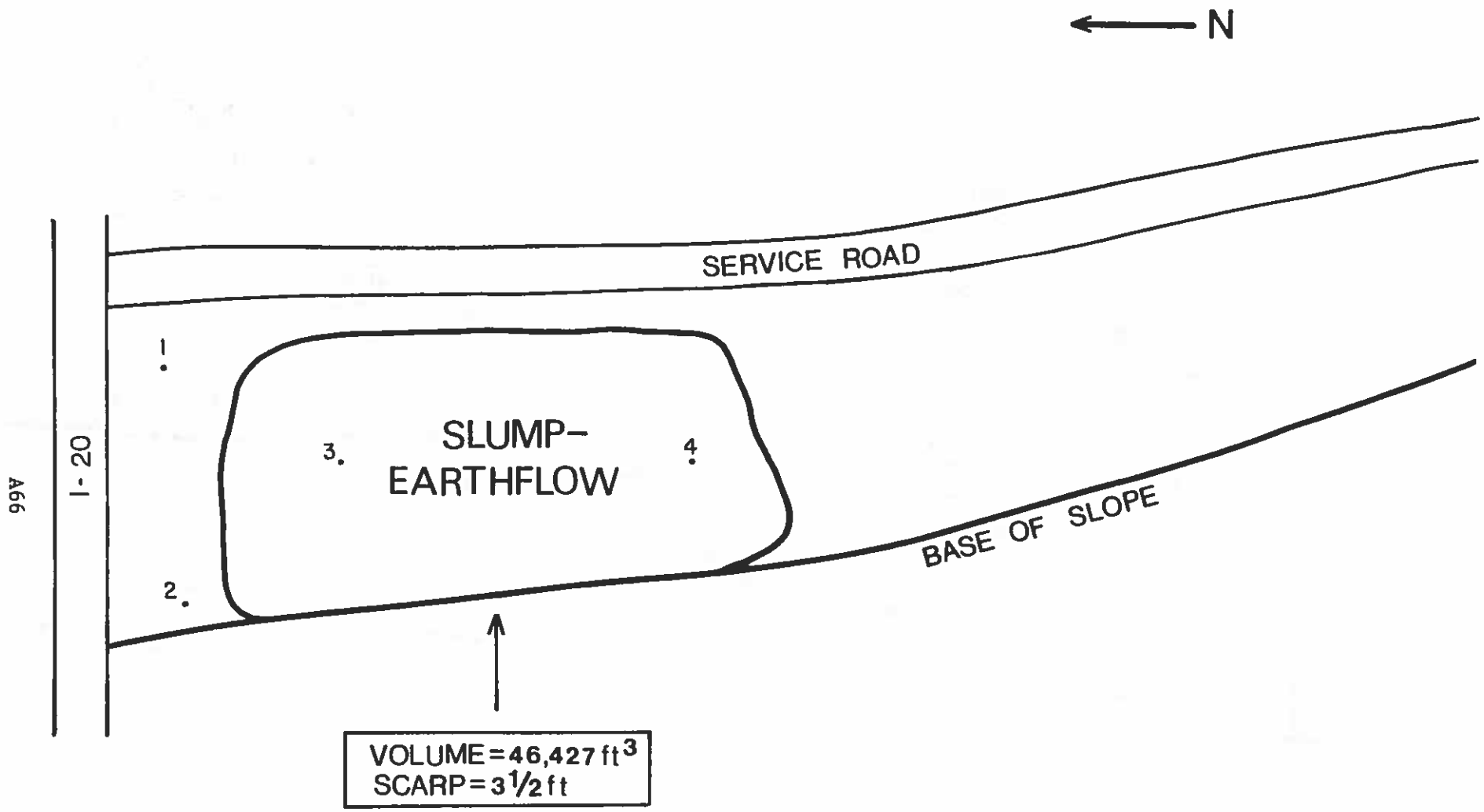

Figure A30. Locality N15, sample location and site map for Tendal, southwest quadrant.

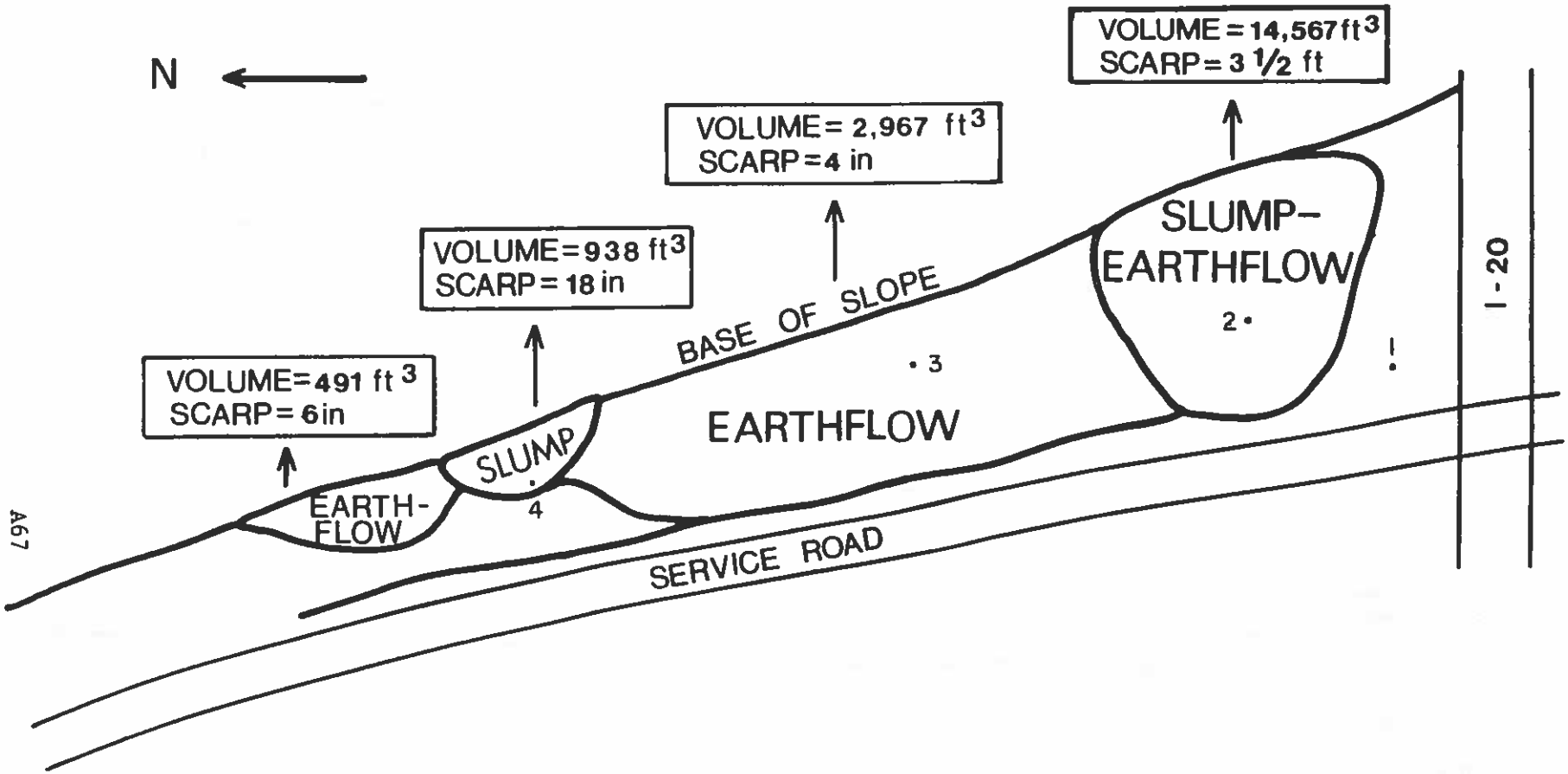

Figure A31. Locality N16, sample location and site map for Quebec, northeast quadrant.

QUEBEC SITE
NE QUADRANT
MADISON PARISH, LA.
SCALE 30'

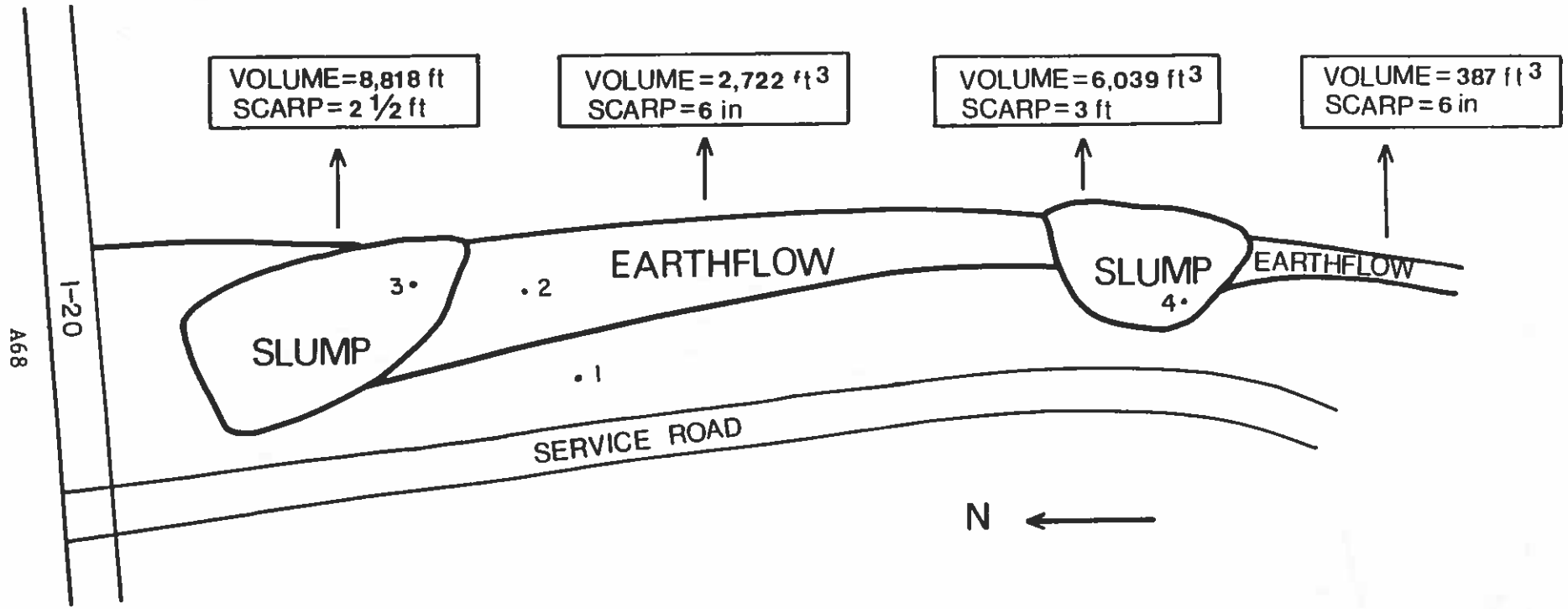

Figure A32. Locality N16, sample location and site map for Quebec, southeast quadrant.

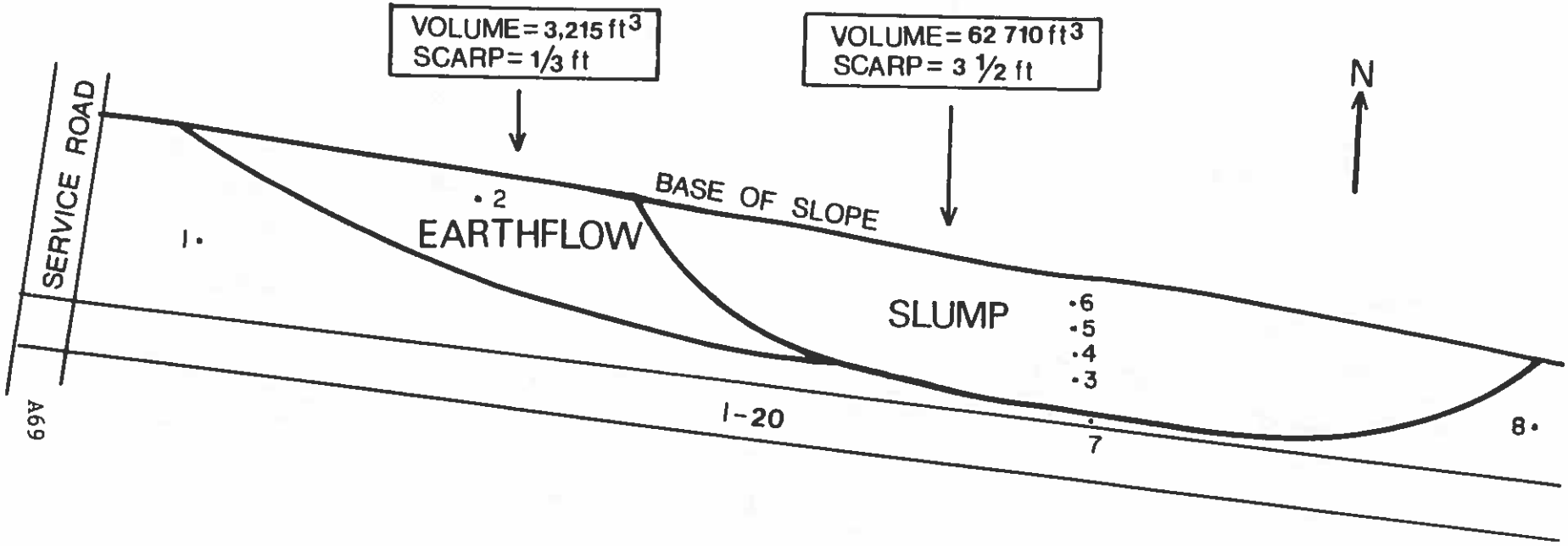

CHICAGO MILL SITE
NE QUADRANT
MADISON PARISH, LA.
MAY 1986
SCALE= 30'

Figure A33. Locality N17, sample location and site map for Chicago Mill, northeast quadrant.

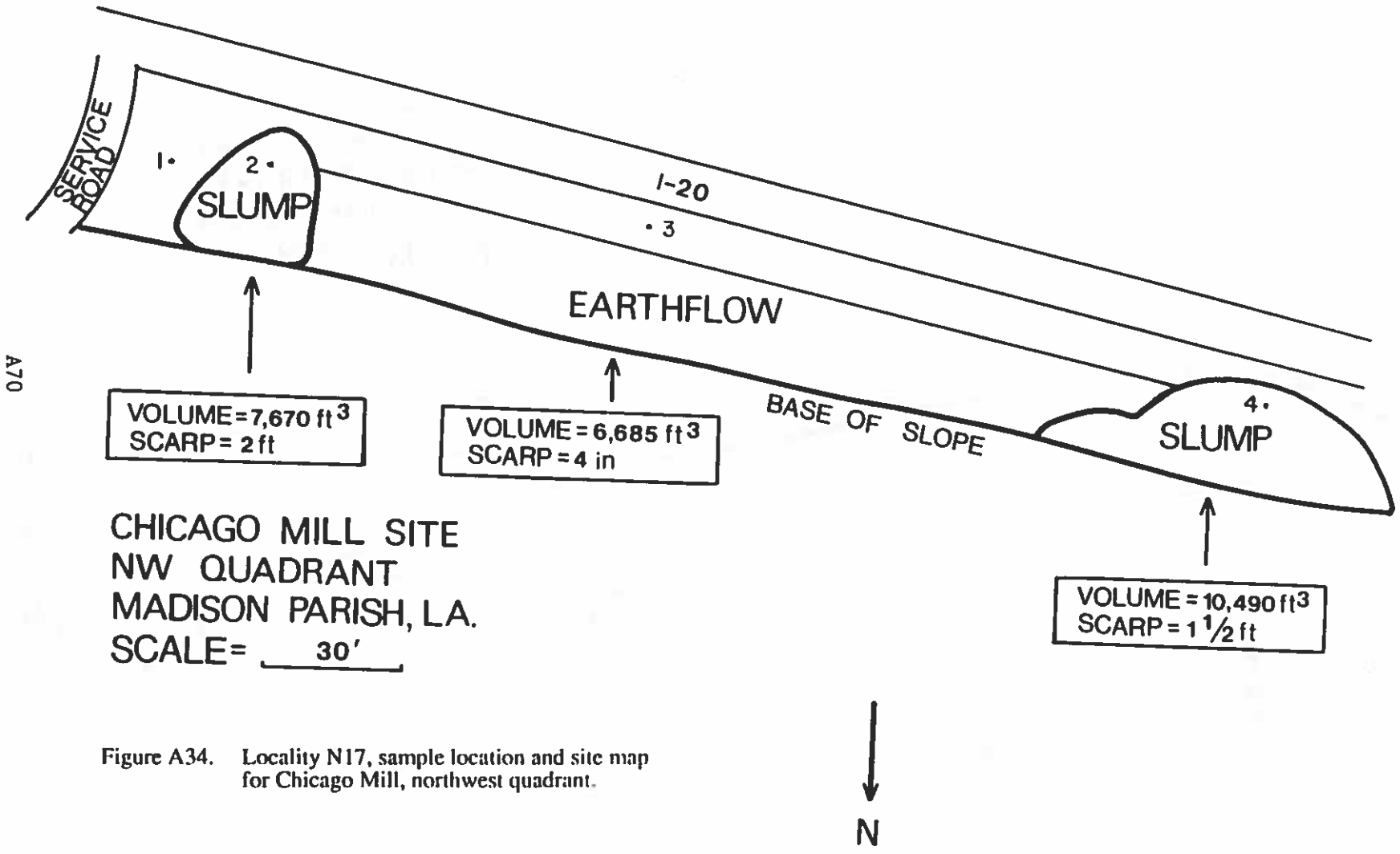

Figure A34. Locality N17, sample location and site map for Chicago Mill, northwest quadrant.

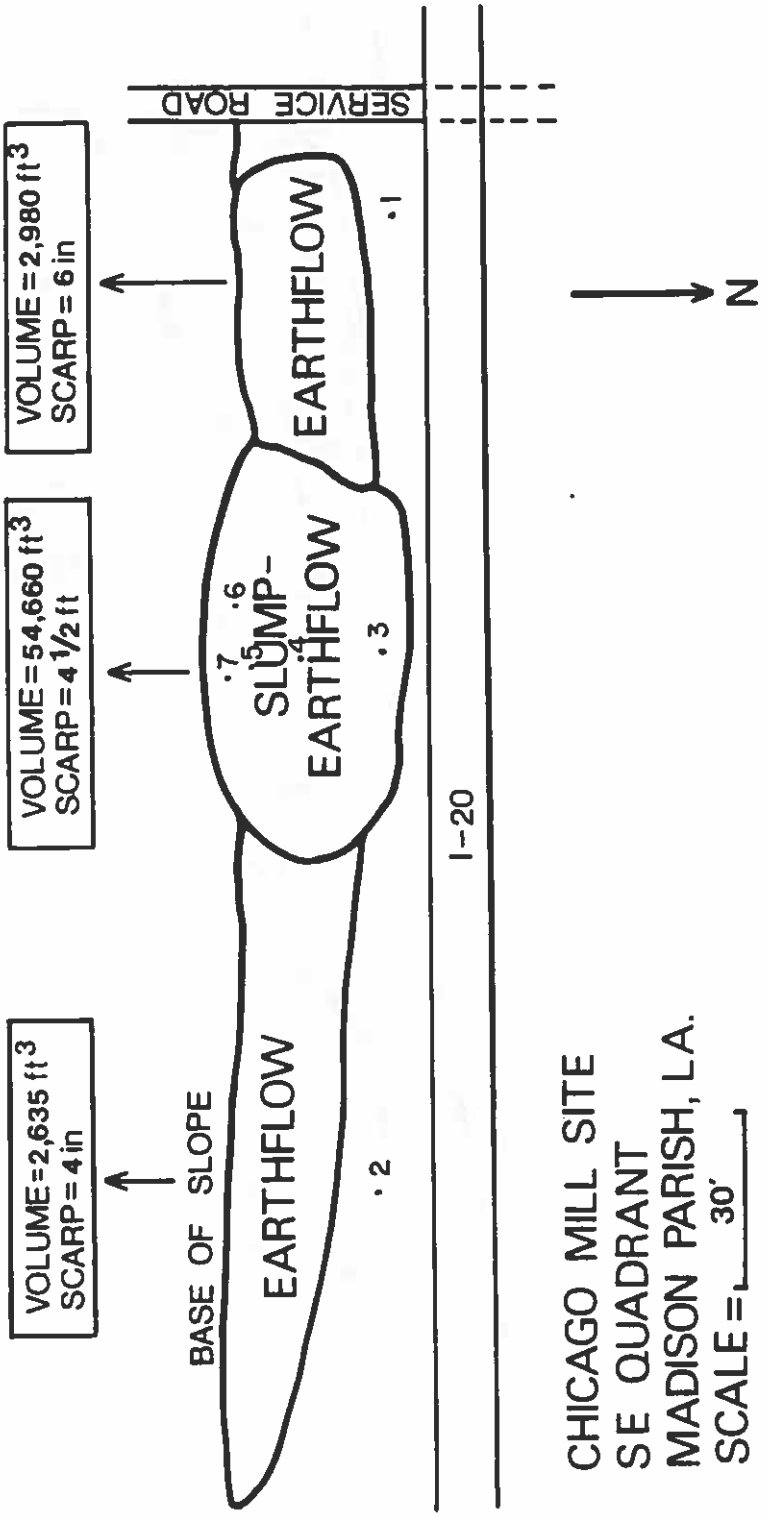

Figure A35. Locality N17, sample location and site map for Chicago Mill, southeast quadrant.

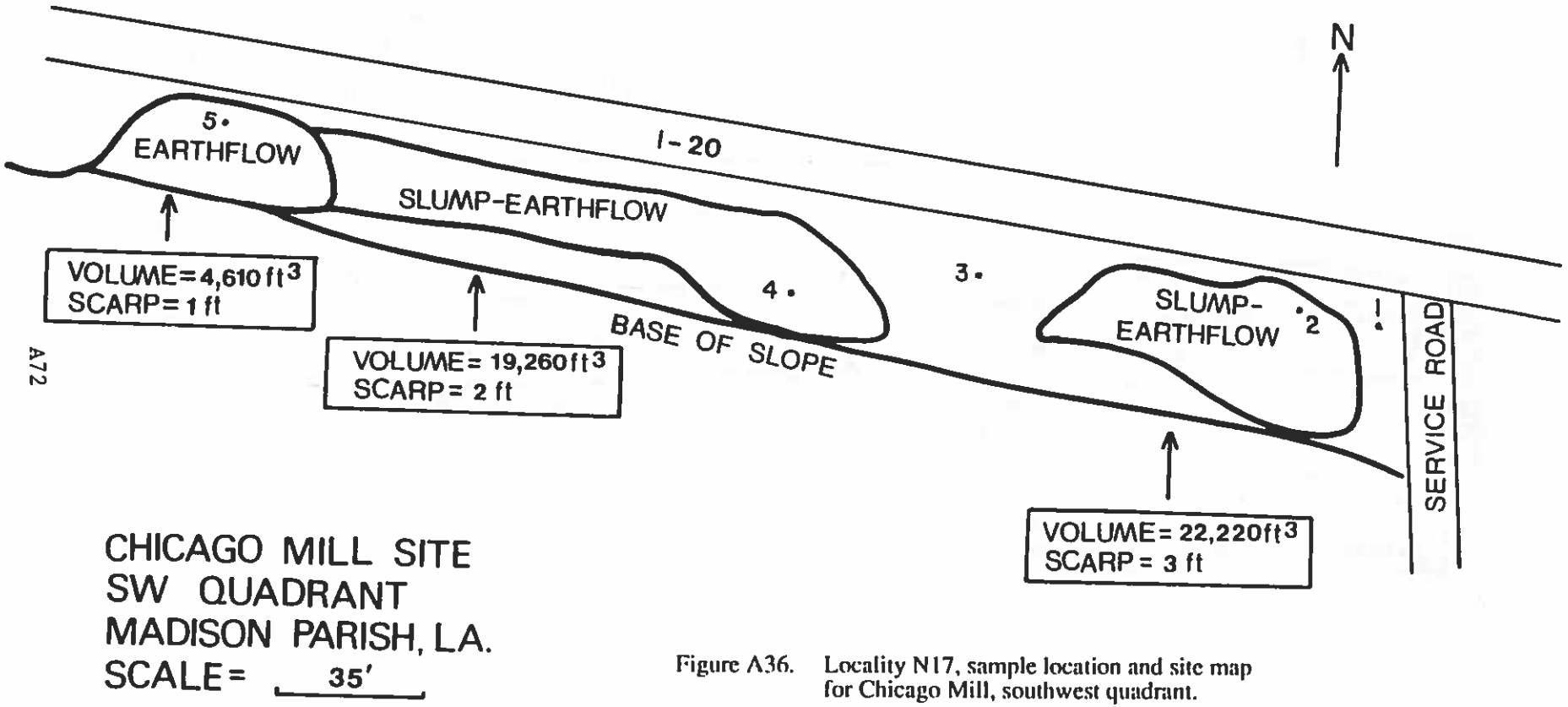

Figure A36. Locality N17, sample location and site map for Chicago Mill, southwest quadrant.

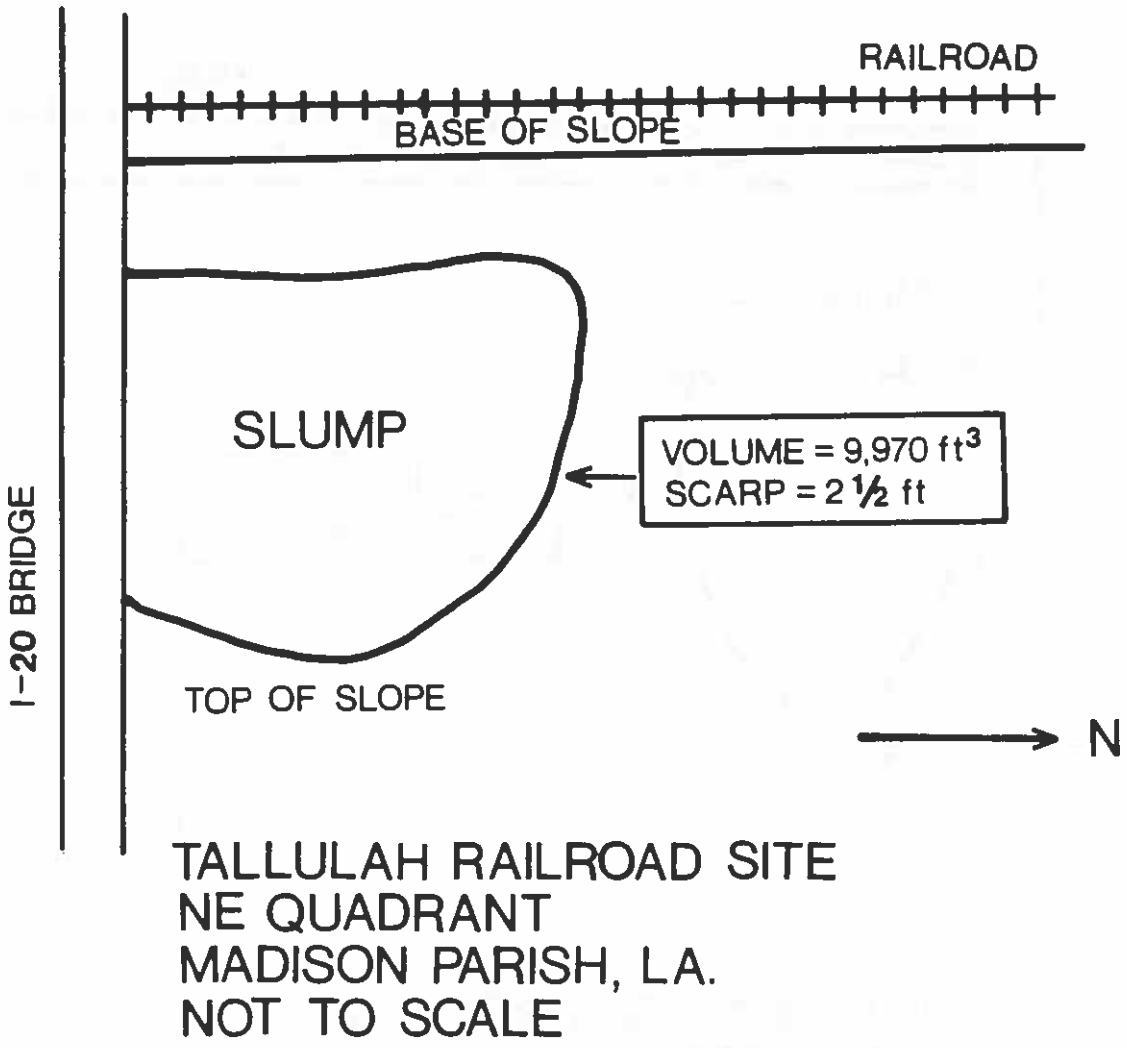

Figure A37. Locality N18, sample location and site map for Tallulah Railroad, northeast quadrant.

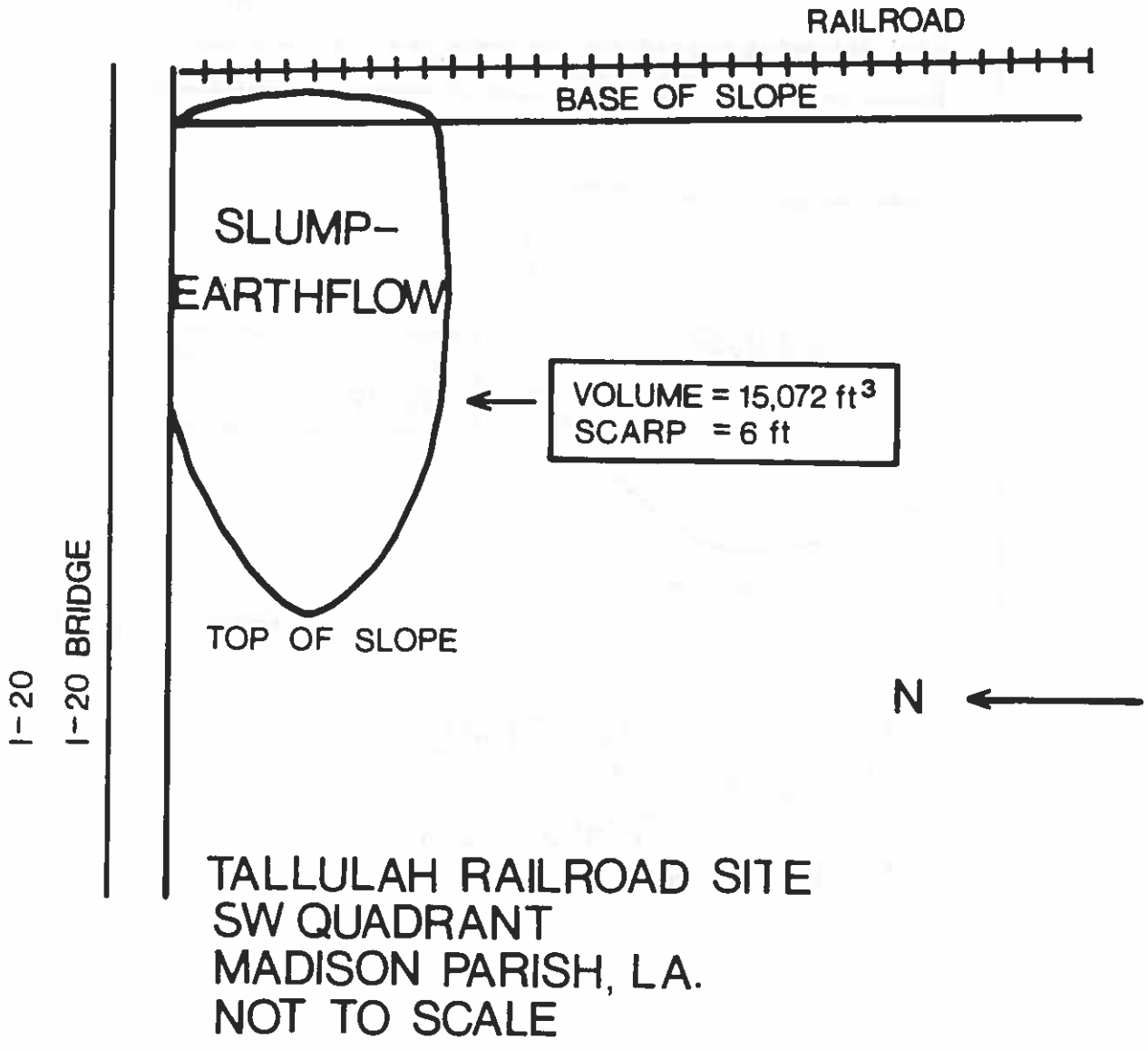

Figure A38. Locality N18, sample location and site map for Tallulah Railroad, southwest quadrant.

APPENDIX 5

DETAILED DESCRIPTIONS OF THE EMBANKMENT FAILURES AND SAMPLES OF THE MISSISSIPPI RIVER FLOOD PLAIN OF THE I-20 STUDY AREA

At the time of mapping, 42 embankment failures had occurred within the Mississippi River flood plain of the I-20 study area. The sample sites of this area in Madison Parish, from east to west, are Cow Bayou, Waverly, Tendal, Quebec, Chicago Mill, and the Tallulah railroad (Fig. A39). Since these sample sites contain nearly all of the failures in the I-20 study area, each site was characterized individually in detail.

Due to remolding of slope material during construction, embankment slopes are fairly uniform in composition. Therefore, the analysis of the slopes should vary only slightly among the samples from a site, with the biggest differences occurring between sites. The only contradiction is where the slopes had been previously repaired. This has been substantiated by T-test data comparing properties of samples taken from failed and non- failed portions of each slope. Properties examined in the T-test were particle size, Atterberg limits, and clay mineralogy. The results of this test suggest that no significant differences exist between the failed and non-failed portions of embankment slopes, which suggests homogeneity. Not only is the slope composition homogeneous, but small inhomogeneities can be masked by the high clay content. Mitchell (65) states that if one-third or more of the soil is clay, as in Madison Parish, then the soil will act as a clay due to the prevention of interparticle contacts between the grains. This occurs at moisture contents normally encountered.

Cow Bayou Locality N13

All four embankments at the Cow Bayou site have failed. The embankments at the Cow Bayou site were constructed in 1970 and failed in December, 1982, after a heavy rainfall of over 12 inches (305 mm). Slope angles vary from 16-18 degrees or 3.5:1 to 3:1 (Table A2). A total of 13 failures have occurred (Table A13). Figures A23 - A26 display the failures on the site maps for this location.

Average values for the properties from the 26 samples collected from the site have been calculated. Particle size distribution is 57% clay (std.dev.= 9.9), 35% silt (std.dev.= 7.1), and 8% sand (std.dev.= 3.7) (Table A4). The liquid limit is 58% (std.dev.= 11.2), plastic limit is 26% (std.dev.= 4.9), plasticity index is 32% (std.dev.= 8.3), and moisture content is 34.6% (std.dev.= 7.0) (Table A5). The moisture content is lower at this site than at the Chicago Mill site due to a smaller amount of clay. The smaller clay content is also responsible for the lower

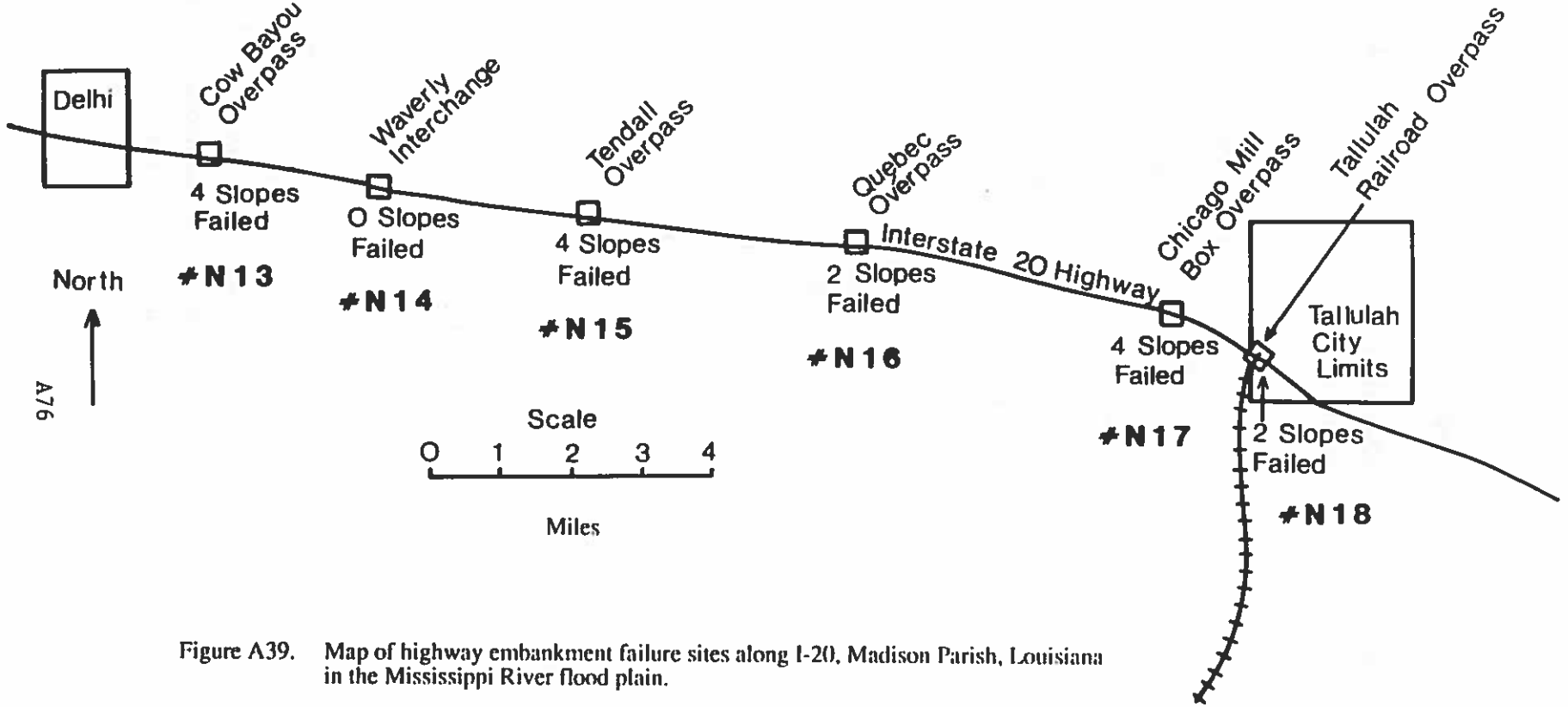

Figure A39. Map of highway embankment failure sites along I-20, Madison Parish, Louisiana in the Mississippi River flood plain.

TABLE A13

Cow Bayou Site Slope Failure Summary

SLOPE	FAILURES	VOLUME ft^3	VOLUME m^3	TOTALS ft^3	TOTALS m^3
NE	Slump	47,685	1,353		
	Slump	9,693	275	66,496	1,887
	Slump-E	9,118	259		
NW	Slump-E	7,221	205		
	Earthflow	8,991	255	19,490	553
	Earthflow	3,278	98		
SE	Slump	6,240	177		
	Slump	3,036	86		
	Slump-E	21,678	615	39,142	1,110
	Slump-E	6,629	188		
	Earthflow	1,559	44		
SW	Slump	29,306	831		
	Earthflow	13,539	384	42,845	1,215
				---	---
				167,973	4,765
	---	---			
	TOTALS	AVERAGES			
	---	---			
	5-Slumps	19,192	544		
	4-Slump-E	11,162	317		
	4-Earthflows	6,842	194		

liquid limits and plasticity index, when compared to the Chicago Mill site. The organic carbon and pH for the site are .48% (std.dev.=.2) and 7.12 (std.dev.= .25) respectively (Table A4).

The average clay mineral composition for this site is 8% kaolinite (std.dev.= 2.8), 20% mica (std.dev.= 4.0), 2% interstratified clays (std.dev.= 3.7), and 70% smectite (std.dev.= 6.1). The net smectite is 40 % (std.dev.= 7.5) (Table A9).

The particle size analysis and Atterberg limits results for the southwest slopes were excluded from statistical analysis. This is because this slope had been previously repaired with imported, sandier material, which subsequently failed. The samples were not representative of the original parent material. Sample 7 from southeast slope was also omitted due to poor sampling. The sample was taken from the top dressing of the slope, which is very silty.

Cow Bayou embankments were constructed from the Sharkey clay soil series (Table A2). Moist colors, according to the Munsell soil color charts, are typically 10YR 4/3-3/2 with mottled colors of 2.5Y 4/0-3/0, 5Y 5/1- 4/1, 5YR 4/5-3/4, and 7.5YR 4/6-3/2. Weems et al (5) report that the Sharkey soil has a moderate to high shrink-swell potential, liquid limits ranging from 32-85%, a plasticity index of 11-50%, and should not be used for embankment construction (5). The sample data fall within these ranges.

Waverly Locality N14

The embankments at Waverly (Fig. A39) were constructed in 1970 and had not failed at the time field work was being conducted. The slope angles at this site are slightly lower than those at the other sites in the Mississippi River flood plain. Slope angles range from 13- 16 degrees or 4.25:1 to 3.5:1 (Table A2).

Average values for the properties from the four samples collected from the site have been calculated. Particle size distribution is 64% clay (std.dev.= 11.0), 34% silt (std.dev.= 10.4), and 2% sand (std.dev.= .8) (Table A4). The liquid limit is 73% (std.dev.= 8.2), the plastic limit is 33% (std.dev.= 3.5), plasticity index is 40% (std.dev.= 7.0), and the moisture content is 30.0% (std.dev.= 3.4) (Table A5). The organic carbon is .55% (std.dev.= .12) and the pH is 7.47 (std.dev.= .21) (Table A4).

The average clay mineral content for this site is 9% kaolinite (std.dev.= 2.5), 18% mica (std.dev.=2.9), interstratified clays 1% (std.dev.= 2.5), and 72% smectite (std.dev.= 6.5). The net smectite is 46% (std.dev.= 4.5) (Table A9).

The embankments at Waverly interchange are also constructed from the Sharkey clay soil series (Table A2). Munsell colors for the Waverly site are typically 2.5Y 4/2-3/2, with mottled colors of 5Y 5/1-3/3, 5YR 3/3, 7.5YR 4/6, and 10YR 5/6. The data agree with the published plasticity ranges for the Sharkey soil.

The Waverly site has a higher clay and smectite content, which in turn increases the liquid limits and the plasticity index, than the Tendal or Cow Bayou sites, which have failed on all four embankments. Why hasn't Waverly failed? The main differences between these sites are the lower slope angles at Waverly. The lower slope angles have only prolonged the failing mechanism. This is supported by the fact that after returning to the Waverly site approximately one year after the original sampling, the southeast slope had failed. The other three slopes are also candidates for failure, based on their physical characteristics.

Tendal, Locality N15

The Tendal site (Fig. A39) was constructed in 1974 and failed in 1982 after a heavy rainfall. A total of 8 failures have occurred on the four slopes (Table A14) and slope angles vary from 16-19 degrees or 3.5:1 to 2.9:1 (Table A2). Figures A27-A30 display the failures on the site maps for this site.

Average values for the properties from the 16 samples collected from the site have been calculated. Particle size distribution is 58% clay (std.dev.= 7.5), 34% silt (std.dev.= 2.5), and 8% sand (std.dev.= 6.7) (Table A4). The liquid limit is 61% (std.dev.= 9.4), the plastic limit is 26% (std.dev.= 2.9), plasticity index is 36% (std.dev.= 8.4), and the moisture content is 34% (std.dev.= 7.0) (Table A5). The organic carbon is .45% (std.dev.= .14) and the pH is 6.80 (std.dev.= .43) (Table A4).

The average clay mineral content for this site is 8% kaolinite (std.dev.= 3.5), 18% mica (std.dev.= 3.1), 1% interstratified clay (std.dev.= 2.0), and 73% smectite (std.dev.= 6.8). The net smectite is 42% (std.dev.= 6.6) (Table A9).

The Tendal embankments were also built from the Sharkey clay soil series (Table A2). Munsell moist colors are typically 10YR 4/2-3/2 with mottled colors of 2.5Y 4/2-4/0, 5Y 5/2-4/1, 5YR 4/6-3/3, and 7.5YR 5/6-4.5/0. Once again, the samples agree with the published ranges, for the Sharkey soil has moderate to high shrink-swell potential, liquid limits ranging from 32-85%, plasticity indices ranging from 11-50% and should not be used in embankment construction (5).

Quebec Locality N16

The Quebec embankments were built in 1974 and also failed in 1982 after the same heavy rainfall (Fig. A39). Only two of the four embankments have failed at this site and these are the northeast and southeast slopes. There are a total of 8 failures at this site (Table A16), and the slope angles range from 16-20 degrees or 3.5:1 to 2.75:1 (Table A2). Figures A31-A32 display the failures on the maps for the two failed slopes at this location.

There are not any significant differences between properties of the failed and non-failed slopes. Average values for the properties from the 14 samples collected from the site have been calculated. Particle size distribution is 46% clay (std.dev.= 4.9), 39% silt (std.dev.= 3.7), and 15% sand (std.dev.= 4.4) (Table A4). Liquid limit is 50% (std.dev.= 5.4), plastic limit is 22% (std.dev.= 2.4), plasticity index is 22% (std.dev.= 4.9), and the moisture content is 25% (std.dev.= 3.3) (Table A5). These properties differ from those of Cow Bayou, Tendal, Chicago Mill, and Waverly in that the clay fraction is smaller, which reduces the liquid limit, plasticity index, and the moisture content. The organic carbon is .55 (std.dev.= .18) and the pH is 6.82 (std.dev.= 1.03) (Table A4).

The average clay mineral content for this site is 10% kaolinite (std.dev.= 3.1), 19% mica (std.dev.= 3.3), 3% interstratified clays (std.dev.= 6.4), and 68% smectite (std.dev.= 7.5). The net smectite is 31% (std.dev.= 4.5) (Table A9).

The Quebec site was constructed mainly of Sharkey clay soil series, but the borrow pit was also located within a small part of the Dundee soil series (Table A2). Munsell moist colors are typically 10YR 4/3.5-3/1 and 2.5Y 3/2 with mottled colors of 2.5Y 4/2, 5Y 6/1.5-2.5/1, 5YR 3/3.5, and 7.5YR 5/7-4/4. The Dundee soil has a low to high shrink-swell potential, liquid limits range from 20-70%, and plasticity indices range from 3-40% (5). The Dundee soil is located on slightly higher elevations than the Sharkey soil, on natural levees and low terraces. Therefore, it contains less clay and slightly more coarse grained material. The presence of the Dundee soil has slightly dampened the nature of the Sharkey soil at this site. The difference between the Quebec site and other sites in this area is in the sand fraction. The clay percentage decreases and the sand content increases. The reduction in clay reduces the Atterberg limits and the net smectite.

Chicago Mill, Locality N17

The Chicago Mill site is different from the others in that instead of the slopes facing the east and west, these slopes face north and south (Fig. A39). Chicago Mill embankments were constructed in 1970, and all four embankments failed in 1982 after a heavy rainfall. A total of 11 failures have occurred on the four embankments (Table A16). Slope angles vary from 13-17 degrees or 4.25:1 to 3.25:1 (Table A2). Figures A33-A36 display the failures on the site maps at this location.

Average values for the properties from the 23 samples collected from the site have been calculated. Particle size distribution for the Chicago Mill site is 77% clay (std.dev.= 7.6), 20% silt (std.dev.= 6.7), and 3% sand (std.dev.= 2.9) (Table A4). The liquid limit is 82% (std.dev.= 7.6), the plastic limit is 40% (std.dev.= 4.6) and the plasticity index is 41% (std.dev.= 5.9).

TABLE A16

CHICAGO MILL SITE SLOPE FAILURE SUMMARY

SLOPE	FAILURES	VOLUME ft^3	VOLUME m^3	TOTALS ft^3	TOTALS m^3
NE	Slump	62,710	1,779		
	Earthflow	3,215	91	65,925	1,870
NW*	Slump	10,490	298		
	Slump	7,670	218	24,845	705
	Earthflow	6,685	190		
SE	Slump-E	54,660	1,551		
	Earthflow	2,980	85	60,275	1,710
	Earthflow	2,635	75		
SW*	Slump-E	22,220	630		
	Slump-E	19,260	546	46,090	1,308
	Earthflow	4,610	131		
				197,135	5,593
	TOTALS	AVERAGES			
	3-Slumps	26,950	765		
	3-Slump-E	32,045	909		
	5-Earthflows	4,025	114		

* = Additional failures have occurred on these slopes since the study began (March 1986).

The moisture content is 44.2% (std.dev.= 5.4) which is rather high due to large amounts of clay retaining water (Table A5). The organic carbon is .49% (std.dev.= .26) and the pH is 7.45 (std.dev.=.26) (Table A4).

The average clay mineral content for this site is 9% kaolinite (std.dev.= 2.3), 16% mica (std.dev.= 4.3), 1% interstratified clays (std.dev.= 3.4), and 73% smectite (std.dev.=6.5). The average percent of net smectite for the site is 56% (std.dev.= 7.8) (Table A9).

Chicago Mill embankments were constructed from the Sharkey clay soil series (Table A2). Munsell moist colors are typically 2.5Y 4/2-3/2 and 10YR3/2 with mottled colors of 5Y 5/1.5-4.5/1, 5YR 3/3, 7.5YR 5/6- 3/2.5, and 10YR 5.5/7. The Soil Conservation Service (5) data for the Sharkey soil agrees with my data for this site. This published data also recommends that the Sharkey soil not be used in embankment construction. These slopes contained the highest amounts of clay and smectites in the study area.

Tallulah Railroad, Locality N18:

These embankments were constructed in 1974 and failed in 1982 after a heavy rainfall (Fig. A39). This site has north-south facing slopes and east-west facing slopes. The east-west slopes are under the bridge facing the railroad tracks and will be designated railroad embankments. The north-south facing slopes parallel the highway, as the slope is built up approaching the bridge. Only the Southwest and Northeast railroad embankments had failed here at the time of field work, for a total of two failures (Table A17). Figures A37-A38 contain site maps with sample locations for the original failed slopes. Slope angles are 16 degrees for the southwest and 17 degrees for the northeast slopes (Table A2).

Average values for the properties from the four samples collected from the site have been calculated. Particle size distribution is 45% clay (std.dev.= 6.6), 45% silt (std.dev.= 5.8), and 10% sand (std.dev.= 2.1) (Table A4). Liquid limit is 55% (std.dev.= 6.9), plastic limit is 26% (std.dev.= 3.5), plasticity index is 29% (std.dev.= 5.1), and the moisture content is 25.4% (std.dev.= 5.3) (Table A5). These properties are very similar to the Quebec site where two failures had occurred. The organic carbon is .54% (std.dev.= .19) and the pH is 7.48 (std.dev.=.19) (Table A4).

The average clay mineral content for this site is 9% kaolinite (std.dev.= 2.5), 16% mica (std.dev.= 4.8), 4% interstratified clays (std.dev.= 2.5), 71% smectite (std.dev.= 7.5), and the net smectite is 33% (std.dev.= 8.1) (Table A9).

The Tallulah railroad site is constructed from the Commerce soil series or that is where the nearest borrow pit is located (Table A2). Liquid limits and plasticity indices for the Commerce soil, as reported by the SIR (National Cooperative Soil Survey, 1985) are 23-50% and non-plastic to 25%, respectively. These numbers are a little lower than the values that we

TABLE A17

TALLULAH RAILROAD SITE SLOPE
FAILURE SUMMARY

SLOPE	FAILURES	VOLUME ft^3	VOLUME m^3	TOTALS ft^3	TOTALS m^3
*NE	Slump	4,970	141	4,970	141
*SW	Slump-E	15,072	428	15,072	428
*NW	NO DATA				
SE	STABLE			--------	----
				20,042	569

TOTALS	AVERAGES	
1-Slump	4,970	141
1-Slump-E	15,072	428

* = Additional failures have occurred on these slopes since the study began (March 1986).

calculated. It is possible that some Sharkey soil was incorporated with the Commerce. A borrow pit of Sharkey soil exists to the northwest of the site. Munsell moist colors of the samples are typically 2.5YR 3/2 and 10YR 3/2 with mottled colors of 5Y 5/1, 7.5YR 5/6, and 10YR 4.5/6.

After returning to this site in March, 1987, approximately one year after the original sampling, additional failures had occurred. The southwest slope, which parallels and slopes away from the highway, had failed and the northwest slope, paralleling the highway, had two failures. The site now contains five failures. The volume of material displaced on the southwest slope is approximately 44,000 cubic feet (1248 cubic meters) and the material displaced on the northwest slope for the two failures totals approximately 55,000 cubic feet (1560 cubic meters). These failures are all classified as slump-earthflows. These failures are not recorded on the location maps (Figs. A37 and A38) or in Table A17.

DETAILED DESCRIPTIONS OF SLOPES AND SAMPLES FROM EMBANKMENTS IN RICHLAND AND OUACHITA PARISHES, I-20 STUDY AREA

Embankments on the Loess Covered Macon Ridge

The embankments included within this area are at the Holly Ridge interchange, Dunn interchange, Dunn-Delhi overpass, and the Dunn overpass (Localities 9-12, Fig. 2). The four embankments in this area were constructed in 1969 and 1970 with none having failed to date. Slope angles range from 10 degrees at the Holly Ridge interchange to 21 degrees at the Dunn-Delhi overpass. The parent material in this area differs considerably from the Mississippi flood plain area. This is expected since Macon Ridge is a loess-covered, valley train deposit (7).

Since there are no significant differences in the properties of the embankment material within the four sites, they will be characterized together. The average grain size distribution is 26% clay (std.dev.= 5.4), 65% silt (std.dev.= 8.0), and 9% sand (std.dev.= 4.8) (Table A4). As can be seen, the silt fraction is high which denotes the large amount of loess present in this area. The liquid limit is 33% (std.dev.= 4.0), the plastic limit is 23% (std.dev.= 2.0), the plasticity index is 10% (std.dev.= 3.8), and the moisture content is 14% (std.dev.= 3.6) (Table A5). This reflects the small amount of clay in the sample and better drainage. The average organic carbon is .39 (std.dev.= .17) and the pH is 6.13 (std.dev.= .88) (Table A4).

The average clay mineral content for this area is 11% kaolinite (std.dev.= 1.9), 21% mica (std.dev.=10.2), 32% interstratified clays (std.dev.= 11.1), and 36% smectite (std.dev.= 6.9). The percentage of net smectite is 10% (std.dev.= 2.1) (Table A9), which results from the low amount of clay and the low smectite percentage.

Unlike the flood plain area to the east, 32% of the clay fraction in this area is mica-smectite interstratified clay. The presence of a significant amount of interstratified clay is attributed to increased weathering in these older soils and therefore, an increased stability of the slopes. When compared to the Mississippi River flood plain soils as a group, these sites can be summarized as being low in clay and high in silt, which in turn lower the Atterberg limits.

The embankments at the Holly Ridge site are constructed from the Grenada-Foley-Calhoun soil association. The Dunn interchange and Dunn-Delhi overpass are constructed from the Grenada-Calhoun soil associations, and the Dunn overpass is constructed from the Grenada-Calhoun-Memphis soil association (Table A2). The Soil Conservation Service (8) reports that these soils have low plasticity indices and liquid limits, which as a group

range between 5-32% and 20-60% respectively. These figures agree with the data. There is little or no risk of slope failures, but due to the high silt content, piping can be prevalent. We noted some surface piping on many of the slopes, but nothing was severe.

Munsell moist colors range typically from 7.5YR4/4 to 10YR 5.5/4-4/3 with mottled colors of 2.5Y 8/0-6/2, 5Y 7.5/2-5.5/2, and 10YR 5/8.

Embankments on Western Part of Macon Ridge

On the western part of Macon Ridge, there is very little loess mixed in with the valley train deposits. The embankments constructed in the area are the Bee Bayou- Holly Ridge overpass, the Bee Bayou interchange, the Rayville East overpass, and the Start interchange (Localities N5-8, Fig. 2). Between the Start and Rayville East site is the Girard site, where Macon Ridge is separated by younger natural levee deposits of the Boeuf River. The Girard site is included in the next section.

The embankments here were constructed in 1969 and 1970. Slope angles range from 17-19 degrees at each site other than the Rayville East site where it is 24 degrees. No failures have occurred in this area to date.

Since these embankments are constructed of the same parent material, their properties will be discussed together. Particle size distribution averages 21% clay (std.dev.= 4.8), 45% silt (std.dev.= 9.1), and 34 % sand (std.dev.= 11.2) (Table A4).

Moisture content has a average value of 15% (std.dev.= 4.0), indicating well-drained soils as compared to the flood plain environments (Table A5).

The average clay mineral content for this area is 11% kaolinite (std.dev.= 5.2), 20% mica (std.dev.= 8.0), 34% interstratified clay (std.dev.=12.2), smectite is 35% (std.dev.= 12.2), and the net smectite is 7% (std.dev.= 3.9) (Table A9).

Stability of the area is attributed to a low amount of net smectite in the slopes, which results from a decreased amount of clay and an increased amount of interstratified clays in the clay fraction.

The embankments at the Bee Bayou-Holly Ridge, Bee Bayou, and the Rayville East sites are constructed of the Grenada-Foley-Calhoun soil association. The Start embankments are constructed of the Rilla-Herbert- Sterlington soil association (Table A2). The plasticity index and liquid limits for the soils of this parent material range from non-plastic to 22% and 22-45%, respectively with averaged values of 27% (std.dev.= 5.1) for liquid limit, 20% for plastic limits (std.dev.= 3.6), and 7% (std.dev.= 4.1) for plasticity index (Table A5). The data, averaged for the area, fit well with the Soil Conservation Service (8) report values for liquid

limit of the Grenada-Calhoun-Foley association of 20-60% and plasticity indices of non-plastic to 32%. Values for the Rilla-Herbert-Sterlington association are 22-45% for liquid limit and non-plastic to 22% for plasticity index.

Munsell moist colors are typically 7.5YR 4/4 to 10YR 5/4-4/4 with mottled colors of 5YR 5.5/0-3.5/4. The average organic carbon and pH are .36% (std.dev.= .26) and 6.58 (std.dev.= .65) respectively (Table A4).

Macon Ridge is stable because the slopes contain approximately equal amounts of interstratified and smectite clays and the clay fraction is about three times less than the Mississippi flood plain sediments. The small amount of clay makes the net amount of interstratified clays and smectite insignificant,and therefore lowers the Atterberg limits. Plasticity index and liquid limit have a strong positive correlation with the percent of clay.

The Macon Ridge areas are very similar to each other, and the only notable difference is in the silt and sand fraction. The loess covered part of the ridge has 65% silt and 9% sand whereas the part not covered by loess has 45% silt and 34% sand. The increase in sand and silt and the subsequent decrease in clay cause a reduction in the Atterberg limits.

Embankments in the Ouachita River Flood Plain

The Ouachita River flood plain constitutes the fourth area of parent material. The Girard, Millhaven, Pecanland Mall, and the State Farm sites are constructed from this parent material (Localities N1-4, Fig.2). These embankments were constructed in 1966 and 1967 with slope angles ranging from 17-23 degrees, and at the time of field work (spring,1986) none of the embankments had failed. A field trip in the winter of 1987 revealed that the State Farm site had experienced two failures. The parent material properties of these sites are discussed together as averaged values because of the similarity of their values.

The grain size distribution averages 52% clay (std.dev.= 21), 36% silt (std.dev.= 11.7), and 12% sand (std.dev.= 13) (Table A4).

The average clay mineral content is 11% kaolinite (std.dev.= 2.3), 21% mica (std.dev.= 3.5), and 40% smectite (std.dev.= 4.2). The interstratified clay is 28% (std.dev.= 2.6) and the net smectite has a value of 20 % (std.dev.= 8.3) (Table A9).

The grain-size distribution is very similar to the Mississippi River flood plain area, but the clay mineral content differs. The Mississippi River flood plain averages 71% smectite and 43% net smectite. A very important difference is the 28% of interstratified mica-smectite clay in the Ouachita River flood plain samples, as compared to the 2% in the Mississippi flood plain.

The Atterberg limits are likewise similar to the those determined for the Mississippi flood plain, just slightly lower. The averaged liquid limit is 56% (std.dev.= 19), the plastic limit is 29% (std.dev.= 7.6), and the plasticity index is 27% (std.dev.= 12.3). The moisture content is 28% (std.dev.= 8.3), indicating a return to clayey soils and poor drainage (Table A5).

Munsell moist colors are typically 10YR 4/2.5 and 7.5YR 5/6-4/4 with mottled colors of 2.5YR 3/4, 2.5Y 6/2, 5YR 4/4, and 7.5YR 4/2. The average organic carbon is .44% (std.dev.= .24) and the pH is 7.59 (std.dev.=.35) (Table A4).

The embankments at the Girard site were constructed of the Rilla-Herbert-Sterlington soil association (Table A2). The Atterberg limits that we calculated are slightly higher than a those determined for this association by the Soil Conservation Service (8). But, due to a lack of soil survey for this parish, a more concise determination of the soil used is at this time not possible. The embankments at the Millhaven site are constructed from either the Herbert or the Portland soil series. Which type is not known definitely, since there are several borrow pits in proximity of the embankments. However, from examining the Atterberg limits data for this site, it seems likely that the Portland series was used. The liquid limits are from 70-88% and the plasticity ranges from 41-46% which is not even close to the values for Herbert as reported by the Soil Conservation Service (8).

The same problem exists at the Pecanland Mall site. The soil is either Portland or Herbert. As above, by examining the Atterberg limits data, it seems probable that the soil is the Herbert. Our liquid limits are 29-35% and the plasticity index is 9-16%, which fits well with the Soil Conservation Service (8) data for the Herbert soil series. The State Farm embankments are constructed from the Portland soil series. The Portland soil, as reported by the Soil Conservation Service (8), has plasticity indices ranging from 20-60% and liquid limits ranging from 55-90%, which coincides with our data.